Identification of Acetylcholinesterase Inhibiting Natural Products From *Buxus natalensis* and *Drypetes gossweileri*.

BY

WADIM LEONARDOVICH MATOCHKO

A thesis submitted to the Faculty of Graduate Studies

The University of Manitoba

In partial fulfillment of the requirements of the degree of

MASTER OF SCIENCE

Department of Chemistry

The University of Manitoba

Winnipeg, Manitoba

Canada

Copyright © 2010 by Wadim L. Matochko

Identification of Acetylcholinesterase Inhibiting Natural Products From *Buxus natalensis* and *Drypetes gossweileri*.

BY

WADIM LEONARDOVICH MATOCHKO

A thesis submitted to the Faculty of Graduate Studies of The University of

Manitoba in partial fulfillment of the requirement of the degree

Master of Science

Wadim Leonardovich Matochko © 2010

Permission has been granted to the University of Manitoba Libraries to lend a copy of this thesis, to Library and Archives Canada (LAC) to lend a copy of this thesis, and to LAC's agent (UMI/ProQuest) to microfilm, sell copies and to publish an abstract of this thesis.

This reproduction or copy of this thesis has been made available by authority of the copyright owner solely for the purpose of private study and research, and may only be reproduced and copied as permitted by copyright laws or with express written authorization from the copyright owner.

Abstract

This thesis describes phytochemical studies on two medically important plants, *Buxus natalensis* and *Drypetes gossweileri*.

Chemical investigation on the acetylcholinesterase inhibiting chloroform extracts, obtained at pH 7.0 and 9.5 resulted in the isolation of seven natural products: O^{10}-natafuranamine (**123**), cyclonataminol A (**124**), 31-demethylbuxaminol A (**125**), buxaminol A (**126**), buxaminol C (**127**), *p*-coumaroylputrescine (**128**) and methyl syringate (**129**). Compound **123** is a member of a rarely occurring class of *Buxus* alkaloids containing a tetrahydrofuran ring incorporated in its structure. Compounds **123-129** were isolated for the first time from this plant. Structures of compounds **123-129** were elucidated with the aid of NMR and MS spectral data. All of these isolates exhibited different levels of AChE inhibitory activities with compound **123** being significantly active in this bioassay with an IC_{50} of 8.5 μM compared to the rest of the isolates. Compounds **123-129** were inactive in antimicrobial assays.

Phytochemical studies on the crude extract of *Drypetes gossweileri* resulted in the isolation of a new *N*-linked aromatic glycoside, *N*-β-glucopyranosyl-*p*-hydroxy phenyl acetamide (**151**), along with two known compounds, *p*-hydroxy phenyl acetic acid (**152**) and *p*-hydroxyphenyl acetonitrile (**153**). Compounds **151-153** exhibited moderate to weak AChE inhibitory activities.

Acknowledgements

I wish to give my thanks and respect to Dr. Ata for allowing me the opportunity to work under his guidance as a graduate student and for the wisdom and knowledge he has imparted unto me so that I may successfully complete this project. I would like to thank the examining committee members for taking the time to read and evaluate this thesis. I thank my mother for all her support throughout my years of study, the many life lessons that she has taught me and the overwhelming amount of patience and love that she has devoted. I appreciate the support of provided by Ramin Vakili, Gundars Reinfelds and all the members of the Chemistry Department at the University of Winnipeg. I would also like to thank Dr. Paul Holloway and Brenda van Dekerkhove from the Biology Department at the University of Winnipeg for their assistance with bioassay and microbiological work. I would like to acknowledge the many great professors that I had the pleasure of meeting and I am grateful for their knowledge that they have passed on. I would like to thank all past and present lab mates I had the opportunity to work with. Lastly I thank my good friends Cathy Marynick and William Kim for their support.

This thesis is dedicated to Wadimism: “I do not believe in a personal God and I have never denied this but have expressed it clearly. If something is in me which can be called religious then it is the unbounded admiration for the structure of the world so far as our science can reveal it.” “True religion is real living, living with all one’s soul, with all one’s goodness and righteousness.” Albert Einstein.

TABLE OF CONTENTS

	Page
Abstract	iv
Acknowledgement	v
Dedication	vi
List of Tables	xi
List of Figures	xiii
List of Schemes	xiv
Glossary	xv
CHAPTER 1: General Introduction	
1.1 Natural Products	1
1.1.1 History of Natural Products	1
1.2 Types of Natural Products and Their Pharmaceutical Application	6
1.2.1 Polyketide Derived Natural Products	8
1.2.2 Shikimic Acid Derived Natural Products	10
1.2.3 Triterpenoidal and Steroidal Natural Products	11
1.2.4 Alkaloid Natural Products	13

1.3 Steroidal Alkaloids and Their Pharmacological Properties 14

1.3.1 Anti-Cancer Steroidal Alkaloids 15

1.3.2 Anti-Microbial Steroidal Alkaloids 19

1.4 Modern Drug Discovery 21

1.4.1 What is Alzheimer's Disease? 22

1.4.2 The Cholinesterase Family. 23

1.4.3 Cholinesterase Inhibitors for the Treatment of AD. 24

1.5 References 28

CHAPTER 2: Phytochemical studies on *Buxus natalensis.*

2.1 Introduction 33

2.2 Results and Discussion 38

2.2.1 O^{10}-Natafuranamine (**123**) 38

2.2.2 Biogenesis of O^{10}-Natafuranamine (**123**) 46

2.2.3 Cyclonataminol A (**124**) 47

2.2.4 31-Demethylbuxaminol A (**125**) 52

2.2.5 Buxaminol A (**126**) 58

2.2.6 Buxaminol C (**127**) 63

2.2.7 *p*-Coumaroylputrescine (**128**) 68

2.2.8 Methyl syringate (**129**) 71

2.2.9 Cholinesterase and Antimicrobial Activities of **123-129** 73

2.3 Experimental 75

2.3.1 General 75

2.3.2 Plant Material 75

2.3.3 Extraction and Isolation of compound (**123-129**) 76

2.3.4 Assay for Cholinesterae Inhibition 79

2.3.5 Antibacterial Activity 80

2.4 References 82

CHAPTER 3: Phytochemical studies on *Drypetes gossweileri*

3.1 Introduction 86

3.1.1 Triterpenoidal Constituents of *Drypetes* 86

3.1.2 Aromatic Constituents from *Drypetes* 88

3.1.3 *Drypetes gossweileri* 89

3.2 Results and Discussion 91

3.2.1 *N*-β-Glucopyranosyl-*p*-hydroxy Phenyl Acetamide (**151**) 91

3.2.2 *p*-Hydroxy Phenyl Acetic Acid (**152**) 95

3.2.3 *p*-Hydroxyphenyl Acetonitrile (**153**) 97

3.2.4 Biogenesis of Isolated Compounds from *Drypetes gossweileri*. 99

3.2.5 Acetylcholinesterase Inhibitory Activity of Compounds **151-153**. 101

3.3 Experimental 102

3.3.1 General 102

3.3.2 Plant Extract 102

3.3.3 Extraction and Isolation 102

3.4 References 104

Conclusion 107

Appendix 108

LIST OF TABLE

Page

Table 1.1. Cytotoxicity against human tumor cell lines and antibacterial .activities. 9

Table 1.2. Cytotoxicity of Cortistatins against various cancer cell lines. 16

Table 1.3. Cytotoxicity of Riterazines against leukemia cancer cells. 16

Table 1.4. Compounds from lilac plants exhibiting cholinesterase inhibitory .activities. 26

Table 2.1. Acetylcholinesterase and butyrylcholinesterase inhibitory activities of steroidal bases from *B. hyrcana*. 35

Table 2.2. ^{1}H and ^{13}C NMR Spectroscopic Data (400 and 100 MHz, respectively) in $CDCl_3$ for O^{10}-natafuranamine (**123**). 44

Table 2.3. ^{1}H and ^{13}C NMR Spectroscopic Data (400 and 100 MHz, respectively) in $CDCl_3$ for cyclonataminol A (**124**). 51

Table 2.4. ^{1}H and ^{13}C NMR Spectroscopic Data (400 and 100 MHz, respectively) in $CDCl_3$ for 31-demethylbuxaminol A (**125**). 56

Table 2.5. ^{1}H and ^{13}C NMR Spectroscopic Data (400 and 100 MHz, respectively) in $CDCl_3$ for buxaminol A (**126**). 63

Table 2.6. ^{1}H and ^{13}C NMR Spectroscopic Data (400 and 100 MHz, respectively) in $CDCl_3$ for buxaminol C (**127**). 68

Table 2.7. ^{1}H and ^{13}C NMR Spectroscopic Data (400 and 100 MHz, respectively) in $CDCl_3$ for *p*-coumaroylputrescine (**128**). 70

Table 2.8. ^{1}H and ^{13}C NMR Spectroscopic Data (400 and 100 MHz, respectively) in $CDCl_3$ for methyl syringate (**129**). 73

Table 2.9. Results of AChE inhibition assay for compounds isolated from *B. natalensis* (**123-129**). Activities reported as IC_{50} (μM) $\pm$ SD. 74

Table 3.1. ^{1}H and ^{13}C NMR Spectroscopic Data (400 and 100 MHz, respectively) in CD_3OD for N-β-glucopyranosyl-*p*-hydroxy phenyl acetamide (**151**). 94

Table 3.2. ^{1}H and ^{13}C NMR Spectroscopic Data (400 and 100 MHz, respectively) in acetone^{d6} for *p*-hydroxy phenyl acetic acid (**152**). 96

Table 3.3. ^{1}H and ^{13}C NMR Spectroscopic Data (400 and 100 MHz, respectively) in acetone^{d6} for *p*-hydroxyphenyl acetonitrile (**153**). 98

Table 3.4. Results of the AChE inhibition assay on compound **151-153** isolated from *D. gossweileri*. 101

LIST OF FIGURES

Page

Figure 2.1. Spin systems determined by COSY and TOCSY spectra for O^{10}-natafuranamine (**123**). 42

Figure 2.2. Spin systems of O^{10}-natafuranamine (**123**) connected through HMBC correlations. 43

Figure 2.3. Perspective illustration of NOESY couplings of O^{10}-natafuranamine (**123**). 45

Figure 2.4. Spin systems determined by COSY spectrum for cyclonataminol A (**124**). 49

Figure 2.5. Spin systems of cyclonataminol A (**124**) connected through HMBC correlations. 52

Figure 2.6. Spin systems determined by COSY and TOCSY spectrum for 31-demethylbuxaminol A (**125**). 55

Figure 2.7. Spin systems of 31-demethylbuxaminol A (**125**) connected through HMBC correlations. 57

Figure 2.8. Spin systems determined by COSY spectrum for buxaminol A (**126**). 60

Figure 2.9. Spin systems of buxaminol A (**126**) connected through HMBC correlations. 62

Figure 2.10. Spin systems determined by COSY spectrum for buxaminol C (**127**). 66

Figure 2.11. Spin sustems of buxaminol C (**127**) connected trough HMBC correlations. 67

Figure 2.12. Spin systems of *p*-coumaroylputrescine (**128**) connected through HMBC correlations. 71

Figure 2.13. Important HMBC couplings of methyl syringate (**129**). 73

Figure 3.1. HMBC correlations of N-β-glucopyranosyl-*p*-hydroxy phenyl acetamide (**151**). 94

Figure 3.2. HMBC correlations of *p*-hydroxy phenyl acetic acid (**152**). 96

Figure 3.3. HMBC correlations of *p*-hydroxyphenyl acetonitrile (**153**). 99

LIST OF SCHEMES

	Page
Scheme 1.1. Biosynthesis of polyketides.	8
Scheme 1.2. Biosynthesis of shikimic acid.	10
Scheme 1.3. Biosynthesis of triterpene skeleton.	12
Scheme 1.4. Biosynthesis of alkaloids.	14
Scheme 1.5. Reaction mechanism of the hydrolysis of ACh catalyzed by AChE.	24
Scheme 2.1. Possible pathway towards the biosynthesis of a furan ring incorporation of compound **123**.	46
Scheme 3.1. Proposed mechanism for the biosynthesis of *p*-hydroxyphenyl acetonotrile	100

GLOSSARY

ACh	Acetylcholine: a neurotransmitter in both the peripheral nervous system and central nervous system.
AChE	Acetylcholinesterase: found in the central nervous system and is responsible to degrade acetylcholine to terminate a nerve impulse.
AD	Alzheimer's Disease: is the most common form of dementia in the elderly population.
BChE	Butyrylcholinesterase: found in the peripheral nervous system, and is more selective in degrading butyrylcholine.
^{13}C-NMR spectrum	Carbon Nuclear Magnetic Resonance: Depicts the electronic environment of carbon atoms in a molecule.
COSY spectrum	Proton-Proton Correlation SpectroscopY: Provides geminal and vicinal proton-proton couplings.
DEPT	Distortionless Enhancement by Polarization Transfer: Helps to distinguish methyl, methylene, methine, and quaternary carbon atoms.
EIMS	Electron Impact MS: High-energy electrons are used to form a radical cation of the molecular species.
HMBC spectrum	Heteronuclear Multiple Bond Coherence: Provides J_2, J_3, and occasional J_4 proton-carbon long range correlations.

^{1}H-NMR spectrum	Proton Nuclear Magnetic Resonance: Depicts the electronic environment of proton atoms in a molecule.
HREIMS	High Resolution EIMS: The sum of the exact masses of the atoms that make up a molecule.
HRESMS	HR Electron Spray MS: The molecule is ionized as a charged droplet upon exiting a capillary as a spray in order to determine the molecular ion.
HSQC spectrum	Heteronuclear Multiple Quantum Correlation: Provides direct geminal (J_1) proton-carbon correlations.
IC_{50}/EC_{50}	Concentration required to inhibit 50% of the enzyme activity.
IR spectrum	InfraRed spectrum: Vibrational characteristics of atoms present in a molecule to provide information regarding functional groups.
NOE	Nuclear Overhauser Effect: Provides proton-proton correlations through-space proximity.
NOESY spectrum	Nuclear Overhauser Effect SpectroscopY: Useful in providing 2D proton-proton correlations through-space proximity of macromolecules.
ROESY spectrum	Rotating-frame Overhauser Effect SpectroscopY: Provides 2D proton-proton correlations through-space proximity.
TLC	Thin layer chromatography

TOCSY spectrum	Totally Correlated SpectroscopY: Provides all proton-proton correlations within the entire spin system.
UV spectrum	UltraViolet spectrum: Provides informations on the type of chromaphore(s) present in a molecule.

CHAPTER 1

General Introduction

1.1 Natural Products

Nature is an inexhaustible source of novel organic compounds. These organic compounds, also known as natural products, have served as a major source of remedies for centuries. Natural products are secondary metabolites derived from pre-cursors of primary metabolism. Secondary metabolities do not play any role in growth, and development of living organisms; however, primary metabolites are the building blocks of life. Secondary metabolites are synthesized by organisms for their protection, identification of their community and attraction of mates. These, secondary metabolites have shown interesting pharmacological activities and are used in treating various human ailments. These compounds exhibit a wide range of biological activities including anti-viral, anti-microbial, anti-leishmanial and anti-cancer[1,2]. These interesting bioactivities of natural products have directed organic chemists to identify these bioactive constituents from different natural sources and to synthesize them.

1.1.1 History of Natural Products.

It is well documented in the literature that plant extracts were used to treat snakebites, fever and pain relief in early days[3]. These plant extract based medicines contain bioactive natural products that are recorded in numerous books and manuscripts around the world. The earliest Egyptian pharmaceutical records dating from 1500 B.C.

include the “Ebers Papyrus”, a document containing over 700 drugs. The ancient Chinese and Greeks also had their own books that included hundreds of herbal drugs for various ailments[1]. These historical collections are full of examples in the use of natural products, such as when the philosopher Socrates, in 399 B.C., drank an extract containing coniine (**1**) from hemlock (*Conium maculatum*) during his execution[3]. Coniine is an extremely toxic alkaloid that causes paralysis of motor nerve endings. It was also said that Queen Cleopatra used extracts from henbane (*Hyoscyamus*) to appear alluring[3]. Extracts from henbane contain atropine (**2**), an anti-cholinergic tropane alkaloid that affects all parasympathetic nerves and organs. Codeine (**3**) and morphine (**4**), constituents of *Papaver somniferum* extracts, are still in clinical practice for pain relief.

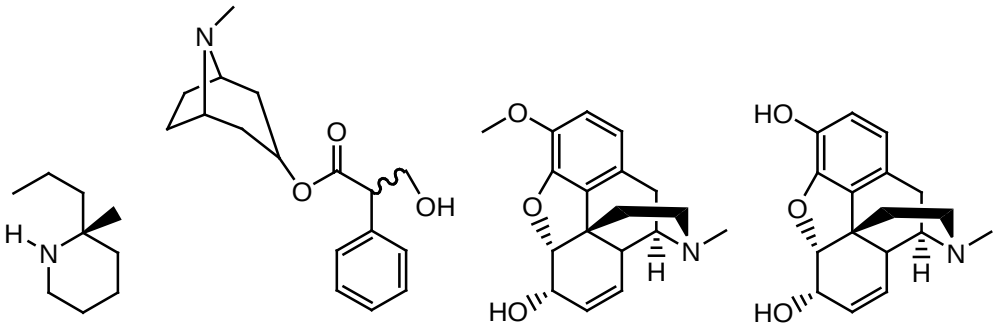

(1) **(2)** **(3)** **(4)**

By the 19th century, morphine (**4**) was isolated as a pure natural product and made commercially available by Merck in 1826. This was followed by the discovery of Aspirin (**5**) by Bayer in 1899, the first semi-synthetic pure drug based on a natural product[4]. These discoveries gave birth to a new branch of organic chemistry, natural products, which still play an important role in the modern pharmaceutical industry. This branch is considered as one of the major contributors to provide lead molecules to drug discovery

programs. It is estimated that between 1981 and 2006 over 45% of 974 small molecules introduced were either natural products, their semisynthetic analogues or synthetic products based on natural product models[4]. Out of this group of molecules, pure natural products consisted of 6%. However, natural products accounted for 14% out of 175 anti-cancer drugs demonstrating their importance to human health and longevity. Out of the same number of anti-cancer drugs it is estimated approximately 50% are either natural products, their semisynthetic analogues or synthetic products based on natural product models[4]. In 1999, 45% of the best selling natural products accounted for over US$16 billion[5]. With the discovery of combinatory chemistry (another branch for drug discovery), it was thought the synthesis of small drug-like molecules through high-throughput screens, could mass produce combinatorial libraries of bioactive compounds. Thus natural product research was deemphasized. However, the failure to materialize new active compounds from this approach has renewed interest in natural product research[6]. To date, only one *de novo*, compound has been discovered through this approach, sorafenib (**6**). The trade name of **6** is Nexavar 1, being manufactured by Bayer and was approved by FDA as an antitumor agent in the treatment of kidney and liver cancer. This drug is also in phase III clinical trial for thyroid cancer[4].

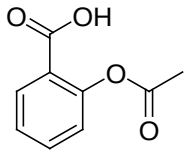

(5)

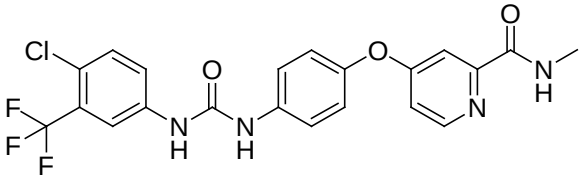

(6)

Traditionally plants have been the focus of the drug discovery program as 80% of the world's population relies predominantly on traditional medicine derived from plants for their primary health care[7]. The economic impact can be seen particularly in 1997, in the US, in which 12% of the population spent US$5.1 billion on herbal remedies[8]. Although it seems a lot of work has already been done on plants, it is only estimated 5-15% of the 250,000 species of higher plants have been investigated chemically and pharmacologically[9]. Natural products have also been isolated from other organisms. A survey of anti-cancer natural products available in 1994 shows that 6 out of 15 drugs originated from one genus of soil bacteria, *Streptomyces*, which include actinomycin D (**7**), bleomycin (**8**), daunomycin (**9**), doxorubicin (**10**), mitomycin C (**11**) and streptozocin (**12**)[10,11]. Natural products have also been isolated from fungi, such as the natural product FTY720 (**13**) (trade name Fingolimod manufactured by Novartis), which was isolated from *Isaria sinclairii* and has shown immune-suppression properties. Natural products derived from plants have also shown significant anti-cancer activities. For instance, vinflunine (**14**) (trade name Javlor manufactured by Pierre Fabre) was isolated from the flowering plant *Catharanthus roseus* exhibiting potent anticancer activity. Fingolimod and Javlor are examples of natural products that are in clinical use. These examples illustrate that even though other organisms possess pharmaceutically active natural products, plant derived natural products will continue to play an important role in human health care systems.

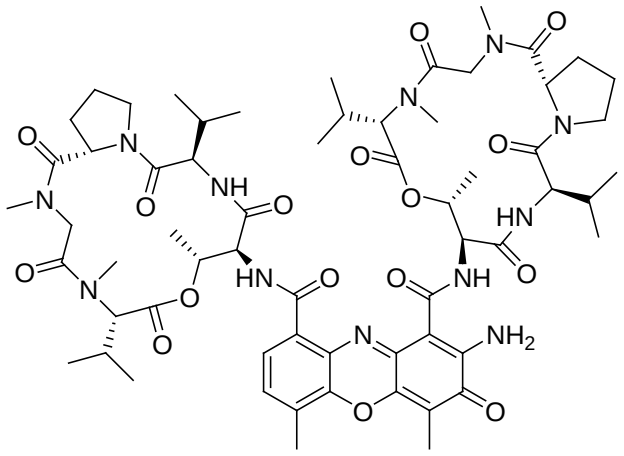

(7)

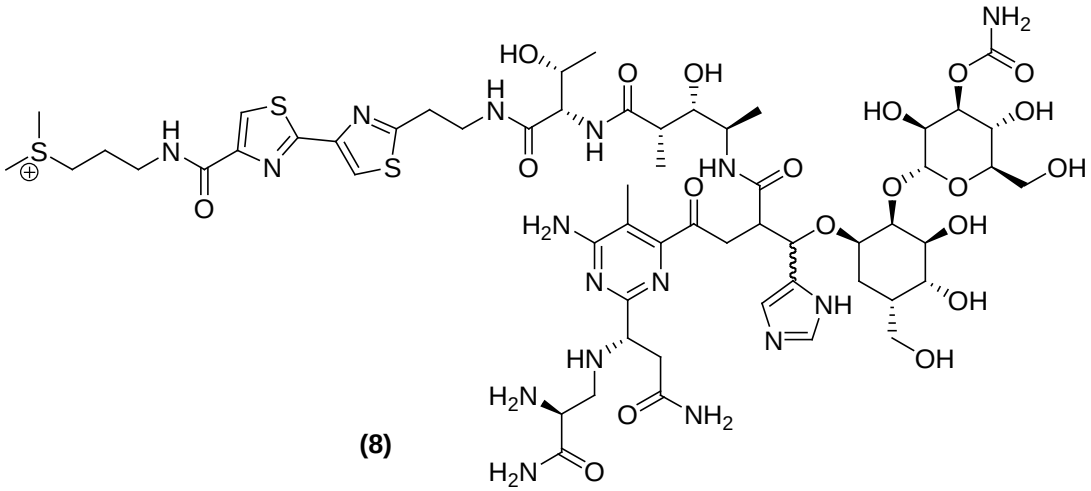

(8)

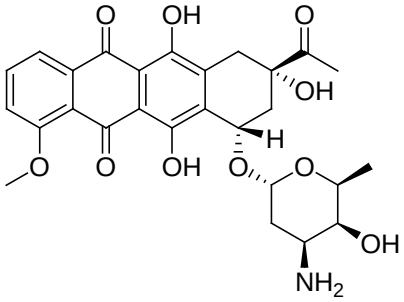

(9)

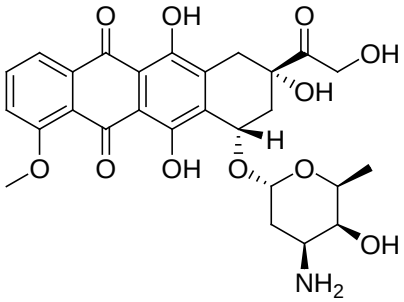

(10)

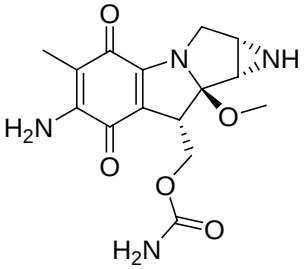

(11)

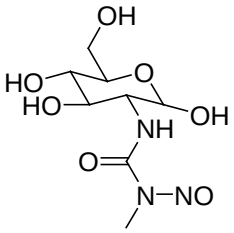

(12)

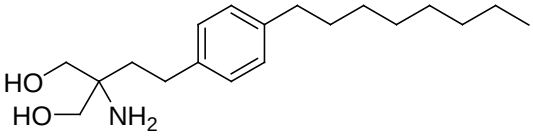

(13)

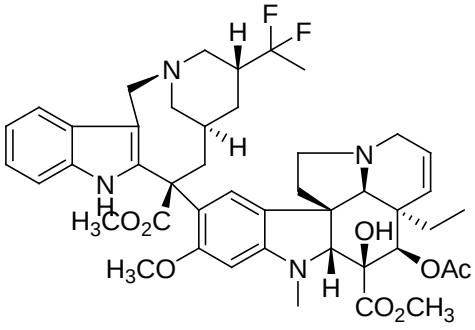

(14)

1.2 Types of Natural Products and Their Pharmaceutical Applications.

Natural products are obtained from different natural sources including plants, microorganisms, marine organisms, and even insects. These compounds can be classified into different classes based on their structural features and biosynthetic origin. The origin

of natural products can be traced to key intermediates of primary metabolism. These intermediates include Acetyl-CoA (**15**), shikimic acid (**16**), and mevaolic acid (**17**). Acetyl-CoA (**15**) is important in polyketide biosynthesis, while shikimic acid (**16**) is an important precursor to many aromatic secondary metabolities, such as lignens and flavanoids[12]. Mevalonic acid (**17**), is responsible for the biosynthesis of terpenoid and steroid metabolities[13], and can be derived from either acetyl-CoA, or methylerythritol phosphate (MEP) (**18**). MEP (**18**) is itself derived from the decarboxylation of pyruvic acid in the presence of the co-factor thiamine pyrophosphate, subsequent attack onto a molecule of glyceraldehydes 3-phosphate will regenerate the co-factor and form MEP (**18**). Another group of natural products are the alkaloids, nitrogen containing compounds derived from amino acids such as tryptophan (**19**) and L-ornithine (**20**). Other natural products can originate from other amino acids and sugars.

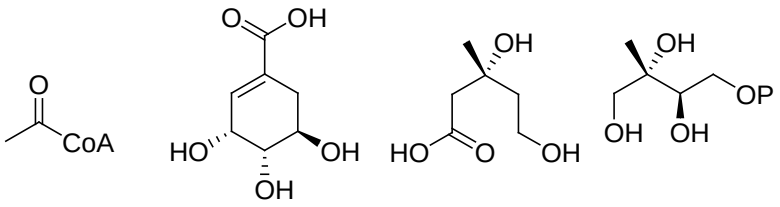

(15) **(16)** **(17)** **(18)**

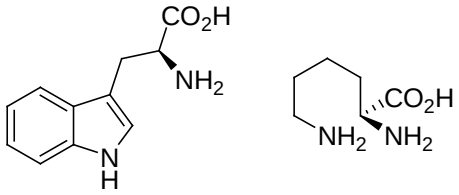

(19) **(20)**

1.2.1 Polyketide Derived Natural Products.

Polyketides derived from acetyl-CoA (**15**) come about from modifications in the fatty acid biosynthetic pathway. In normal fatty acid biosynthesis two molecules of acetyl-CoA undergo a Claisen reaction to form a ketoester. The pathway continues with a reduction to a hydroxyl group, followed by dehydration to a double bond and a final reduction to a reduced ester. This process is repeated many more times to form fatty acids. In polyketide synthesis, the process can be stopped at any of the steps and a further acetyl-CoA loaded onto the chain, thus maintaining a functional group in the growing chain as seen in **Scheme 1.1**.

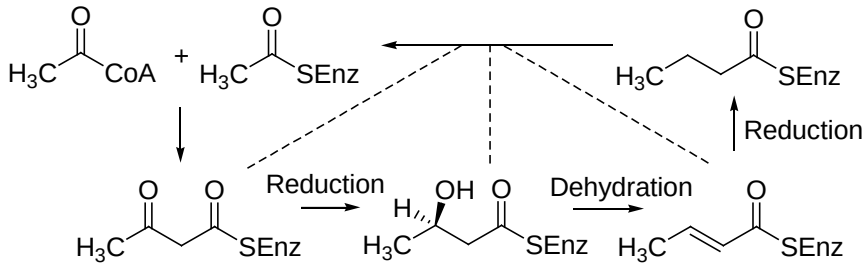

Scheme 1.1. Biosynthesis of polyketides.

Numerous isolated polyketides have shown to be pharmacologically active, such as 2,4-dihydroxy-6-((*R*)-4-hydroxy-2-oxopentyl)-3-methylbenzaldehyde (**21**), sterigmatocystin (**22**), averantin (**23**) and averufin (**24**) isolated from the fungus *Aspergillus versicolor* have shown cytotoxic and antibacterial activities, as shown in **Table 1.1**[14].

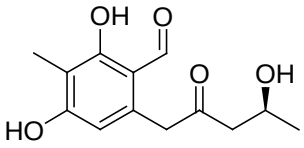

(21)

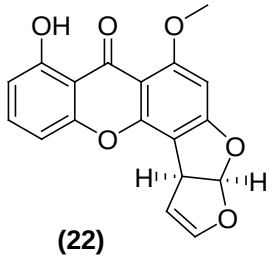

(22)

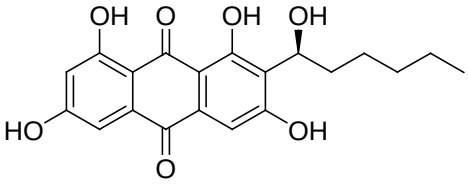

(23)

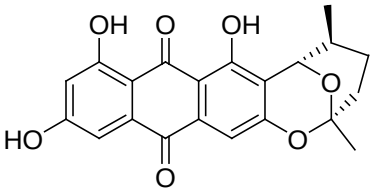

(24)

Table 1.1. Cytotoxicity against human tumor cell lines and antibacterial activities[14].

	Compound	(**21**)	(**22**)	(**23**)	(**24**)
Tumor Cell Lines IC_{50} (µg/ml)	A549	>30.0	1.86	3.15	14.92
	SK-OV-3	>30.0	2.53	3.88	14.07
	SK-MEL-2	>30.0	1.22	3.57	14.56
	XF498	>30.0	2.75	3.04	12/04
	HCT15	>30.0	4.61	3.13	11.97
Bacterial Strains IC_{50} (µg/ml)	*Streptococcus pyogenes* (308A)	-	-	0.78	6.25
	Staphylococcus aureus (SG511)	-	-	3.13	>12.50

Polyketides have also been isolated from marine organisms. Examples include plakortin (**25**), purified from the sponge *Plakortis angulospiculatus*. It has shown cytotoxicity against cancer cell lines MDA-MB435, HCT-8, SF295 and HL60 with IC_{50} values of 10.4, 3.0, 9.8 and 13.3 µg/ml, respectively[15].

In polyketide biosynthesis, varying amounts of reduction and dehydration could lead to macrolide formation. Peloruside B (**26**) is an example of a macrolide isolated from the marine sponge *Mycale hentscheli*[16].

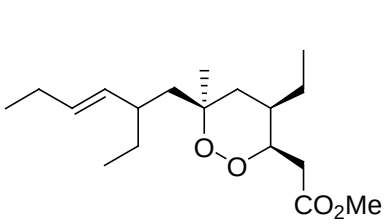

(25)

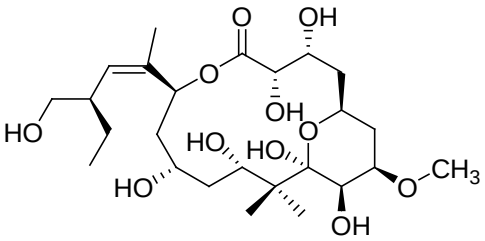

(26)

1.2.2 Shikimic Acid Derived Natural Products.

Shikimic acid (**16**) is a precursor to flavanoids, lignans and some amino acids, therefore it can serve as an alternative route to aromatic compounds. Shikimic acid is formed from the intermediate 3-deoxy-D-*arabino*-heptulosonic acid 7-phosphate (**29**) which is a product of the coupling between phosphoenolpyruvate (PEP) (**27**) and D-erythrose 4-phosphate (**28**) from the pentose phosphate cycle according to **Scheme 1.2**[13].

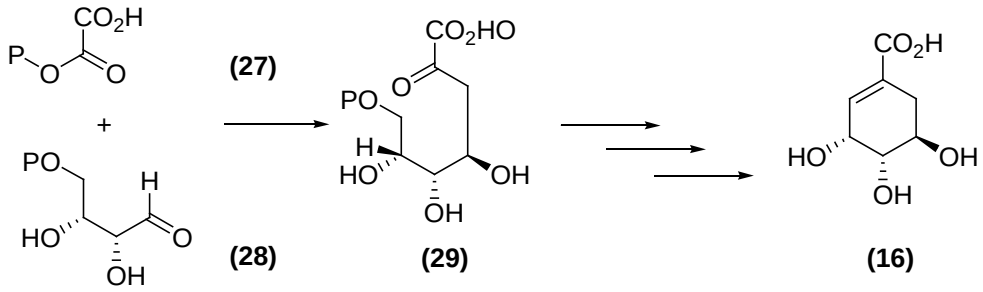

Scheme 1.2. Biosynthesis of shikimic acid.

Like polyketides, this class of natural products exhibit pharmacological activities. Recent phytochemical investigations on the herb *Dalbergia odorifera* have lead to the isolation of pinocembrin (**30**), dalparvone (**31**), mucronulatol (**32**) and sativanone (**33**); all of which have shown cytotoxicity against human cervical cancer cells (cell line KB)[17].

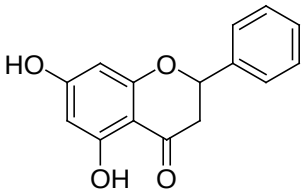

(30)

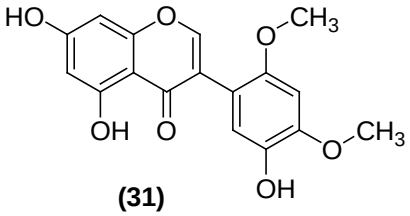

(31)

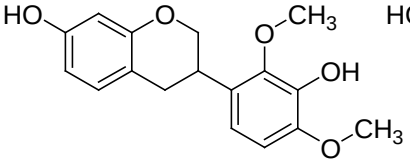

(32)

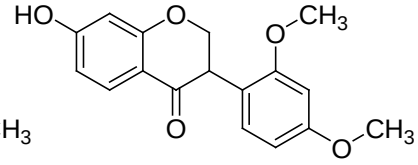

(33)

Lignans have shown to exhibit anti-HIV properties. Examples include Peperomin A (**34**), B (**35**), and C (**36**), which were isolated from the Chinese herb *Peperomia heyneana*, and found to reduce viral load in C8166 cells with an EC_{50} value of 5.3, 5.4 and 42.6 µM, respectively[18].

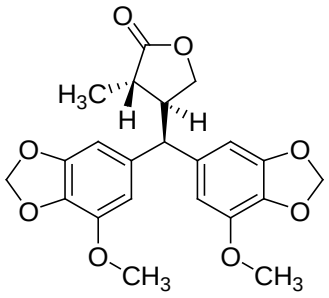

(34)

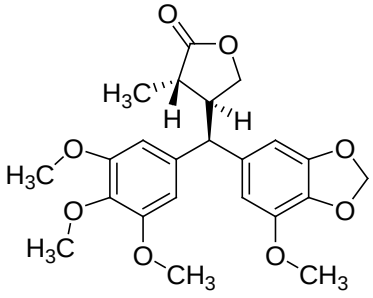

(35)

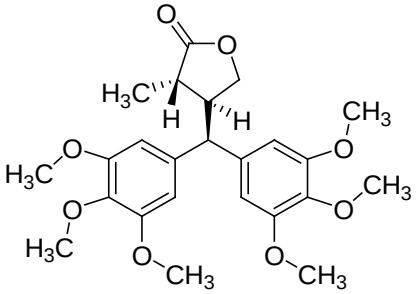

(36)

1.2.3 Triterpenoidal and Steroidal Natural Products.

Triterpenes are formed when two molecules of farnesyl pyrophosphate (FPP) (**37**) are joined tail to tail to give squalene (**38**). Once squalene is epoxidized and folded into

the proper orientation it undergoes cyclization to yield a protosteryl cation (**39**). This cation undergoes successive Wagner-Meerwein 1,2-hydride and methyl shifts to yield lanosterol (**40**) in animals and fungi and cycloartenol (**41**) in plants as seen in **Scheme 1.3**[13].

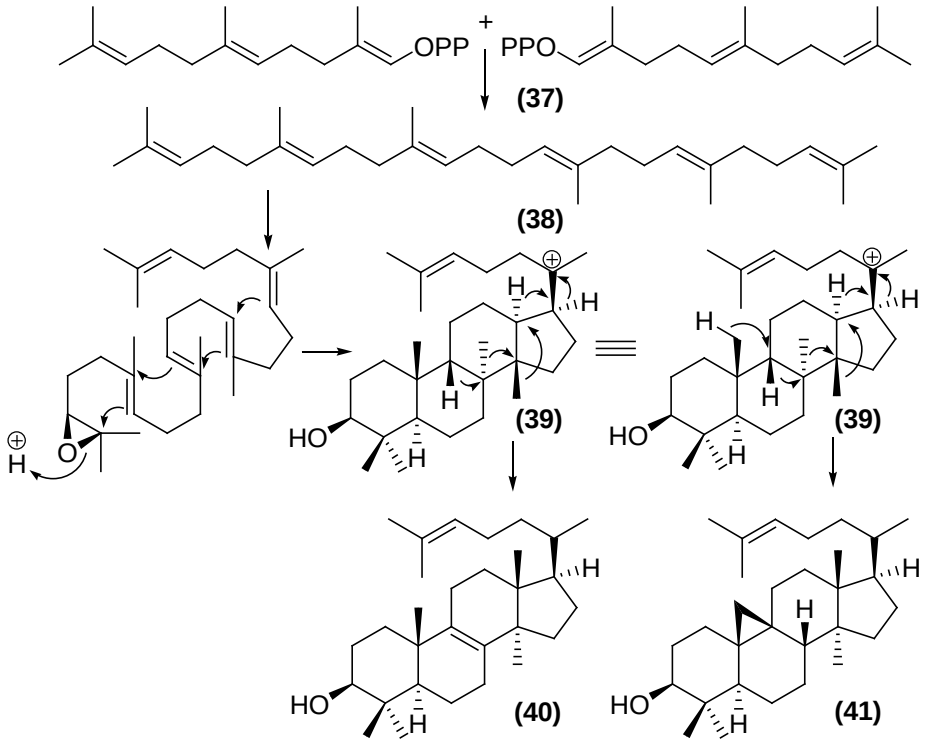

Scheme 1.3. Biosynthesis of triterpene skeleton.

Steroids and terpenes have also shown to possess biological activities. Examples include the steroids **42** and **43** isolated from the brown alga *Sargassum carpophyllum*. Compound **42** was found to be cytotoxic against HL-60 cancer cell lines with an IC_{50} value of 7.8 µg/mL and compound **43** was active against P-388 at 0.7 µg/mL[19]. Likewise, terpenes such as 23-*trans*-*p*-coumaroyloxy-2α,3α-dihyroxyolean-12-en-28-oic acid (**44**),

3-*O*-*trans*-*p*-coumaroyltormentic acid (**45**) and 3β-*trans*-caffeate (**46**), isolated from the Korean shrub *Berberis koreana*, were cytotoxic against various cancer cell lines.

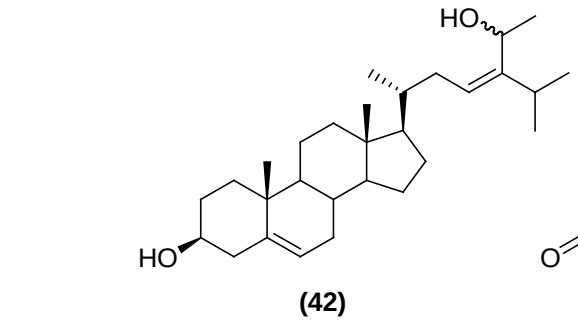

(42)

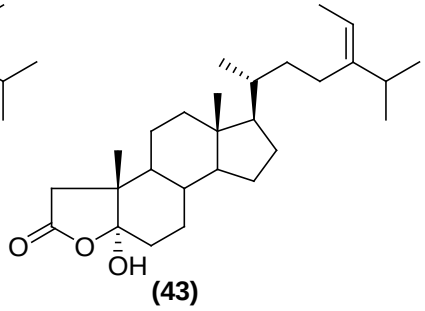

(43)

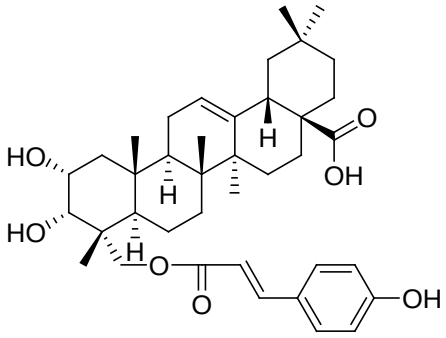

(44)

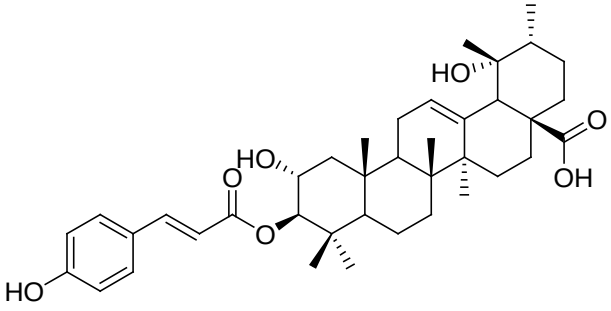

(45)

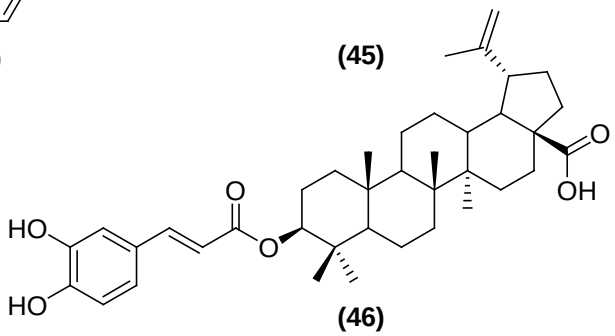

(46)

1.2.4 Alkaloid Natural Products.

Alkaloids constitute a class of nitrogen containing natural products with a variety of structural features that can be further divided into subclasses. One such subclass would be ornithine (**20**) derived natural products. L-Ornithine, in animals, is formed from the

urea cycle, while plants synthesize it from L-glutamic acid (**47**). Decarboxylation can lead to putrescine (**48**), a substituent of a natural product such as *p*-coumaroylputrescine (**128**). Putrescine (**48**) can also be further modified to *N*-methyl-Δ^1-pyrrolinium cation (**49**), which can be used in the synthesis of tropine (**50**) a precursor to atropine (**2**) as seen in **Scheme 1.4**[13].

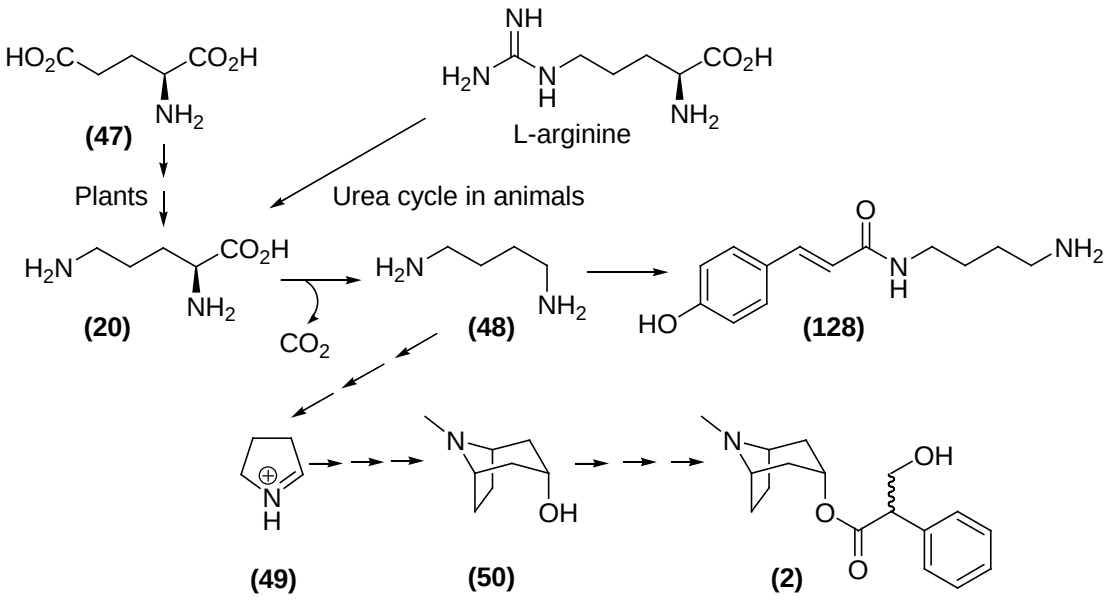

Scheme 1.4. Biosynthesis of alkaloids.

1.3 Steroidal Alkaloids and Their Pharmacological Properties.

One class of alkaloids that has been repeatedly found in plants, fungi and marine organisms are the "steroidal alkaloids". Steroidal alkaloids possess biological activities that range from anti-microbial to anti-cancer. This class of natural products has also demonstrated its potential in the treatment of Alzheimer's Disease[20,21].

1.3.1 Anti-Cancer Steroidal Alkaloids.

As soon as doctors started diagnosing cancer there has been a search for drugs to treat and cure the different types of cancers that are present. Unfortunately, many of the drugs used to eradicate cancer are not able to selectively target cancer cells, causing healthy cells to be damaged as well. Currently, the search continues for a new anti-cancer drug that is able to selectively target cancer cells without harming healthy cells.

Steroidal alkaloids showing anti-cancer activities have been isolated from numerous sources, including common plants such as lilacs. Veratramine (**51**), and rubijervervine (**52**) isolated from the roots of a lilac plant (*Veratrum nigrum*) are examples that show weak cytotoxicity against brain tumors (SF-188 cell line)[22].

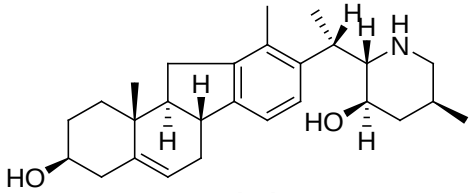

(51)

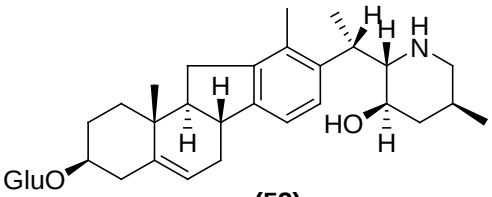

(52)

Marine organisms have proven to be an equally important source for steroidal alkaloids as plants. Numerous steroidal alkaloids have been isolated from the sea sponge, *Corticium simplex*, which include cortistatin A (**53**), B (**54**), C (**55**), D (**56**), E (**57**), F (**58**), G (**59**), H (**60**), J (**61**), K (**62**) and L (**63**) with the most cytotoxic cortistatins being A, C, J, K and L. with IC_{50} values of 1.8, 19, 8, 40 and 23 nM, respectively, as seen in **Table 1.2**[23].

Table 1.2. Cytotoxicity of Cortistatins against various cancer cell lines[23].

Compound IC_{50} (μM)	HUVAC	KB3-1	Neuro2A	K562	NHDF
53	0.0018	7.0	6.0	7.0	6.0
54	1.1	120	160	200	>300
55	0.019	150	180	>300	>300
56	0.15	55	>300	>300	>300
57	0.45	2.5	1.9	2.8	1.9
58	1.9	10.8	4.0	4.0	4.1
59	0.80	8.9	4.0	3.8	2.9
60	0.35	2.3	2.2	2.7	2.7
61	0.008	9.1	3.3	3.3	2.4
62	0.04	10.2	3.0	3.9	2.5
63	0.023	14	2.8	4.3	2.4

The most interesting steroidal alkaloids with anti-cancer activities came from the invertebrate marine chordates *Cephalodiscus gilchristi* and *Ritterella tokioka*. These compounds are referred to as steroidal pyrazines which are made up of two steroidal fragments referred to as the Southern and Northern fragments. Compounds isolated from *Ritterella tokioka* include Ritterazine A (**64**) - U (**75**), which showed IC_{50} values ranging from 0.17nM to 2.38μM against the P388 cancer cell line (**Table 1.3**).

Table 1.3. Cytotoxicity of Riterazines against leukemia cancer cells.

Compound	P388 EC_{50} (nM)	ref	Compound	P388 EC_{50} (nM)	ref
A (**64**)	14.2	24	K (**70**)	10.4	26
B (**65**)	0.17	25	L (**71**)	11.1	26
C (**66**)	102.3	25	N (**72**)	522	27
D (**67**)	17.5	25	O (**73**)	2383	27
E (**68**)	3.8	26	T (**74**)	522	27
F (**69**)	0.81	26	U (**75**)	2341	27

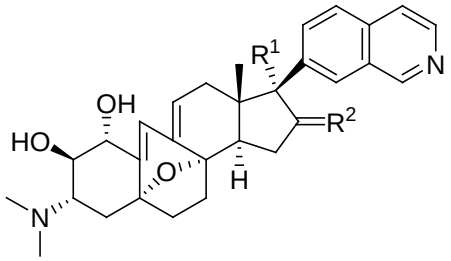

(53): R^1 = H, R^2 = H, H
(54): R^1 = H, R^2 = H (a), OH (b)
(55): R^1 = H, R^2 = O
(56): R^1 = OH, R^2 = O

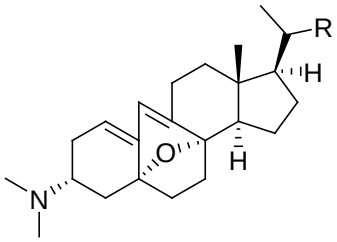

(57): R = S^1
(59): R = S^2
(60): R = S^3

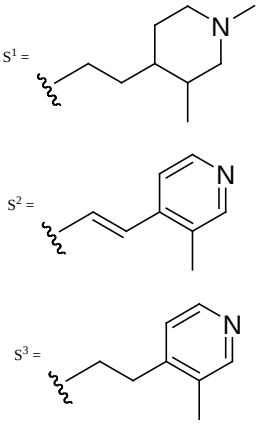

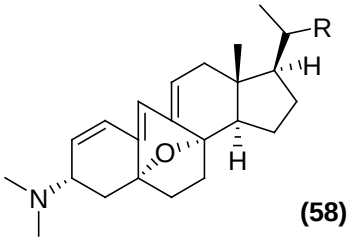

(58): R = S^1

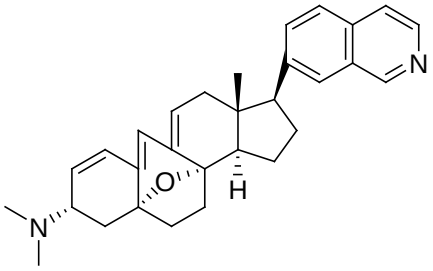

(61)

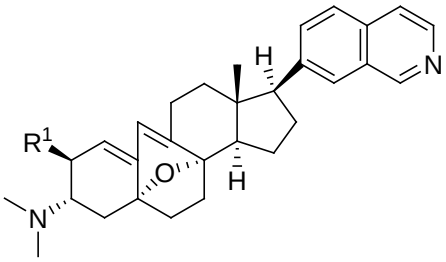

(62): R^1 = H
(63): R^1 = OH

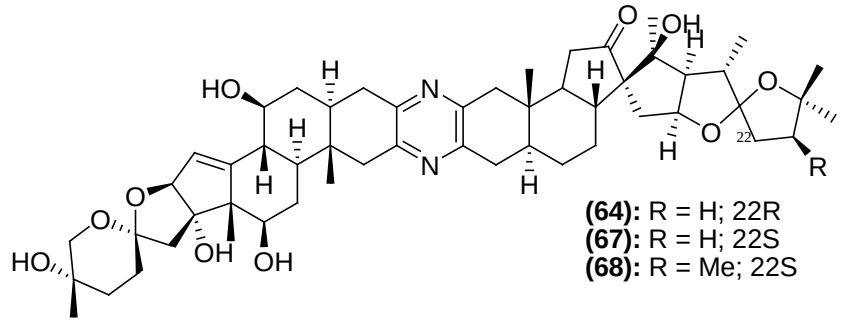

(64): R = H; 22R
(67): R = H; 22S
(68): R = Me; 22S

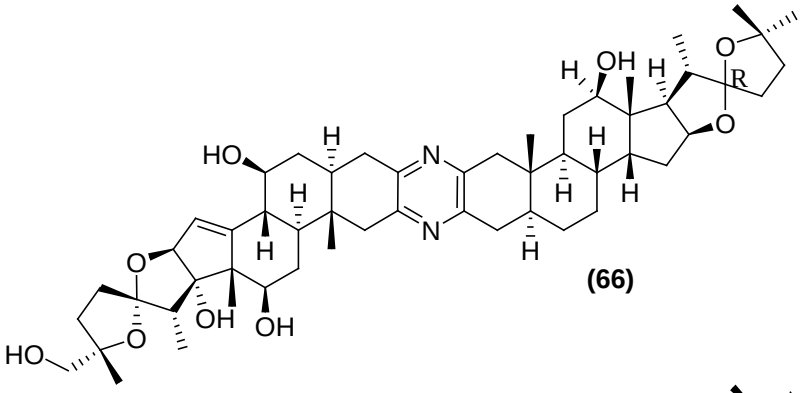

(66)

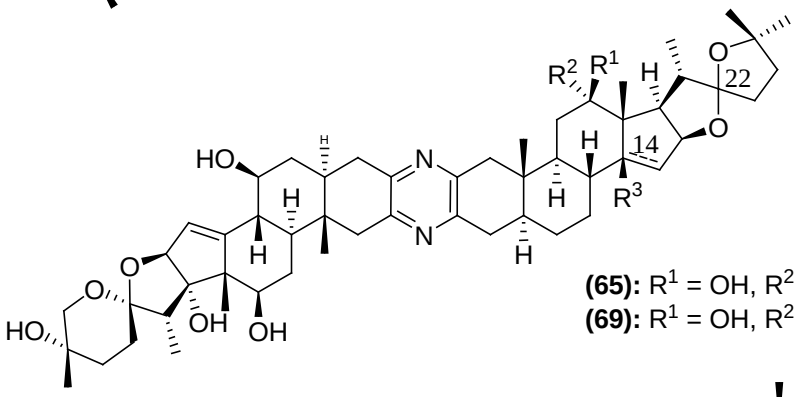

(65): R^1 = OH, R^2 = H, R^3 = H; 22R
(69): R^1 = OH, R^2 = H, R^3 = H; 22S

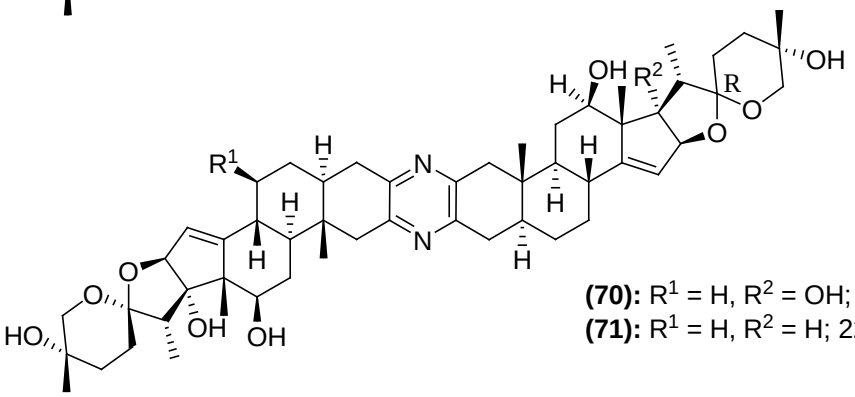

(70): R^1 = H, R^2 = OH; 22R
(71): R^1 = H, R^2 = H; 22R

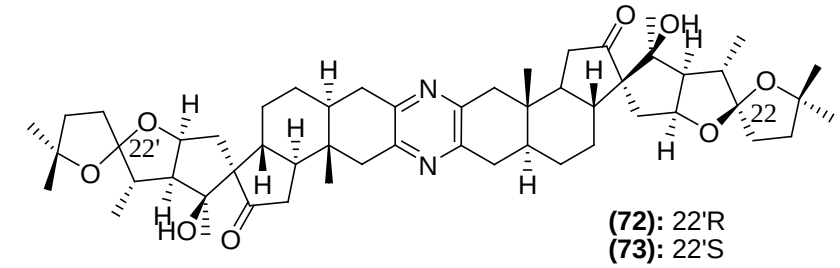

(72): 22'R
(73): 22'S

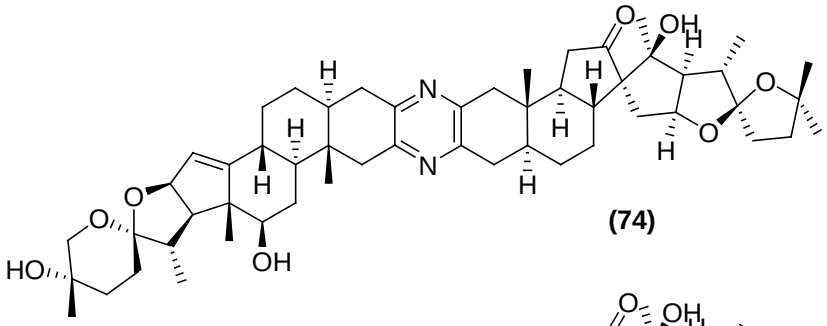

(74)

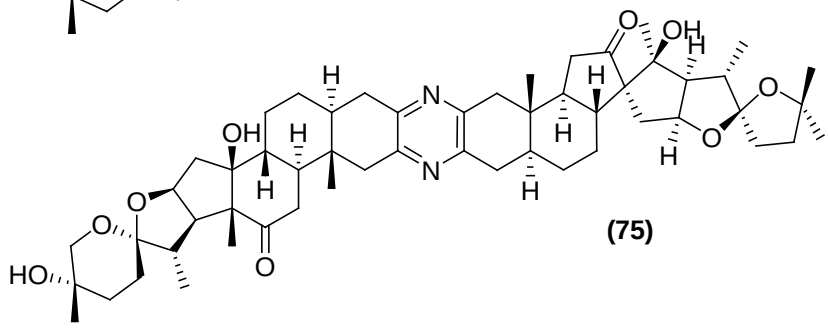

(75)

1.3.2 Anti-Microbial Steroidal Alkaloids.

Penicillin's were the first drugs introduced to the market to treat bacterial infections. Since these anti-microbial drugs came out, they have been over-prescribed and otherwise used improperly, which has led to these drugs becoming ineffective; bacteria that once were susceptible are now resistant. This has also led to the appearance of "superbugs": micro-organisms that are resistant to most types of drugs. Recent headlines have shown the appearance of resistant malaria strains as well as drug resistant forms of

bacteria in hospitals and animals. Hence, new drugs are needed to treat individuals infected by new strains of bacteria and other micro-organisms.

Steroidal alkaloids, isolated from *Veratrum taliense*, have shown potential for anti-bacterial activity. These compounds include: neoverataline A (**76**), B (**77**), stenophylline-B (**78**), 2-*O*-β-D-glucopyranoside (**79**), veramiline-3-*O*-β-D-glucopyranoside (**80**), veramitaline (**81**), jervine (**82**) and jervine-3-*O*-β-D-glucopyranoside (**83**). Compounds **76** and **77** have shown an MIC value at 200µg/ml against *Phytophthora capisis*. Compounds **79** and **81** have exhibited an MIC value of 160µg/ml, **78** and **83** at 120µg/ml, and **80** and **82** at 80µg/ml[28].

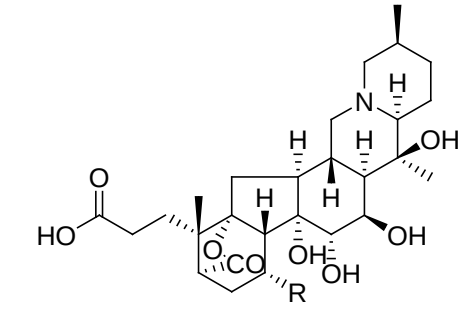

(76): R = H
(77): R = OH

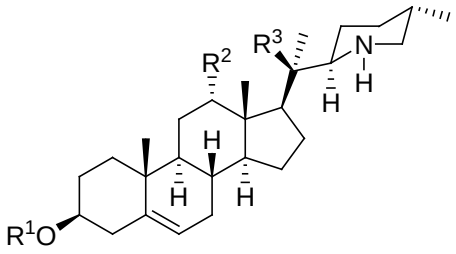

(78): $R^1 = R^2 = H$, $R^3 = OH$
(79): R^1 = Glu, $R^2 = H$, $R^3 = OH$
(80): R^1 = Glu, $R^2 = R^3 = H$
(81): $R^1 = R^3 = H$, $R^2 = OH$

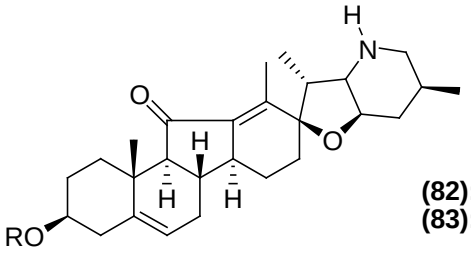

(82): R = H
(83): R = Glu

The *Funtumia elastic*, native to central Africa was subjected to phytochemical studies to reveal four steroidal alkaloids with anti-plasmodial activity against one of the most virulent malaria causing protozoa, *Plasmodium falciparum*. These isolates include holarrhetine (**84**), conessine (**85**), holarrhesine (**86**) and isoconessimine (**87**) have shown anti-plasmodial activity against *P. falciparum* ranging from 0.97 to 3.39 μM[29].

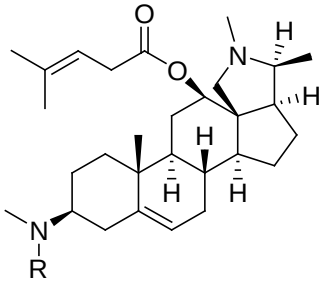

(84): R = CH_3
(85): R = H

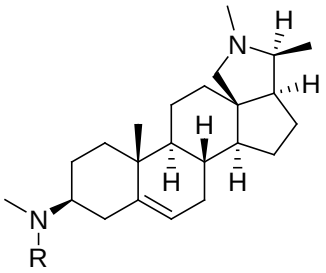

(86): R = CH_3
(87): R = H

1.4 Modern Drug Discovery.

The modern drug discovery program has focused on the screening of large numbers of natural products against many biological assays. This was made possible through high-throughput screening, using automation to quickly analyze and process many samples at one time with microplates. Microplate assays have several advantages over cuvette assays in that multiple assays can be performed, smaller assay volume are used and data is automatically recorded and easily exported to data processing software. Detection of the biological or chemical events in the assay can be achieved using absorbance, fluorescence, luminescence, and time-based readings. There are two distinct microtiter plate assay methods used; cell based and enzyme based assays. Enzyme based

assays have risen to be the preferred method as they require less time in preparation, fewer safety precautions need to be taken and fewer variables need to be considered. In our program we use enzyme based assays to study Alzheimer's Disease, a neurological disease that is growing in interest in the research community. Today 69% of all dementia cases affecting 20 million individuals worldwide have been diagnosed with Alzheimer's Disease[30].

1.4.1 What is Alzheimer's Disease?

Dr. Alois Alzheimer was the pioneer to discover Alzheimer's Disease (AD) in 1907. The disease was first reported by observations of similar neurophysiological appearances; these included neural fibre tangles and plaques in brain tissue. AD is seen as a gradual and progressive neuro-degenerative disease leading to a breakdown in memory retention and absence of cognitive reasoning and language skills[31]. Besides the neuropathological signs of AD, it is also characterized neurochemically by a consistent deficiency in cholinergic neurotransmission in neurons of the basal forebrain[32,33], particularly in the neocortex and hippocampus. These areas of the brain are associated with learning and memory, executive functioning, behavior and emotional responses[34].

The cholinergic neurotransmitor responsible for signal transduction between neurons is acetylcholine (**88**). Its deficiency is seen as a result of the excess degradation by acetylcholinesterase (AChE)[35,36,37]. AChE is a member of the enzyme family of cholinesterases. AChE is found predominantly in the Central Nervous System (CNS)

with its activity located almost entirely within cholinergic axons coming from the basal forebrain implicating AChE as a cause to AD[38]. Butyrylcholinesterase (BChE), the other member of the cholinesterase family, is found predominantly in the Peripheral Nervous System (PNS). Early investigations linked BChE with the maturation of senile plaques, which are associated with AD[39]. However, recent studies have found BChE does not play a major role in AD, as high levels of BChE are seen to improve cognitive function[40]. Since the role of BChE is not clearly understood, treatment strategies are focused on the inhibition of AChE to treat AD.

1.4.2 The Cholinesterase Family.

Acetylcholinesterase (AChE) is a 76 kD protein belonging to the α/β-hydrolase family[41]. The catalytic site of AChE is found in a gorge which contains key amino acids responsible for the selective recognition of acetylcholine over all other molecules. These amino acids play a role in recognition of the *tert*-butyl group, basic nitrogen and the ester of acetylcholine[42]. Three amino residues are key to the hydrolysis of acetylcholine (**88**). These amino acids include Glu327, which orients acetylcholine (**88**) into the proper orientation within the active site so that it can abstract a hydrogen from a neighboring His amino acid. This His440 can then abstract a hydrogen from Ser200 making it a good nucleophile to attack the ester carbonyl carbon acetylcholine (**88**). This leads to choline (**89**) being released and further introduction of a water molecule releases a molecule of acetic acid (**90**)[41] as seen in **Scheme 1.5**.

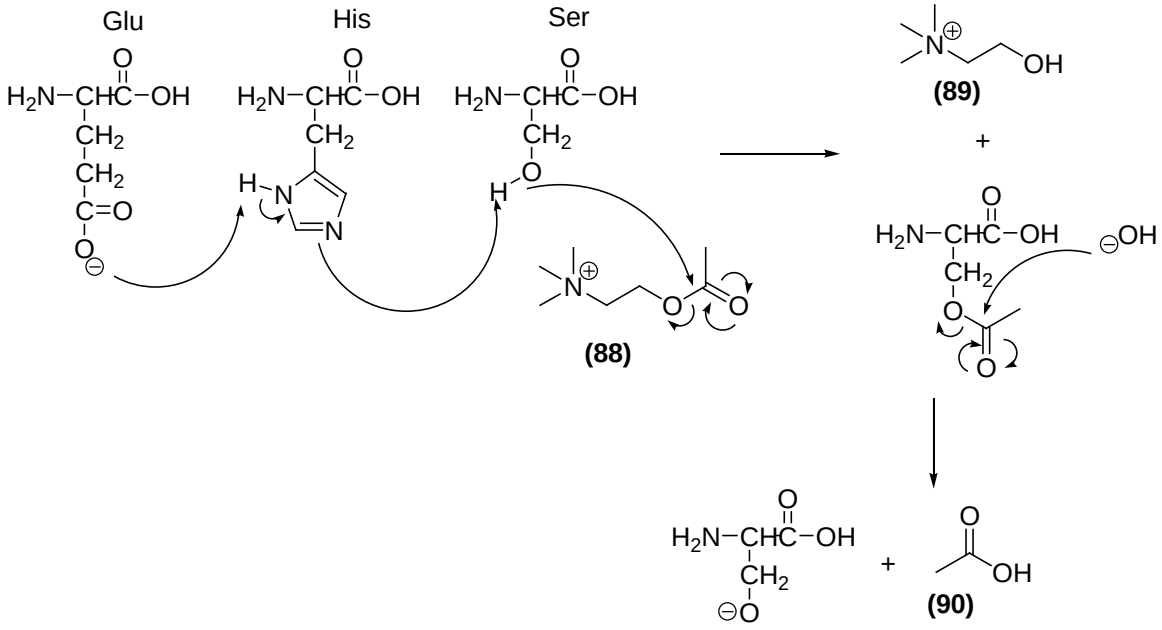

Scheme 1.5. Reaction mechanism of the hydrolysis of ACh catalyzed by AChE.

1.4.3 Cholinesterase Inhibitors for the Treatment of AD.

Currently there are four drugs available to treat AD, tacrine (Cognex) (**91**), dionepezil (Aricept) (**92**), rivastigmine (Exelon) (**93**) and galanthamine (Reminyl) (**94**)[38,43]. However, all except galanthamine have adverse side effects and problems associated with bioavailability[44]. Galanthamine is more selective for AChE than BChE and is completely bioavailable. It is a reversible competitive inhibitor, and has an elimination half-life of six hours. Its metabolities include four products, one of which is more active as a cholinesterase inhibitor than galanthamine itself[21].

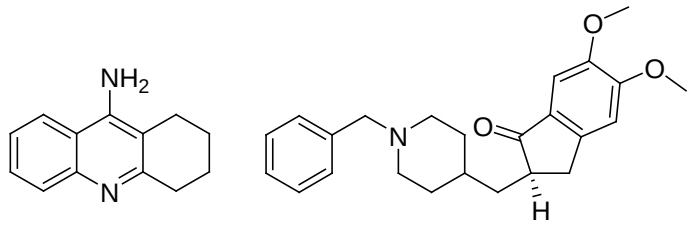

(91) **(92)**

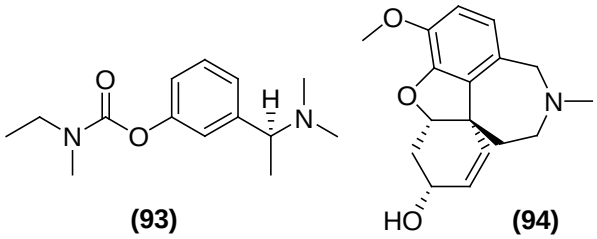

(93) **(94)**

Based on problems aforementioned, there is a need to find new AChE inhibitors that are more selective, exhibiting better bio-availability and more potent than galanthamine. The search has led researchers to a number of steroidal alkaloids that could be candidates for AChE inhibition. Compounds **95** to **99** have been isolated from various species of lilac plants, *Fritillaria*, and have shown good cholinesterase inhibitory activities[45].

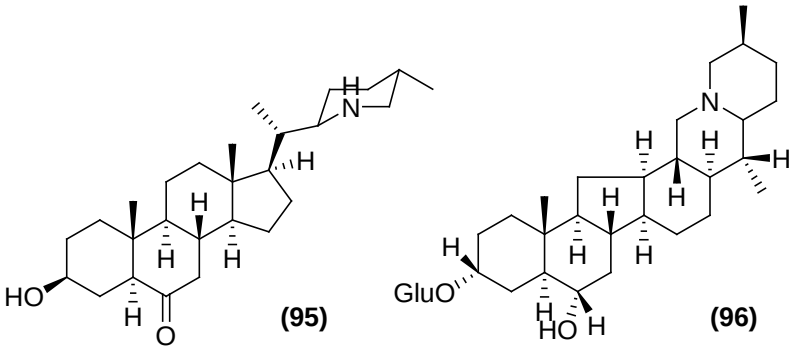

(95) **(96)**

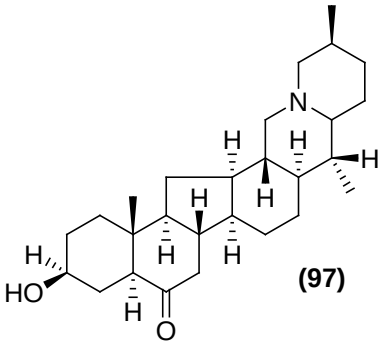

(97)

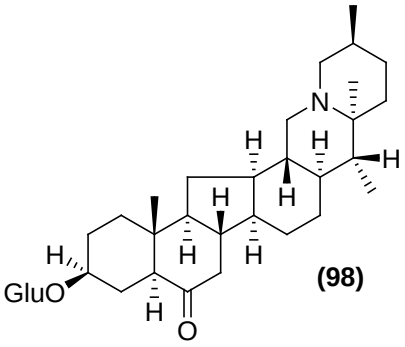

(98)

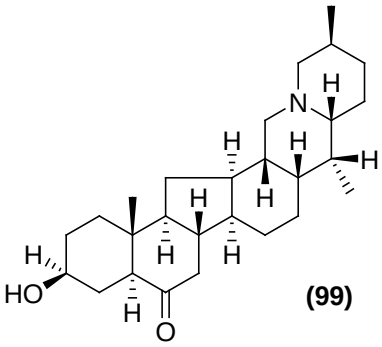

(99)

Table 1.4. Compounds from lilac plants exhibiting cholinesterase inhibitory activities.

Compound	AChE IC_{50} (µM) ± S.D.	BChE IC_{50} (µM) ± S.D.
95	6.4 ± 0.003	12.5 ± 0.026
96	16.9 ± 0.018	2.1 ± 0.005
97	5.7 ± 0.004	5.2 ± 0.002
98	6.5 ± 0.013	7.3 ± 0.005
99	7.7 ± 0.001	0.7 ± 0.001

Phytochemical studies on the marine sponge *Corticium* have yielded a steroidal alkaloid 4-acetoxy-plakinamine B (**100**) which has shown AChE inhibitory activity at an IC_{50} of 3.75µM[46].

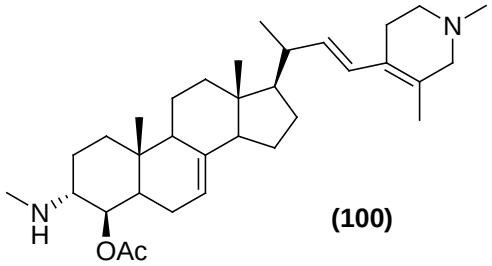

(100)

Three compounds, epoxynepapakistamine-A (**101**), Funtumafrine C (**102**) and *N*-methylfuntumine (**103**), were isolated from a shrub from the Buxaceae family, *Sarcococca coriacea*, have shown potential anti-AChE and anti-BChE activities from 6.56 to > 200µM[47].

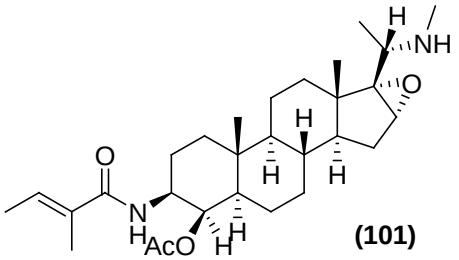

(101)

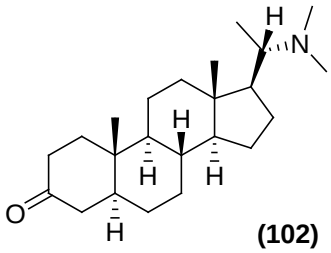

(102)

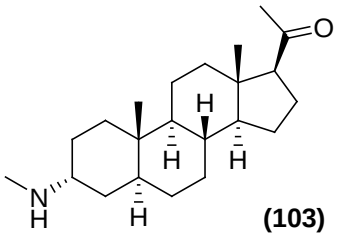

(103)

Thus, based on the importance of steroidal alkaloids in their ability to inhibit enzymes of the cholinesterase family, this project was designed to identify AChE inhibitory steroidal bases from *Buxus natalensis* and nitrogen containing compounds from *Drypetes gossweileri*.

In summary, the literature presented indicates that natural product chemistry is an important part of research that contributes lead molecules not only to drug discovery but also to the agricultural industry. This feature makes this branch very interesting to chemists to discover novel chemical structures.

1.5 REFERENCES

1. Newman, D. J.; Cragg, G. M.; Snaderb, K. M. *Nat. Prod. Rep.* **2000**, *17*, 215.

2. Clark, A. M. *Pharm. Res.* **1996**, *13*, 1133.

3. Croteau, R.; Kutchan, T. M.; Lewis N. G. *Biochemistry & Molecular Biology of Plants*; Buchanan, B.; Gruissem, W., Jones, R., Ed.; John Wiley and Sons: New York, 2000, Chapter 24, pp 1250- 1318.

4. Newman, D. J.; Cragg G. M. *J. Nat. Prod.* **2007**, *70*, 461.

5. Harvey, A. *Drug Discovery Today*. **2000**, *5*, 294.

6. Newman, D. J.; Cragg, G. M.; Snader K. M. *J. Nat. Prod.* **2003**, *66*, 1022.

7. Farnsworth, N. R.; Akerele, A. S.; Bingel, A. S.; Soejarto, D. D.; Guo,Z. *Bulletin of the WHO*. **1985**. *63*. 965.

8. De Smet, P. A. G. M. *Clin. Pharmacol. Ther*. **2004**, *74*, 1.

9. Brahmachari, G. *Natural Products: Chemistry, Biochemistry and Pharmacology*. Alpha Science International. Oxford, UK. 2009; p 1.

10. Cragg, G. M.; Newman, D. J.; Snader, K. M. *J. Nat. Prod.* **1997**, *60*, 52.

11. Boyd, M. R. *In Current Therapy in Oncology*; Niederhuber, J., Ed.; B.C. Decker: Philadelphia, 1993; pp 11-22.

12. Stanforth, S. P. *Natural Product Chemistry at a glance*. Blackwell Publishing Ltd: Malden, MA. 2006; p 2-6.

13. Dewick, P. M. *Medicinal Natural Products: A Biosynthetic Approach*. 3rd Ed.; John Wiley and Sons: New York. 2009; p 8.

14. Lee, Y. M.; Li, H.; Hong, J.; Cho, H. Y.; Bae, K. S.; Kim, M. A.; Kim, D. K.; Jung, J. H. *Arch. Pharm. Res.* **2010**, *33*, 231.

15. Kossuga, M. H.; Nascimento, A. M.; Reimao, J. Q.; Tempone, A. G.; Taniwaki, N. N.; Veloso, K.; Ferreira, A. G.; Cavalcanti, B. C.; Pessoa, C.; Moraes, M. O.; Mayer, A. M. S.; Hajdu, E.; Berlinck, R.G.S. *J. Nat. Prod*. **2008**, *71*, 334.

16. Singh, A. J.; Xu, C. X.; Xu, X.; West, L. M.; Wilmes, A.; Chan, A.; Hamel, E.; Miller, J. H.; Northcote, P. T.; Ghosh, A. K. *J. Org. Chem*. **2010**, *75*, 2.

17. Songsiang, U.; Wanich, S.; Pitchuanchom, S.; Netsopa, S.; Uanporn, K.; Yenjai, C. *Fitoterapia* **2009**, *80*, 427.

18. Zhang, G. L; Li, N.; Wang, Y. H.; Zheng, Y. T.; Zhang, Z.; Wang, M. W. *J. Nat. Prod*. **2007**, *70*, 662.

19. Tang, H. F.; Yi, Y. H.; Yao, X. S.; Xu, Q. Z.; Zhang, S. Y.; Lin, H. W. *J. of Asian Nat. Prod. Res*. **2002**, *4*, 95.

20. Simons, V.; Morrissey, J. P.; Latijnhouwers, M.; Csukai, M.; Cleaver, A.; Yarrow, C.; Osborn, A. *Antimicrob. Agents and Chemother*. **2006**, *50*, 2732.

21. Mukherjee, P. K.; Kumar, V.; Mal, M.; Houghton, P. J. Acetylcholinesterase inhibitors from plants. *Phytomedicine* **2007**, *14*, 289.

22. Cong, Y.; Jia, W.; Chen, J.; Song, S.; Wang, J. H.; Yang, Y. H. *Helv. Chim. Acta*. **2007**, *90*, 1038.

23. Aoki, S.; Watanabe, Y.; Tanabe, D.; Arai, M.; Suna, H.; Miyamoto, K.; Tsujibo, H.; Tsujikawa, K.; Yamamoto H.; Kobayashi, M. *Bioorg. Med. Chem.* **2007**, *15*, 6758.

24. Fukuzawa, S.; Matsunaga, S.; Fusetani, N. *J. Org. Chem.* **1994**, *59*, 6164.

25. Fukuzawa, S.; Matsunaga, S.; Fusetani, N. *J. Org. Chem.* **1995**, *60*, 608.

26. Fukuzawa, S.; Matsunaga, S.; Fusetani, N. *Tetrahedron* **1995**, *51*, 6707.

27. Fukuzawa, S.; Matsunaga, S.; Fusetani, N. *J. Org. Chem.* **1997**, *62*, 4484.

28. Zhou, C. Z.; Liu, J. Y.; Ye, W. C.; Liu, C. H.; Tana, R.X. *Tetrahedron* **2003**, *59*, 5743.

29. Zirihi, G. L.; Grellier, P.; Guede-Guina, F.; Bodo, B.; Mambu, L.; *Bioorg. Med. Chem. Lett*. **2005**, *15*, 2637.

30. Andrade, C.; Radhakrishnan, R. *Indian J. Psychiatry*. **2009**, *51*, 12.

31. Selkoe, D. *Science* **2002**, *298*, 789.

32. Price, D. L. *J. Neurosci*. **1986**, *9*, 489.

33. Kasa, P.; Rakonczay, Z.; Gulya, K. *Neurobiology*. **1997**, *52*, 511.

34. Katzman, R. *N. Engl. J. Med*. **1986**, *314*, 964.

35. Davis, P.; Maloney, A.J. *Lancet* **1976**, *2*, 1403.

36. Sims, N. R.; Bowen, D. M.; Allen, S. J.; Smith, C. C.; Neary, D.; Thomas, D. J. *J. Neurochem*. **1983**, *40*, 503.

37. DeKosky, S. T.; Harbough, R. E.; Shmitt, F. A.; Bakay, R. A.; Chui, H. C.; Knopman, D. S. *Ann. Neurol*. **1992**, *32*, 625.

38. Mesulan, M.; Guillozet, A.; Shaw, P.; Quinn, B. *Neurobiol. Dis*. **2002**, *9*, 88.

39. Ballard, C. G. *Eur. Neurol*. **2002**, *47*, 64.

40. Darreh-Shori, T.; Brimijoin, S.; Kadir, A.; Almkvist, O.; Nordberg, A. *Neurobiol. Dis*. **2006**, *24*, 326.

41. Weinstock, M. *CNS Drugs*. **1999**, *12*, 307.

42. Sussman, J.; Silman, I. *Chem-Biol Interact*. **2008**, *175*, 3.

43. Oh, M. H.; Houghton, P. J.; Whang, W. F.; Cho, S. H. *Phytomedicine*. **2004**, *11*, 544.

44. Schulz, V. *Phytomedicine* **2003**, *10*, 74.

45. Lin, B. Q.; Ji, H.; Li, P.; Fang, W.; Jiang, Y. *Planta Med*. **2006**, *72*, 814.

46. Langjae, R.; Bussarawit, S.; Yuenyongsawad, S.; Ingkaninan, K.; Plubrukarn A. *Steroids* **2007**, *72*, 682.

47. Kalauni, S. K.; Choudhary, M. I.; Khalid, A.; Manandhar, M. D.; Shaheen, F.; Atta-ur-Rahman; Gewall, M. B. *Chem. Pharm. Bull.* **2002**, *50*, 1423.

CHAPTER 2

Pytochemical studies on *Buxus natalensis*

2.1 INTRODUCTION

The genus *Buxus* is a rich source of steroidal alkaloids found all over the world. Although *Buxus natalensis* has not been studied, extensive phytochemical studies on other species of the genus *Buxus* including *B. sempervirens, B. papillosa, B. microphylla, B. longifolia, B. hildebrandtii,* and *B. hyrcana* have afforded over 200 new steroidal bases[1]. Plants of this genus are widely distributed throughout Eurasia and North America. These plants are used in folk medicine to treat various ailments including malaria, rheumatism and skin infections[2,3]. Ethanolic extracts from *Buxus* species are shown to exhibit anti-bacterial properties[4]. The ethanolic extract of *B. sempervirens* is reported to exhibit anti-HIV activity, and postpone the progression in HIV-infected asymptomatic patients[5,6]. The powdered wood of the trunk of *Buxus microphylla* has long been used in Chinese folk medicine to treat heart disease[7].

Buxus alkaloids have unique triterpenoid-steroidal pregnane type structures with C-4α, C-4β methyl groups, 9β,10β-cycloartenol system and C-20 degraded side chains[8]. Generally, *Buxus* alkaloids have two types of structures, as shown below.

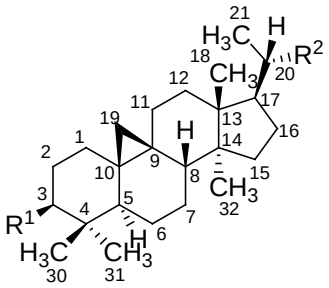

(104)

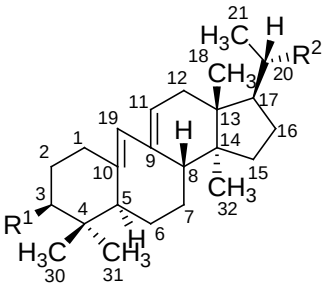

(105)

R^1 and R^2 in both structures represent different amino or keto functionalities. Both structures can easily be distinguished in the ^{1}H-NMR spectrum. Alkaloids with structures similar to **104** exhibit AB doublets at δ 0.1-0.5 (J = 4.0 Hz) for cyclopropyl methylene (C-19) protons. While alkaloids similar to **105** have a 9(10→19) *abeo*-diene system, with the methine C-19 proton resonating in the olefinic range of ^{1}H-NMR spectrum. The 9(10→19) *abeo*-diene system of these compounds can also be identified by UV spectrum that shows absorption maxima at 238 and 245 nm with shoulders at 228 and 252 nm in the UV spectrum[8].

Other structural features of *Buxus* alkaloids include oxidation of C-31 methyl group or the presences of double bonds at C_1=C_{10}, C_5=C_6 and C_6=C_7. Some of these features are exemplified in cyclomicrophylline A-C (**106-108**), and cyclomicrophyllidine-A (**109**)[9,10].

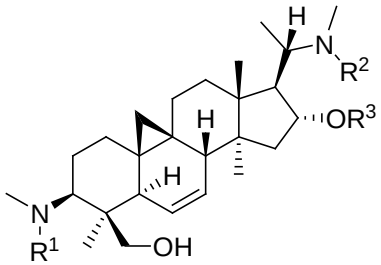

(106): $R^1 = R^2 = CH_3$, R^3 = H
(107): $R^1 = CH_3$, $R^2 = R^3$ = H
(108): $R^1 = R^3$ = H, $R^2 = CH_3$
(109): $R^1 = R^2 = CH_3$, R^3 = COPh

Buxus alkaloids have shown various biological activities including anti-acetylcholinesterase (AChE) and anti-butyrylcholinesterase (BChE). For instance, *N*-benzoylbuxahyrcanine (**110**), *N*-tigloylbuxahyrcanine (**111**), *N*-isobutyroylbuxahyrcanine (**112**), 2α,16β,31-triacetylbuxiran (**113**), 2α,16β,31-triacetyl-9-11-dihydrobuxiran (**114**), O^6-buxafurandiene (**115**), 7-deoxy-O^6-buxafurandiene (**116**), benzoylbuxidienine (**117**), buxapapillinine (**118**), buxaquamarine (**119**) and irehine (**120**) purified from *B. hyrcana*[11,12,13], exhibit anti-AChE and anti-BChE activities. These bioactivities are listed in **Table 2.1**.

Table 2.1. Acetylcholinesterase and butyrylcholinesterase inhibitory activities.

Compound	AChE	BChE	Compound	AChE	Compound	AChE
110	>1000	310.6	**115**	17	**118**	80
111	443.6	31.2	**116**	13	**119**	76
112	>1000	53.7	**117**	35	**120**	100

(110) R =

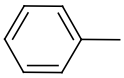

(111) R =

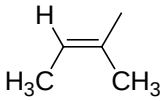

(112) R =

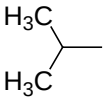

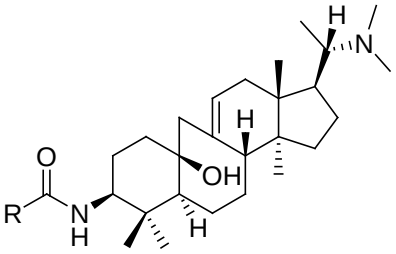

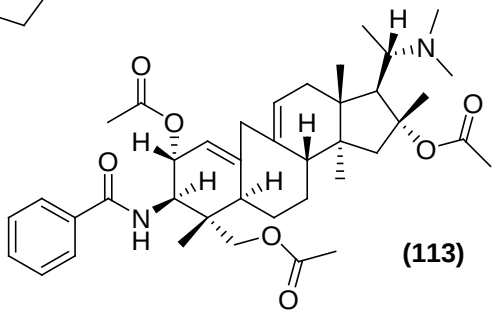

(113)

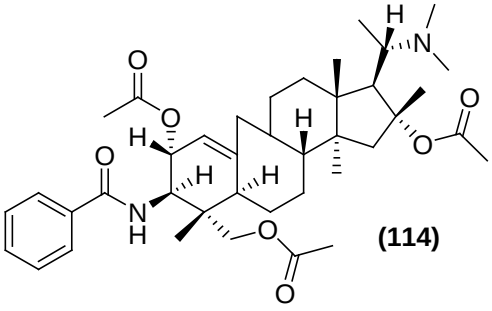

(114)

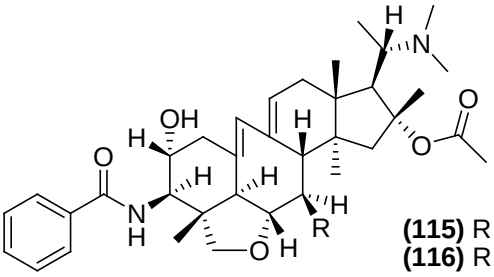

(115) R = OH
(116) R = H

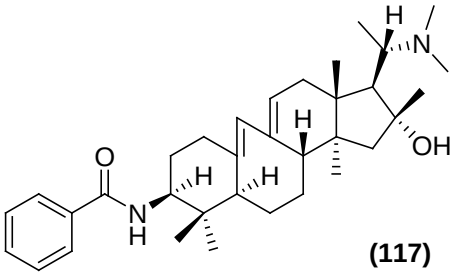

(117)

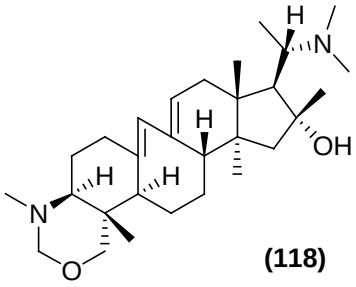

(118)

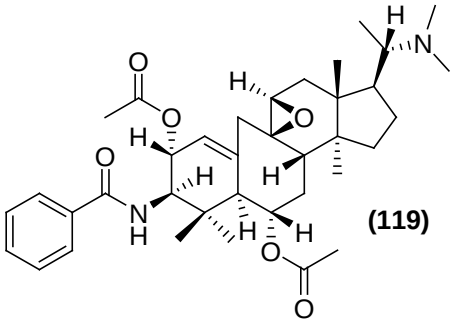

(119)

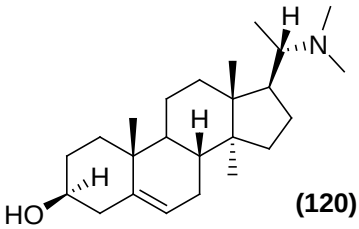

(120)

Cyclovirobuxine D (**121**) is found to be as potent as hydrocortisone (**122**), a prescribed anti-inflammatory drug[14]. Cyclovirobuxine D was also found to relieve tension in smooth muscle by inhibiting potassium-activated calcium channels needed to initiate muscle contraction[15]. Later investigations led researchers to propose cyclovirobuxine D helps prevent and treat mycocardial ischemia when it was observed it was responsible for opening ATP sensitive potassium channels, enhancing nitric oxide (NO) release and inhibiting venous thrombosis all factors in myocardial ischemia[16].

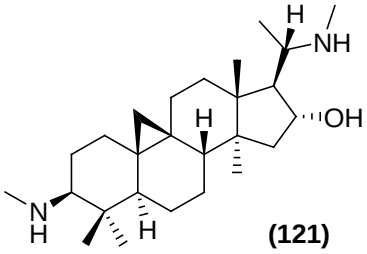

(121)

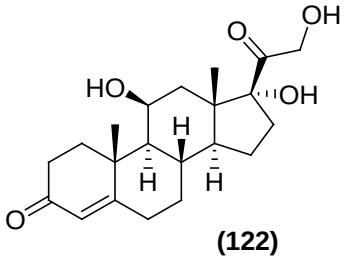

(122)

Buxus natalensis, a shrub native to South Africa, was the focus of our phytochemical investigations. Previous studies reported the crude extracts displayed antimicrobial activity from this plant[17]. According to South African traditional healers, this plant is used to enhance memory of elderly people. The methanolic extract of this plant was active in our AChE inhibitory assay. This chapter describes the isolation, structure elucidation and bioactivity data of steroidal bases, O^{10}-natafuranamine (**123**), cyclonataminol A (**124**), 31-demethylbuxaminol A (**125**), buxaminol A (**126**), buxaminol C (**127**), and aromatics *p*-coumaroylputrescine (**128**), and methyl syringate (**129**) isolated during the course of the study.

2.2 RESULTS AND DISCUSSION

Buxus natalensis was collected from uMhalanga Rocks nature reserve, Durban, South Africa. The methanolic extract of *B. natalensis* exhibited AChE inhibitory activity with an IC_{50} value 28 µg/ml. AChE inhibiting guided fractionation was carried out, as described in the experimental section, to afford compounds **123-129**.

2.2.1 O^{10}-Natafuranamine (123).

O^{10}-Natafuranamine (**123**) was isolated as yellow colored solid. Its UV spectrum showed the absorption maximum at 221 nm was due to the benzamide functionality[18]. The IR spectrum displayed intense absorption bands at 3356 (OH), 2925 (CH), 1730 (C=O), 1650, 1528 and 1459 (aromatic), and 1246 and 1027 (unsymmetrical ether) cm^{-1}. The high resolution electron impact mass spectrum (HREIMS) of **123** showed the molecular ion peak $[M+H]^+$ *m/z* 535.3523 that was in agreement with the molecular formula $C_{33}H_{46}N_2O_4$ indicating the twelve degrees of unsaturation in this compound. The EIMS also showed the molecular ion peak at *m/z* 534. An ion at *m/z* 519 was due to the loss of a methyl from the molecular ion. The base peak at *m/z* at 72 was due to the cleavage of ring D side chain containing *N*,*N*-dimethyl substituent at C-20[19]. Another intense ion at *m/z* 105 was due to the loss of a benzoyl cation.

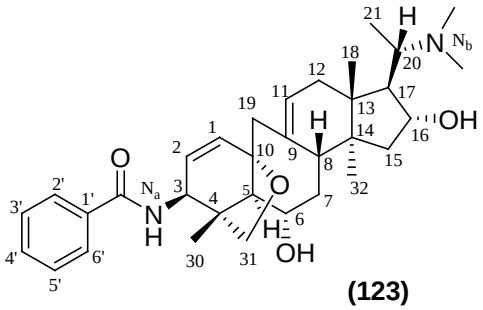

(123)

The ^{1}H-NMR spectrum ($CDCl_3$, 400MHz) of compound **123** featured three three-proton singlets at δ 0.66, 1.36 and 0.92 and were assigned to the protons of three tertiary methyl protons on C-18, C-30 and C-32 respectively. A doublet, intergrating for three protons, centered at δ 0.90 (J = 6.8 Hz) was due to the secondary C-21 methyl group. A six-proton broad singlet at δ 2.28 was ascribed to the *N*,*N*-dimethyl protons. A two-proton broad singlet appeared at δ 2.69 was due to the C-19 methylene protons flanked by two quaternary carbons. Two AB doublets, integrating for one-proton each, resonated at δ 3.60 (J = 8.7 Hz) and 3.69 (J = 8.8 Hz) were due to the C-31 methylene protons. This carbon usually contains either hydroxyl group, aldehyde or ether functionalities. To distinguish between an ether or hydroxyl group, the ^{1}H-NMR spectra of **123** was recorded in pyridine-d_5. The chemical shift of these AB doublets remains unaffected suggesting the presence of an ether functionality at C-31. It has been reported in literature that protons, geminal to hydroxyl group, showed prounced paramagnetic shift (~0.2ppm)[19,20]. A downfield one-proton multiplet appeared at δ 3.81 was due to the C-6 methine proton, geminal to the oxygen moiety. This proton was present geminal to a hydroxyl group as this signal resonated downfield at δ 4.20 when the ^{1}H-NMR spectrum was recorded in pyridine^{d5}. A downfield one-proton multiplet at δ 4.52 was assigned to the C-3 (δ 55.0) methine proton, geminal to the benzamide group. The C-11 proton resonated as a broad singlet at δ 5.40. The C-1 olefinic proton resonated as a doublet at δ 5.74 (J = 9.5) and C-2 appeared as a double doublet at δ 6.06 (J_{dd} = 9.5, J_2 = 3.9 Hz) respectively. The amidic N*H* resonated as a doublet at δ 7.27 (J = 7.6 Hz). Aromatic protons resonated as two set of multiplets at δ 7.43 - 7.85.

The ^{13}C-NMR spectrum ($CDCl_3$, 100 MHz) of **123** showed the resonance of all 33 carbons. A combination of ^{13}C-NMR broad-band and DEPT spectra revealed the presence of six methyl, five methylene, fifteen methine and seven quaternary carbons in this compound. The HSQC spectrum of **123** was used to establish ^{1}H/^{13}C one-bond shift correlation of all protonated carbons. Complete ^{1}H and ^{13}C chemical shift assignments and ^{1}H/^{13}C one-bond shift correlations determined from HSQC spectrum are presented in **Table 2.2**.

The COSY-45° spectrum of **123** revealed the presence of five isolated spin systems **123*a-e*** in the molecule as seen in **Figure 2.1**. The first spin system **123*a*** represents a phenyl moiety. The C-2'/C-6' proton (δ 7.85) exhibited cross-peaks with C-3'/C-5' (δ 7.44). The latter exhibited ^{1}H-^{1}H spin correlation with the *para* C-4' proton (δ 7.48). The presence of a phenyl moiety was further suggested by the ^{13}C-NMR spectrum that showed signals at δ 127.3 (C-2'/C-6'), δ 128.9 (C-3'/C-5') and δ 131.8 (C-4'), respectively. The second spin system, **123*b*** started with the C-1 olefinic proton (δ 5.74) that showed a cross-peak with the C-2 vinylic proton (δ 6.06). The latter in turn exhibited vicinal coupling with the C-3 methine proton (δ 4.52) that was coupled with the amidic N*H* (δ 7.27) in the COSY-45° spectrum. The DEPT spectra showed the olefinic signals at δ 131.3 (C-1) and 129.5 (C-2) that exhibited HSQC correlations with H-1 (δ 5.74) and H-2 (δ 6.06), respectively. A methine carbon signal at δ 55.0 in the DEPT spectra showed direct ^{1}H/^{13}C connectivity with H-3 (δ 4.52) in the HSQC spectrum. The third spin system **123*c*** began with the C-5 methine proton (δ 1.60). This proton exhibited vicinal coupling with the C-6 methine proton (δ 3.81). The latter exhibited vicinal couplings with the C-7 methylene protons (δ 1.60 and 1.85), that in turn showed COSY-45° interaction

with the C-8 methine proton (δ 1.93). The TOCSY spectrum also confirmed the presence of this spin system. The DEPT spectra displayed methine signals at δ 60.8 (C-5), 75.5 (C-6), 43.4 (C-8) and methylene resonance at δ 38.7 (C-7). The HSQC spectrum revealed direct connectivities of H-5 (δ 1.60), H-6 (δ 3.81), H_2-7 (δ 1.60 and 1.85) and H-8 (δ 1.93) with C-5 (δ 60.8), C-6 (δ 75.5), C-7 (δ 38.7), and C-8 (δ 43.4), respectively. The fourth spin system **123*d*** consisted of C-11 and C-12 protons. The C-11 olefinic proton (δ 5.40) showed cross-peaks with the C-12 methylene protons (δ 1.81 and 2.02). The allylic coupling of the C-19 methylene protons (δ 2.69) with the C-11 olefinic proton was observed in the TOCSY spectrum. The DEPT spectra featured signals at δ 124.8 (C-11), δ 39.1 (C-12) and δ 44.6 (C-19). H-11 (δ 5.40) displayed one-bond HSQC coupling with C-11 (δ 124.8), while H_2-19 and H_2-12 were bonded with C-19 (δ 44.6) and C-12 (δ 39.1), respectively. The largest spin system **123*e*** was deduced by observing the C-16 methine proton (δ 4.09) showing cross-peaks with the C-15 methylene (δ 1.40 and 1.92) and C-17 methine (δ 1.83) protons. The latter showed vicinal couplings with the C-20 methine proton (δ 2.69) that in turn exhibited cross-peaks with the C-21 methyl protons (δ 0.90). The TOCSY spectrum was in agreement with the COSY-45° spectrum confirming the presence of **123*e*** spin system. DEPT spectra showed resonances at δ 14.4, 42.5, 77.4, 56.0 and 63.7 due to C-21 methyl, C-15 methylene, C-16, C-17, and C-20 methine carbons, respectively. The HSQC spectrum showed direct ^{1}H- and ^{13}C-NMR chemical shift correlations of H_2-15 (δ 1.40 and 1.92), H-16 (δ 4.09), H-17 (δ 1.83), H-20 (δ 2.69) and H_3-21 (δ0.90) with C-15 (δ 42.5), C-16 (δ 77.4), C-17 (δ 56.0), C-20 (δ 63.7) and C-21 (δ 14.4) respectively.

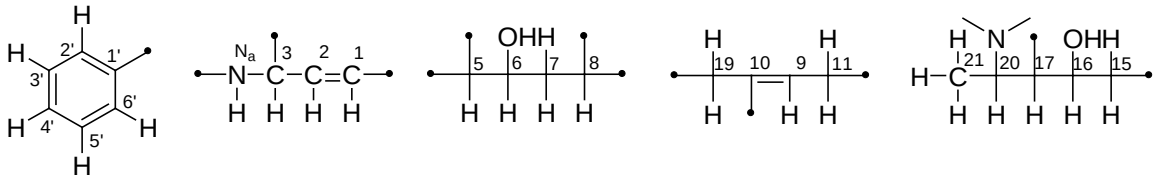

(123*a*) **(123*b*)** **(123*c*)** **(123*d*)** **(123*e*)**

Figure 2.1. Spin systems determined by COSY and TOCSY spectra for O^{10}-natafuranamine (**123**).

The HMBC spectrum of **123** was useful in determining the chemical shifts of quarternary carbons and in connecting partial structures **123*a*-*e***, as obtained from the COSY-45° and TOCSY spectra. The H-2'/H-6' (δ 7.85) of fragment **123*a*** showed HMBC interactions with C-1' (δ 134.5) and the amidic carbonyl carbon (δ 166.7). The amidic hydrogen (δ 7.27) in turn showed long-range heteronuclear correlations with the amidic carbonyl carbon (δ 166.7). These HMBC spectral data helped to connect spin system **123*a*** with **123*b*** through an amidic bond. H-3 showed cross-peaks with C-4 (δ 46.1) and C-5 (δ 60.8) of fragment **123*c***. H-5 (δ 1.60) showed cross-peaks with C-3 (δ55.0), C-4 (δ46.1) and C-10 (δ 80.3). H-30 showed cross-peaks with C-3 (δ 55.0) and C-31 (δ 78.2). H_2-31 (δ 3.69 and δ 3.60) showed cross-peaks with C-3 (δ 55.0), C-10 (δ 80.3) and C-30 (δ 22.0). These HMBC interactions suggested a bond connecting C-3 and C-5 through C-4 quaternary carbon. The C-31 was bonded with C-10 through an ether linkage. These linkages afforded partial structure **123*f***. The methylene H_2-19 (δ 2.69) protons of fragment **123*d*** exhibited cross-peaks with C-8 (δ 43.4), C-9 (δ 113.6), C-10 (δ 80.3) and C-11 (δ 124.8). As well, H-1 (δ 5.74) and H-2 (δ 6.06) displayed cross peaks

with C-10 (δ 80.3). These observations were important in connecting C-19 methylene carbon of fragment **123*d*** with C-1 of fragment **123*b*** and C-5 of fragment **123*c*** through a quaternary C-10 carbon. These observations also helped connect C-19 with C-8 of fragment **123*c*** which expanded the structure **123*f*** into **123*g***. Fragment **123*e*** was connected to fragment **123*c*** by observing the H_3-32 (δ 0.92) HMBC correlation with C-8 (δ 43.4), C-14 (δ 43.8) and C-15 (δ 42.5). These observations suggested C-15 of fragment **123*e*** was connected to C-8 of fragment **123*c*** through a quaternary C-14. Fragment **123*e*** was also connected to fragment **123*d***. H_3-18 (δ 0.66) showed cross-peaks with C-12 (δ 37.1), C-13 (δ 47.9), C-14 (δ 43.8) and C-17 (δ 56.0). Indicating C-17 of fragment **123*e*** was connected to C-12 of fragment **123*d*** through a quaternary C-13. All HMBC correlations are depicted in **Figure 2.2**.

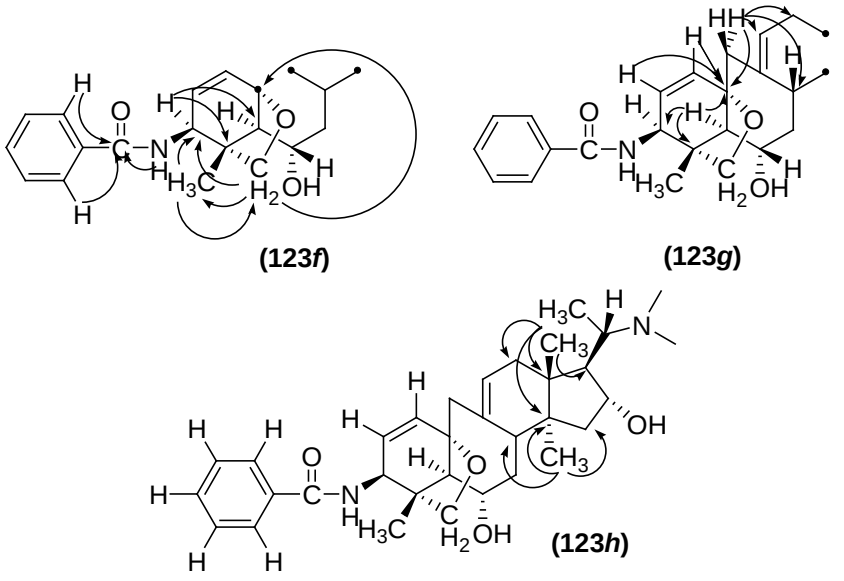

Figure 2.2. Spin systems of *O*[10]-natafuranamine (**123**) connected through HMBC correlations.

Table 2.2. ^{1}H and ^{13}C NMR Spectroscopic Data (400 and 100 MHz, respectively) in $CDCl_3$ for O^{10}-natafuranamine (**123**).

	O^{10}-natafuranamine (**123**)		
Position	**δ_C**	**Multiplicity †**	**δ_H (*J* in Hz)**
1	131.3	CH	5.74, *d* (9.5)
2	129.5	CH	6.06, *dd* (3.9, 3.8)
3	55.0	CH	4.52, *m*
4	46.1	C	-
5	60.8	CH	1.60, *m*
6	75.5	CH	3.81, *m*
7	38.7	CH_2	1.85, *m*, 1.60, *m*
8	43.4	CH	1.93, *m*
9	133.6	C	-
10	80.3	C	-
11	124.8	CH	5.40, *s*
12	37.1	CH_2	2.02, *m*, 1.81, *m*
13*	43.8	C	-
14*	47.9	C	-
15	42.5	CH_2	1.92, *m*, 1.40, *m*
16	77.4	CH	4.09, *m*
17	56.0	CH	1.83, *m*
18	16.8	CH_3	0.66, *s*
19	44.6	CH_2	2.69, *m*
20	63.7	CH	2.69, *m*
21	14.4	CH_3	0.90, *s* (6.8)
30	22.0	CH_3	1.36, *s*
31	78.2	CH_2	3.69, *d* (8.8), 3.60, *d*
32	18.7	CH_3	0.92, *s*
O*C*NH	166.7	C	-
OCN*H*	-		7.27, *d* (7.6)
$N_b(CH_3)_2$	44.5	CH_3	2.28, *s*
1’	134.5	C	-
2’	127.3	CH	7.85, *d* (7.1)
3’	128.9	CH	7.44, *m*
4’	131.8	CH	7.48, *m*
5’	128.9	CH	7.44, *m*
6’	127.3	CH	7.85, *d* (7.1)

*Assignments are interchangeable. †Multiplicity as determined by DEPT spectra.

After establishing the gross structure of **123**, the relative configurations of chiral centers were established using NOESY spectrum. It has been documented in the literature the α-orientation of H-3, H-5, and H-17, and β-orientation of H-8, and H-16 in *Buxus* alkaloids[21]. H-3 (δ 4.52) showed NOESY correlations with the $H_{2\alpha}$-31 proton (δ 3.60). H_3-32 (δ 0.92) showed cross-peaks with H-5 (δ 1.60) and H-17 (δ 1.83). Based on these observations, H-3, H-5, H-17, H_3-31 and H_3-32 were established to have α-orientation. H-16 (δ 4.09) showed NOESY correlations with H-6 (δ 3.81), H_3-8 (δ 1.93), H-18 (δ 0.66) and H-20 (δ 2.69). Based on these observations H-6, H-8, H-16 and H_3-18 were placed in the β-orientation. It is reported in literature the α-oriented methyl, H_3-31, undergoes oxidation whereas the β-oriented methyl, H_3-30, does not[22,23]. Based on these literature precedents, α-stereochemistry was proposed for the ether linkage between C-31 and C-10. The probable conformation of **123** obtained from the NOESY spectrum is shown in **Figure 2.3**. Based on these spectral data, structure **127** was proposed for this new steroidal base.

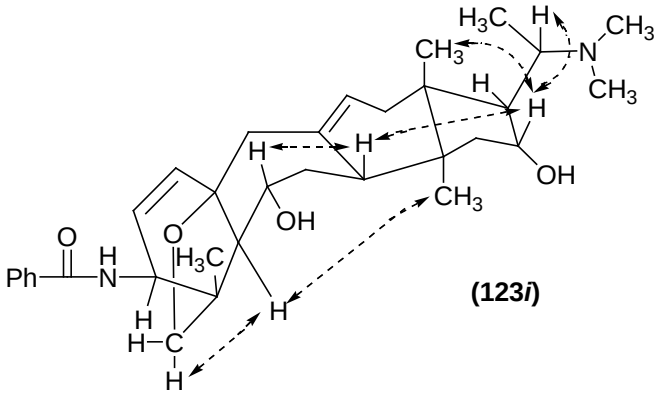

Figure 2.3. Probable configuration of rings A, B, C, D, and E of compound **123** as obtained from NOESY spectrum.

2.2.2 Biogenesis of O^{10}-Natafuranamine (123).

Only six compounds have been reported in the literature containing a tetrahydrofuran ring incorporated in ring A of *Buxus* alkaloids[13,19,24,25,26]. These compounds might be produced in nature from buxanoldine (**130**), previously isolated from *Buxus papilosa*[27]. Buxanoldine can undergo oxidation at C-2 and C-6 to give the intermediate (**131**), which can be susceptible to an attack by the C-31 hydroxyl on $\Delta^{1,10}$ double bond, followed by the elimination of C-2 hydroxyl group to generate a $\Delta^{1,2}$ double bond, as outlined in **Scheme 2.1**.

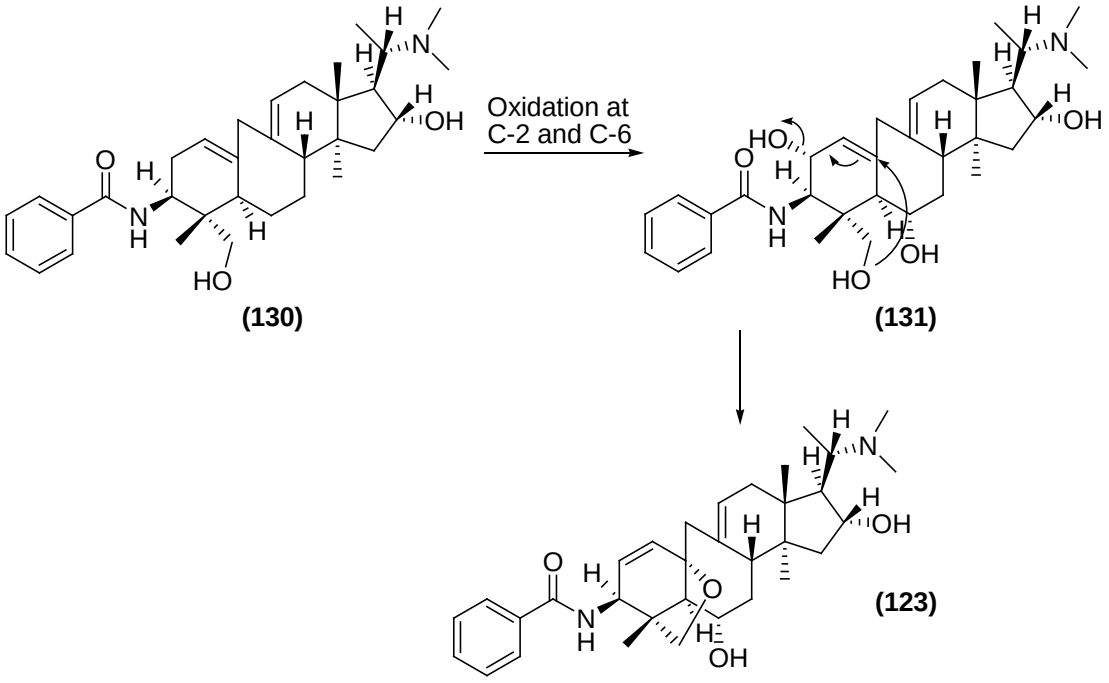

Scheme 2.1. Possible pathway towards the biosynthesis of a furan ring incorporation of compound **123**.

2.2.3 Cyclonataminol A (124)

Compound **124** was isolated as a yellow amorphous powder. Its UV spectrum showed terminal absorption indicating the lack of conjugated π systems. The IR spectrum displayed absorption bands at 3435 (OH), 2936 (CH), and 1452 (C=C) cm^{-1}. The HREIMS of **124** showed a molecular ion peak at *m/z* 444.3708 that provided a molecular formula $C_{28}H_{48}N_2O_2$ (calcd. 444.3716) and suggested the presence of six degrees of unsaturation in this alkaloid. An ion at *m/z* 429.34738 (calcd. for $C_{27}H_{45}N_2O_2$) arose due to the loss of a methyl group from the molecular ion. The base peak at *m*/*z* 72.08132 (calcd. for $C_4H_{10}N$) was indicative for the presence of an *N*,*N*-dimethyl substituent at C-20.

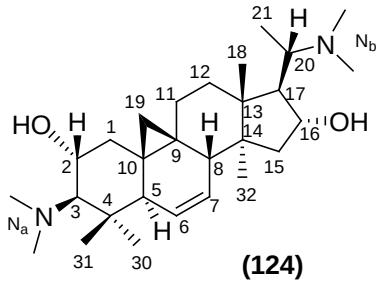

(124)

The ^{1}H-NMR spectrum ($CDCl_3$, 400MHz) of **124** showed the resonance of two doublets integrating for one proton each at δ -0.13 (*J* = 4.1Hz) and 0.73 (*J* = 3.4Hz) due to C-19 cyclopropyl methylene protons. It has been reported in the literature that *Buxus* alkaloids containing C-6/C-7 double bond show the upfield resonance for one of the C-19 cyclopropyl methylene protons while the second C-19 methylene proton resonates in the methyl/methylene region[28]. In compound **124**, resonance of two doublets at δ -0.13 and 0.74 indicated the presence of a double bond at C-6 and C-7. It was confirmed by the ^{1}H-

NMR spectrum that displayed two olefinic signals at δ 5.56 and 5.44 due to H-6 and H-7, respectively. Four three-proton singlets at δ 0.88, 1.07, 0.89 and 0.94 were due to the C-18, C-30, C-31 and C-32 methyl protons, respectively. One three-proton doublet at δ 0.86 (J = 6.6 Hz) was assigned to C-21 secondary methyl protons.

The ^{13}C-NMR spectrum ($CDCl_3$, 100 MHz) of **124** showed the resonance of all 28 carbons. Broad-band ^{13}C-NMR spectral data along with the DEPT spectra revealed the presence of nine methyl, five methylene, nine methine and five quaternary carbons in this compound. The HSQC spectrum of **124** was used to establish ^{1}H/^{13}C one-bond shift correlation of all protonated carbons. Complete ^{1}H and ^{13}C chemical shift assignments and ^{1}H/^{13}C one-bond shift correlations determined from HSQC spectrum are presented in **Table 2.3**.

The COSY-45° spectrum of **124** showed the presence of four isolated spin systems **124*a-d*** as seen in **Figure 2.4**. The first spin system **124*a*** was traced by the downfield resonace of H-2 (δ 3.75) which showed cross-peaks with the H_2-1 methylene (δ 1.86 and 1.55) and H-3 methine (δ 2.09) protons. DEPT spectra showed resonances at δ 39.7, 66.2, and 78.0 due to the C-1 methylene, C-2 and C-3 methine carbons, respectively. The HSQC spectrum showed direct ^{1}H- and ^{13}C-NMR chemical shift correlations of H_2-1 (δ 1.86 and 1.55), H-2 (δ 3.75) and H-3 (δ 2.09) with C-1 (δ 39.7), C-2 (δ 66.2), and C-3 (δ 78.0), respectively. Spin system **124*b*** included the vinylic protons H-6 (δ 5.56) and H-7 (δ 5.44). H-6 was coupled with H-5 (δ 1.92) and H-7 was found to be coupled to H-8 (δ 2.53) as indicated by the COSY spectrum of **124**. DEPT spectra showed resonances at δ 49.1, 126.3, 129.3, and 43.5 due to C-5, C-6, C-7, and C-

8 methine carbons, respectively. The HSQC spectrum showed direct correlations of H-5 (δ 1.92), H-8 (δ 2.53) with C-5 (δ 49.1), C-8 (δ 43.5) aliphatic carbons and H-6 (δ 5.56), H-7 (δ 5.44) with C-6 (δ 126.3), C-7 (δ 129.3) olefinic carbons. Spin system **124*c*** comprised of H-11 and H-12 methylene protons and showed vicinal coupling of H_2-11 with H_2-12 in the COSY spectrum. The DEPT spectra showed resonances at δ 25.0, and 31.9 due to C-11 and C-12 methylene carbons. The HSQC spectrum showed direct correlations of H_2-11 (δ 1.83 and 1.42) and H_2-12 (δ 1.65 and 1.30) with C-11 (δ 25.0) and C-12 (δ 31.9), respectively. Spin system **124*d***, the largest of the spin systems, was the same as to that of **123*e***. The C-16 methine proton (δ 4.09) showed cross-peaks with the C-15 methylene (δ 1.24 and 1.98) and C-17 methine (δ 1.80) protons. The latter showed vicinal coupling with the C-20 methine proton (δ 2.63) which in turn exhibited cross-peaks with the C-21 methyl protons (δ 0.86). The TOCSY spectrum was in agreement with the COSY-45° spectrum confirming the presence of this spin system. DEPT spectra showed resonances at δ 10.3, 41.7, 79.3, 56.9 and 62.8 due to C-21 methyl, C-15 methylene, C-16, C-17, and C-20 methine carbons, respectively. The HSQC spectrum showed direct $^{1}H/^{13}C$-NMR chemical shift correlations of H_2-15 (δ 1.24 and 1.98), H-16 (δ 4.09), H-17 (δ 1.80), H-20 (δ 2.63) and H_3-21 (δ0.86) with C-15 (δ 41.7), C-16 (δ 79.3), C-17 (δ 56.9), C-20 (δ 62.8) and C-21 (δ 10.3) respectively.

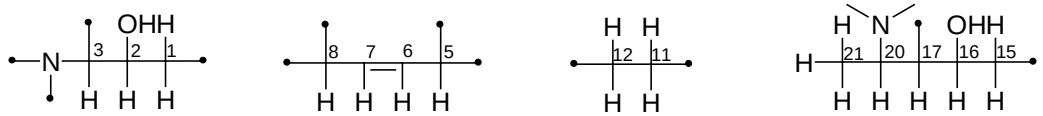

(124*a*) **(124*b*)** **(124*c*)** **(124*d*)**

Figure 2.4. Spin systems determined by COSY spectra for cyclonataminol A (**124**).

The HMBC spectrum of **124** helped connect spin systems **124*a*** and **124*b*** whereby $^{1}H/^{13}C$ long-range coupling of H-3 (δ 2.09) with C-1 (δ 39.7), C-2 (δ 66.2), C-4 (δ 43.7), C-5 (δ 49.1), and C-30 (δ 27.3) was observed. H_3-30 (δ 1.07) showed coupling with C-3 (δ 78.0), C-4 (δ 42.7) and C-5 (δ 49.1), likewise H_3-31 (δ 0.89) showed coupling with C-3 (δ 78.0) and C-30 (δ 27.3). These observations led to the connection of C-3 of fragment **124*a*** with C-5 of fragment **124*b*** through the quaternary C-4 carbon. C-8 of **124*b*** was connected to C-15 of **124*d*** through the quaternary C-14 carbon based on the HMBC cross-peaks of H-8 (δ 2.53) with C-6 (δ 126.3), C-7 (δ 129.3), C-9 (20.2), C-14 (δ 49.9), C-15 (δ 41.9), and C-32 (δ 18.6). Likewise, H_2-15 (δ 1.94 and δ 1.24) showed couplings with C-13 (δ 45.4), C-16 (δ 79.3) and C-32 (δ 18.6) and H_3-32 showed couplings with C-13 (δ 45.4), C-14 (δ 49.9) and C-15 (δ41.7). Spin system **124*d*** was connected to **124*c*** by observing the $^{1}H/^{13}C$ long-range coupling of H-17 (δ1.80) with C-12 (δ 31.9), C-13 (δ 45.4), C-16 (δ 4.09), C-18 (δ 19.3), C-20 (δ 2.63) and C-21 (δ 10.3). Spin system **124*c*** was connected to **124*b*** when it was observed that H_2-11 (δ 1.83 and 1.42), and H_2-12 (δ 1.65 and δ 1.30) both showed HMBC correlations with C-9 (δ 20.2). It was also observed that H_2-1 (δ 1.86 and 1.55) and the cyclopropyl methylene protons H_2-19 (δ 0.73 and -0.13) showed long-range coupling to C-9/C-10 (δ 20.2). This observation helped connect spin system **124*a*** to **124*c*** through the quaternary carbons of the cyclopropyl group. Complete HMBC couplings can be seen in **Figure 2.5**.

Table 2.3. ^{1}H and ^{13}C NMR Spectroscopic Data (400 and 100 MHz, respectively) in $CDCl_3$ for cyclonataminol A (**124**).

		cyclonataminol A (**124**)	
Position	**δ_C**	**Multiplicity †**	**δ_H (*J* in Hz)**
1	39.7	CH_2	1.86, *d* (5.0), 1.55, *m*
2	66.2	CH	3.75, *m*
3	78.0	CH	2.09, *d* (10.3)
4	43.7	C	-
5	49.1	CH	1.92, *m*
6	126.3	CH	5.56, *d* (10.5)
7	129.3	CH	5.44, *m*
8	43.5	CH	2.53, *m*
9	20.2	C	-
10	20.2	C	-
11	25.0	CH_2	1.83, *m*, 1.42, *dd* (3.52,
12	31.9	CH_2	1.65, *m*, 1.30, *m*
13	45.4	C	-
14	49.9	C	-
15	41.7	CH_2	1.98, *m*, 1.24, *m*
16	79.3	CH	4.09, *m*
17	56.9	CH	1.80, *m*
18	19.3	CH_3	0.88, *s*
19	18.8	CH_2	0.73, *d* (3.4), -0.13, *d* (4.1)
20	62.8	CH	2.63, *m*
21	10.3	CH_3	0.86, *d* (6.6)
30	27.3	CH_3	1.07, *s*
31	15.6	CH_3	0.89, *s*
32	18.6	CH_3	0.94, *s*
$N_a(CH_3)_2$	43.5	CH_3	2.23
$N_b(CH_3)_2$	43.5	CH_3	2.54

†Multiplicity as determined by DEPT spectra.

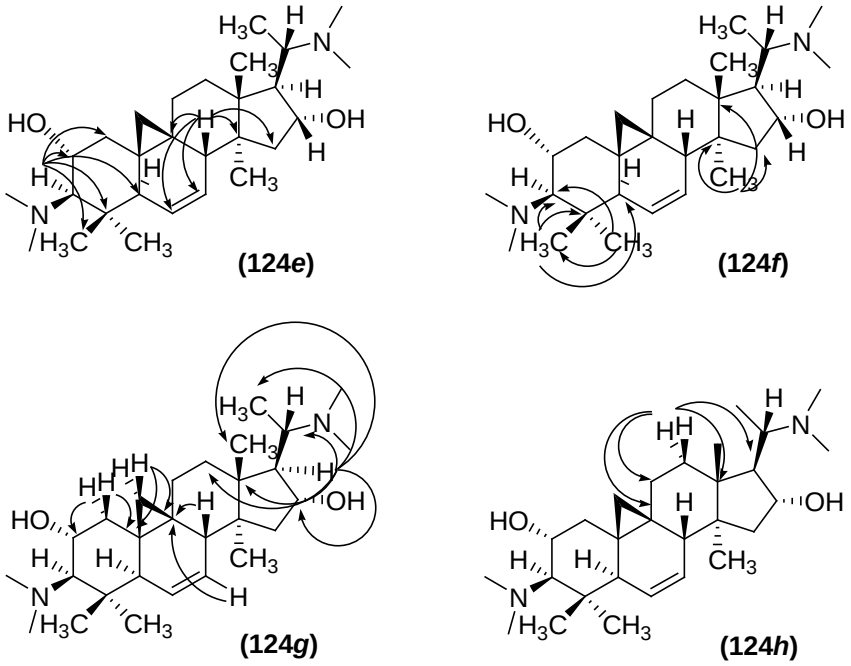

Figure 2.5. Spin systems of cyclonataminol A (**124**) connected through HMBC correlations.

The NOESY spectrum exhibited the same stereochemistry at chiral centers C-3, C-5, C-8, C-13, C-14, C-16, C-17, and C-20 as those determined in compound **123**. It has been documented from studies on cycloartenol that show the β stereochemistry of the cyclopropyl methylene (C-19)[22,23,29]. Based on these spectroscopic data, structure **124** was proposed for this new natural product characterized as cyclonataminol-A.

2.2.4 31-Demethylbuxaminol A (125)

31-Demethylbuxaminol A (**125**) was isolated as a white amorphous powder. The UV spectrum of **125** showed absorption maxima at 238, and 245, with a shoulder peak at

254 nm indicating the presence of a 9(10→19) *abeo*-diene system[30]. The IR spectrum displayed intense absorption bands at 3301 (OH), 2933 (CH), 1452 (C=C) cm^{-1}. The HREIMS of **125** showed a molecular ion peak at *m/s* 414.36135 $[M]^+$ corresponding to a molecular formula of $C_{27}H_{46}N_2O$ (calcd. 414.36102). The base peak at *m*/*z* 72.08132 was due to the loss of a *N*,*N*-dimethylethylamine group resulting from the cleavage of the C-17/C-20 bond. The EIMS showed a molecular ion at *m/z* 414 $[M]^+$, together with NMR stectral data corresponded to the molecular formula $C_{27}H_{46}N_2O$, indicating six degrees of unsaturation in compound **125**. The EIMS showed an ion at *m*/*z* 399 was due to the loss of a methyl group from the molecular ion.

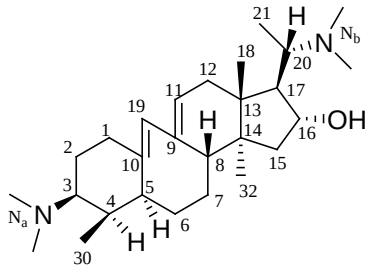

(125)

The ^{1}H-NMR spectrum ($CDCl_3$, 400MHz) of compound **125** showed the resonance of two singlets, integrating for one proton each, at δ 5.52 and 5.87 due to the C-11 and C-19 protons, respectively. A combination of UV spectrum and these signals in the ^{1}H-NMR spectrum confirmed the presence of a 9(10→19) *abeo*-diene system in compound **125**. Two three-proton singlets at δ 0.91 and 0.66 were due to the C-18 and C-32 methyl protons, respectively. Two three-proton doublets at δ 0.92 (*J* = 6.4 Hz) and δ 1.05 (*J* = 5.6 Hz) were assigned to C-21 and C-30 methyl protons, respectively. A multiplet integrating for one proton at δ 4.43 was due to the C-16 methine, while an

upfield multiplet at δ 3.00 was ascribed to H-20. Two singlets, integrating for six protons each, at δ 2.24 and 2.27 were due to the N_a and N_b dimethyl protons, respectively.

The broad-band ^{13}C-NMR spectrum ($CDCl_3$, 100 MHz) together with the DEPT spectra revealed the presence of eight methyl, six methylene, nine methine and four quaternary carbons in compound **125**. Complete ^{1}H and ^{13}C chemical shift assignments and ^{1}H/^{13}C one-bond shift correlations of all protonated carbons as determined from the HSQC spectrum are presented in **Table 2.4** for compound **125**.

The COSY-45° spectrum of **125** displayed the presence of three spin systems **125*a-c*** as seen in **Figure 2.6**. Spin system **125*a***, the largest of the three spin systems, was elucidated with the help of both COSY and TOCSY spectra. H_2-1 (δ 2.07) displayed COSY interactions with H_2-2 (δ 1.24 and 1.85). The H-3 (δ 2.19) proton showed cross peaks with H_2-2 (δ 1.24 and 1.85) and H-4 (δ 1.24). H-4 showed COSY interactions with H_3-30 (δ 1.05) methyl protons and H-5 (δ 1.79) methine proton. The H_2-6 methylene protons (δ 2.40 and 1.23) showed cross peaks with H-5 and H_2-7 (δ 1.25 and 1.62). The latter in turn showed cross peaks with H-8 (δ 2.19). These interactions were also visible in the TOCSY spectrum. The DEPT spectra indicated that C-30 (δ 16.1) was a methyl carbon,; C-1 (δ 40.1), C-2 (δ 23.1), C-6 (δ 34.8), C-7 (δ 26.0) were methylene carbons,; and C-3 (δ 68.3), C-4 (δ 42.9), C-5 (δ 48.4), and C-8 (δ 49.8) were methine carbons. The HSQC showed direct correlations of H_2-1 (δ 2.07), H_2-2 (δ 1.85 and 1.24), H-3 (δ 2.19), H-4 (δ 1.24), H-5 (δ 1.79), H_2-6 (δ 1.23 and 2.40), H_2-7 (δ 1.25 and 1.62), H-8 (δ 2.19), and H_3-30 (δ 1.05) with C-1 (δ 40.1), C-2 (δ 23.1), C-3 (δ 68.3), C-4 (δ 42.9), C-5 (δ 48.4), C-6 (δ 34.8), C-7 (δ 26.0), C-8 (δ 49.8), and C-30 (δ 16.1), respectively. The

second spin system **125*b*** consisted of H-11 (δ 5.52) showing COSY interactions with H_2-12 methylene protons (δ 1.95 and 2.05). Allylic coupling between the H-8 methine proton (δ 2.19) and H-11 (δ 5.52) was also observed in the COSY spectrum. H-19 (δ 5.87) also showed these cross peaks with H_2-1 (δ 2.07) and H-5 (δ 1.79). The DEPT spectra confirmed C-12 (δ 39.1) was a methylene carbon and C-11 (δ 129.5) and C-19 (δ 127.7) were methine carbons. The HSQC showed direct correlations of H-11 (δ 5.52), H_2-12 (δ 1.95 and 2.05), and H-19 (δ 5.87) with C-11 (δ 129.5), C-12 (δ 39.1), and C-19 (δ 127.7), respectively. It was also seen that H-11 and H-19 methine protons of spin system **125*b*** showed TOCSY correlations with the protons of spin system **125*a***. The last spin system **125*c*** was easily elucidated as it was the same as **123*e***. The H-16 methine proton (δ 4.43) showed COSY interactions with H_2-15 (δ 1.51 and 2.03) and H-17 (δ 1.83), with H-20 (δ 3.00) showing cross peaks with H-17 (δ 1.83) and H_3-21 methyl protons (δ 0.92). The DEPT spectra displayed C-21 (δ 9.6) was a methyl, C-15 (δ 43.7) was methylene, and C-16 (δ 72.4), C-17 (δ 52.9), C-20 (δ 57.6) were methine carbons. The HSQC showed direct correlations of H_2-15 (δ 1.51 and 2.03), H-16 (δ 4.43), H-17 (δ 1.83), H-20 (δ 3.00), and H_3-21 (δ 0.92) with C-15 (δ 43.7), C-16 (δ 72.4), C-17 (δ 52.9), C-20 (δ 57.6), and C-21 (δ 9.6), respectively.

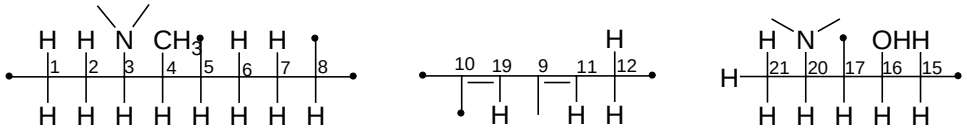

(125*a*) **(125*b*)** **(125*c*)**

Figure 2.6. Spin systems determined by COSY and TOCSY spectra for 31-demethylbuxaminol A (**125**).

Table 2.4. ^{1}H and ^{13}C NMR Spectroscopic Data (400 and 100 MHz, respectively) in $CDCl_3$ for 31-demethylbuxaminol A (**125**).

	31-demethylbuxaminol A (**125**)		
Position	**δ_C**	**Multiplicity †**	**δ_H (*J* in Hz)**
1	40.1, CH_2	CH_2	2.07, *m*
2	23.1, CH_2	CH_2	1.85, *m*, 1.24, *m*
3	68.3, CH	CH	2.19, *m*
4	42.9, CH	CH	1.24, *m*
5	48.4, CH	CH	1.79, *m*
6	34.8, CH_2	CH_2	2.40, *m*, 1.23, *m*
7	26.0, CH_2	CH_2	1.62, *m*, 1.25, *m*
8	49.8, CH	CH	2.19, *m*
9	138.5, C	C	-
10	138.5, C	C	-
11	129.5, CH	CH	5.52, *s*
12	39.1, CH_2	CH_2	2.05, *m*, 1.95, *m*
13	43.4, C	C	-
14	46.4, C	C	-
15	43.7, CH_2	CH_2	2.03, 1.51, *dd* (6.2,
16	72.4, CH	CH	4.43, *m*
17	52.9, CH	CH	1.83, *m*
18	17.5, CH_3	CH_3	0.91, *s*
19	127.7, CH	CH	5.87, *s*
20	57.6, CH	CH	3.00, *m*
21	9.6, CH_3	CH_3	0.92, *d* (5.6)
30	16.1, CH_3	CH_3	1.05, *d* (6.4)
31	-	-	-
32	17.8, CH_3	CH_3	0.66, *s*
$N_a(CH_3)_2$	40.3, CH_3	CH_3	2.27, *s*
$N_b(CH_3)_2$	40.3, CH_3	CH_3	2.24, *s*

†Multiplicity as determined by DEPT spectra.

The HMBC spectrum of **125** showed $^{1}H/^{13}C$ long-range coupling of H_2-15 (δ 2.01 and 1.49) with C-8 (δ 49.6), C-13 (δ 43.7), C-14 (δ 46.3), C-16 (δ 72.6), C-17 (δ 53.0) and C-32 (δ 0.64); which aided in connecting spin system **125*a*** with **125*c***. The HMBC spectrum displayed long-range coupling of H-17 (δ 1.81) with C-12 (δ 39.1), C-13

(δ 43.4), C-16 (δ 72.6), C-18 (δ 17.4), C-20 (δ 57.4) and C-21 (δ 9.5). These observations helped to connect spin system **125*b*** with **125*c***. H-5 (δ 1.93) exhibited $^{1}H/^{13}C$ long-range coupling with C-3 (δ 71.7), C-4 (δ 43.2), C-6 (δ 30.2), C-10 (δ 137.0), C-19 (δ 128.6) and C-30 (δ 15.3). H-8 (δ 2.19) showed long range coupling with C-9 (δ 138.5), C-11 (δ 129.5), C-19 (δ 127.7), and C-32 (δ 17.8). These observations along with the aforementioned COSY and TOCSY correlations between protons of spin system **125*b*** and **125*a*** helped connect these two spin systems. The position of C-13 (δ 43.4) was confirmed through the observed long range coupling of H-20 (δ 2.97) with C-13 (δ 43.7). The N_a methyl protons (δ 2.27) showed HMBC coupling with C-3 (δ 68.3) and N_b methyl protons (δ 2.24) showed HMBC coupling with C-20 (δ 57.6). These important $^{1}H/^{13}C$ HMBC long range couplings can be seen in **Figure 2.7**.

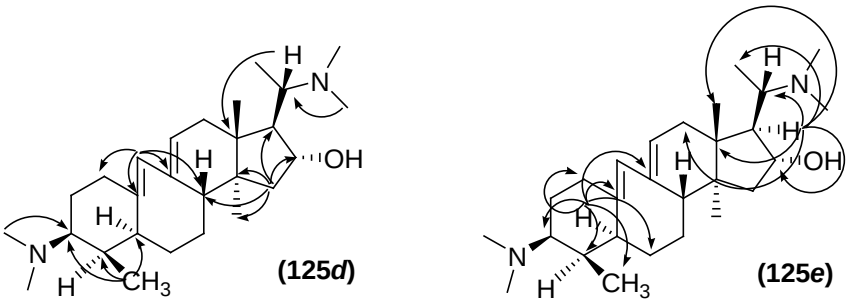

Figure 2.7. Spin systems of 31-demethylbuxaminol A (**125**) connected through HMBC correlations.

The relative stereochemistry at C-3, C-5, C-8, C-13, C-14, C-16, C-17, and C-20 was found to be the same as those of compound **123** as indicated by the NOESY spectrum. An NOE between H_3-18 with H_3-30 helped assign the C-30 methyl to be β-

oriented, thus indicating the H-4 was α-oriented. Based on these spectroscopic data, structure **125** was proposed for this new natural product, which was named nataminol-A.

2.2.5 Buxaminol A (126)

Buxaminol A (**126**) exhibited spectral data closely resembling that of 31-demethylbuxaminol A (**125**). Compound **126** displayed the same absorption maxima at 239, 246, and 254 nm in its UV spectrum characteristic for a 9(10→ 19) *abeo*-diene system. The IR spectrum displayed the same intense absorption bands at 3298 (OH), 2940 (CH) and 1453 (C=C) cm^{-1}. The HREIMS displayed an ion at *m/z* 413.34949 (calcd. for $C_{27}H_{25}N_2O$) which was due to the loss of a methyl group from the molecular ion. The base ion at *m/z* 72.08132 was due to the loss of a *N*,*N*-dimethyl group. The molecular ion was found at *m/z* 428.37668 [M^+], and together with NMR spectral data the molecular formula was determined to be $C_{28}H_{48}N_2O$, indicating six degrees of unsaturation.

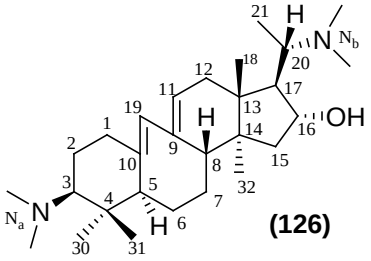

(126)

The ^{1}H-NMR spectrum ($CDCl_3$, 400MHz) of **126** was slightly different from compound **125** in that the appearance of a fifth methyl signal was observed. Four three-proton singlets resonated at δ 0.89, 0.99, 0.70 and 0.66 were due to the C-18, C-30, C-31

and C-32 methyl protons, respectively. One three-proton doublet was observed at δ 0.88 (J = 6.4 Hz) and was assigned to the C-20 methyl protons. Two singlets, integrating for one proton each, at δ 5.47 and 5.89 were ascribed to C-11 and C-19 respectively. A multiplet, integrating for one proton, at δ 4.22 was due to the C-16 methine proton, while an upfield multiplet at δ 2.97 was ascribed to the H-20. Two singlets, integrating for six protons each, at δ 2.23 and 2.26 were due to the N_a and N_b dimethyl protons, respectively.

The broad-band ^{13}C-NMR spectrum ($CDCl_3$, 100 MHz) together with the DEPT spectra revealed the presence of nine methyl, six methylene, nine methine and four quaternary carbons in the compound **126**. Complete ^{1}H and ^{13}C chemical shift assignments and ^{1}H/^{13}C one-bond shift correlations determined from the HSQC spectrum of compound **126** are presented in **Table 2.5**.

Unlike 31-demethylbuxaminol A (**125**), the COSY-45° spectrum of **126** displayed the presence of four spin systems, **126*a-d*** as shown in **Figure 2.8**. The first spin system comprised of C-1 to C-3 (**126*a***) and the second spin system consisted of C-5 to C-8 (**126*b***) coupled protons. Spin system **126*a***, displayed COSY interactions of the H_2-2 methylene protons (δ 1.48 and 1.70) with H_2-1 (δ 2.10 and 2.26) and H-3 (δ 2.08). DEPT spectra indicated C-1 (δ 41.5), and C-2 (δ 23.2) were methylene while C-3 (δ 71.7) was a methine carbon. The HSQC spectrum showed direct correlations of H_2-1 (δ 2.10 and 2.26), H_2-2 (δ 1.48 and 1.70), and H-3 (δ 2.08) with C-1 (δ 41.5), C-2 (δ 23.2), and C-3 (δ 71.7), respectively. The second spin system **126*b*** H-5 (δ 1.93) exhibited COSY cross-peaks with H_2-6 (δ 1.39 and 2.11), which in turn showed cross peaks with the H_2-7 (δ 1.52) methylene protons. H_2-7 showed cross peaks with H-8 (δ 2.13), thus connecting all

protons of spin system **126*b***. DEPT spectra indicated that C-6 (δ 30.2), C-7 (δ 25.8) were methylene and C-5 (δ 52.2), C-8 (δ 49.6) were methine carbons. The HSQC spectrum showed direct correlations of H-5 (δ 1.93), H_2-6 (δ 1.39 and 2.11), H_2-7 (δ 1.52), and H-8 (δ 2.13) with C-5 (δ 52.5), C-6 (δ 30.2), C-7 (δ 25.8), and C-8 (δ 49.6), respectively. The third spin system **126*c*** was based on H-11 (δ 5.47) and H_2-12 (δ 1.93 and 2.04) displaying COSY interactions between each other. H-19 (δ 5.89) also showed cross peaks with H-11, representing vinylic coupling between them. The DEPT spectra confirmed C-12 (δ 39.1) was methylene and C-11 (δ 128.5), C-19 (δ 128.6) were methine carbons. The HSQC spectrum showed direct correlations of H-11 (5.47), H_2-12 (δ 1.93 and 2.04) and H-19 (δ 5.89) with C-11 (δ 128.5), C-12 (δ 39.1), and C-19 (δ 128.6). The last spin system **126*d*** was easily elucidated as it was the same as **125*c***. The H-16 methine proton (δ 4.22) showed COSY interactions with H_2-15 (δ 1.49 and 2.01) and H-17 (δ 1.81), while H-20 (δ 2.97) displayed cross peaks with H-17 (δ 1.81) and H_3-21 methyl protons (δ 0.88). The DEPT spectra displayed C-21 (δ 9.5) was a methyl, C-15 (δ 43.5) was methylene, and C-16 (δ 72.6), C-17 (δ 53.0), C-20 (δ 57.4) were methine carbons. The HSQC showed direct correlations of H_2-15 (δ 1.49 and 2.01), H-16 (δ 4.22), H-17 (δ 1.81), H-20 (δ 2.97), and H_3-21 (δ 0.88) with C-15 (δ 43.4), C-16 (δ 72.6), C-17 (δ 53.0), C-20 (δ 57.4), and C-21 (δ 9.5), respectively.

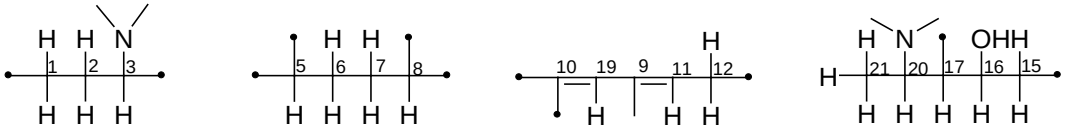

(126*a*) **(126*b*)** **(126*c*)** **(126*d*)**

Figure 2.8. Spin systems determined by COSY spectra for buxaminol A (**126**).

It was important to connect spin systems **126*a*** and **126*b*** as they were the only distinct difference from compound **125**. The HMBC spectrum of **126** showed $^{1}H/^{13}C$ long-range coupling of the H-5 methine proton (δ 1.93) with C-3 (δ 71.7), C-4 (δ 43.2), C-6 (δ 30.2), C-10 (δ 137.0), C-19 (δ 128.6) and C-31 (δ 15.3). The H_3-30 displayed HMBC cross-peaks with C-3 (δ 71.7), C-4 (δ 43.2), C-5 (δ 52.2) and C-31 (δ 15.3). Likewise the H_3-31 displayed HMBC cross-peaks with C-3 (δ 71.7), C-4 (δ 43.2), C-5 (δ 52.2) and C-30 (δ 25.1). These observations led to the connection of spin systems **126*a*** and **126*b***. Other HMBC interactions include exhibiting long-range coupling of H-19 (δ 5.89) with C-1 (δ 41.5), C-5 (δ 52.2), C-8 (δ 49.6), C-10 (137.0), C-11 (128.5). These observations helped connect C-19 of spin system **126*c*** with C-1 from **126*a*** and C-5 and C-8 from **126*b***. H-11 (δ 5.47) showed long range coupling with C-8 (δ 49.6), C-13 (δ 43.7), and C-19 (δ 128.6). H_2-12 also showed long range coupling with C-9 (δ 138.8) and C-11 (δ 128.5). These observations led to the confirmation C-8 of **126*b*** was connected to C-19 of **126*c*** through the quaternary C-9 (δ 138.8). The H_2-15 (δ 2.01 and 1.49) proton exhibited HMBC correlations with C-8 (δ 49.6), C-13 (δ 43.7), C-14 (δ 46.3), C-16 (δ 72.6), C-17 (δ 53.0) and C-32 (δ 17.7). The coupling between H_2-15 with C-8 help connect two spin system, **126*b*** with **126*d***. The HMBC spectrum showed other $^{1}H/^{13}C$ long- range couplings of H-17 (δ 1.81) with C-12 (δ 39.1), C-16 (δ 72.6), C-18 (δ 17.4), C-20 (δ 57.4) and C-21 (δ 9.5). These observations led to the connection of C-17 from spin system **126*d*** with C-12 of spin system **126*c***. The position of C-13 was confirmed through the observed long range coupling of H-20 (δ 2.97) with C-13 (δ 43.7). The N_a methyl protons (δ 2.26) showed HMBC coupling with C-3 (δ 71.7) and N_b methyl

protons (δ 2.23) showed HMBC coupling with C-20 (δ 57.4). These important $^{1}H/^{13}C$ HMBC long range couplings can be seen in **Figure 2.9**.

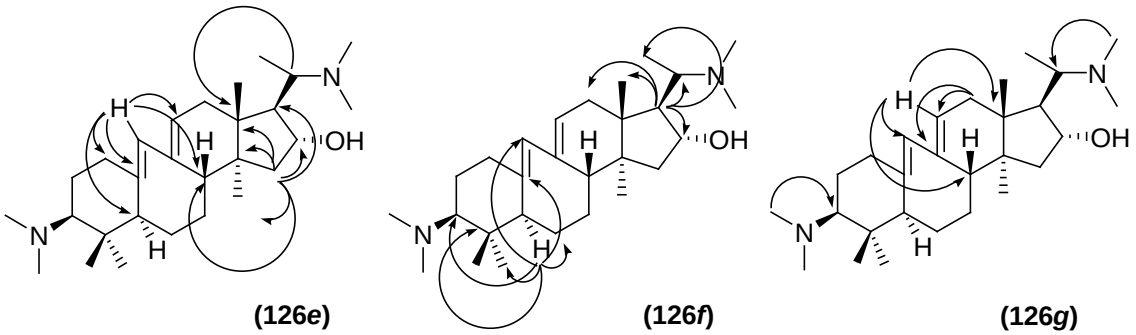

Figure 2.9. Spin systems of buxaminol A (**126**) connected through HMBC correlations.

NOESY and ROESY spectra were used to establish the relative configurations of chiral centers for **126**. H-3, H-5, H-17, H_3-30 and H_3-32 are in the α-orientation as they exhibited NOE with each other. While H-8, H-16, H_3-18, H_3-31 were placed in the β-orientation as they displayed coupling in the NOESY spectrum. Based on these spectroscopic data, structure **126** was proposed for this new natural product characterized as buxaminol A (**126**).

This is the first isolation of buxaminol A (**126**) as a natural product. Previously this compound was synthesized by performing *N*-methylation of buxaminol E, isolated from *B. sempervirens*[31].

Table 2.5. ^{1}H and ^{13}C NMR Spectroscopic Data (400 and 100 MHz, respectively) in $CDCl_3$ for buxaminol A (**126**).

	buxaminol A (**126**)		
Position	**δ_C**	**Multiplicity †**	**δ_H (*J* in Hz)**
1	41.5	CH_2	2.26, *m*, 2.10, *m*
2	23.2	CH_2	1.70, *m*, 1.48, *m*
3	71.7	CH	2.08, *m*
4	43.2	C	-
5	52.2	CH	1.93, *m*
6	30.2	CH_2	2.11, *m*, 1.39, *m*
7	25.8	CH_2	1.52, *m*
8	49.6	CH	2.13, *m*
9	138.8	C	-
10	137.0	C	-
11	128.5	CH	5.47, *s*
12	39.1	CH_2	2.04, *m*, 1.93, *m*
13	43.7	C	-
14	46.3	C	-
15	43.4	CH_2	2.01, *m*, 1.49, *m*
16	72.6	CH	4.22, *m*
17	53.0	CH	1.81, *m*
18	17.4	CH_3	0.89, *s*
19	128.6	CH	5.89, *s*
20	57.4	CH	2.97, *m*
21	9.5	CH_3	0.88, *d* (6.4)
30	25.1	CH_3	0.99, *s*
31	15.3	CH_3	0.70, *s*
32	17.7	CH_3	0.64, *s*
$N_a(CH_3)_2$	44.7	CH_3	2.26, *s*
$N_b(CH_3)_2$''	44.7	CH_3	2.23, *s*

†Multiplicity as determined by DEPT spectra.

2.2.6 Buxaminol C (127)

Buxaminol C's (**127**) spectral data was nearly identical to that of buxaminol A (**126**) and 31-demethylbuxaminol A (**125**). Its UV spectrum displayed the same chromophore, the 9(10→19) *abeo*-diene system, with absorption peaks at 238, 245, and a

shoulder peak at 254 nm. Its IR spectrum showed the same absorption bands at 3345 (OH), 2936 (CH) and 1454 (C=C) cm^{-1}. Its molecular ion was found by EIMS at *m/z* 414, to be the same as 31-demethylbuxaminol A (**125**). Together with NMR spectral data the molecular formula was determined to be $C_{27}H_{46}N_2O$, indicating six degrees of unsaturation. The ion at 399 was due to the loss of a methyl group from the molecular ion. The base peak at *m/z* 72 suggested the presence of a *N*,*N*-dimethyl group at C-20.

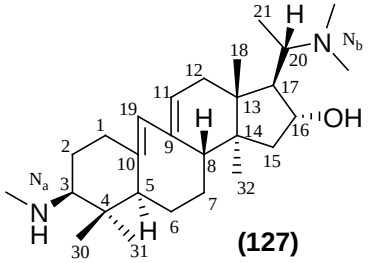

(127)

The ^{1}H-NMR spectrum ($CDCl_3$, 400MHz) of **127** was similar to **126** except for the integration of the *N*-methyl protons. One singlet integrating for three protons at δ 2.44, and another for six proton singlet at δ 2.26 were due to the N_a-methyl and N_b-dimethyl protons, respectively. The rest of the ^{1}H-NMR showed the same spectral features, which included the resonance of two singlets integrating for one proton each at δ 5.49 and 5.93 due to C-11 and C-19 olefinic protons, respectively. Four three-proton singlets were observed at δ 0.90, 1.01, 0.69 and 0.66 due to the C-18, C-30, C-31 and C-32 methyl protons, respectively. A three-proton doublet was observed at δ 0.90 (J = 6.3 Hz) that was assigned to the C-21 methyl protons. A multiplet integrating for one proton at δ 4.41 was assigned to H-16. An upfield multiplet at δ 2.99 was ascribed to the H-20.

The broad-band ^{13}C-NMR spectrum ($CDCl_3$, 100 MHz) together with the DEPT spectra revealed the presence of eight methyl, six methylene, eight methine and five

quaternary carbons in the compound **127**. Complete ^{1}H and ^{13}C chemical shift assignments and $^{1}H/^{13}C$ HSQC correlations of compound **127** are presented in **Table 2.6**.

The COSY-45° spectrum of buxaminol C (**127**) revealed the same four spin systems, **127*a-d***, as in buxaminol A (**127**), as shown in **Figure 2.10**. The first spin system, **127*a***, displayed COSY coupling of the H_2-2 methylene protons (δ 1.28 and 1.56) with H_2-1 (δ 2.14 and 2.19) and H-3 (δ 2.07). DEPT spectra exhibited C-1 (δ 40.6), C-2 (δ 25.8) were methylene and C-3 (δ 68.6) methine carbons. The HSQC spectrum showed direct correlations of H_2-1 (δ 2.14 and 2.19), H_2-2 (δ 1.28 and 1.56), and H-3 (δ 2.07) with C-1 (δ 40.6), C-2 (δ 25.8), and C-3 (δ 68.6), respectively. The second spin system **127*b*** revealed H-5 (δ 1.99) showed COSY cross-peaks with H_2-6 (δ 1.41 and 2.18), which in turn showed cross peaks with the H_2-7 (δ 1.28 and 1.56) methylene protons. The latter (H-7) showed cross-peaks with H-8 (δ 2.14), thus connecting all protons of spin system **127*b***. DEPT spectra indicated C-6 (δ 30.3), C-7 (δ 25.8) were methylene and C-5 (δ 51.6), C-8 (δ 49.7) were methine carbons. The HSQC spectrum showed direct correlations of H-5 (δ 1.99), H_2-6 (δ 1.41 and 2.18), H_2-7 (δ 1.28 and 1.56), and H-8 (δ 2.14) with C-5 (δ 51.6), C-6 (δ 30.3), C-7 (δ 25.8), and C-8 (δ 49.7), respectively. The third spin system **127*c*** consisted of H-11 (δ 5.49) exhibting COSY interactions with H_2-12 methylene protons (δ 1.93 and 2.07), which also showed cross-peaks with H-8 (δ 2.14). H-19 (δ 5.93) exhibited olefinic coupling with H_2-1 (δ 2.14 and 2.19) and H-5 (δ 1.99). The DEPT spectra confirmed C-12 (δ 39.1) was methylene and C-11 (δ 128.8), C-19 (δ 129.2) were methine carbons. The HSQC spectrum showed direct correlations of H-11 (5.49), H_2-12 (δ 1.93 and 2.07) and H-19 (δ 5.93) with C-11 (δ 128.8), C-12 (δ 39.1), and C-19 (δ 129.2). The last spin system **127*d*** was easily elucidated as it was the same as

126*d*. The H-16 methine proton (δ 4.41) showed COSY interactions with H_2-15 (δ 1.50 and 2.02) and H-17 (δ 1.83), with H-20 (δ 2.99) exhibiting COSY coupling with H-17 (δ 1.83) and H_3-21 methyl protons (δ 0.90). The DEPT spectra displayed C-21 (δ 9.6) was a methyl, C-15 (δ 43.8) was methylene, and C-16 (δ 72.5), C-17 (δ 53.1), C-20 (δ 57.5) were methine carbons. The HSQC showed direct correlations of H_2-15 (δ 1.50 and 2.02), H-16 (δ 4.41), H-17 (δ 1.83), H-20 (δ 2.99), and H_3-21 (δ 0.90) with C-15 (δ 43.8), C-16 (δ 72.5), C-17 (δ 53.1), C-20 (δ 57.5), and C-21 (δ 9.6), respectively.

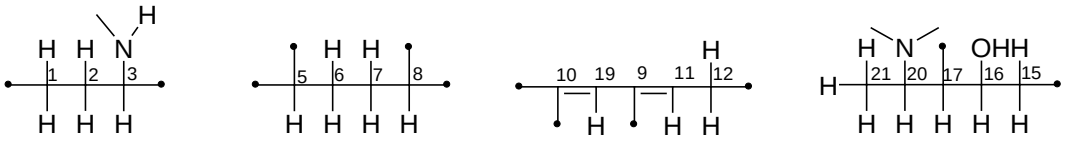

(127*a*) **(127*b*)** **(127*c*)** **(127*d*)**

Figure 2.10. Spin systems determined by COSY spectrum for buxaminol C (**127**).

The HMBC spectrum of **127** depicted the same $^1H/^{13}C$ long-range couplings as buxaminol A (**126**). The important HMBC couplings show the position of the *N*-methyl groups. The N_a-methyl protons (δ 2.44) showed long-range coupling with the C-3 methine carbon (δ 68.6). The N_b-dimethyl protons (δ 2.26) showed HMBC cross-peaks with C-20 (δ 57.5). Together with the mass spectral data, these observations helped confirm the N_a-methyl is geminal to C-3, while the N_b-dimethyl group is geminal to C-20. The HMBC correlation of the H-18 (δ 0.90) with C-12 (δ 39.1), C-13 (δ 43.3), C-14 (δ 46.4), and C-17 (δ 53.1) aided in connecting C-12 of spin system **127*c*** with C-17 of spin system **127*d***. The HMBC spectrum also showed the $^1H/^{13}C$ long- range couplings of H_3-32 (δ 0.66) with C-8 (δ 49.7), C-14 (δ 46.4), and C-15 (δ 43.8). These observations

helped connect C-15 from spin system **127*d*** with C-8 of spin system **127*b***. Other HMBC interactions include the H-19 methine proton (δ 5.93) exhibiting long-range coupling with C-1 (δ 40.6), C-5 (δ 51.6), and C-8 (δ 49.7). This observation helped connect spin system **127*c*** with **127*b***, as well as **127*c*** with **127*a***. The H_3-30 (δ 0.69) and H_3-31 (δ 1.01) methyl protons both showed long range coupling with C-3 (δ 68.6), C-4 (δ 41.4), and C-5 (δ 51.6). These observations helped connect spin system **127*a*** with **127*b***. These important $^{1}H/^{13}C$ HMBC long range couplings are illustrated in **Figure 2.11**.

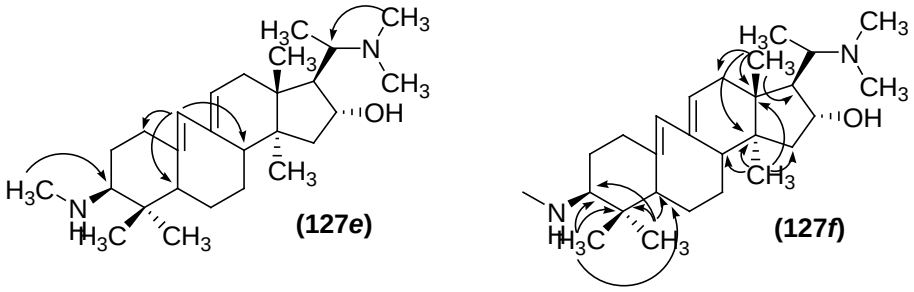

Figure 2.11. Spin systems of buxaminol C (**127**) connected through HMBC correlations.

The NOESY spectrum was used to establish the relative configurations of chiral centers for **127**. H-3, H-5, H-17, H_3-30 and H_3-32 were in the α-orientation as they exhibited NOE with each other. While H-8, H-16, H_3-18, H_3-31 were placed in the β-orientation as they displayed coupling in the NOESY spectrum. These spectral data led us to identify compound **127** as buxaminol C. The ^{1}H, ^{13}C, and MS spectral data of **127** matched the data reported in literature for buxaminol C. Previously this compound was isolated from *B. sempervirens*[19].

Table 2.6. ^{1}H and ^{13}C NMR Spectroscopic Data (400 and 100 MHz, respectively) in $CDCl_3$ for buxaminol C (**127**).

		buxaminol C (**127**)	
Position	**δ_C**	**Multiplicity †**	**δ_H (*J* in Hz)**
1	40.6	CH_2	2.14, *m*, 2.19, *m*
2	25.8	CH_2	1.28, *m*, 1.56, *m*
3	68.6	CH	2.07, *m*
4	41.4	C	-
5	51.6	CH	1.99, *m*
6	30.3	CH_2	1.41, *m*, 2.18, *m*
7	25.8	CH_2	1.28, *m*, 1.56, *m*
8	49.7	CH	2.14, *m*
9	138.6	C	-
10	138.6	C	-
11	128.8	CH	5.49, *s*
12	39.1	CH_2	1.93, *m*, 2.07, *m*
13	43.3	C	-
14	46.4	C	-
15	43.8	CH_2	1.50, *m*, 2.02, *m*
16	72.5	CH	4.41, *m*
17	53.1	CH	1.83, *m*
18	17.5	CH_3	0.90, *s*
19	129.2	CH	5.93, *s*
20	57.5	CH	2.99, *m*
21	9.6	CH_3	0.90, *d* (6.3)
30	14.9	CH_3	0.69, *s*
31	25.0	CH_3	1.01, *s*
32	17.8	CH_3	0.66, *s*
N_aCH_3	35.8	CH_3	2.44, *s*
$N_b(CH_3)_2$	39.1	CH_3	2.26, *s*

†Multiplicity as determined by DEPT spectra.

2.2.7 *p*-Coumaroylputrescine (128)

A yellow colored gum was isolated by preparative TLC and determined to be *p*-coumaroylputrescine (**128**). Its UV spectrum showed absorption peaks at 309, 294 and 224 nm indicating the presence of amide carbonyl and aromatic chromaphores in the

molecule. The IR spectrum displayed intense absorption bands at 3286 (OH), 1655 (amide carbonyl), 1608, 1514, and 1437 (aromatic) cm^{-1}. The EIMS indicated the molecular ion was at *m/z* 234 [M^+], and together with NMR spectral data, the molecular formula of **128** was determined to be $C_{13}H_{18}N_2O_2$. An ion at *m/z* 119 was due to a styrene moiety, while another ion *m/z* 147 was due to a loss of the putrescine group.

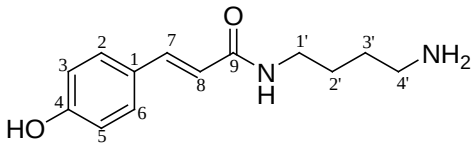

(128)

The ^{1}H-NMR spectrum (DMSO-d_6, 400MHz) of compound **128** showed the presence of AB doublets at δ 6.80 (*J* = 8.6 Hz) and 7.37 (*J* = 8.6 Hz) due to the C-3 and C-2 methine protons, respectively. Another set of AB doublets at δ 6.43 (*J* = 15.8 Hz) and 7.31 (*J* = 15.7 Hz) were due to C-8 and C-7 respectively. The large coupling constant indicated H-7 and H-8 are *trans* to one another. Four two-proton multiplets were observed at δ 1.49, 1.57, 2.78 and 3.17 assigned to the C-2', C-3', C-4' and C-1' methylene protons, respectively. The one-proton signal at δ 8.15, was assigned to the N*H* proton. The COSY-45° spectrum revealed coupling of H-2 (δ 7.37) with H-3 (δ 6.80) and H-7 (δ 7.31) with H-8 (δ 6.43). The H_2-1' (δ 3.17) exhibited COSY correlations with *N*H and H_2-2' (δ 1.49). The H_2-2' (δ 1.49) methylene protons showed cross-peaks with H_2-3' (δ 1.57), which in turn showed coupling with H_2-4' (δ 2.78). The TOCSY spectrum confirmed the connectivity of hydrogens H_2-1' to H_2-4'. The ^{13}C NMR (DMSO-d_6, 100 MHz) spectrum confirmed the presence of all 13 carbon atoms present in the molecule.

HSQC spectrum determined all $^{1}H/^{13}C$ one-bond correlations with complete ^{1}H and ^{13}C NMR chemical shift assignments presented in **Table 2.7**.

Table 2.7. ^{1}H and ^{13}C NMR Spectroscopic Data (400 and 100 MHz, respectively) in DMSO-d_6 for *p*-coumaroylputrescine (**128**).

	p-coumaroylputrescine (**128**)		
Position	**δ_C**	**Multiplicity †**	**δ_H (*J* in Hz)**
1	126.3	C	-
2	129.3	CH	7.37, *d* (8.6)
3	116.2	CH	6.80, *d* (8.6)
4	159.3	C	-
5	116.2	CH	6.80, *d* (8.6)
6	129.3	CH	7.37, *d* (8.6)
7	139.0	CH	7.31, *d* (15.7)
8	119.1	CH	6.43, *d* (15.8)
9	165.9	C	-
1’	38.4	CH_2	3.17, *m*
2’	25.0	CH_2	1.49, *m*
3’	26.7	CH_2	1.57, *m*
4’	38.9	CH_2	2.78, *m*
N*H*	-		8.15, *m*

†Multiplicity as determined by DEPT spectra.

The HMBC spectrum of **128** showed $^{1}H/^{13}C$ long-range couplings of H-2 (δ 7.37) with C-3 (δ 116.2), C-4 (δ 159.3), C-6 (δ 129.6) and C-7 (δ 139.0), whereas H-3 did not show coupling with C-7. This observation led to H-2 placed *ortho* to the H-7. H_2-1’ (δ 3.17) showed HMBC long-range coupling with C-9 (δ 165.9). Both H-7 (δ 7.31) and H-8 (δ 6.43) showed coupling to C-9. This observation helped to connect the purescine fragment with the coumaroyl moiety through an amide group as seen in **Figure 2.12**.

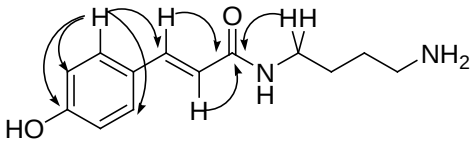

(128)

Figure 2.12. Spin systems of *p*-coumaroylputrescine (**128**) connected through HMBC correlations.

This compound was isolated for the first time from *B. natalensis*, and confirmed to be *p*-coumaroylputrescine (**128**), a known compound, which was similar to sinapic acid methyl ester isolated from *B. papilosa*[32]. *p*-coumaroylputrescine has been isolated from plants such as *Nicotiana tabacum*[33], and found in potato plants[34].

2.2.8 Methyl syringate (129)

Compound **129** was isolated as light yellow solid. Its UV spectrum showed absorption peaks at 218, and 275 nm indicating the presence of ester carbonyl and benzene chromaphores. The IR spectrum displayed intense absorption bands at 3401 (OH), 1714 (ester carbonyl), 1608, 1512 and 1450 (aromatic) cm^{-1}. The EIMS showed a molecular ion peak at *m/z* 212, and together with NMR spectral data suggested its molecular formula was $C_{10}H_{12}O_4$. The EIMS also showed fragments at *m/z* 197 indicating the loss of a methyl group and at *m/z* 181 representing the loss of a methoxy group.

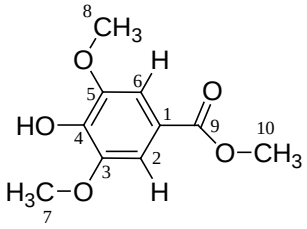

(129)

The ^{1}H-NMR spectrum ($CDCl_3$, 400MHz) of **129** displayed one two-proton singlet at δ 7.28 due to the C-2/C-6 methine protons. A three-proton singlet at δ 3.86 was assigned to the H_3-10 methoxy protons. A six-proton singlet resonated at δ 3.90, and was assigned to the H_3-7 and H_3-8 methoxy protons on the benzene ring. The ^{13}C NMR spectrum ($CDCl_3$, 100 MHz) of compound **129** showed seven carbon signals due to the symmetry in the molecule. DEPT spectra confirmed one methine, two methyl, and four quaternary carbons. HMBC spectrum showed ^{1}H/^{13}C long-range coupling of H_3-10 (δ 3.86) with C-9 (δ 166.9), whereas H_3-7/H_3-8 (δ 3.90) showed coupling to C-3/C-5 (δ 139.1). The H-2/H-6 (δ 7.28) protons showed HMBC couplings to all aromatic carbon atoms on the benzene ring in addition to C-9 (δ 166.9), thus indicating the H-2/H-6 protons are *ortho* to the ester carbonyl carbon as depicted in **Figure 2.13**. The HSQC spectrum was used in the determination of ^{1}H/^{13}C direct one-bond correlations. These correlations in addition to all ^{1}H and ^{13}C NMR chemical shift assignments for methyl syringate (**129**) can be found in **Table 2.8**.

All ^{1}H and ^{13}C chemical values corresponded to previously synthesized and isolated methyl syringate (**129**)[35]. Compound **129** has been isolated from *B. sempervirens*[36], *Tagetes minuta*[37], and from Manuka (*Leptosperunum scoparium*) honey[38]. Methyl syringate (**129**) was also found to possess anti-bacterial properties[39].

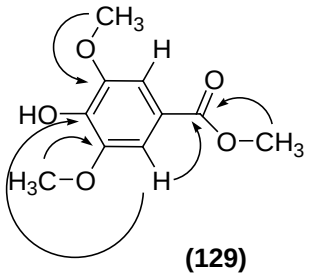

(129)

Figure 2.13. Important HMBC couplings of methyl syringate (**129**).

Table 2.8. ^{1}H and ^{13}C NMR Spectroscopic Data (400 and 100 MHz, respectively) in $CDCl_3$ for methyl syringate (**129**).

	methyl syringate (**129**)		
Position	**δ_C**	**Multiplicity †**	**δ_H (*J* in Hz)**
1	121.0	C	-
2	106.6	CH	7.28, *s*
3	139.1	C	-
4	146.6	C	-
5	139.1	C	-
6	106.6	CH	7.28, *s*
7	56.4	CH_3	3.90, *s*
8	56.4	CH_3	3.90, *s*
9	166.9	C	-
10	52.1	CH_3	3.86, *s*

†Multiplicity as determined by DEPT spectra.

2.2.9 Cholinesterase and Antimicrobial Activities of 123-129.

Compounds **123-129** were evaluated for AChE Inhibitory activity and all of the isolates were active to different levels. Compound **123** was significantly active in this assay with an IC_{50} value of 8.5 µM compared to the rest of the isolates. The higher potency of **123** compared to compounds **124-127** might be due to the presence of a

tetrahydrofuran ring. In BChE Inhibition assays, all of the isolates were moderately active suggesting the compounds **123-129** are selective towards AChE Inhibition over BChE.

Table 2.9. Results of AChE and BChE Inhibition assays for compounds isolated from *B. natalensis* (**123-129**). Activities reported as IC_{50} (µM) ± SD.

Compound	AChE IC_{50} (µM)	BChE IC_{50} (µM)
123	8.5 ± 1.5	74.74 ± 3.243
124	22.9 ± 2.2	56.42 ± 13.082
125	25.8 ± 1.8	131.61 ± 7.284
126	29.8 ± 4.4	103.09 ± 6.224
127	40.8 ± 4.0	90.13 ± 7.840
128	NA	NT
129	NA	NT
Galanthamine	0.9 ± 0.2	9.2 ± 1.6
Huperzine	2.0 ± 0.5	NT

Anti-bacterial and anti-fungal properties of the isolated compounds were performed by Kirby Bauer Disk Diffusion method and MIC method using microtiter plates (as described in Section 2.3.4 and 2.3.5). It was found none of the isolated compounds were active in the antimicrobial assay except buxaminol C (**127**), which was very weakly active at 0.2 µg/ml against *C. albicans*.

2.3 EXPERIMENTAL

2.3.1 General

The UV spectra were recorded in methanol on a *Shimadzu UV-2501 PC* spectrophotometer. IR spectra were acquired on *Varian 1000 FT-IR* (Scimitar Series) with the use of salt plates. Optical rotation data were measured on an Autopal IV Automatic polarimeter. The 1D-NMR (^{1}H, ^{13}C, DEPT) and 2D-NMR (COSY-45°, HSQC, HMBC, NOESY, ROESY, TOCSY) spectra were acquired using a *Bruker Avance-3 400MHz* spectrometer; chemical shifts are in (δ) ppm and coupling constants (*J*) are in Hz. EIMS were measured on *Hewlett-Packard 5989B MS*. Column chromatography was carried out on 60Å silica gel (230-400mesh). Thin-layer chromatography was performed on *EMD* silica gel $60F_{254}$ pre-coated plates. Bioassays were carried out using *Synergu HT multidetection BioTek* microplate reader. Acetylcholinesterase (from electric eel), butyrylcholinesterase (from equine serum), and acetylcholine were purchased from *Sigma-Aldrich*. Butyrylthiocholine iodide was purchased from *Fluka Analytical*. 5,5'-Dithio-*bis*-(2-nitrobenzoic Acid) (DTNB) was purchased from *Calbiochem*.

2.3.2 Plant Material

Buxus natalensis was collected from uMhalanga Rocks nature reserve, Durban, South Africa on 14/02/07 in collaboration by Robert Gengan, Department of Chemistry, Durban University, South Africa. The plant was identified by Mkhipheni A Ngwenya, Scientific Officer, South Africa National Biodiversity Institute, South Africa. A voucher

specimen (132176) was deposited in the South Africa National Biodiversity Institute, Durban, South Africa.

2.3.3 Extraction and Isolation of compound (123-129).

Root bark (1.754 kg) of *Buxus natalensis* was dried and ground into a powder. The powder was extracted by Abin James, and was subjected to solvent/solvent partitioning by Zahid[40]. The acetylcholinesterase inhibition assay conducted on different fractions of the extract was also performed by Zahid.[40]

The methanolic extracted (pH 9.5) was loaded onto a silica gel column (230-400 mesh, Merk) and was eluted with hexane-chloroform (0-100%) and chloroform-methanol (0-100%). This yielded several fractions and were pooled on the bases of analytical TLC results. Column chromatography (0-100% $CHCl_3$-MeOH) was again performed on a fraction obtained at 20%MeOH-80%$CHCl_3$ (FMC20) to yield several fractions which were pooled based on similar R_f values. A fraction obtained at 20% methanol in chloroform (FMC20-39) showed the presence of one major compound, which was separated by preparative TLC using MeOH-$CHCl_3$-acetic acid (15:85:0.1) as a mobile phase to afford *p*-coumaroylputrescine (**128**) (FMC-20-39-e, 20mg, R_f = 0.18). Another fraction obtained on elution of the silica gel column with MeOH-$CHCl_3$ was subjected to preparative TLC using hexane-Et_2O-diethylamine (90:5:5) to afford cyclonataminol-A (**124**) (16mg, R_f = 0.28).

The chloroform extract at pH 7.0 was also subjected to column chromatography in order to determine the source of its bioactivity. The extract was loaded over a silica gel column and eluted with hexane-$CHCl_3$ (0-100%) and $CHCl_3$-MeOH (0-100%). The fraction collected at 100% chloroform showed the presence of one major compound on the bases of analytical TLC. This major compound was purified using acetone-hexane-diethylamine (25:75:0.1) to yield methy syringate (**129**) **(**BNMe7-XM-6B, 40mg, R_f = 0.16).

Several fractions collected at low polarities of hexane-$CHCl_3$ showed promise for further purification. One fraction (BNMe-7HJ-8-14) contained two compounds which were separated by preparative TLC using hexane-Et_2O-diethylamine (95:5:5) to give buxaminol A (**126**) (BNMe7-HJ-8-14A, 14mg) and 31-demethylbuxaminol A (**125**) (BNMe7-HJ-8-14B, 8mg) with R_f values of 0.27 and 0.22, respectively. Buxaminol C (**127**) (BNMe7-HJ-27-D, 2.3mg, R_f = 0.16) was isolated from preparative TLC of another fraction (BNMe7-HJ-27) using hexane-Et_2O-diethylamine (75:25:5). A fraction (BNMe-7HJ-15-26) obtained from the primary column was further subjected to column chromatography and was eluted with hexane-Et_2O (0-100%) and Et_2O-MeOH (0-35%). A fraction obtained at 85%Et_2O-15%MeOH contained one major compound which was purified using preparative TLC to yield O^{10}-natafuranaminol (**123**) (2.7mg, R_f = 0.33). A solvent mixture of acetone-hexane-diethylamine (80:20:5) was used as the developing solvent for this TLC.

O^{10}-Natafuranamine (**123**)**:** yellow amorphous powder (2.7 mg); $[\alpha]^{25}$ = +21 (*c* = 0.048, $CHCl_3$), UV (MeOH) λ_{max} 221 nm; IR ($CHCl_3$) 3356, 2925, 1730, 1650, 1528 and 1459

cm^{-1}; ^{1}H NMR ($CDCl_3$, 400 MHz) Refer to Table 2.2; ^{13}C NMR ($CDCl_3$, 100 MHz) Refer to Table 2.2; EIMS *m/s* 534 $[M]^+$, 519, 517, 105, 72; HRESMS *m/s* 535.3523 $[M+H]^+$ (calcd for $C_{33}H_{47}N_2O_4$, 535.353).

Cyclonataminol-A (**124**): yellow amorphous powder (16 mg); $[\alpha]^{25}$ = -70 (*c* = 0.05, $CHCl_3$), UV (MeOH) λ_{max} 282, 247 nm; IR ($CHCl_3$) 3434 and 2935 cm^{-1}; 1H NMR ($CDCl_3$, 400 MHz) Refer to Table 2.3; 13C NMR ($CDCl_3$, 100 MHz) Refer to Table 2.3; EIMS *m/s* 444 $[M]^+$, 429, 72; HREIMS *m/s* 444.3708 $[M]^+$ (calcd for $C_{28}H_{48}N_2O_2$, 444.3716).

31-Demethylbuxaminol A (**125**): white amorphous powder (8 mg); $[\alpha]^{25}$ = +9.4 (*c* = 0.05, $CHCl_3$), UV (MeOH) λ_{max} 254, 245 and 238 nm; IR ($CHCl_3$) 3301, 2933 and 1452 cm^{-1}; 1H NMR ($CDCl_3$, 400 MHz) Refer to Table 2.4; 13C NMR ($CDCl_3$, 100 MHz) Refer to Table 2.4; EIMS *m/s* 414 $[M]^+$, 399, 369, 352, 72; HREIMS *m/s* 414.36135 $[M]^+$ (calcd for $C_{27}H_{46}N_2O$, 414.36102).

Buxaminol A (**126**): white amorphous powder (14 mg); UV (MeOH) λ_{max} 254, 246 and 239 nm; IR ($CHCl_3$) 3298, 2940 and 1453 cm^{-1}; 1H NMR ($CDCl_3$, 400 MHz) Refer to Table 2.5; 13C NMR ($CDCl_3$, 100 MHz) Refer to Table 2.5; EIMS *m/s* 428 $[M]^+$, 413, 383, 366, 72.

Buxaminol C (**127**): white amorphous powder (2.3 mg); UV (MeOH) λ_{max} 254, 245 and 238 nm; IR ($CHCl_3$) 3345, 2936 and 1454 cm^{-1}; 1H NMR ($CDCl_3$, 400 MHz) Refer to Table 2.6; 13C NMR ($CDCl_3$, 100 MHz) Refer to Table 2.6; EIMS *m/s* 414 $[M]^+$, 399, 369, 72.

p-Coumaroylputrescine (**128**): yellow colored gum (20 mg); UV (MeOH) λ_{max} 309, 294 and 224 nm; IR ($CHCl_3$) 3286, 1655, 1608, 1514, and 1437 cm^{-1}; 1H NMR ($CDCl_3$, 400 MHz) Refer to Table 2.7; 13C NMR ($CDCl_3$, 100 MHz) Refer to Table 2.7; EIMS *m/s* 234 $[M]^+$, 217, 119, 147.

Methyl syringate (**129**): yellow amorphous powder (40 mg); UV (MeOH) λ_{max} 275 and 218 nm; IR ($CHCl_3$) 3401, 2928, 2859, 1714, 1608, 1512 and 1450 cm^{-1}; 1H NMR ($CDCl_3$, 400 MHz) Refer to Table 2.8; 13C NMR ($CDCl_3$, 100 MHz) Refer to Table 2.8; EIMS *m/s* 212 $[M]^+$, 197, 181.

2.3.4 Assay for Cholinesterae Inhibition.

The inhibitory activity of *B. natalensis* fractions and isolated compounds were tested against AChE using the method by Ellman[39] with slight modifications for microtiter plates[41]. This assay measures the activity of the enzyme by conjugation of thiocholine with DTNB, the resulting thiocholine-DTNB (2-5-mercapto-thiocholine-nitrobenzoate) adduct has a distinct absorbance maxima at 406nm. Various concentrations of the compounds were incubated with the enzyme at 22°C for 30 min after which the assay was performed. The assay mixture contains 5 mM DTNB, 3.75 mM AChI, 100 mM phosphate (pH 8.0) and 2.5 mU/mL of enzyme in a 200µL total assay volume. The rate of 2-5-mercapto-thiocholine-nitrobenzoate adduct formation was measured at 406 nm after 3 min using the *Synergu HT multidetection BioTek* microplate reader. The percent inhibition was calculated by Formula 1. The effects of the

compounds as inhibitors of AChE was calculated as an IC_{50} value, which is the concentration of the inhibitor required to reduce enzyme activity to 50%. Galanthamine was used as a positive control in this assay.

Formula 1: % Inhibition = $[(A_O - A_I) / A_O] \times 100$; where A_O is the absorbance of the blank with no test compound and A_I are the average absorbance values for each concentration tested.

The inhibition of isolated compounds was tested against BChE as well. In this assay butyrylthiocholine iodide is used as the substrate for butyrylcholinesterase. The butyrylcholine-DTNB adduct was measured at 406 nm. The isolated compounds were incubated with the enzyme for 30 min at 37°C. The assay mixture contains 5 mM DTNB, 10 mM BChI, 100 mM phosphate (pH 8.0) and 5 mU/mL of enzyme in a 200µL total assay volume. The rate of butyrylcholine-DTNB adduct formation was measured at 406 nm after 30 min at 37°C using *Synergu HT multidetection BioTek* microplate reader. The IC_{50} was calculated with galanthamine used as a positive control in this assay as well.

2.3.5 Antibacterial Activity.

Antibacterial activities of compounds isolated were first tested by Kirby Bauer Disk Diffusion method[42]. *Staphylococcus aureus* (ATCC 25923), *Pseudomonas aeruginosa* (ATCC 27853), *Escherichia coli* (ATCC 25922), *Mycobacterium goodii* (ATCC 87709813), *Streptococcus mitis* (ATCC 9811), *Streptococcus bovis* (ATCC

9809), and *Streptococcus mutans* (ATCC 25175) were used to test against bacterium in this assay. Two strains of *Candida albicans* (ATCC 14053 and 90028) were used to test for anti-fungal activity in this assay. These bacterial strains were obtained from the Department of Biology, the University of Winnipeg. Blank discs, 6 mm diameter (BBL^{TM}) were impregnated with 100µg of compound dissolved in a soluble solvent. The solvent was evaporated and the discs placed in Mueller Hinton agar for bacteria and SAB agar for fungi. These plates were then incubated for 24 hours at 37°C for the bacteria and 31°C for the fungi. The antibacterial activity was determined by measuring the diameters of the inhibitory zone around each disc. Ceftriaxone and Ciprofloxacin were used as positive controls for bacterial cultures and Nystatin was used as a positive control for fungal cultures.

The anti-fungal activities were also tested by MIC method taken from Devkota[43]. MIC is the lowest concentration which inhibits growth of the test organism, which is *C. albicans* (ATCC 90028). Fungal broth was used as the media in this test. The fungi were grown in fungal broth for 24 hours after which time they were diluted to optically match a McFarland two standard. 100µL of fungal from the dilution culture was added to each well with the first well having 198µl. 2µL of test compound was added to the first well at a final concentration of 50µg/mL. The test compound was diluted two fold across the microtiter plate. The plates were incubated for eight hours at 31°C with absorbance readings taken at 540 nm every 15 min using the *Synergu HT multidetection BioTek* microplate reader.

2.4 REFERENCES

1. Atta-ur-Rahman; Naz, S.; Noor-e-ain, F.; Ali, R. A.; Choudhary, M. I.; Sener, B.; Turkoz, S. *Phytochemistry* **1992**, *31*, 2933.
2. Atta-ur-Rahman; Ahmed, D.; Asif, E.; Jamal, S. A.; Choudhary, M. I.; Sener, B.; Turkoz, S. *Phytochemistry* **1991**, *30*, 1295.
3. Atta-ur-Rahman; Asif, E.; Ali, S. S.; Nasir, H.; Jamal, S. A.; Ata, A.; Farooq, A.; Choudhary, M. I. *J. Nat. Prod.* **1992**, *55*, 1063.
4. Weller, L. E.; Redemann, C. T.; Gottshall, R. Y.; Roberts J. M.; Lucas E. H.; Sell, H. M. *Antibiot Chemother*. **1953**, *3*, 603.
5. Durant, J.; Dellamonica, P.; Rebouillat, A. PCT Int. Appl. WO Patent 9300916, 1993.
6. Durant, J.; Chantre, P.; Gonzalez, G.; Vandermander, J.; Halfon, P.; Rousse, B.; Guedon, D.; Rahelinirina, V.; Chamaret, S.; Montagnier, L.; Dellamonica, P. *Phytomedicine* **1998**, *5*, 1.
7. Fan, S. F. *Trends Pharmacol. Sci*. **1983**, *4*, 208.
8. Ata, A.; Andersh, B. J. *The Alkaloids: Chemistry and Biology*; Cordell, G.A., Ed.; Natural products Inc.: Evanston, IL USA, 2008; Vol.66, Chapter 3, pp 191-213.
9. Nakano, T.; Terao, S.; *Tetrahedron Lett*. **1964**, *17*, 1035.
10. Nakano, T.; Terao, S. *J. Chem. Soc.* **1965**, 4512.
11. Choudhary, M. I.; Shahnaz, S.; Parveen, S.; Khalid, A.; Ayatollahi, S. A. M.; Atta-ur-Rahman; Parvez, M. *J. Nat. Prod*. **2003**, *66*, 739.
12. Meshkatalsadat, M. H.; Abass, M.; Ata, A. *Z. Naturforsch., B: Chem. Sci*. **2006**, *61*, 201.

13. Babar, Z. U.; Ata, A.; Meshkatalsadat, M. H. *Steroids* **2006**, *71*, 1045.

14. Lee, J. H.; Park, Y. H.; Cho, B. H.; Kim, Y. J.; Kim, J. B.; Kim, C. M.; Kim, C. S.; Cha, Y. D.; Kim, Y. S. *Korean J. Pharmacol*. **1987**, *23*, 151.

15. Kwon, J. T.; Lee, J. H.; Park, Y. H.; Cho, B. H.; Choi, K. H.; Kim, Y. J.; Kim, C. M.; Kim, C. S.; Cha, Y. D.; Kim, Y. S. *Korean J. Pharmacol*. **1988**, *24*, 103.

16. Hu, D.; Liu, Z.; Wang, Y.; Chen, S. *Eur. J. Pharmacol*. **2007**, *569*, 103.

17. Kaikabo, A. A. Isolation and characterization of antibacterial compounds from a *Garcinia livingstonei* (Clusiaceae) leaf extract. M.Sc. Thesis, University of Pretoria, Onderstepoort, South Africa, 2009.

18. Kupchan, S. M.; Kennedy, R. M.; Schleigh, W. R.; Ohata, G. *Tetrahedron* **1967**, *23*, 4563.

19. Atta-ur-Rahman; Choudhary, M. I.; Naz, S.; Ata, A.; Sener, B.; Turkoz, S. *J. Nat. Prod*. **1997**, *60*, 770.

20. Demarco, P. V.; Farkas, E.; Doddrell, D.; Mylari, B. L.; Wenkert, E. *J. Am. Chem. Soc*. **1968**, *90*, 5480.

21. Brown, K. S.; Kupchan, S. M. *J. Am. Chem. Soc*. **1962**, *84*, 4592.

22. Sangare, M.; Khuong, H. L. F.; Herlem, D.; Milliet, A.; Septe, B.; Berenger, G.; Lukacs, G. *Tetrahedron Lett*. **1975**, *22*, 1791.

23. Guilhem, J. *Tetrahedron Lett*. **1975**, *34*, 2937.

24. Atta-ur-Rahman; Alam, M.; Nasir, H.; Dagne, E.; Yenesew, A. *Phytochemistry* **1990**, *29*, 1293.

25. Atta-ur-Rahman; Choudhary, M. I.; Ata, A. *Heterocycles* **1992**, *34*, 157.

26. Atta-ur-Rahman; Noor-e-ain, F.; Choudhary, M. I.; Parveen, Z. *J. of Nat. Prod*. **1997**, *60*, 976.

27. Choudhary, M. I.; Atta-ur-Rahman; Freyer, A. J.; Shamma, M. *Tetrahedron* **1986**, *42*, 5747.

28. Iqbal Z. Studies on the steroidal alkaloids of *Buxus papillosa* and other related plants. Ph.D. Thesis, University of Karachi, Karachi. 1990.

29. Dewick, P. M. *Medicinal Natural Products: A Biosynthetic Approach*. 3rd Ed.; John Wiley and Sons, New York. 2009.

30. Atta-ur-Rahman. *Studies in natural products chemistry*; University of Karachi: Pakistan, 1988; Vol. 2, Chapter , pp 175-189.

31. Voticky, Z.; Bauerova, O.; Paulik, V. *Collect. Czech. Chem. Commun*. **1975**, *40*, 3055.

32. Choudhary, M. I.; Atta-ur-Rahman; Shamma, N. *Phytochemistry* **1988**, *27*, 1561.

33. Mizusaki, S.; Tanabe, Y.; Noguchi, M.; Tamaki, E. *Phytochemistry* **1970**, *10*, 1347.

34. Leubner-Metzger, G.; Amrhein, N. *Phytochemistry* **1993**, *32*, 551.

35. Hristea, E. N.; Covaci-Cimpeanu, I. C. C.; Ionita, G.; Ionita, P.; Draghici, C.; Caproiu, M. T.; Hillebrand, M.; Constantinescu, T.; Balaban, A. T. *Eur. J. Org. Chem*. **2009**, 626.

36. Atta-ur-Rahman; Ahmed, D.; Asif, E.; Ahmad, S. *J. of Nat. Prod*. **1991**, *54*, 79.

37. Ickes, G. R.; Fong, H. H. S.; Schiff, P. L.; Perdue, R. E.; Farnsworth, N. R. *J. Pharm. Sci*. **1973**, *62*, 1009.

38. Russell, K. M.; Molan, P. C.; Wilkins, A. L.; Holland, P. T. *J. Agric. Food Chem*. **1990**, *38*, 10.

39. Ellman, G. L.; Courtney, K. D.; Andres, V.; Featherstone, R.M. *Biochem. Pharmacol*. **1961**, *7*, 88.

40. Zahid, S. Isolationand structure elucidation of bioactive chemical constituents from *Vitex pinnata, Artocarpus nobilis, Barleria prionitis, Buxus natalensis* and *Coprinus micaceus*. M.Sc. Thesis, University of Manitoba, Manitoba, Canada, 2009.

41. Ingkaninam, K.; Temkitthawan, P.; Chuenchon, K.; Yuyaem, P.; Thongnoi, W. *J. Ethnopharmacol*. **2003**, *89*, 261.

42. National Committee for Clinical Laboratory Standards *Performance Standards for Antimicrobial Disc Susceptibility Tests*, 5th ed; approved standard, NCCLS document M2-A5; NCCLS: Vilanova, Pensylvania, 1993.

43. Devkota, K. P; Lenta, B. N.; Wansi, J. D.; Sewald, N. *Phytochem. Lett*. **2010**, *3*, 24.

CHAPTER 3

Phytochemical studies on *Drypetes gossweileri.*

3.1 INTRODUCTION

The genus *Drypetes* (Putranjivaceae) is composed of over 200 species worldwide; many of which are found in Africa, as well as other tropical and subtropical regions of the world. These plants are extensively utilized in African folk medicine to treat various diseases such as bronchitis, ailments of the digestive tract, fever, rheumatism and kidney pain[1,2]. In the Congo, a dark decoction from *D. capillipes* is used as a mouthwash to treat toothache. Extracts from *D. klainei* are used to treat rheumatism while extracts from *D. natalensis* are used to treat malaria induced fever[2]. Compounds isolated from *Drypetes* have shown anti-inflammatory, analgesic[3], antileishmanial[4] and antimicrobial[5] activities. The genus *Drypetes* has not been extensively explored for phytochemicals as *Buxus*.

3.1.1 Triterpenoidal Constituents of Drypetes.

Plants *Drypetes* have been reported to produce terpenes. Recent studies have found 12α-hydroxyfriedelane-3,15-dione (**132**) and 3β-hydroxyfriedelan-25-al (**133**), isolated from *D. paxii*, to exhibit anti-bacterial activity against *Staphylococcus aureus*[6].

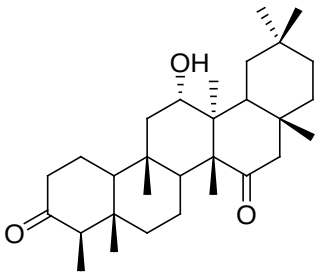

(132)

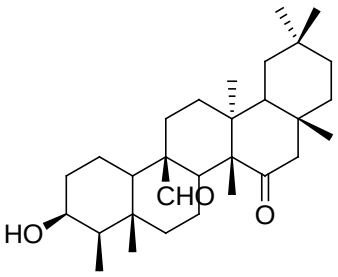

(133)

Triterpenes isolated from *D. inaequalis* have also shown antibacterial properties including lup-20(29)-en-3β,6α-diol (**134**), 3β-acetoxylup-20(29)-en-6α-ol (**135**), 3β-caffeoyloxyup-20(29)-en-6α-ol (**136**) and D-glucopyranosyl-30-methyl 3β-hydrooxyolean-12-en-28,30-dioate (**137**). Compound **134** has shown anti-bacterial activity against *S. aureus*, while compound **137**, a triterpene glycoside, has shown activities against *S. aureus*, *Escherichia coli* and *Salmonella typhi*[5].

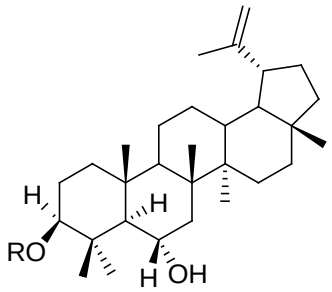

(134): R = H

(135): R = $COCH_3$

(136): R =

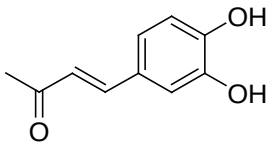

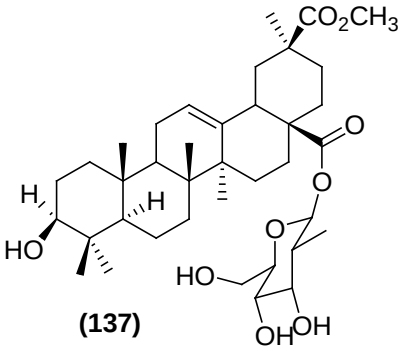

(137)

Unique structural triterpene natural products were isolated from *D. gerrardii*, such as a 5β,24-cyclofriedelan-3-one (**138**)[7], which has a cyclopropane ring between C-25 and C-5, and 3β-*O*-(E)-3,5-dihydroxycinnamoyl-11-oxo-olean-12-ene (**139**), a triterpene with a cinnamic acid moiety isolated from *D. tessmanniana*[8].

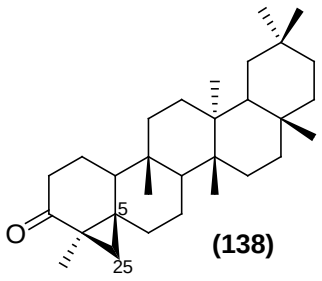

(138)

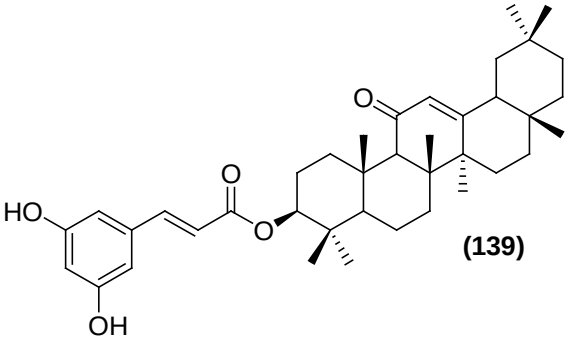

(139)

3.1.2 Aromatic Constituents from Drypetes.

Phytochemical investigations of the genus *Drypetes* have also yielded a wide variety of unique aromatic compounds. One such example is the diflavonoid amentoflavone (**140**), isolated from *D. gerrardii*[7]. Isolates purified from extracts of *D. littoralis* and *D. molunduana* have yielded lignans boehmenan D (**141**)[9] and syringaresinol (**142**)[10]. Investigation of extracts from the shrub *D. parvifolia* from Cameroon led to the isolation of the flavan glycoside, 7-hydroxy-5-*O*-(β-D-glucopyranoside) flavan (**143**), and the chalcone glycoside, (Z)-4',6'-dihydroxy-2'-*O*-(β-D-glucopyranoside) chalcone (**144**)[11].

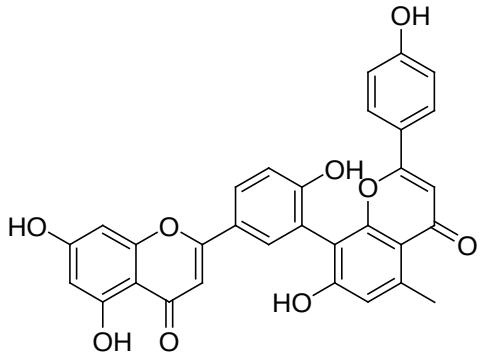

(140)

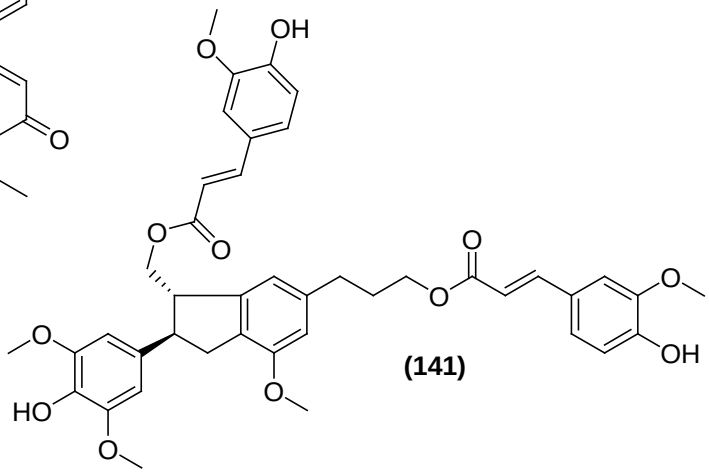

(141)

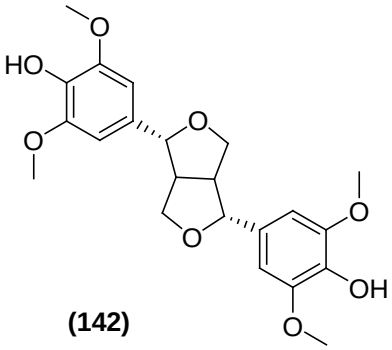

(142)

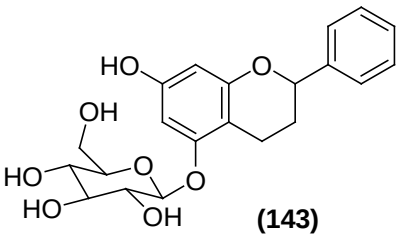

(143)

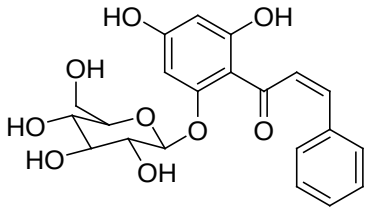

(144)

3.1.3 Drypetes gossweileri.

Drypetes gossweileri is a large tree found in the dense humid forests of Africa and is known for its smell of horseradish. The main essential oils of the stem bark are composed of benzyl isothiocyanide (**145**), benzyl cyanide (**146**) and benzaldehyde (**147**)[12]. Minor components include triterpenes such as friedelin (**148**), stearic acid (**149**) and β-sitosterol (**150**). The crude ethanolic extract of the stem bark have shown anti-bacterial activity against *Staphylococcus aureus, Pseudomonas aeruginosa, Klebsiella sp.* and *Proteus sp*. Methanolic extracts have also shown phytotoxic properties against *Lemna minor* L. as well as anti-fungal activity against *Microsporum canis* and *Trichophyton longiformis*.[2]

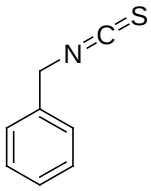

(145)

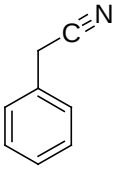

(146)

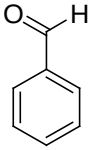

(147)

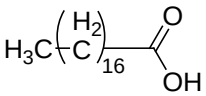

(149)

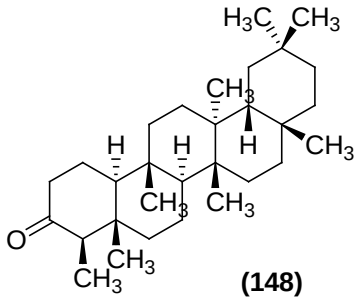

(148)

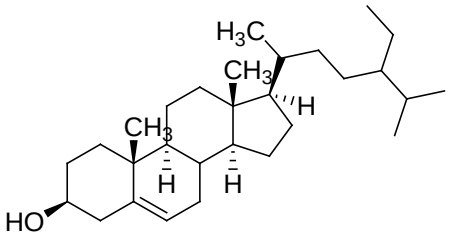

(150)

Recent phytochemical studies on *D. gossweileri* yielded three natural products **151-153**. In this chapter, isolation, characterization, and the bioactivity data for compounds **151-153** will be discussed.

3.2 RESULTS AND DISCUSSION

The bark of *Drypetes gossweileri* was collected from South Africa in 2006 and was shipped to the University of Winnipeg. Phytochemical studies on the crude methanolic extract resulted in the isolation of three aromatic compounds; N-β-glucopyranosyl-*p*-hydroxy phenyl acetamide (**151**), *p*-hydroxyphenyl acetic acid (**152**), and *p*-hydroxyphenyl acetonitrile (**153**). Compound **151** was found to be a novel *N*-linked glycoside. All compounds, **151-153**, were evaluated for their anti-AChE activity.

3.2.1 *N*-β-Glucopyranosyl-*p*-hydroxy Phenyl Acetamide (151).

Compound **151** was isolated as a brown amorphous solid. Its UV spectrum showed absorption maxima at 226, 279, and 383, nm indicating the presence of a phenolic chromophore. The IR spectrum showed intense absorption bands for hydroxyl (3423 cm^{-1}), amidic carbonyl (1643 cm^{-1}) and benzene (1557 and 1416 cm^{-1}) functionalities.

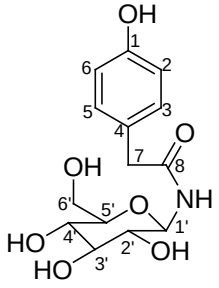

(151)

The ^{1}H-NMR spectrum ($CD_{3,}OD$, 400 MHz) of **151** showed two pairs of AB doublets, one set in the aromatic region, at δ 7.22 (*J* = 8.3 Hz) and 6.76 (*J* = 8.3 Hz) and other set was in the aliphatic region, at δ 4.15 (*J* = 15.7 Hz) and 3.95 (*J* = 15.7 Hz). The

latter doublets, which integrated for one proton each, were ascribed to the homotopic C-7 methylene protons connecting the benzene ring with the amidic carbonyl. The former doublets integrated for two protons each, indicated the presence of a *para*-substituted benzene ring. These signals were assigned to H-3/H-5 (δ 7.22) and H-2/H-6 (δ 6.76), respectively. A one-proton doublet at δ 4.55 (J = 9.3 Hz) was ascribed to the anomeric proton (H-1'). Other signals resonating between δ 3.10 and 4.56 were ascribed to the sugar moiety. The COSY-45° spectrum displayed the presence of three isolated spin systems: one being the benzene ring, the second due to the C-7 methylene protons, and the last spin system corresponded to the sugar moiety. The benzene spin system showed a coupling between H-2/6 (δ 6.76) and H-3/5 (δ 7.22). This coupling was due to the chemical equivalence of H-2/H-6, and H-3/H-5. The spin system of the sugar moiety includes COSY interactions between H-1' (δ 4.55) and H-2' (δ 3.15), H-3' (δ 3.13) and H-4' (δ 3.24), and H-5' (δ 3.23) and the H-6' methylene protons (δ 3.64 and 3.88).

The broad-band ^{13}C-NMR spectrum (CD_3OD, 100 MHz) showed the resonance of all 12 carbons. The DEPT spectra indicated the presence of two methylene, seven methine and three quaternary carbons. The ^{13}C-NMR spectrum showed the resonance of four aromatic carbons, with two methine carbons being chemically equivalent. This was due to symmetry in the benzene ring which was confirmed by both ^{1}H and ^{13}C-NMR spectra, thereby indicating C-3/C-5 (δ 130.5) and C-2/C-6 (δ 116.8) were chemically equivalent methine carbons. The three quaternary carbons C-1, C-4, C-8 resonated at C-1 (δ 157.9), C-4 (δ 128.0), and C-8 (δ 161.5), respectively. A downfield chemical shift at δ 157.9 (C-1) indicated the presence of a geminal hydroxyl group. The quaternary carbon

resonating at δ161.5 (C-8) suggested the presence of an amide carbonyl functionality. The six carbon signals between δ 62.9 and 82.9 were due to the sugar moiety.

The HMBC spectrum was essential in connecting the three spin systems in compound **151**. The HMBC spectra showed $^{1}H/^{13}C$ long-range coupling of H-3/H-5 (δ7.22) with C-7 (δ 39.1) and C-1 (δ 157.9). H-2/H-6 (δ 6.76) showed HMBC coupling with C-1 (δ 157.9) and C-4 (δ 128.0). This indicated the C-7 methylene group was *ortho* to H-3/H-5. Since the ^{1}H-NMR chemical shifts of the sugar moiety were very close to each other, HMBC was utilized to determine the chemical shift of all the carbons in the sugar moiety. The H-1' anomeric proton (δ 4.55) showed HMBC cross-peaks with C-2' (δ 79.5), C-3' (δ 74.4) and C-8 (δ 161.5). The H-6' (δ 3.64 and 3.88) showed coupling to C-4' (δ 71.4) and C-5' (δ 82.3). H-5' (δ 3.23) showed coupling with C-2' (δ 79.5) and H-3' (δ 3.13) showed coupling to C-1' (δ 82.9) and C-5' (δ 82.3). The H-7 methylene protons showed coupling to C-4 (δ 128.0), C-3/C5 (δ 130.5), and C-8 (δ 161.5). This HMBC correlation led to the connection of the aromatic fragment to the sugar moiety through an amide linkage. Important HMBC long range couplings are shown in **Figure 3.1**. Complete ^{1}H, ^{13}C, and HSQC one-bond chemical shift assignments of N-β-glucopyranosyl-*p*-hydroxy phenyl acetamide (**151**) are shown in **Table 3.1**.

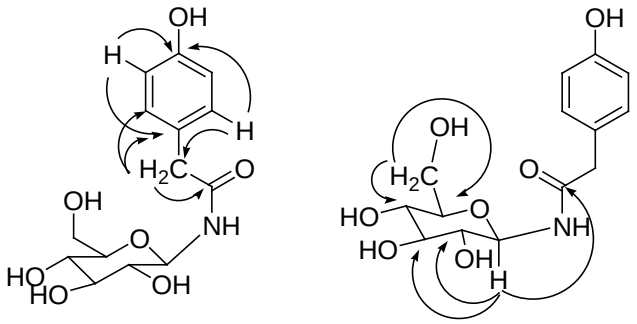

(151*a*) **(151*b*)**

Figure 3.1. HMBC correlations of N-β-glucopyranosyl-*p*-hydroxy phenyl acetamide (**151**).

The sugar moiety in this compound, **151**, was determined to be glucose based on comparison of the ^{1}H-, and ^{13}C-NMR data with glucose data reported in the literature[11,13]. Based on these spectroscopic studies, a tentative structure was proposed for this compound and was named *N*-β-glucopyranosyl-*p*-hydroxy phenyl acetamide (**151**).

Table 3.1. ^{1}H and ^{13}C NMR Spectroscopic Data (400 and 100 MHz, respectively) in CD_3OD for N-β-glucopyranosyl-*p*-hydroxy phenyl acetamide (**151**).

	N-β-glucopyranosyl-*p*-hydroxy phenyl acetamide (**151**)		
Position	**δ_C**	**†Multiplicity**	**δ_H (*J* in Hz)**
1	157.9	C	-
2	116.8	CH	6.76, *d* (8.3)
3	130.5	CH	7.22, *d* (8.3)
4	128.0	C	-
5	130.5	CH	7.22, *d* (8.3)
6	116.8	CH	6.76, *d* (8.3)
7	39.1	CH_2	3.93, *d* (15.7), 4.13, *d* (15.7)
8	161.5	C	-
1’	82.9	CH	4.55, *d* (9.3)
2’	79.5	CH	3.15, *m*
3’	74.4	CH	3.13, *m*
4’	71.4	CH	3.24, *m*
5’	82.3	CH	3.23, *m*
6’	62.9	CH_2	3.64, *m*, 3.88, *m*

†Multiplicity as determined by DEPT spectra.

3.2.2 *p*-Hydroxy Phenyl Acetic Acid (152)

Compound **152** was isolated as a white powder. The UV spectrum was similar to that of **151** indicating the presence of the same phenolic chromophore with absorption maxima at 223, 263, and 281 nm. The IR spectrum showed intense absorption bands at 3339 (OH), 2932 and 2959 (C-H), and 1708 (COOH) cm^{-1}. The IR spectrum of **152** also showed bands at 1614, 1598, and 1516 cm^{-1}, values characteristic for a benzene ring. EIMS showed a molecular ion peak at *m/z* 152. This MS data in combination with NMR spectral data suggested a molecular formula of $C_8H_8O_3$. An ion at *m/z* 135 was due to the loss of a hydroxyl group, while an ion at *m/z* 107 indicated the loss of a carboxyl group.

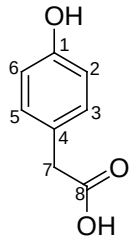

(152)

The ^{1}H-NMR spectrum (acetone-d_6, 400 MHz) of **152** showed two AB doublets, integrating for two protons each, at δ 6.78 (J = 8.5 Hz) and δ 7.13 (J = 8.5 Hz). These signals indicated the presence of a *para*-substituted benzene ring and were assigned to H-3/H-5 and H-2/H-6 respectively. A two-proton singlet resonated at δ 3.50 was due to the C-7 methylene protons. The COSY-45^o spectrum showed ^{1}H-^{1}H coupling between H-2/H-6 and H-3/H-5.

A combination of ^{13}C-NMR (acetone-d_6, 100 MHz) and DEPT spectra indicated the presence of one methylene, two methine (each representing two methines due to symmetry in molecule) and three quaternary carbons in **152**. The HMBC spectrum of **152**

showed $^{1}H/^{13}C$ long-range coupling of H-3/H-5 (δ 7.12) with C-7 (δ 40.5) and C-1 (δ 157.2). The C-7 methylene protons (δ 3.50) showed coupling to the C-3/C-5 (δ 131.3) methine, and C-4 (δ 126.7), C-8 (δ 173.3) quaternary carbons. These HMBC correlations indicated that C-7 was flanked by an aromatic ring and an acid group. Important HMBC long range couplings are shown in **Figure 3.2**. The complete ^{1}H, ^{13}C, and HSQC one-bond chemical shift assignments for *p*-hydroxy phenyl acetic acid (**152**) are shown in **Table 3.2**.

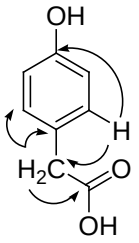

(152)

Figure 3.2. HMBC correlations of *p*-hydroxy phenyl acetic acid (**152**).

Table 3.2. ^{1}H and ^{13}C NMR Spectroscopic Data (400 and 100 MHz, respectively) in acetone-d_6 for *p*-hydroxy phenyl acetic acid (**152**).

	p-hydroxy phenyl acetic acid (**152**)		
Position	**δ_C**	**†Multiplicity**	**δ_H (*J* in Hz)**
1	157.2	C	-
2	116.0	CH	6.78, *d* (8.5)
3	131.3	CH	7.13, *d* (8.5)
4	126.7	C	-
5	131.3	CH	7.13, *d* (8.5)
6	116.0	CH	6.78, *d* (8.5)
7	40.5	CH_2	3.50, *s*
8	173.3	C	-

†Multiplicity as determined by DEPT spectra.

Based on these spectroscopic studies, this compound was confirmed to be *p*-hydroxy phenyl acetic acid **(152)**, a known compound that has been isolated from plants including *Sonchus oleraceus*[14] and lupine seed[15]. *p*-hydroxy phenyl acetic acid has also been found from fungi such as *Cladosporium* sp.[16] and has been found to enhance the growth of the red alga *Porphyra tenera*[17].

3.2.3 *p*-Hydroxyphenyl Acetonitrile (153)

Compound **153** was isolated as a green amorphous solid. The IR spectrum showed intense absorbance bands at 3416 (OH), 2256 (CN) 1624, 1511 and 1449 (C=C) cm^{-1}. The EIMS showed a molecular ion peak at *m/z* 133, which corresponded to a molecular formula of C_8H_7NO with six degree of unsaturation. Two ions at *m/z* = 107 and 90 indicated the loss of cyanide and methylene-cyanide groups from the molecular ion.

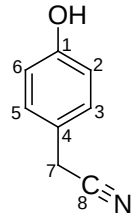

(153)

The ^{1}H-NMR spectrum (acetone-d_6, 400 MHz) of **153** showed two two-proton doublets in the aromatic region at δ 6.87 (*J* = 8.6) and δ 7.21 (*J* = 8.5 Hz). These signals indicated a *para*-substituted benzene ring, and were assigned to H-3/H-5 and H-2/H-6 respectively. A two-proton singlet at δ 3.80 indicated the presence of the C-7 methylene

protons. The COSY-45^{o} spectrum showed coupling for protons between H-2/H-6 and H-3/H-5.

Table 3.3. ^{1}H and ^{13}C NMR Spectroscopic Data (400 and 100 MHz, respectively) in acetone^{d6} for *p*-hydroxyphenyl acetonitrile (**153**).

p-hydroxyphenyl acetonitrile (**153**)

Position	**δ_C**	**†Multiplicity**	**δ_H (*J* in Hz)**
1	157.9	C	-
2	116.7	CH	6.87, *d* (8.6)
3	130.2	CH	7.21, *d* (8.5)
4	122.8	C	-
5	130.2	CH	7.21, *d* (8.5)
6	116.7	CH	6.87, *d* (8.6)
7	22.6	CH_2	3.80, *s*
8	119.6	C	-

†Multiplicity as determined by DEPT spectra.

Combination of ^{13}C-NMR and DEPT spectra indicated the presence of one methylene, two methine (each representing two methine carbons due to symmetry in the molecule) and three quaternary carbons. The HMBC spectrum showed the ^{1}H/^{13}C long-range coupling of H-3/H-5 (δ 7.21) with the C-7 (δ 22.6) methylene and C-1 (δ 157.9) quaternary carbon. H-2/H-6 (δ 7.21) showed HMBC cross-peaks with C-4 (δ 122.8). This indicated C-7 is *ortho* to H-3 and H-5. The methylene protons H-7 (δ 3.80) showed HMBC couplings to C-4 (δ 122.8), C-3 and C-5 (δ 130.2) and C-8 (δ 119.6) indicating the cyanide group was geminal to the methylene carbon. HMBC long range couplings are shown in **Figure 3.3**. The complete ^{1}H-NMR, ^{13}C-NMR and HSQC one-bond chemical shift assignments for *p*-hydroxyphenyl acetonitrile (**153**) are shown in **Table 3.3**.

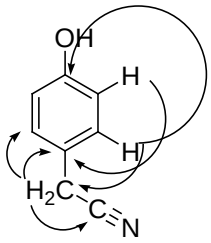

(153)

Figure 3.3. HMBC correlations of *p*-hydroxyphenyl acetonitrile (**153**).

Based on these spectroscopic studies, this compound was confirmed to be *p*-(hydroxyphenyl) acetonitrile (**153**), a known compound that has been isolated from the oil in *Brassica campestris* seeds[18] and from the flowers of *Angelica furcijuga*[19]. The seeds of *Brassica hirta* also contained *p*-(hydroxyphenyl) acetonitrile and was found to have an antitussive, cough suppressant, effect[20].

3.2.4 Biogenesis of Isolated Compounds from *Drypetes gossweileri.*

Previous studies have elucidated the biosynthesis of cyanogenic glucosides in which *p*-hydroxyphenyl acetonitrile (**153**) is an intermediate for these compounds. Work was done on sorghum (*Sorghum bicolor*) as a plant model to study this biosynthetic pathway. It was found that two cytochrome P450 monooxygenases are needed to convert L-tyrosine (**154**) into *p*-hydroxymandelonitrile (**156**)[21]. The first enzyme is a member of the CYP79 family that converts L-tyrosine into (Z)-*p*-hydroxyphenyl-acetaldoxime (**155**)[22]. The second P450 converts (**155**) into (**156**) through an intermediate *p*-hydroxyphenyl acetonitrile (**153**)[23,24] as depicted in **Scheme 3.1**. Compound (**152**) can

be thought of being derived from *p*-hydroxyphenyl-pyruvic acid with compound (**152**) further used to make the *N*-glycoside.

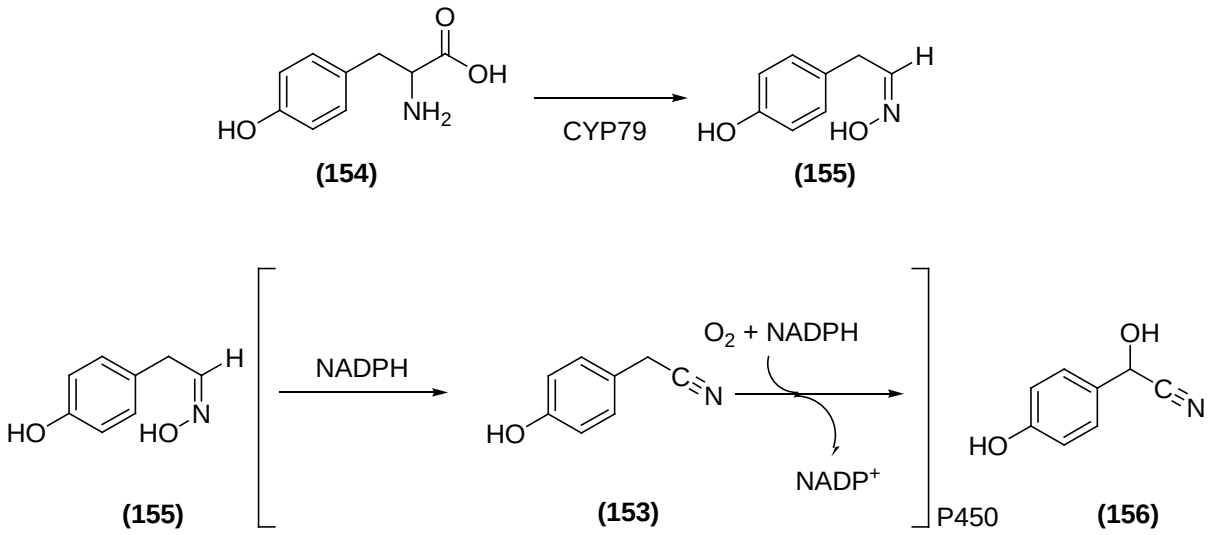

Scheme 3.1. Proposed mechanism for the biosynthesis of *p*-hydroxyphenyl acetonitrile (**153**).

3.2.5 Acetylcholinesterase Inhibitory Activity of Compounds 151-153.

Compounds **151-153** were evaluated for AChE Inhibitory activity with all isolates exhibiting different levels of activity (**Table 3.4**). Compound **151** showed the highest activity of these compounds with a moderate IC_{50} value of 78.1 μM. From these bioactivity data, the higher potency of **151** might be hypothesized to be the result of the presence of amide or glucose functionalities.

Table 3.4. Results of the AChE inhibition assay on compound **151-153** isolated from *D. gossweileri*.

Compound	AChE IC50 (μM) ± SD
151	78.1 ± 1.3
152	127.2 ± 7.5
153	207.9 ± 10.2
Galanthamine	0.9 ± 0.2

3.3 EXPERIMENTAL

3.3.1 General

The general experimental procedures of chromatography and spectroscopy were the same as discussed in Chapter 2 (section 2.3.1).

3.3.2 Plant Material

The bark of *Drypetes gossweileri* was collected from South Africa in 2006 and was shipped to the University of Winnipeg, Department of Chemistry.

3.3.3 Extraction and Isolation

The bark was extracted with methanol, then filtered and evaporation of solvent was performed *in vacuo*. This methanolic extract was loaded onto a silica gel column for further fractionation. This column was eluted with $CHCl_3$:CH_3OH (0-100%). 298 fractions were obtained for primary fractionation. These fractions were pooled based on the bases of analytical TLC results. Three fractions, DG-19, DG-109, and DG-224, were chosen to be further purified as they contained major products different from one another.

DG-19 collected at a 96%$CHCl_3$-4%CH_3OH was subjected to secondary column chromatography and was eluted with $CHCl_3$:CH_3OH (0-100%). Fractions at 98%$CHCl_3$-2%MeOH appeared to contain one major compound, therefore they were pooled. The major constituent was purified by preparative TLC using chloroform-methanol (99:1) to give compound **153**, *p*-hydroxyphenyl acetonitrile (81.4mg). Fraction DG-109 (89%$CHCl_3$-11%MeOH) was subjected to a secondary column as well, and eluted with

the same solvent system as before. Eight fractions from eluted at 99%$CHCl_3$-1%MeOH and pooled based on TLC results (DG-109-17). Preparative TLC was performed on this fraction using $CHCl_3$-MeOH (95:5) which afforded *p*-hydroxyphenyl acetic acid (**152**) (14.9mg). A third fraction, DG-224 (75%$CHCl_3$-25%MeOH), from the primary column was loaded onto a secondary column and once again eluted with the same solvent system $CHCl_3$:CH_3OH (0-100%). Several fractions collected at 75%$CHCl_3$-25%MeOH were pooled based on similar R_f values. This fraction (DG-224-51) was subjected to preparative TLC using $CHCl_3$-MeOH-Acetic acid (50:50:5) to yield *N*-β-glucopyranosyl-*p*-hydroxy phenyl acetamide (**151**) (7.00mg).

N-β-glucopyranosyl-*p*-hydroxy phenyl acetamide (**151**): brown amorphous solid (70 mg); UV (MeOH) λ_{max} 383, 279 and 226 nm; IR ($CHCl_3$) 3423, 1643, 1557, and 1416 cm^{-1}; 1H NMR Refer to Table 3.1; 13C NMR Refer to Table 3.1.

p-hydroxy phenyl acetic acid (**152**): white powder (14.9 mg); UV (MeOH) λ_{max} 381, 263 and 223 nm; IR ($CHCl_3$) 3338.8, 2932.2, 2959.2, 1614.4, 1598.0, 1516.1, and 1708 cm^{-1}; 1H NMR Refer to Table 3.2; 13C NMR Refer to Table 3.2; EIMS *m/s* 152 $[M]^+$, 135, 107.

p-hydroxyphenyl acetonitrile (**153**): green colored gum (64.6 mg); IR ($CHCl_3$) 3416, 2256, 1624, 1511 and 1449 cm^{-1}; 1H NMR Refer to Table 3.3; 13C NMR Refer to Table 3.3; EIMS *m/s* 133 $[M]^+$, 107, 90.

3.4 REFERENCES

1) Bouquet, A.; Debray, L. *Plantes Medicinales de la Cote-d'Ivoire*; Orstom, Paris, 1974; Vol. 32, pp 82-87.

2) Schmelzer, G. H.; Gurib-Fakim, A. *Medicinal Plants*. Khuys Publishers, Wageningen, Netherlands, 2008; p 233-236.

3) Chungag-Anye, N. B.; Njamen, D.; Dingma, A. B.; Wandji, J.; Nguelefack, T. B.; Wansi, J. D.; Kamanyi, A.; Fomum, Z. T. *Pharmacol. Lett*. **2001**, *11*, 61.

4) Wansi, J. D.; Wandji, J.; Lallemand, M. C.; Chiozem, D. D.; Iqbal, M. C.; Tillequin, F.; Fomum, T. Z. *Bol. Latinoam. Caribe Plant. Med. Aromat*. **2007**, *6*, 5.

5) Awanchiri, S. S.; Dufat, H. T. V.; Shirri, C. J.; Dongfack, J. M. D.; Nguenang, G. M.; Boutefnoucher, S.; Fomum, Z. T.; Seguin, E.; Verite, P.; Tillequin, F.; Wandji, J. *Phytochemistry*. **2009**, *70*, 419.

6) Chiozen, D. D.; Van-dufat, H. T.; Wansi, J. D.; Djama, C. M.; Fannang, V. S.; Seguin, E.; Tillequin, F.; Wandji, J. *Chem. Pharm. Bull.* **2009**, *57*, 1119.

7) Nganga, M. M.; Chhabra, S.; Langat-Thoruwa, C.; Hussain, H.; Krohn, K. *Biochem. Syst. Ecol*. **2008**, *36*, 320.

8) Dongfack, M. D. J.; Van-dufat, H. T.; Lallemand, M. C.; Wansi, J. D.; Sequin, E.; Tillequin, F.; Wandji, J. *Chem. Pharm. Bull.* **2008**, *56*, 1321.

9) Lin, M. T.; Chen, L. C.; Chen, C. K.; Liu, K. C. S.; Lee, S. S. *J. Nat. Prod.* **2001**, *64*, 707.

10) Fomuma, Z. T.; Sondengama, B. L.; Nkehf, B. C.; Njamen, D. *Phytochemistry*. **2000**, *54*, 811.

11) Nenkeo, V. N.; Shirri, J. C.; Van-dufat, H. T.; Sipepnou, F.; Verite, P.; Sequin, E.; Tillequin, F.; Wandji, J. *Chin. Chem. Lett*. **2008**, *19*, 943.

12) Mve-Mba, C. E.; Menut, C.; Bessiere, J. M.; Lamaty, G.; Ekekang, L. N.; Denamganai, J. *J. Essent. Oil Res.* **1997**, *9*, 367.

13) Du, Q.; Jerz, G.; Winterhalter, P.; *J. Chromatog.* **2004**, *1045*, 59.

14) Hu, P.; Zou, C.; Zhu, Y. *Xibei Zhiwu Xuebao*, **2005**, *25*, 1234.

15) Stobiecki, M.; Ciesiotka, D.; Peretiatkowicz, M.; Gulewicz, K. *J. Chem. Ecol*. **1993**, *19*, 325.

16) Ding, L.; Qin, S.; Li, F.; Chi, X.; Laatsch, H. *Curr. Microbiol*. **2008**, *56*, 229.

17) Fries, L.; Iwasaki, H. *Plant Sci. Lett*. **1976**, *6*, 634.

18) Nagatsu, A.; Sugitani, T.; Mori, Y.; Okuyama, H.; Sakakibara, J.; Mizukami, H. *Nat. Prod. Res.* **2004**, *18*, 231.

19) Matsuda, H.; Morikawa, T.; Ohgushi, T.; Ishiwada, T.; Nishida, N.; Yoshikawa, M. *Chem. Pharm. Bull.* **2005**, *53*, 387.

20) Feng, B.; Wang, H.; Wnag, Y. Patent CN 101531616, 2009.

21) Kahn, R. A.; Bak, S.; Svendsen, I.; Halkier, B. A.; Moller, B.L. *Plant Physiol*. **1997**, *115*, 1661.

22) Sibbesen, O.; Koch, B.; Halkier, B. A.; Moller, B. L. *J. Biol. Chem*. **1995**, *270*, 3506.

23) McFarlene, I. J.; Lees, E. M.; Conn, E. E. *J. Biol. Chem*. **1975**, *250*, 4708.

24) Halkier, B. A.; Moller, B.L. *Plant Physiol*. **1991**, *96*, 10.

CONCLUSION

In conclusion, phytochemical studies on the extracts of *B. natalensis* resulted in the isolation of O^{10}-natafuranamine (**127**), cyclonataminol A (**128**), 31-demethylbuxaminol A (**129**), buxaminol A (**130**), buxaminol C (**131**), *p*-coumaroylputrescine (**132**) and methyl syringate (**133**). O^{10}-Natafuranamine (**127**), cyclonataminol A (**128**), and 31-demethylbuxaminol A (**129**) were found to be novel compounds while buxaminol A (**130**) was isolated for the first time as a natural product. O^{10}-Natafuranamine (**127**) was a member of a rarely occurring class with a tetrahydrofuran ring incorporated in its structure. Only six *Buxus* bases of this series has been reported in literature thus far. This compound was significantly active in out AChE inhibitory assay (IC_{50} = 8.5 µM). Further structure activity relationship studies on this compound are warranted to improve its bioactivity.

In addition, phytochemical studies on the methanolic extract of *D. gossweileri* resulted in the isolation of *N*-β-glucopyranosyl-*p*-hydroxy phenyl acetamide (**151**), along with two known compounds, *p*-hydroxy phenyl acetic acid (**152**) and *p*-hydroxyphenyl acetonitrile (**153**). Compound **151** was found to be a new *N*-linked aromatic glycoside. Compound **151** was moderately active while compounds **152** and **153** displayed weak anti-AChE activities.

APPENDIX

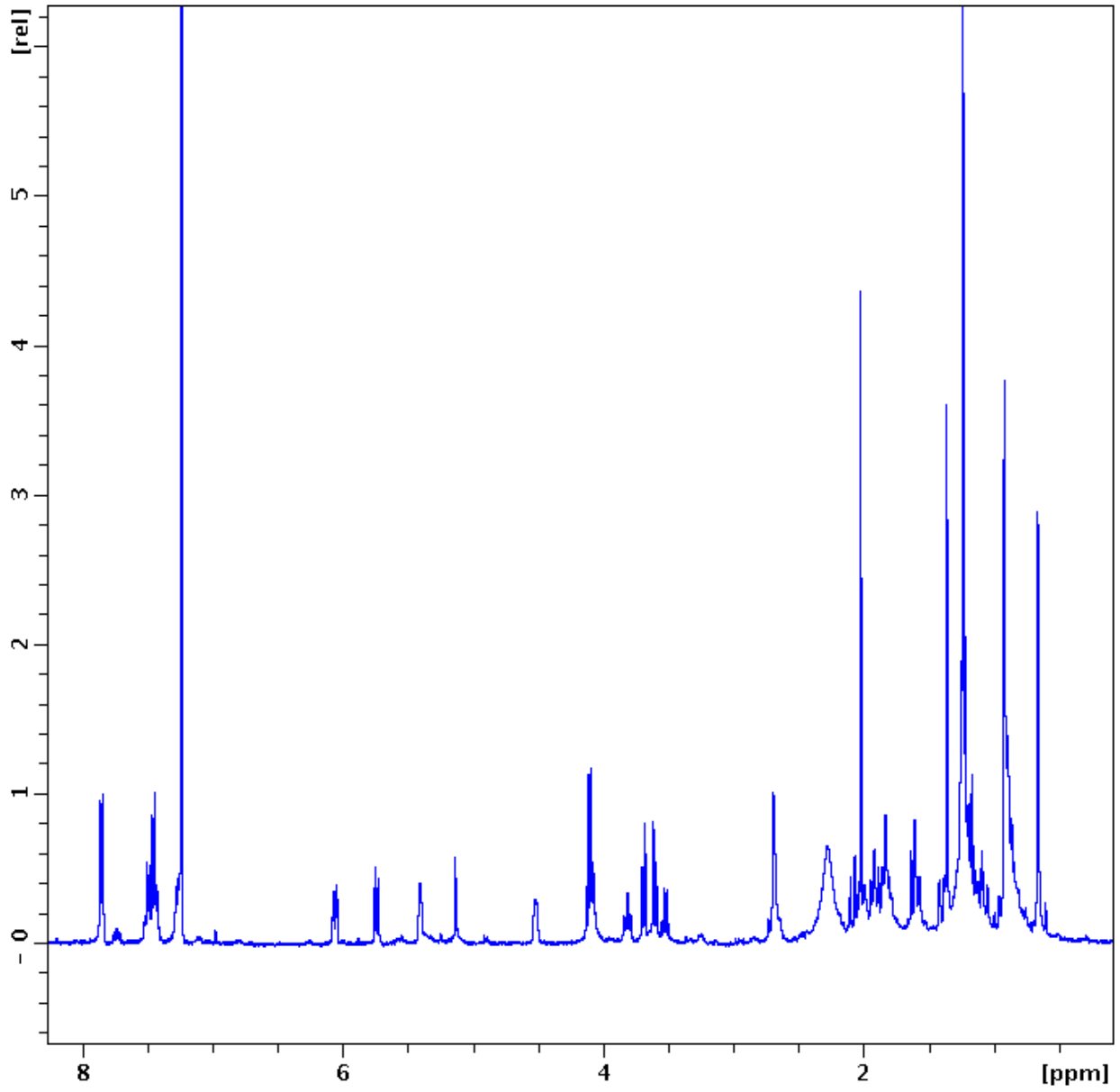

A1. ^{1}H-NMR spectrum of compound **(123)** in $CDCl_3$.

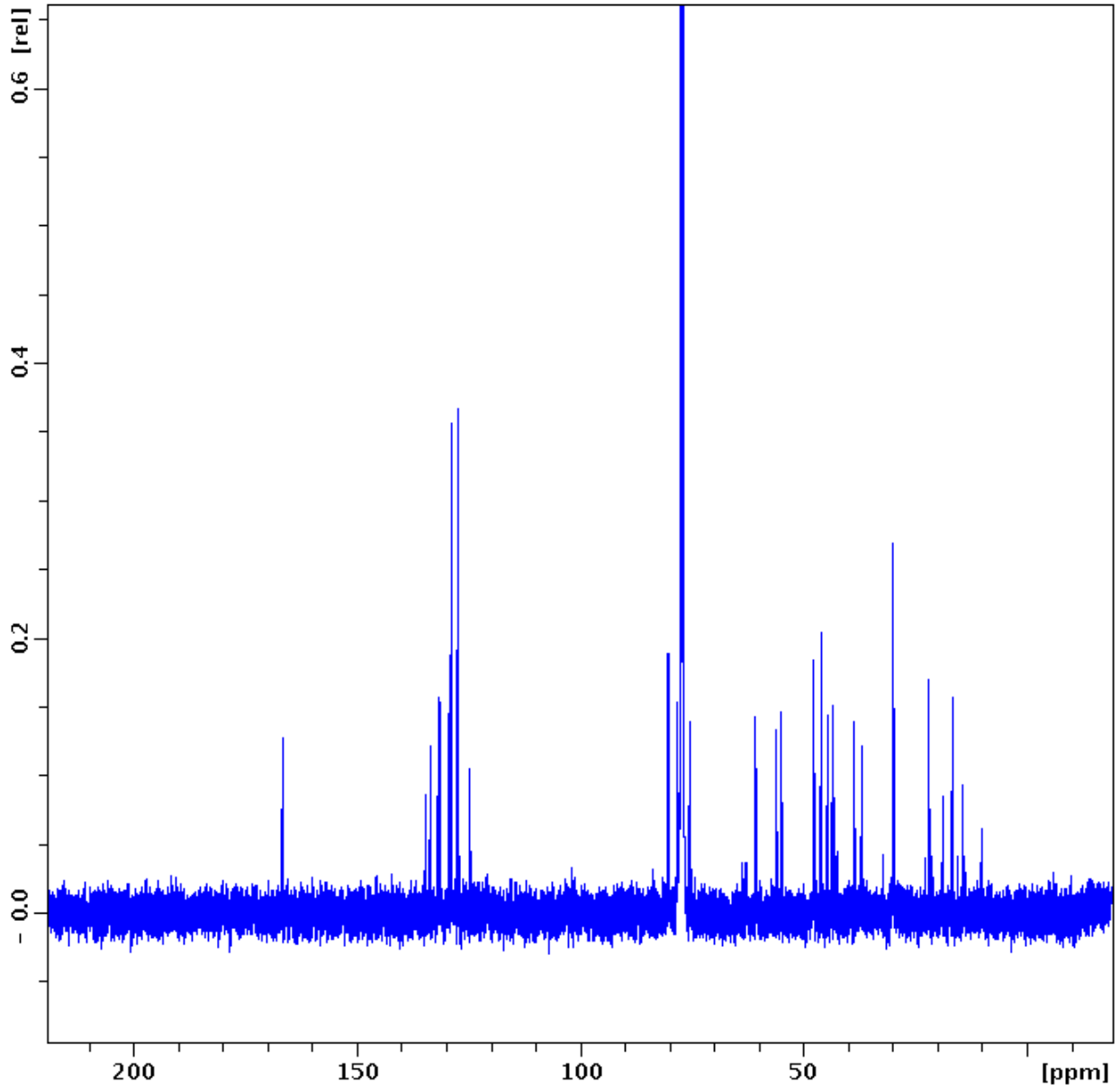

A2. ^{13}C-NMR spectrum of compound **(123)** in $CDCl_3$.

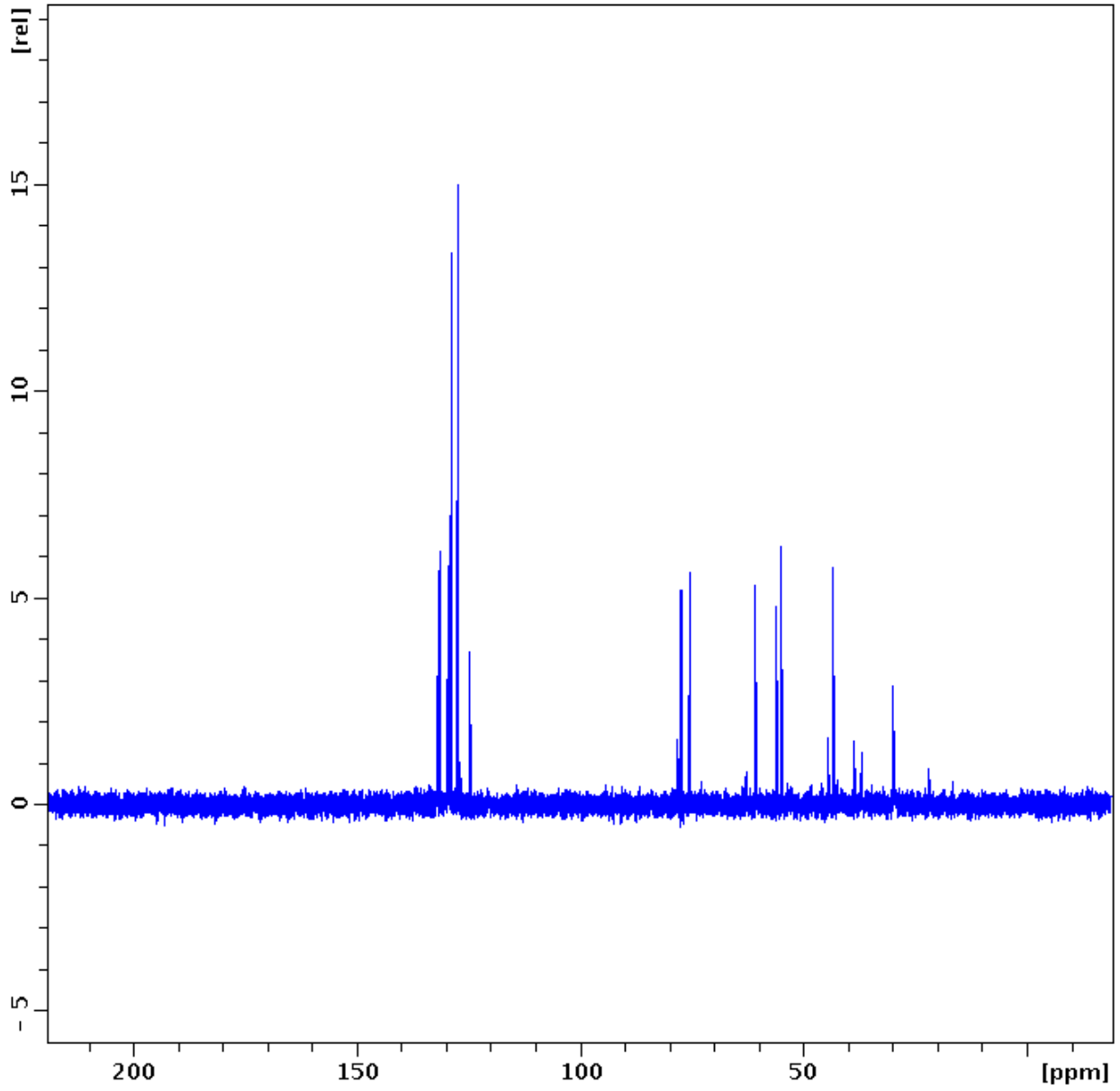

A3. DEPT 90 spectrum of compound **(123)** in $CDCl_3$.

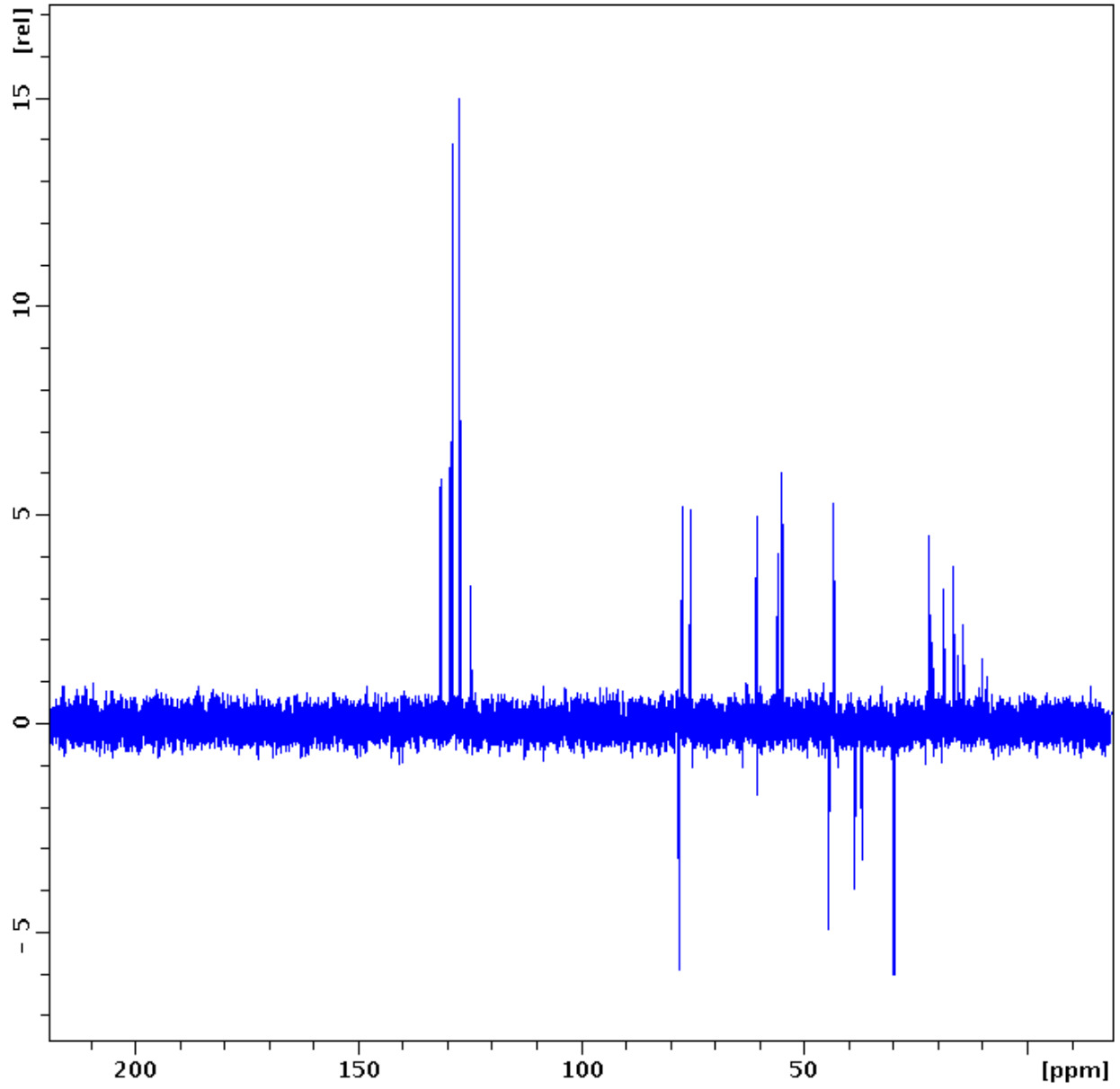

A4. DEPT 135 spectrum of compound **(123)** in $CDCl_3$.

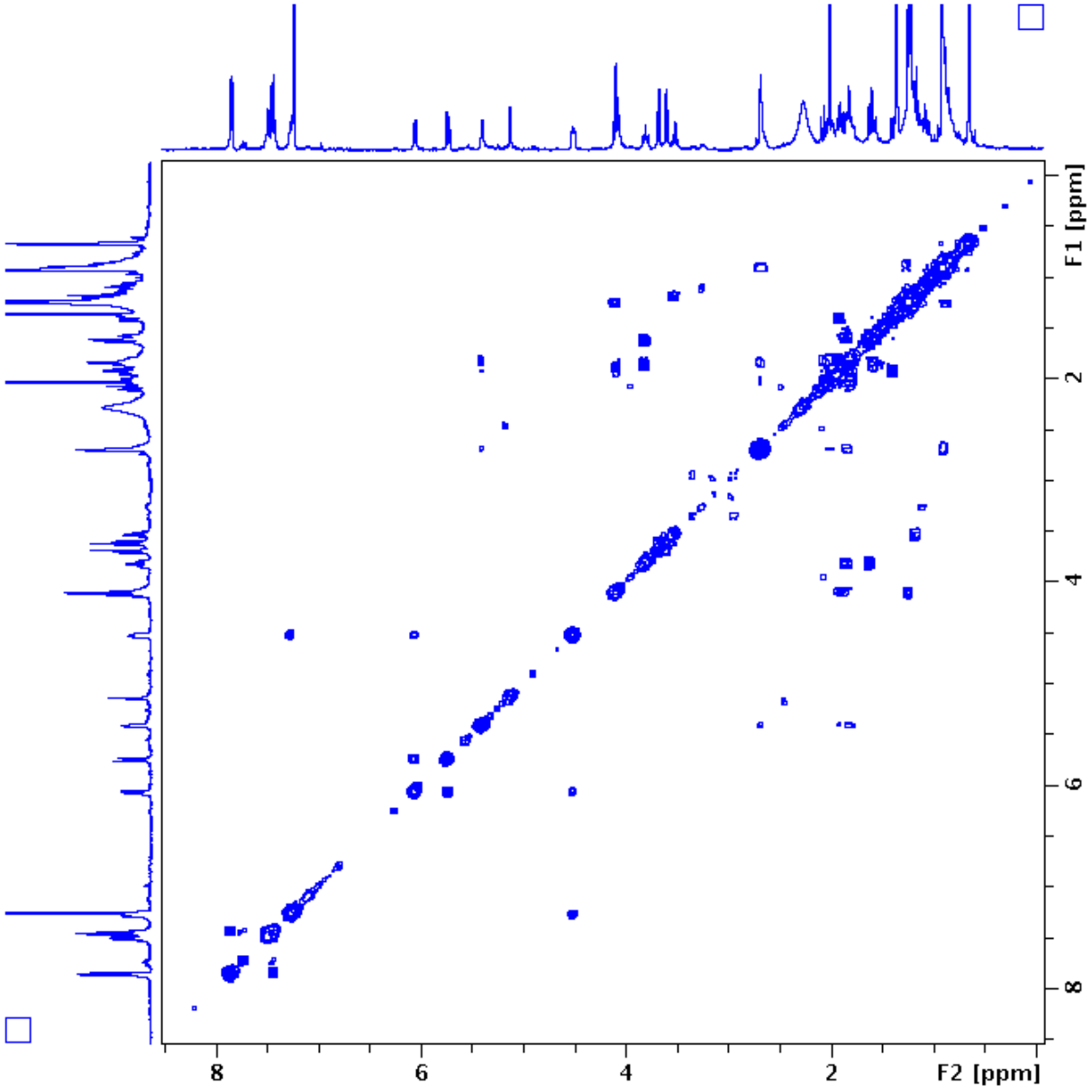

A5. COSY spectrum of compound **(123)** in $CDCl_3$.

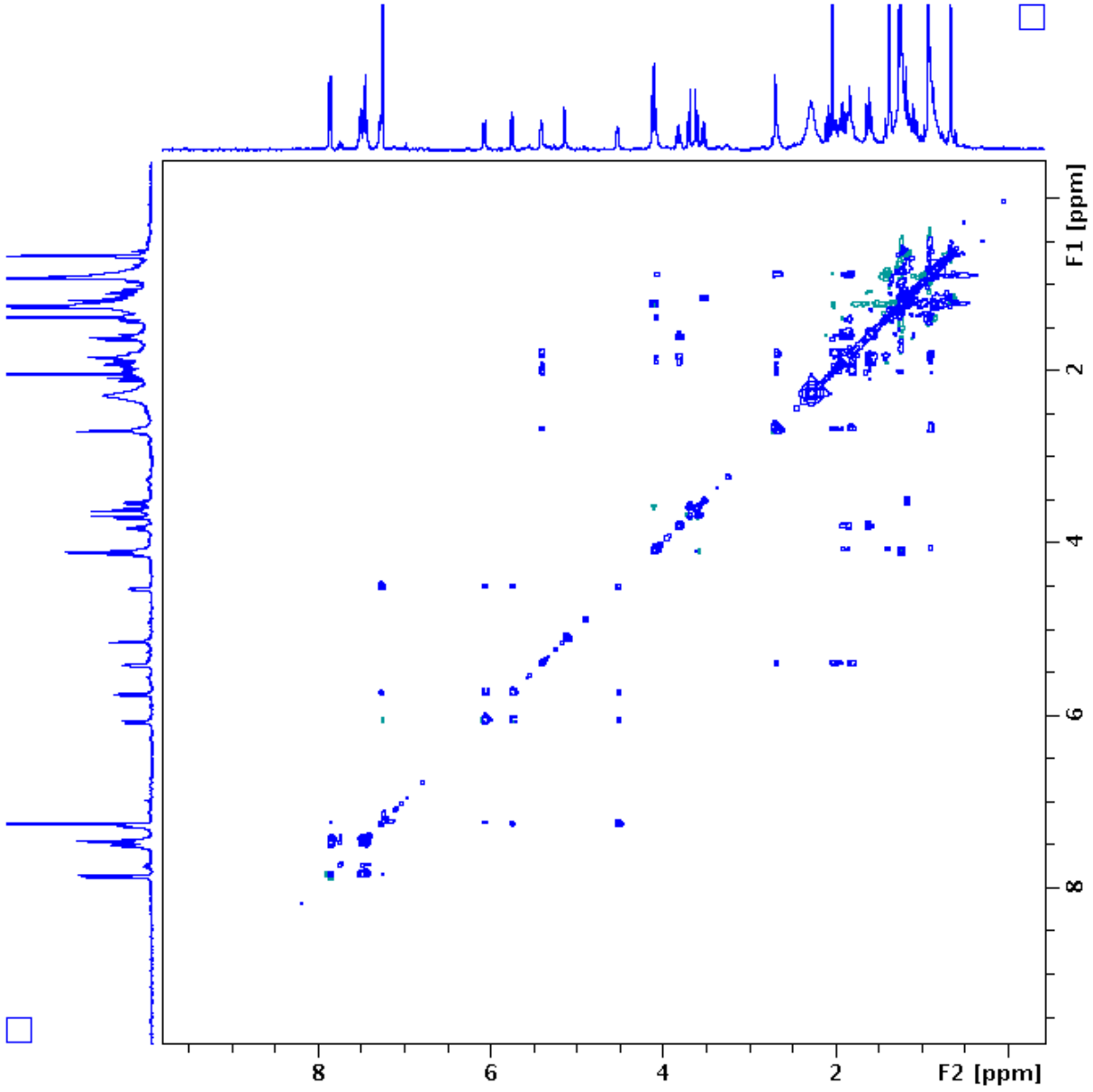

A6. TOCSY spectrum of compound **(123)** in $CDCl_3$.

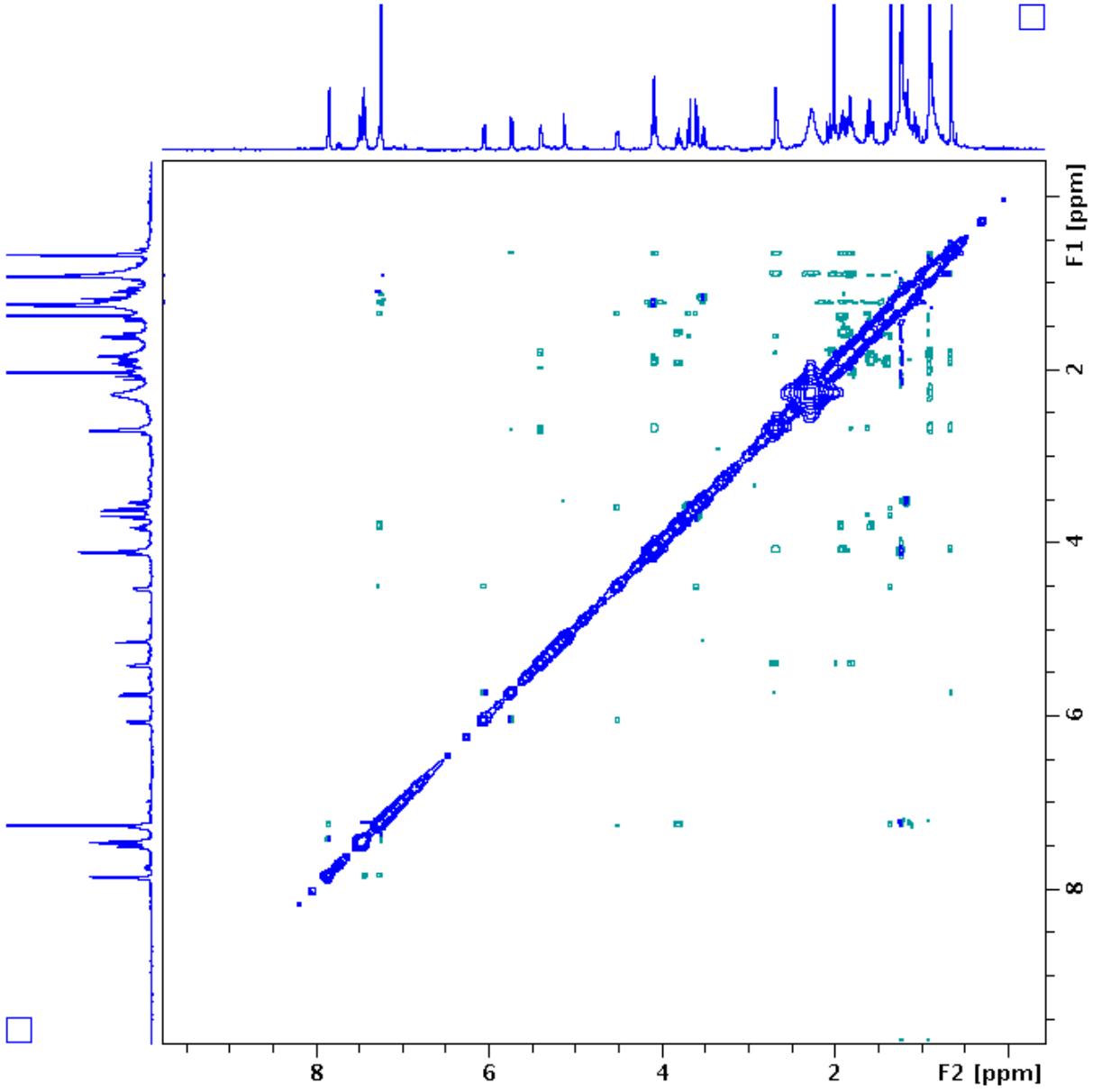

A7. NOESY spectrum of compound **(123)** in $CDCl_3$.

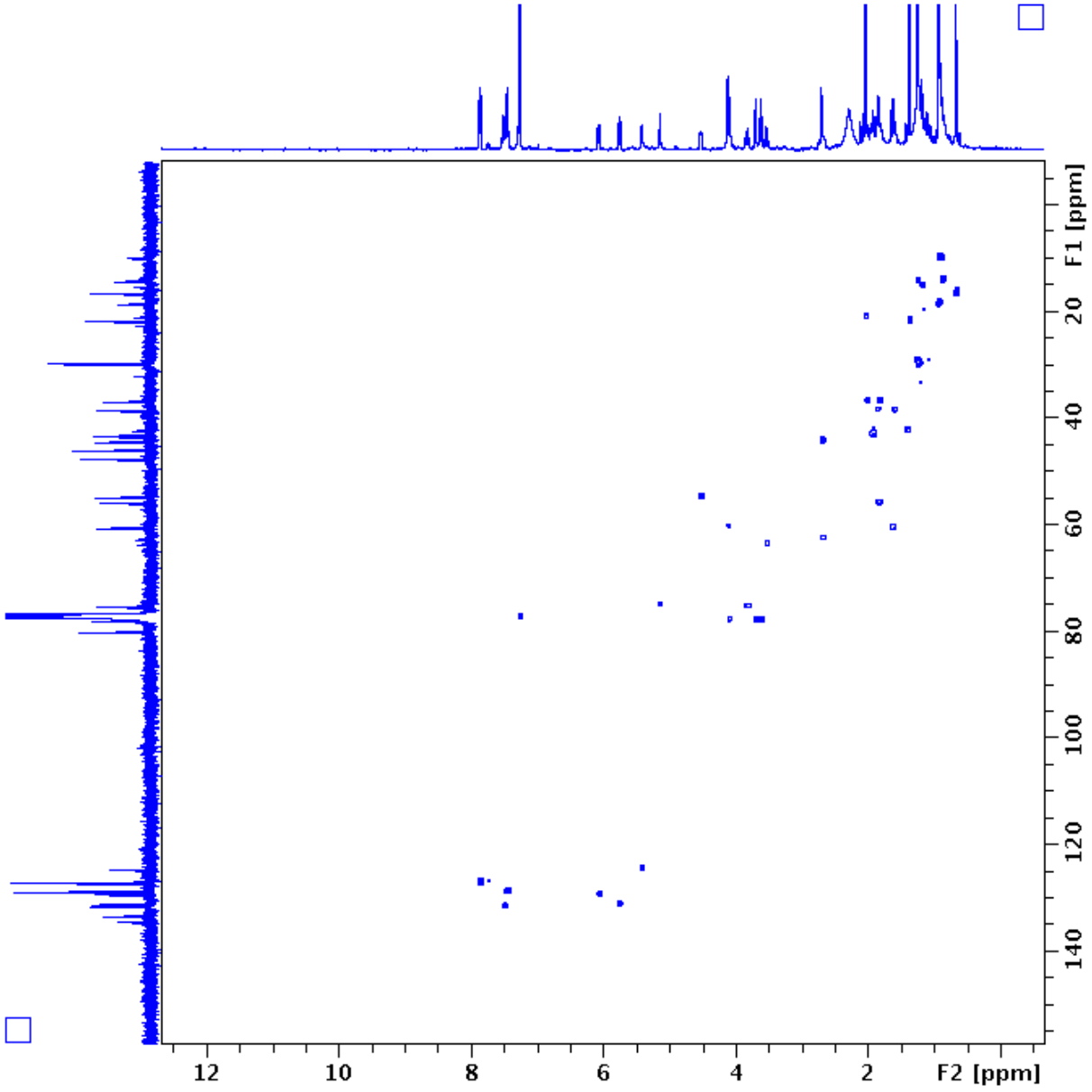

A8. HMBC spectrum of compound **(123)** in $CDCl_3$.

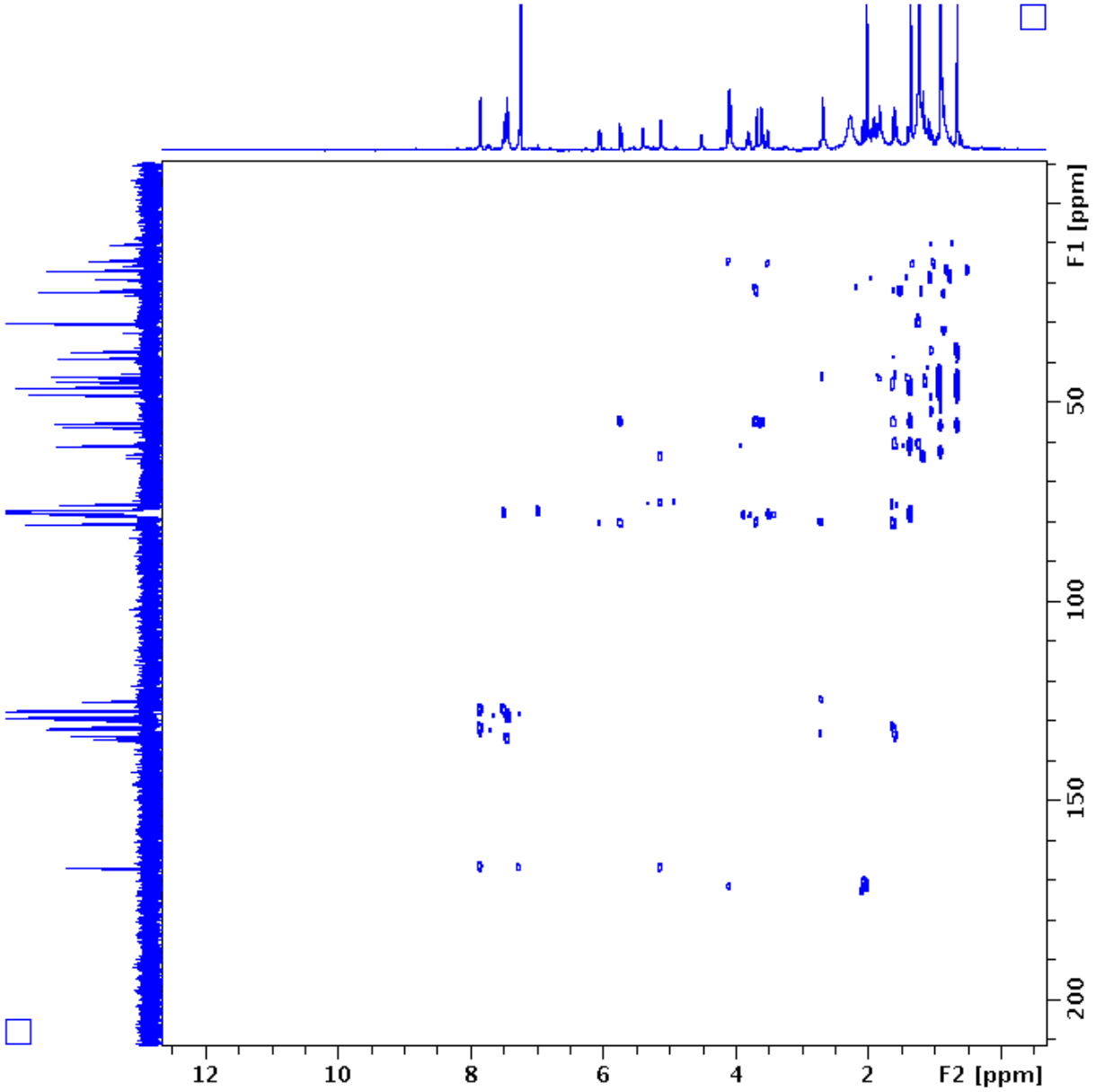

A9. HMBC spectrum of compound **(123)** in $CDCl_3$.

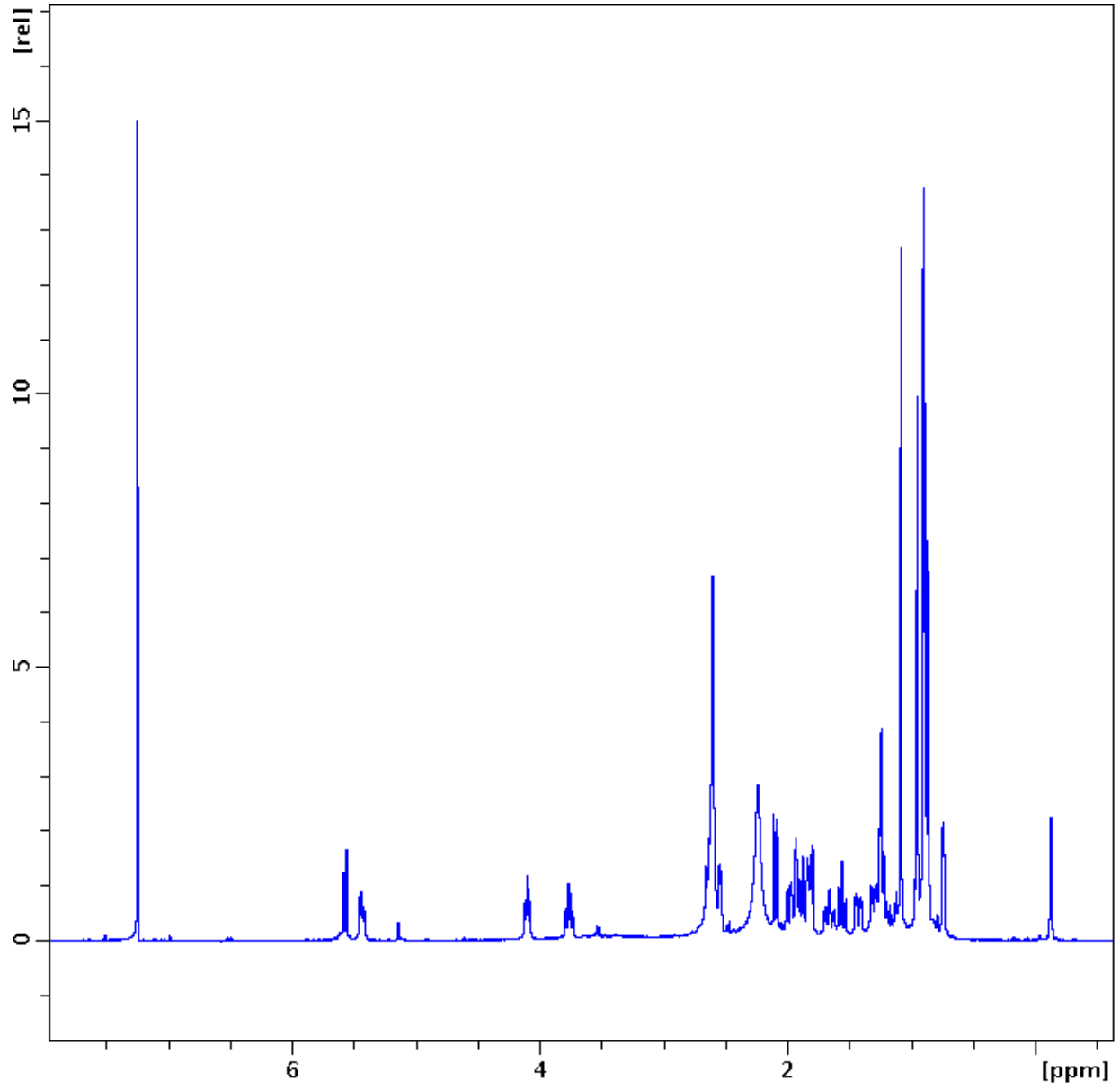

A10. ^{1}H-NMR spectrum of compound **(124)** in $CDCl_3$.

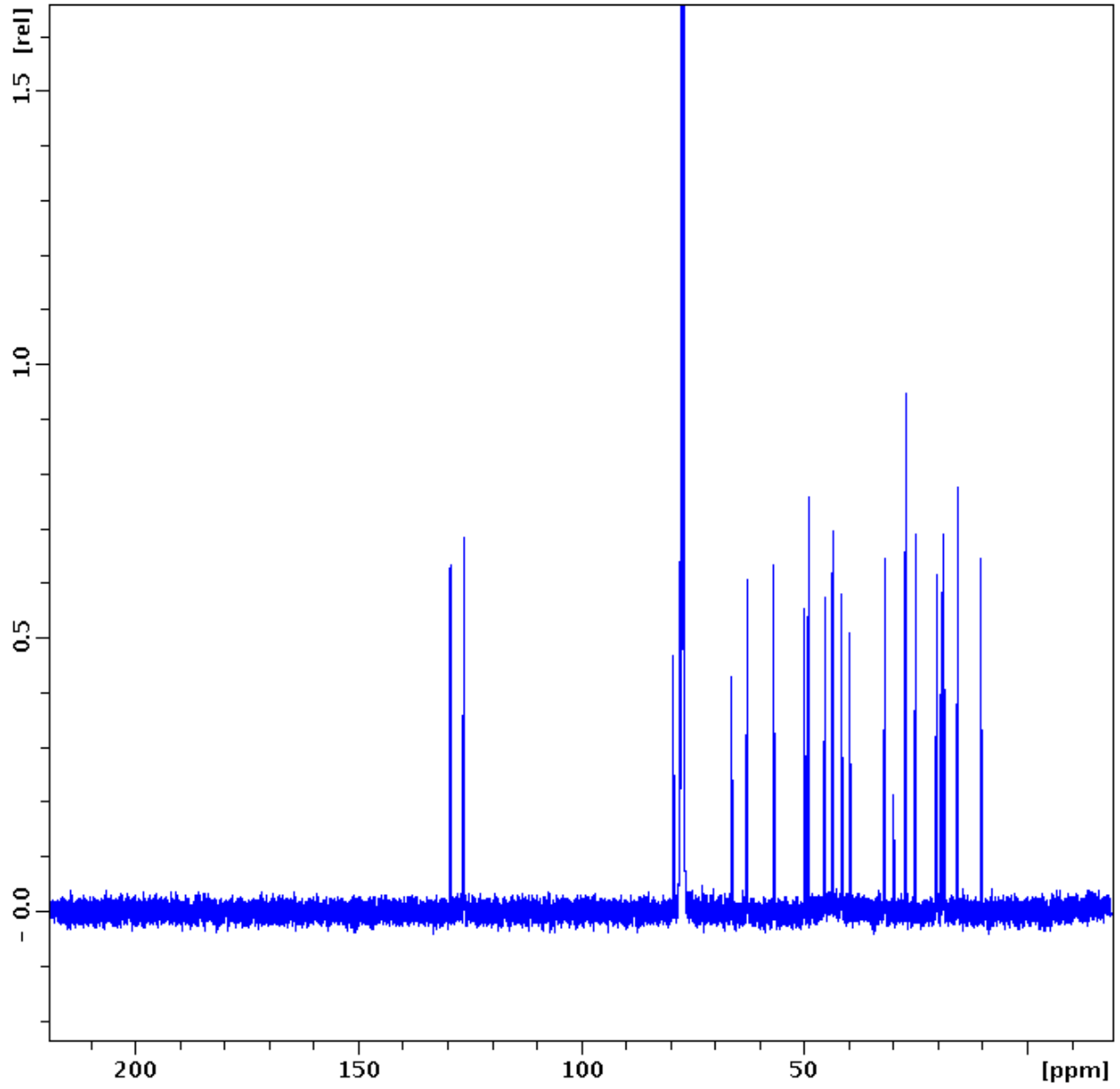

A11. ^{13}C-NMR spectrum of compound **(124)** in $CDCl_3$.

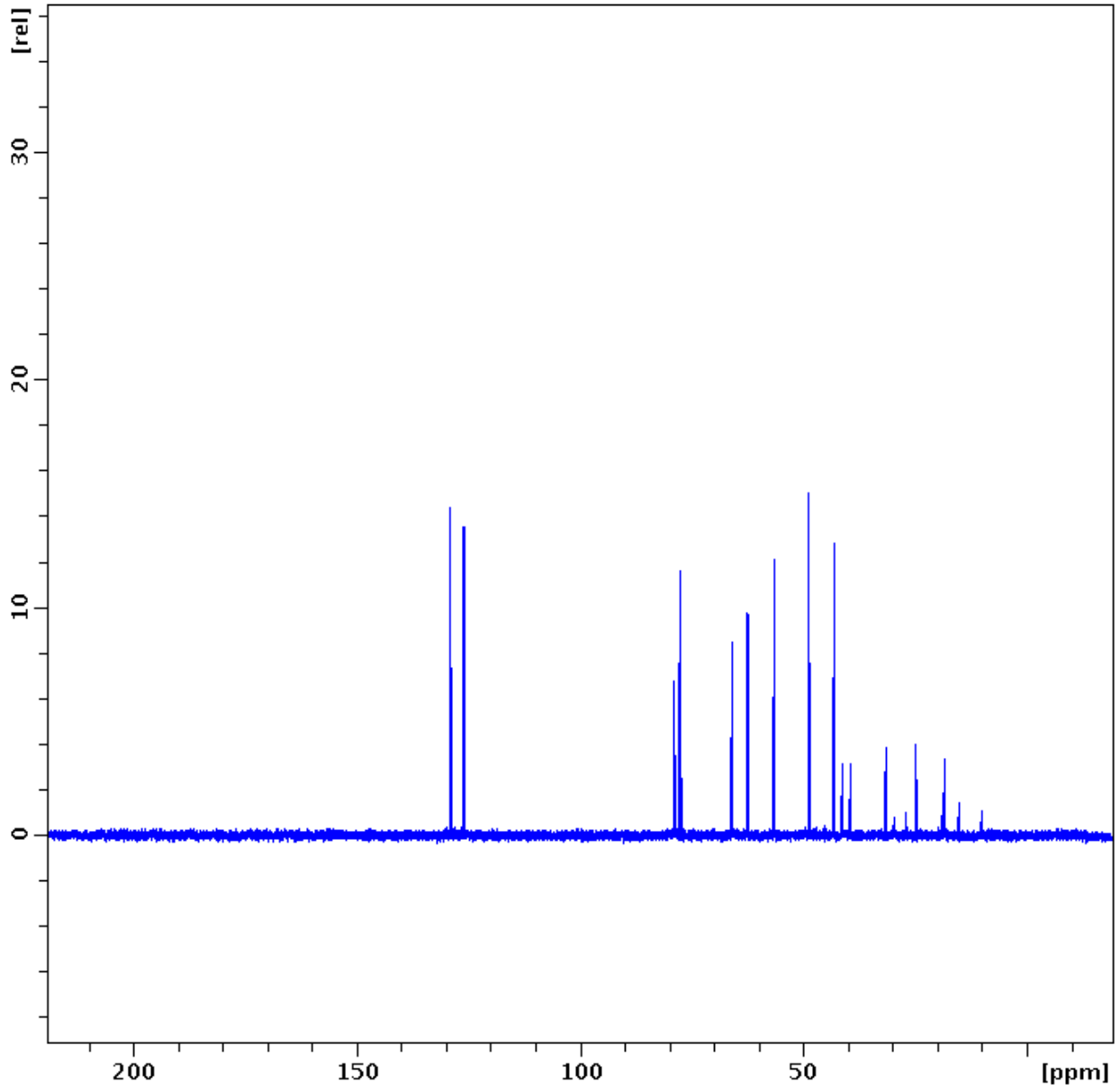

A12. DEPT 90 spectrum of compound **(124)** in $CDCl_3$.

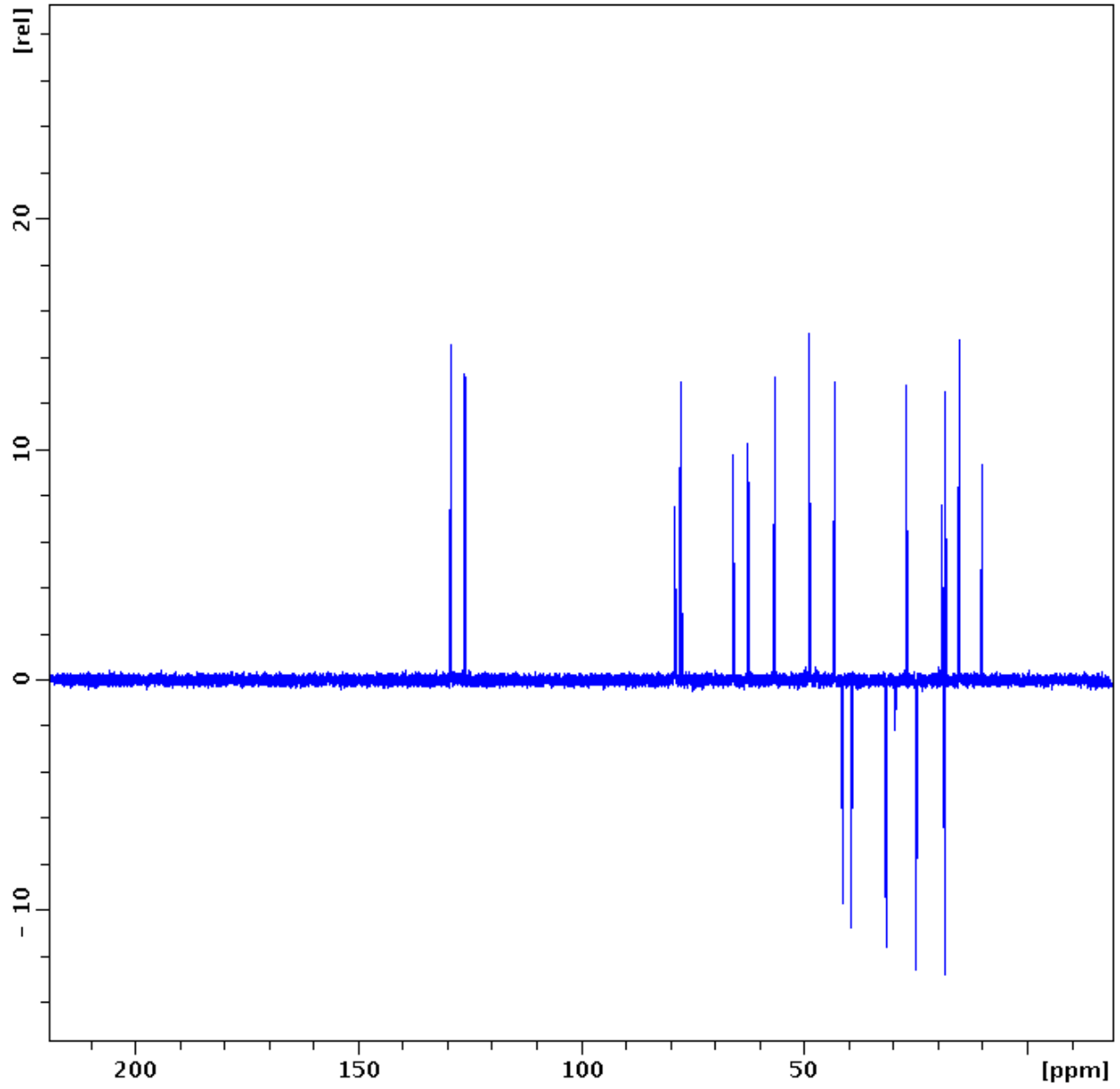

A13. DEPT 135 spectrum of compound **(124)** in $CDCl_3$.

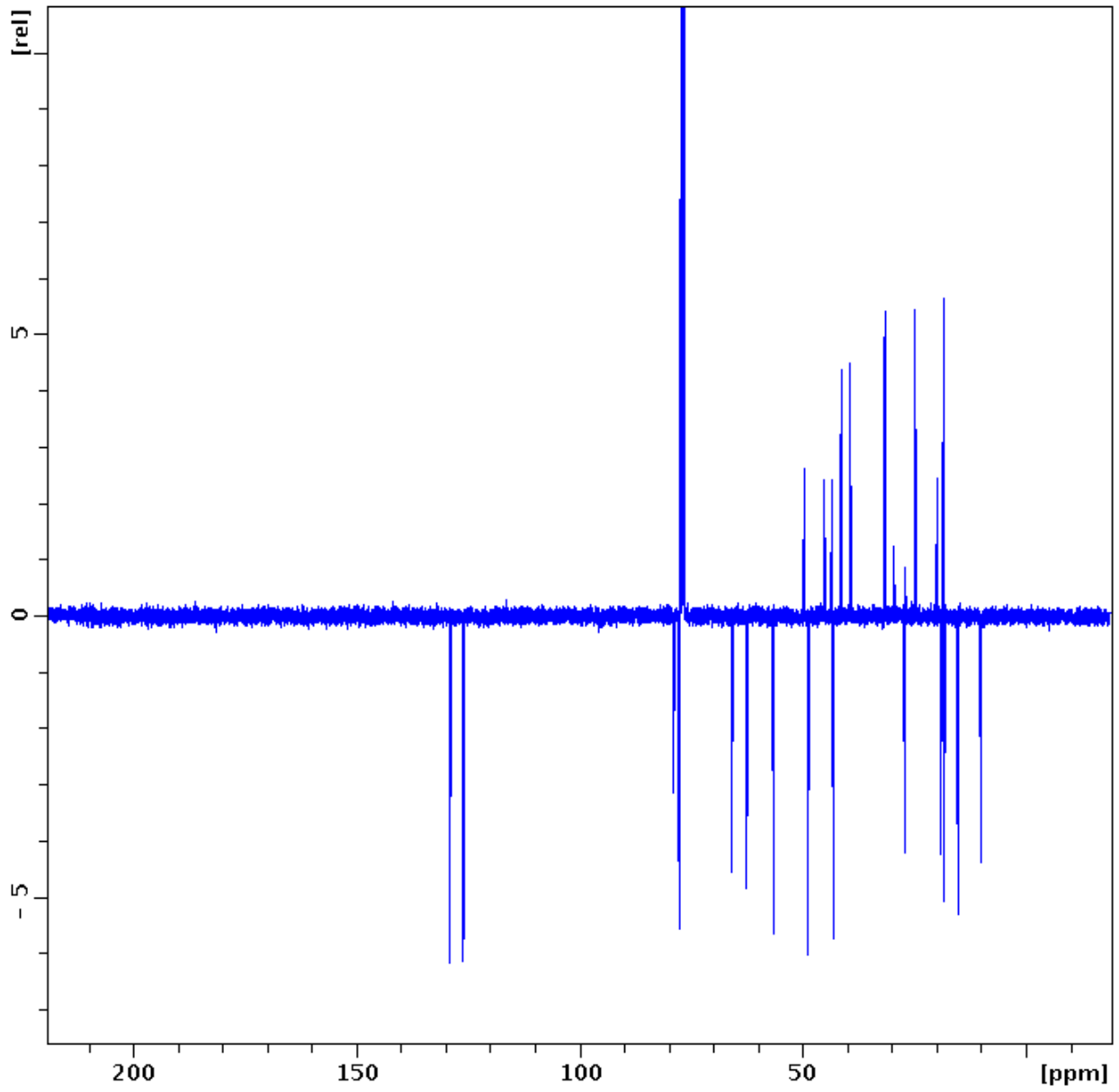

A14. APT spectrum of compound **(124)** in $CDCl_3$.

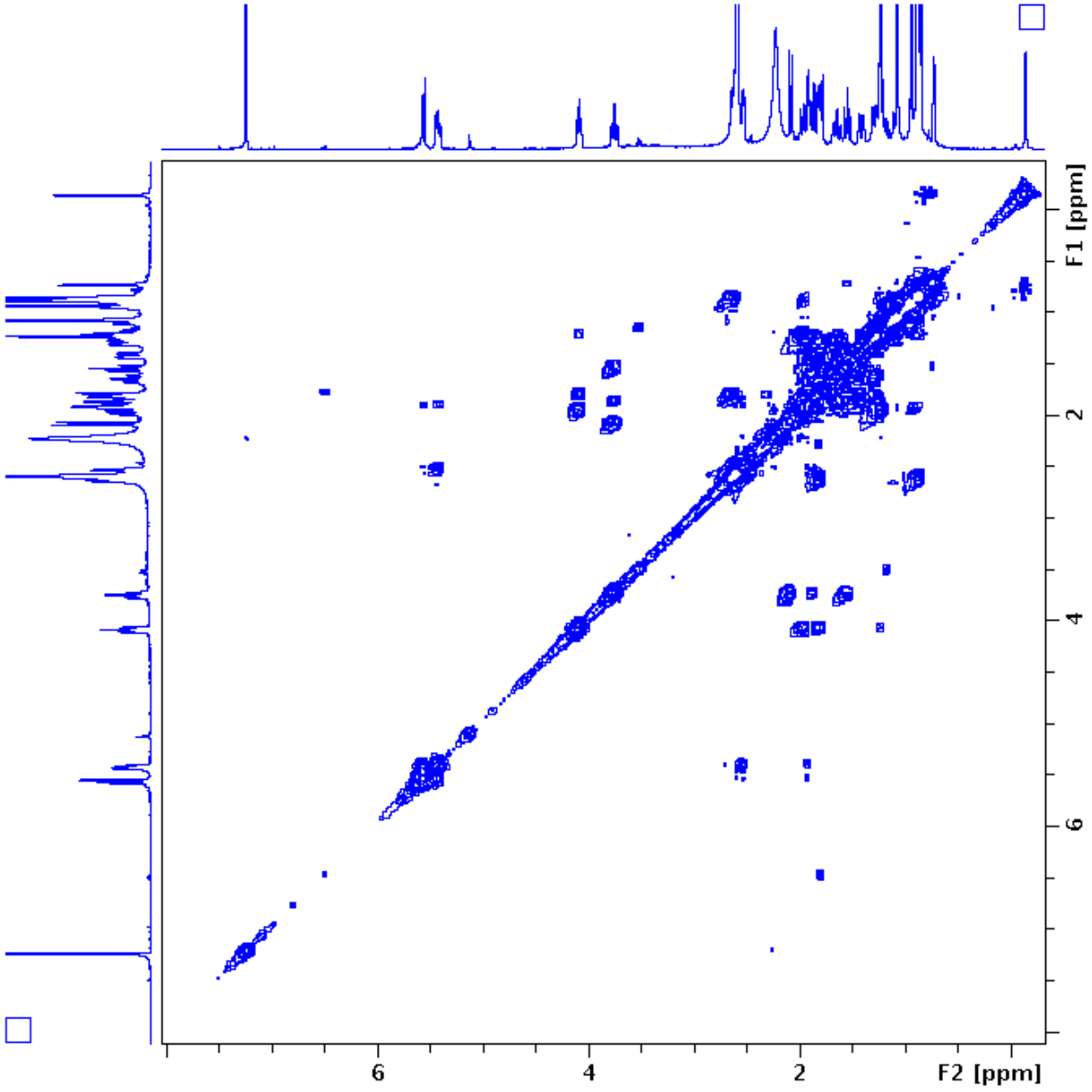

A15. COSY spectrum of compound **(124)** in $CDCl_3$.

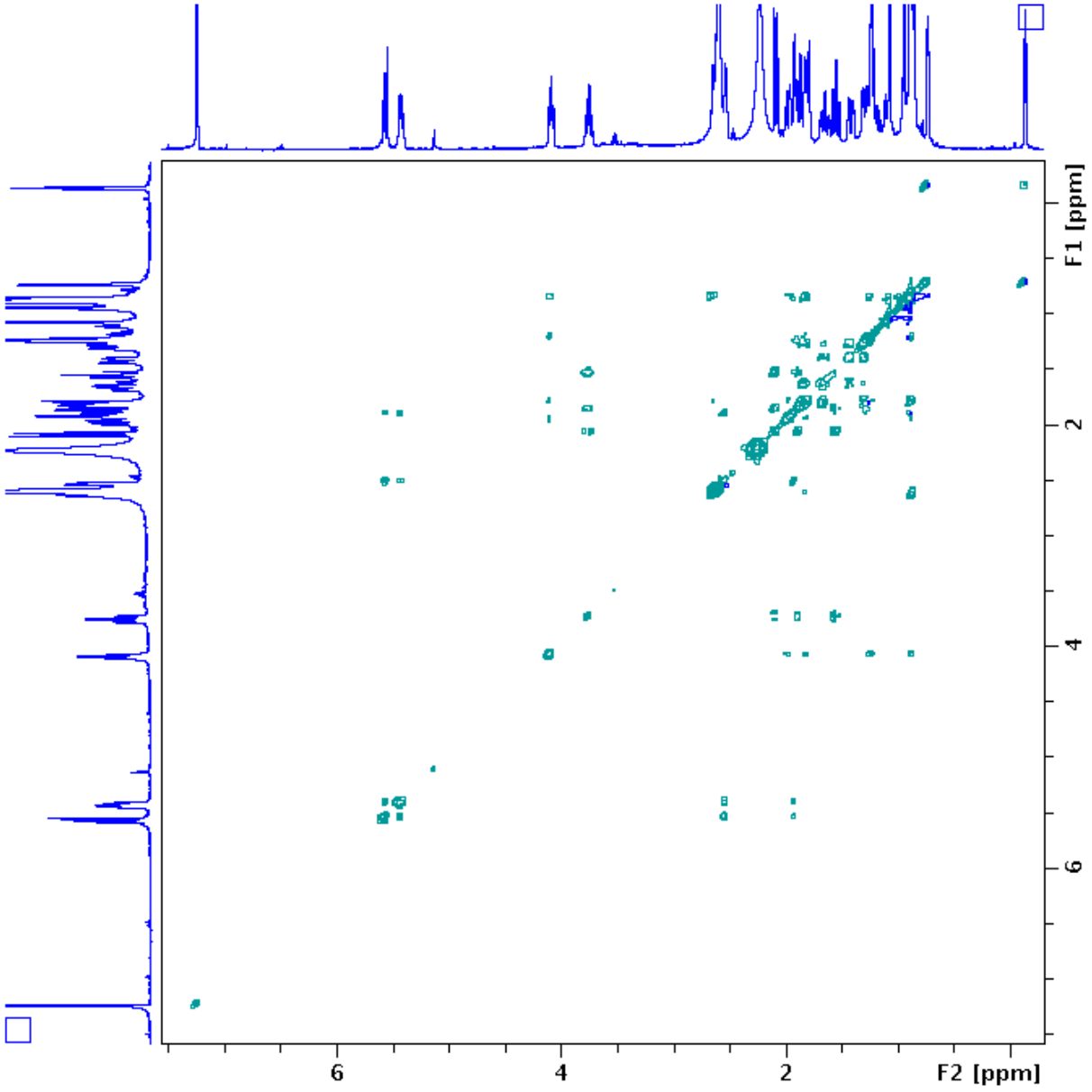

A16. TOCSY spectrum of compound **(124)** in $CDCl_3$.

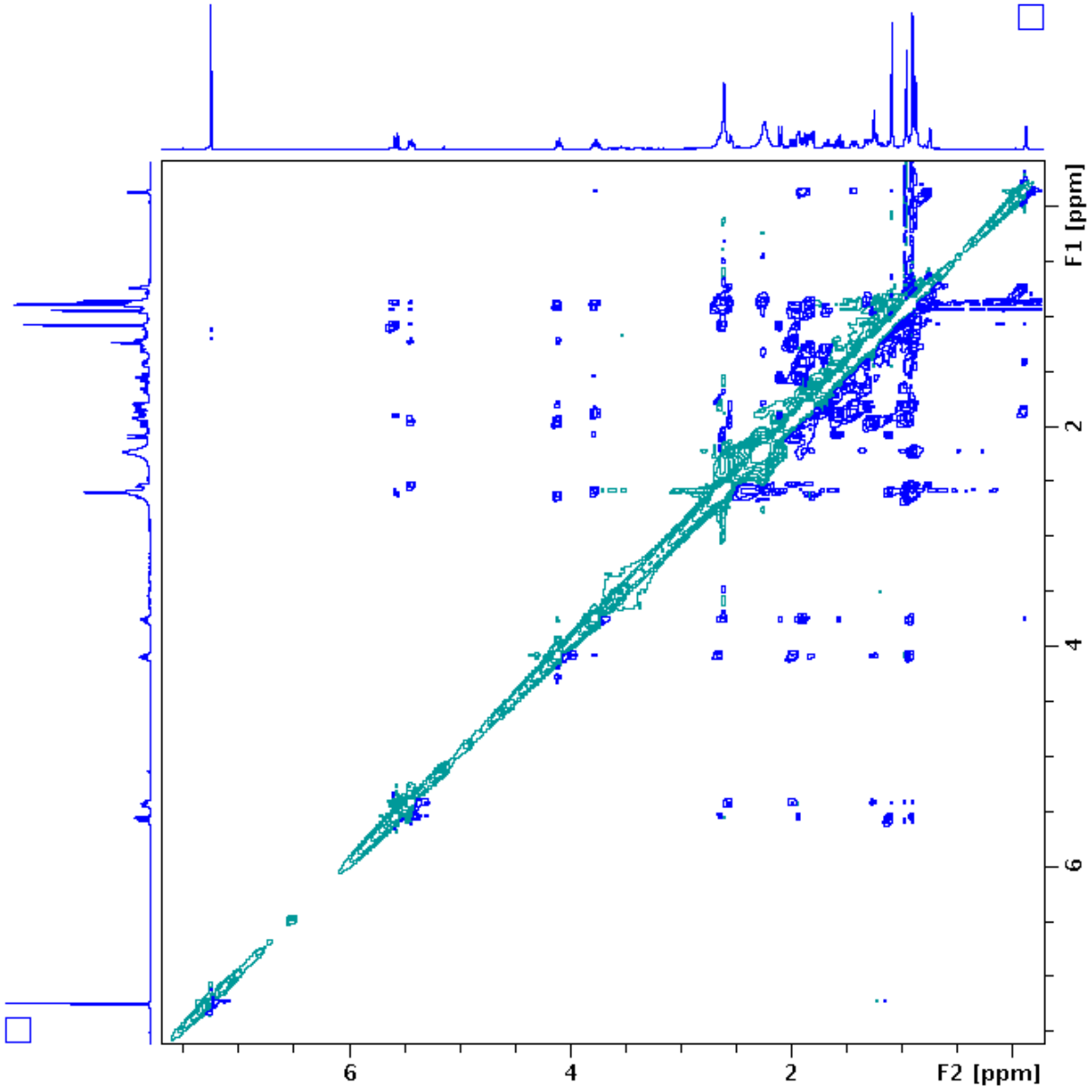

A17. NOESY spectrum of compound **(124)** in $CDCl_3$.

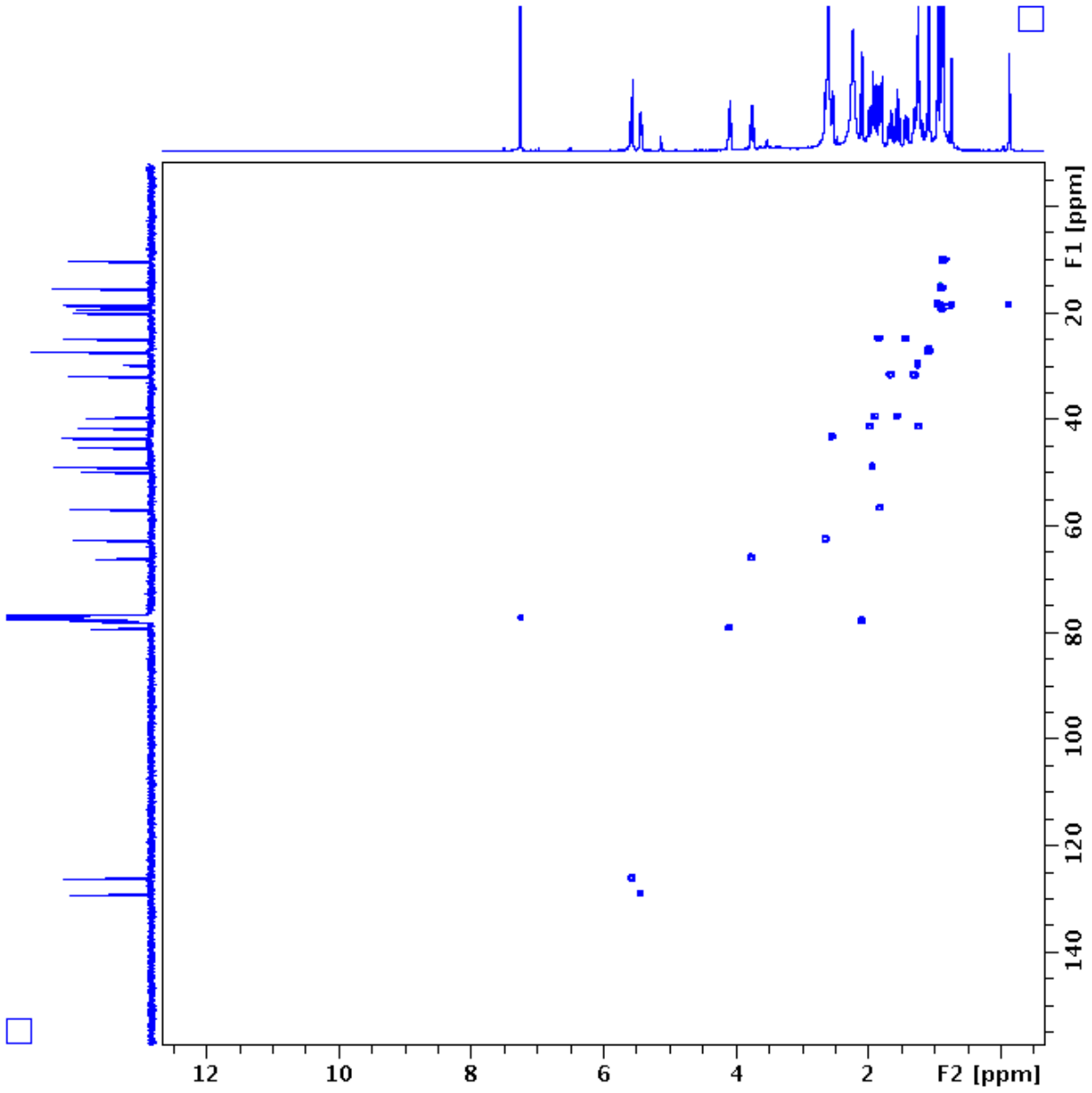

A18. HSQC spectrum of compound **(124)** in $CDCl_3$.

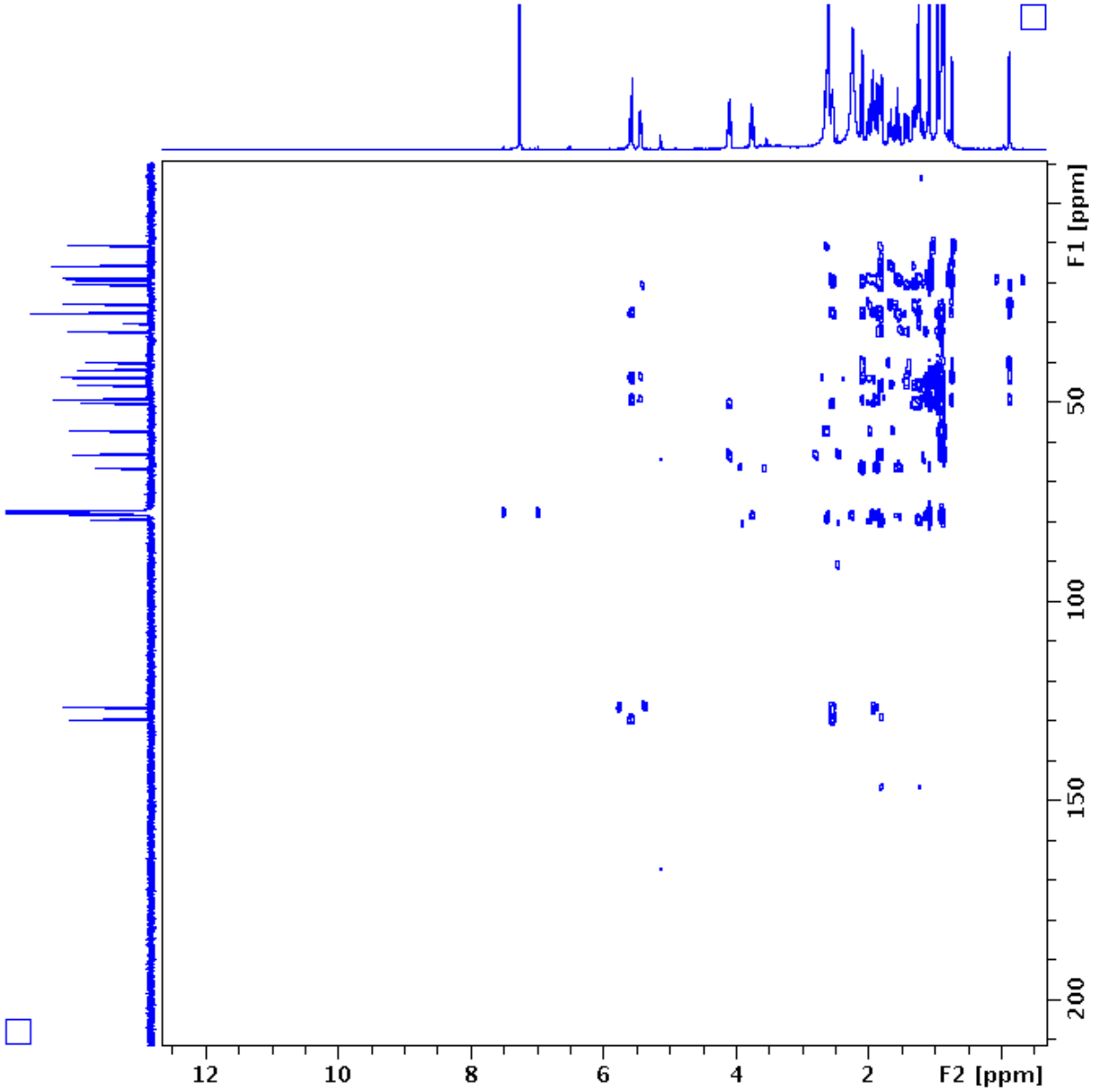

A19. HMBC spectrum of compound **(124)** in $CDCl_3$.

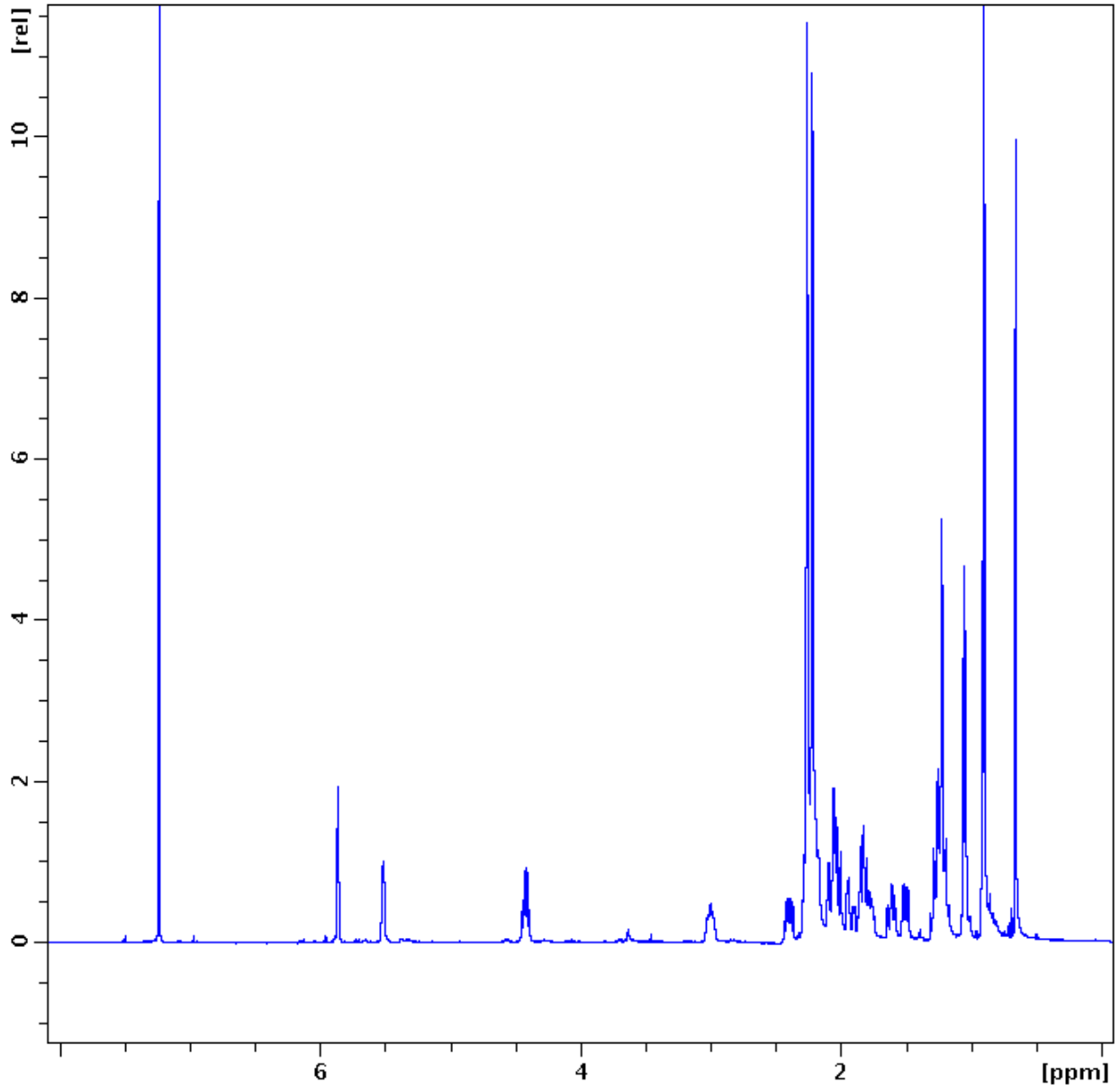

A20. ^{1}H-NMR spectrum of compound **(125)** in $CDCl_3$.

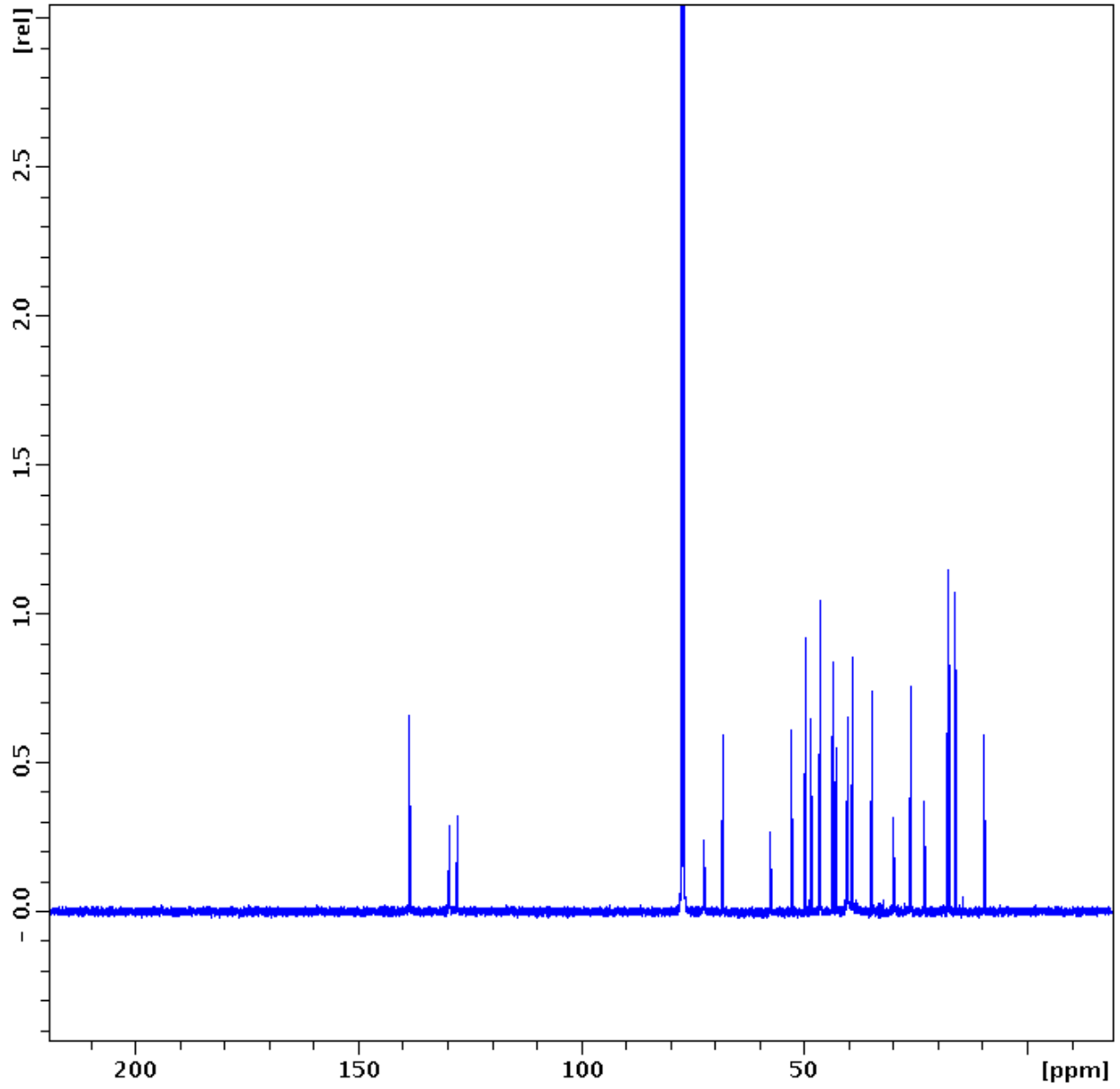

A21. ^{13}C-NMR spectrum of compound **(125)** in $CDCl_3$.

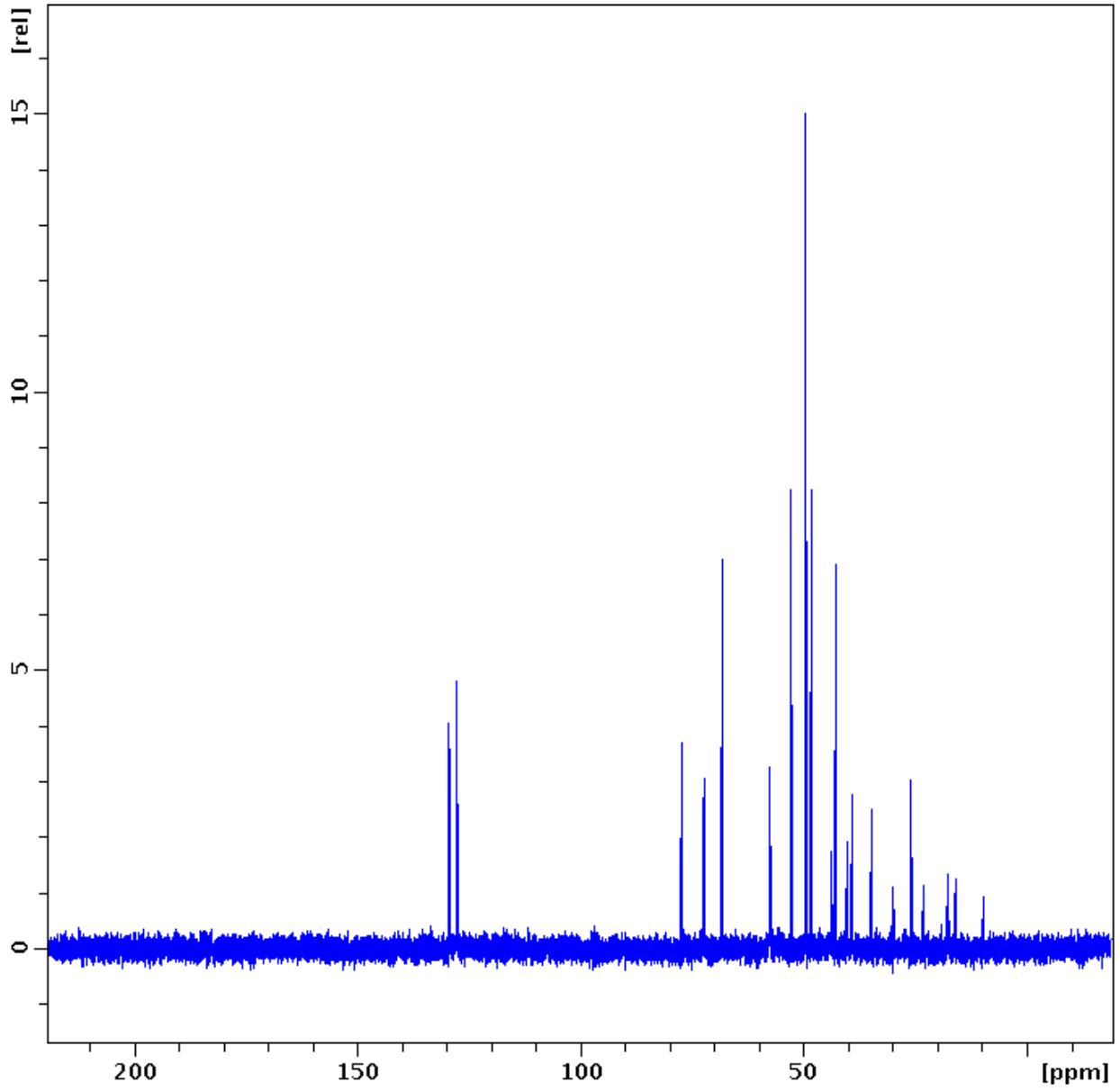

A22. DEPT 90 spectrum of compound **(125)** in $CDCl_3$.

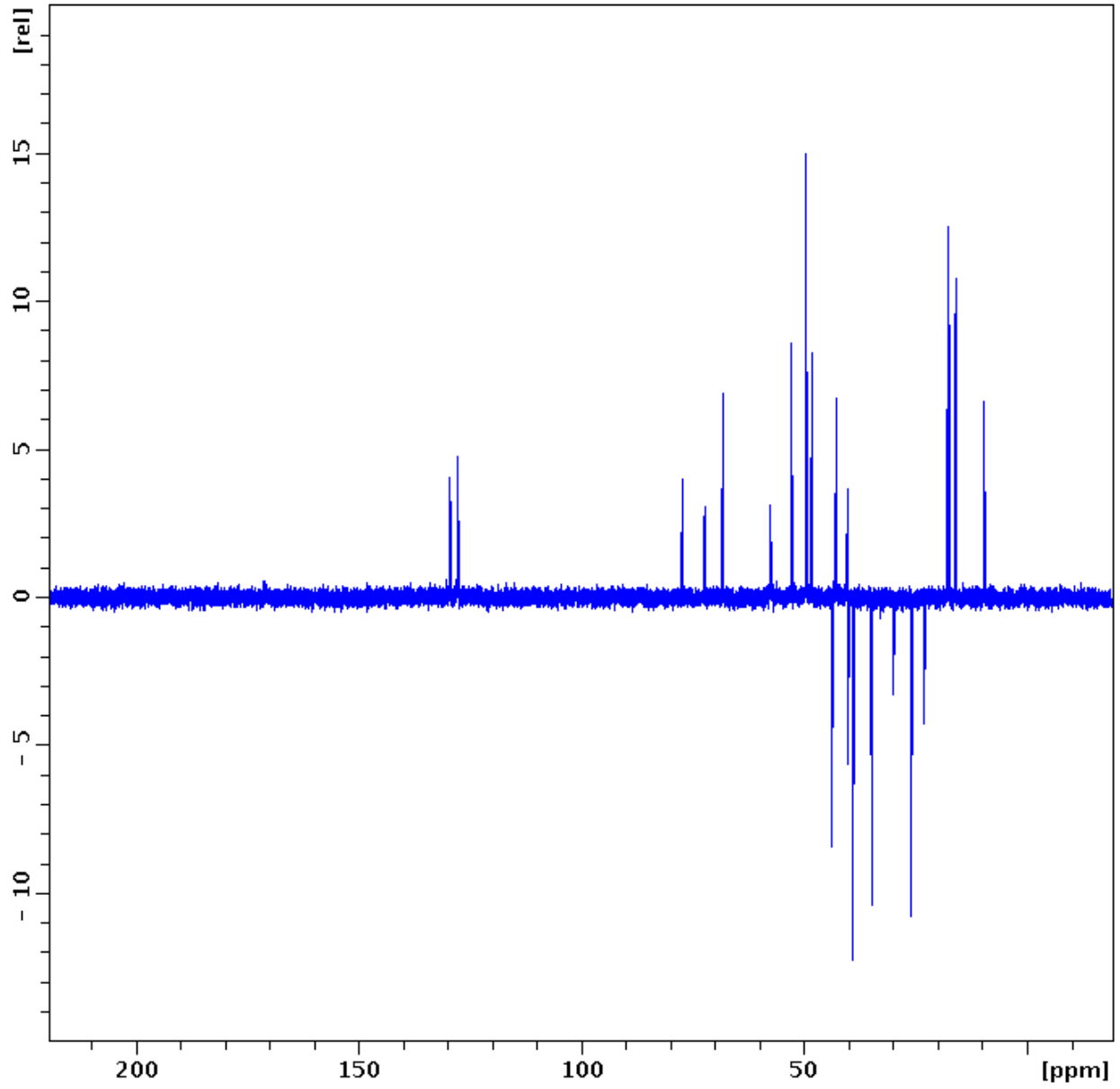

A23. DEPT 135 spectrum of compound **(125)** in $CDCl_3$.

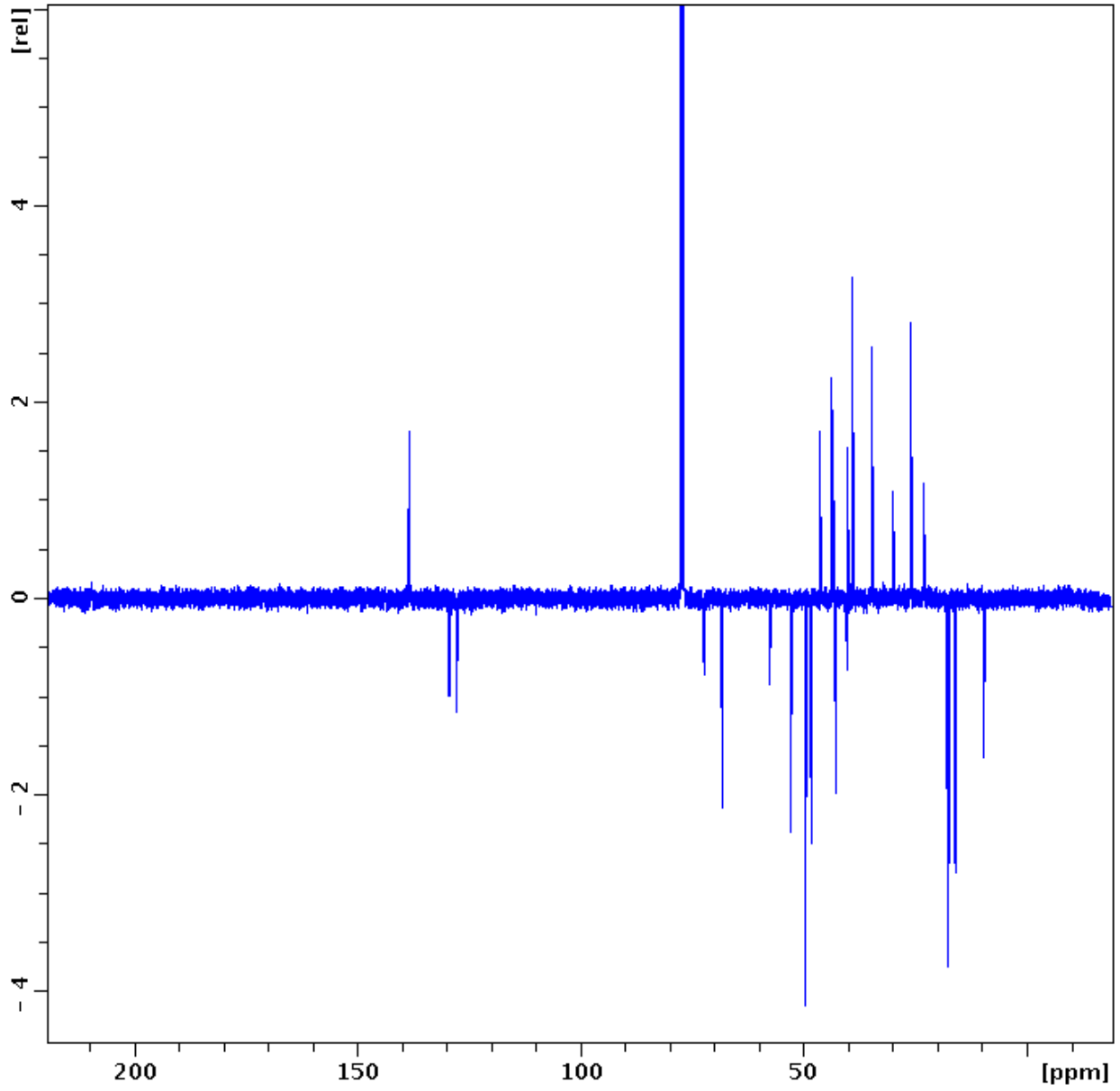

A24. APT spectrum of compound **(125)** in $CDCl_3$.

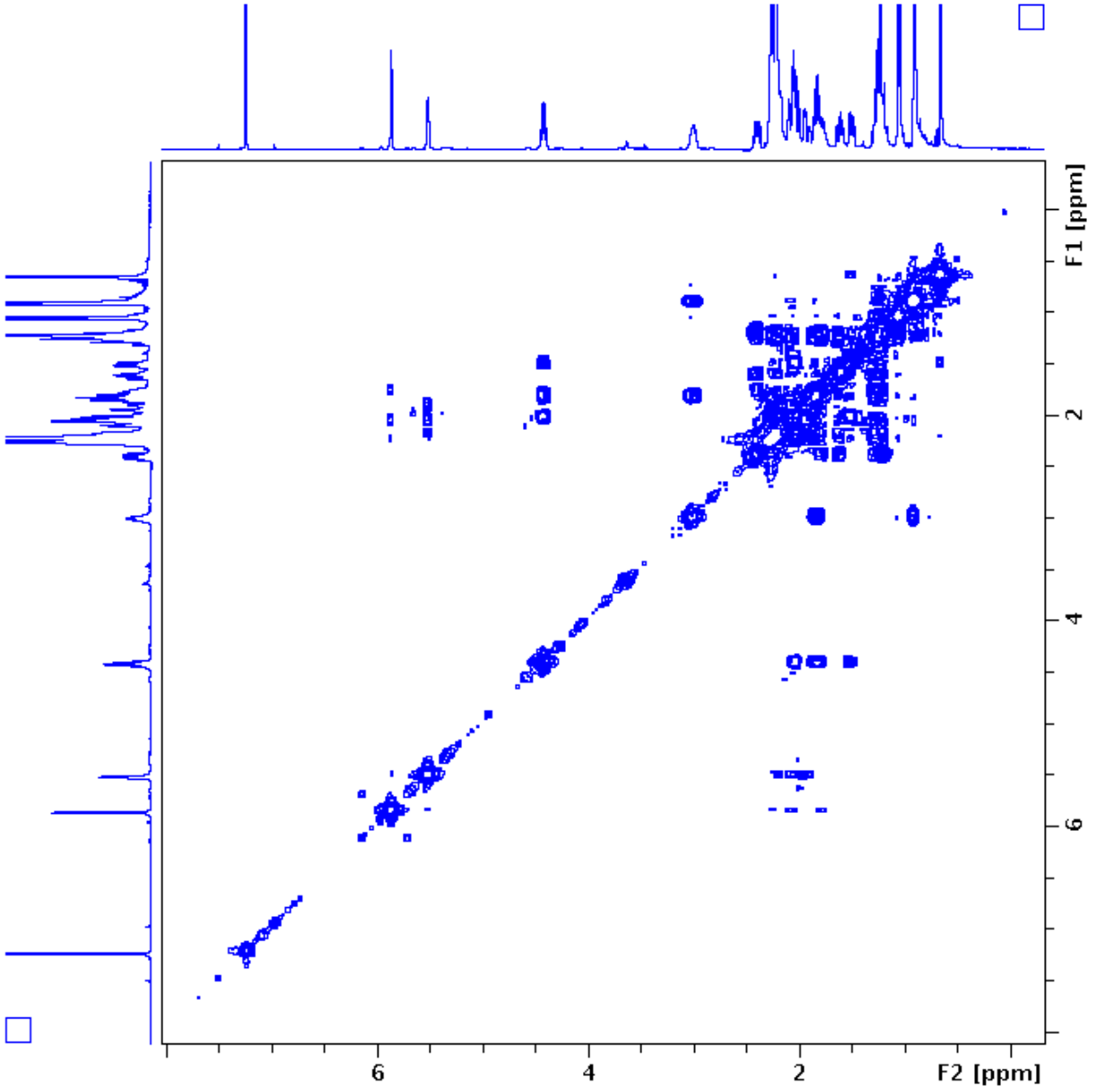

A25. COSY spectrum of compound **(125)** in $CDCl_3$.

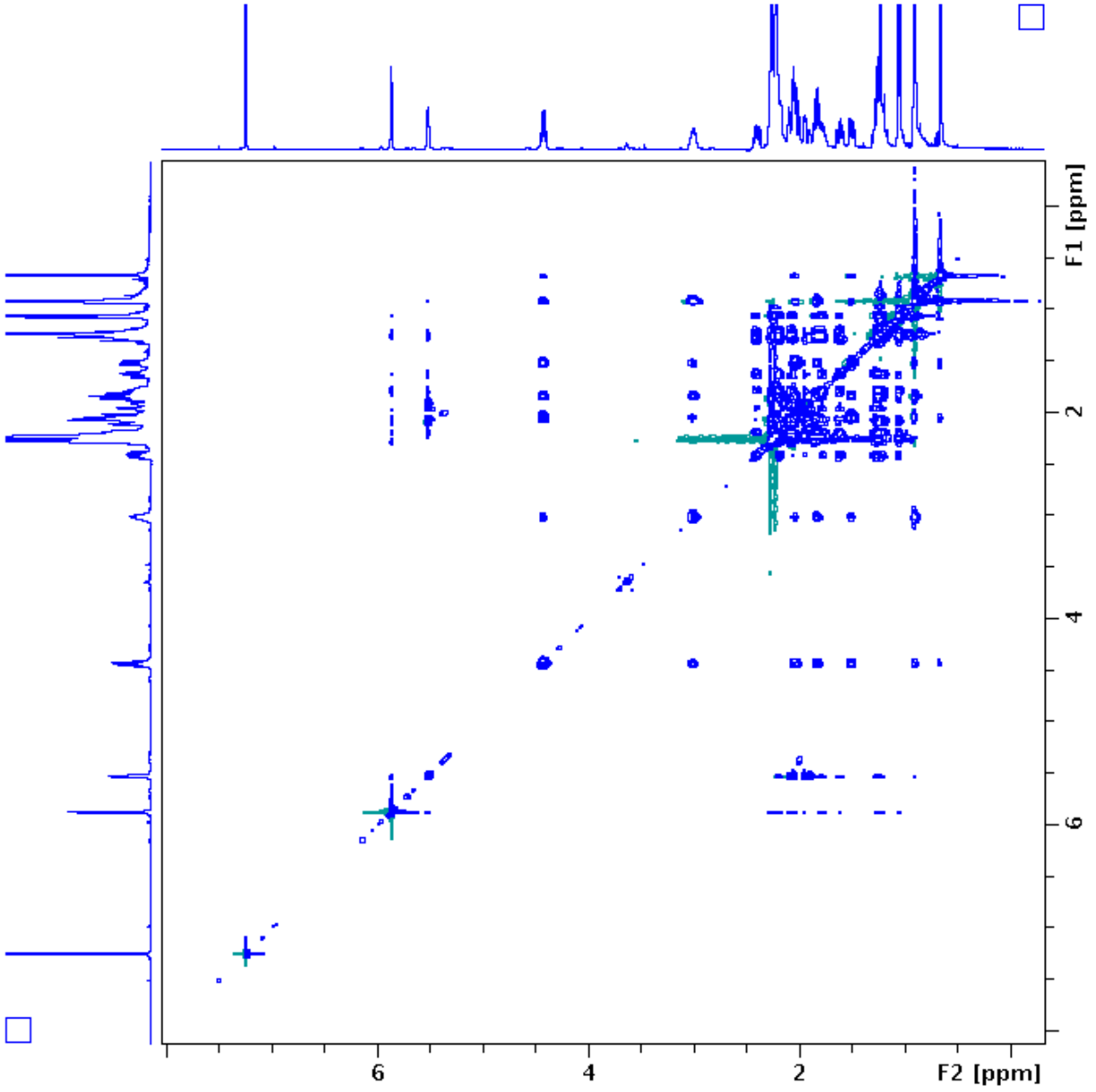

A26. TOCSY spectrum of compound **(125)** in $CDCl_3$.

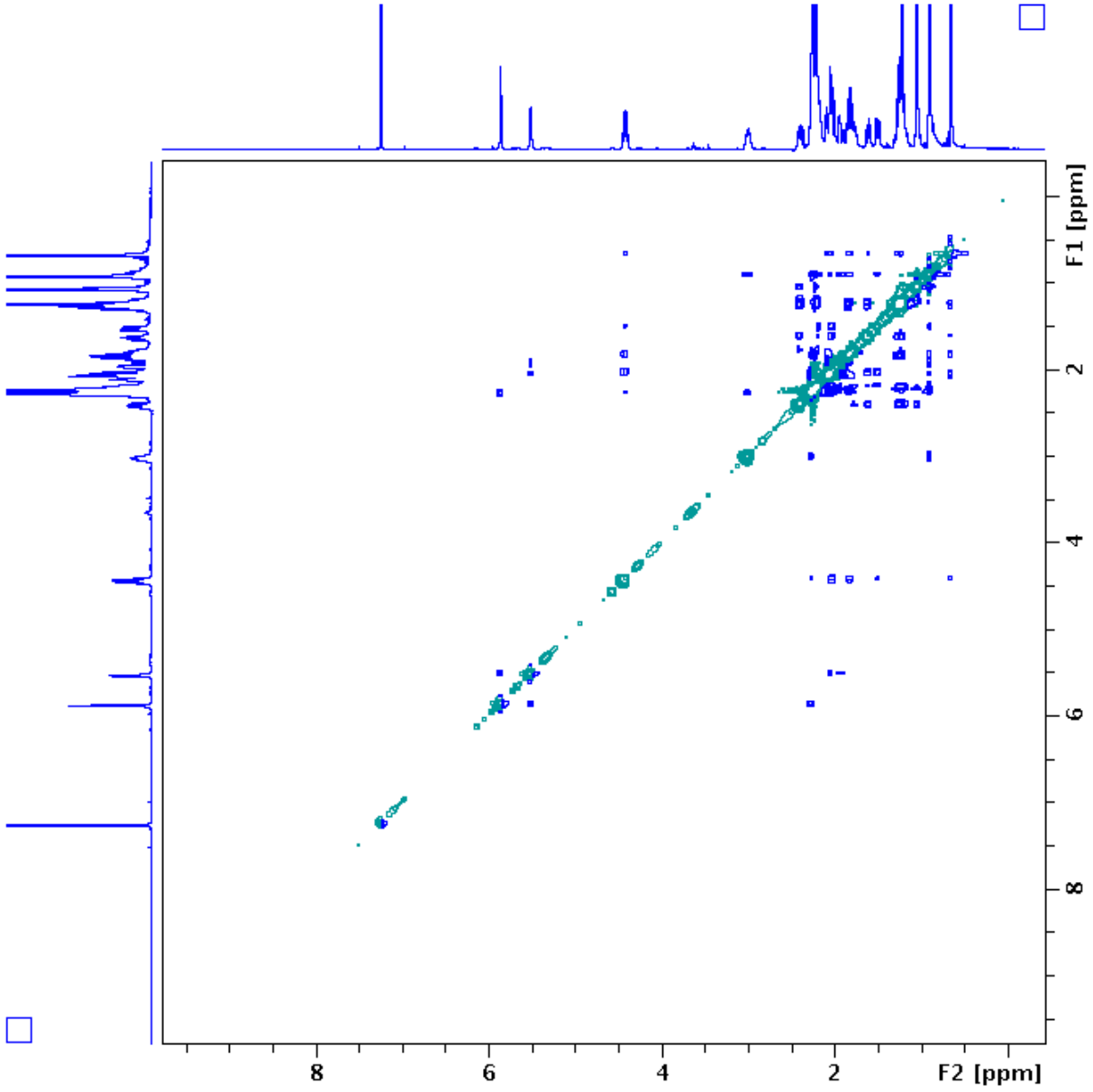

A27. NOESY spectrum of compound **(125)** in $CDCl_3$.

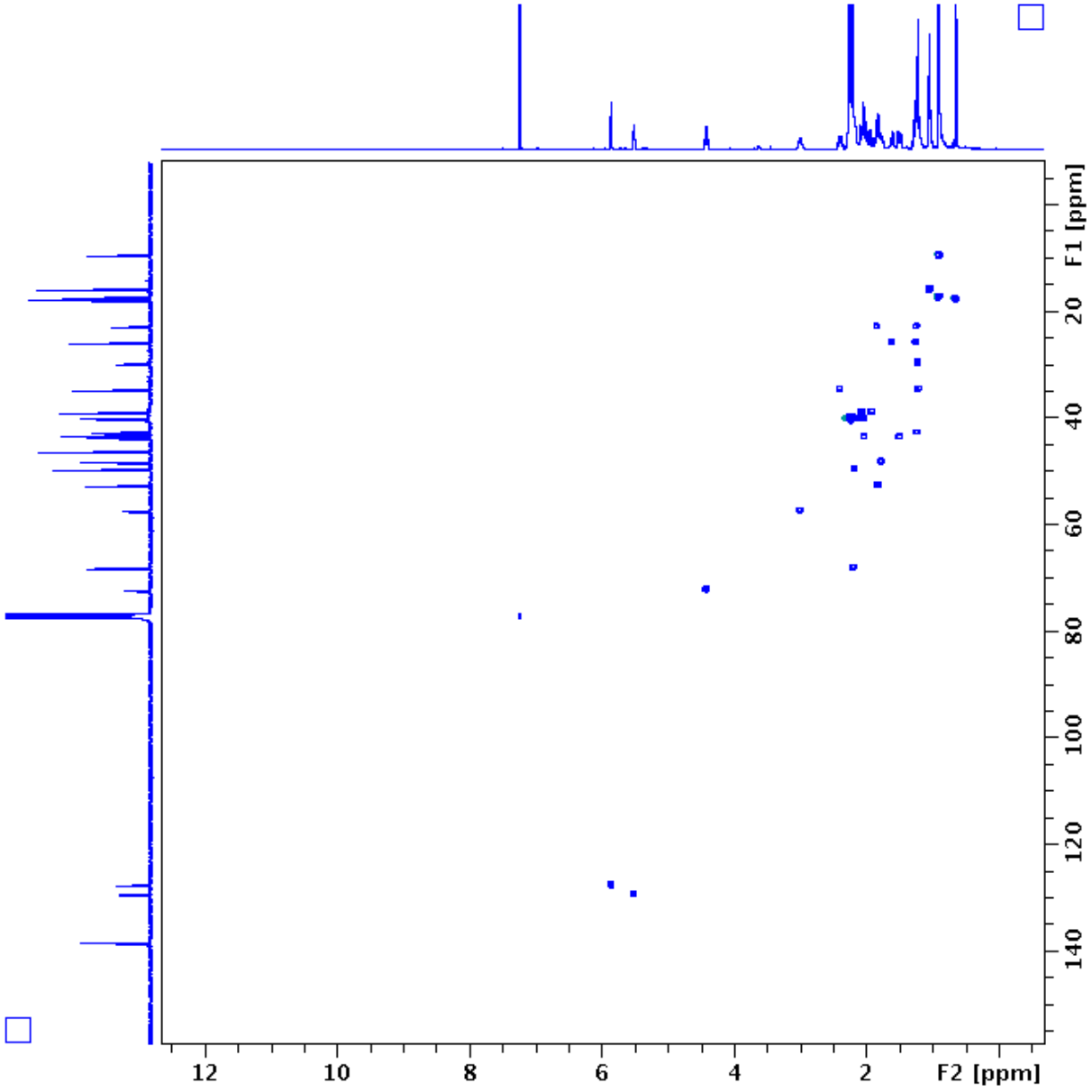

A28. HSQC spectrum of compound **(125)** in $CDCl_3$.

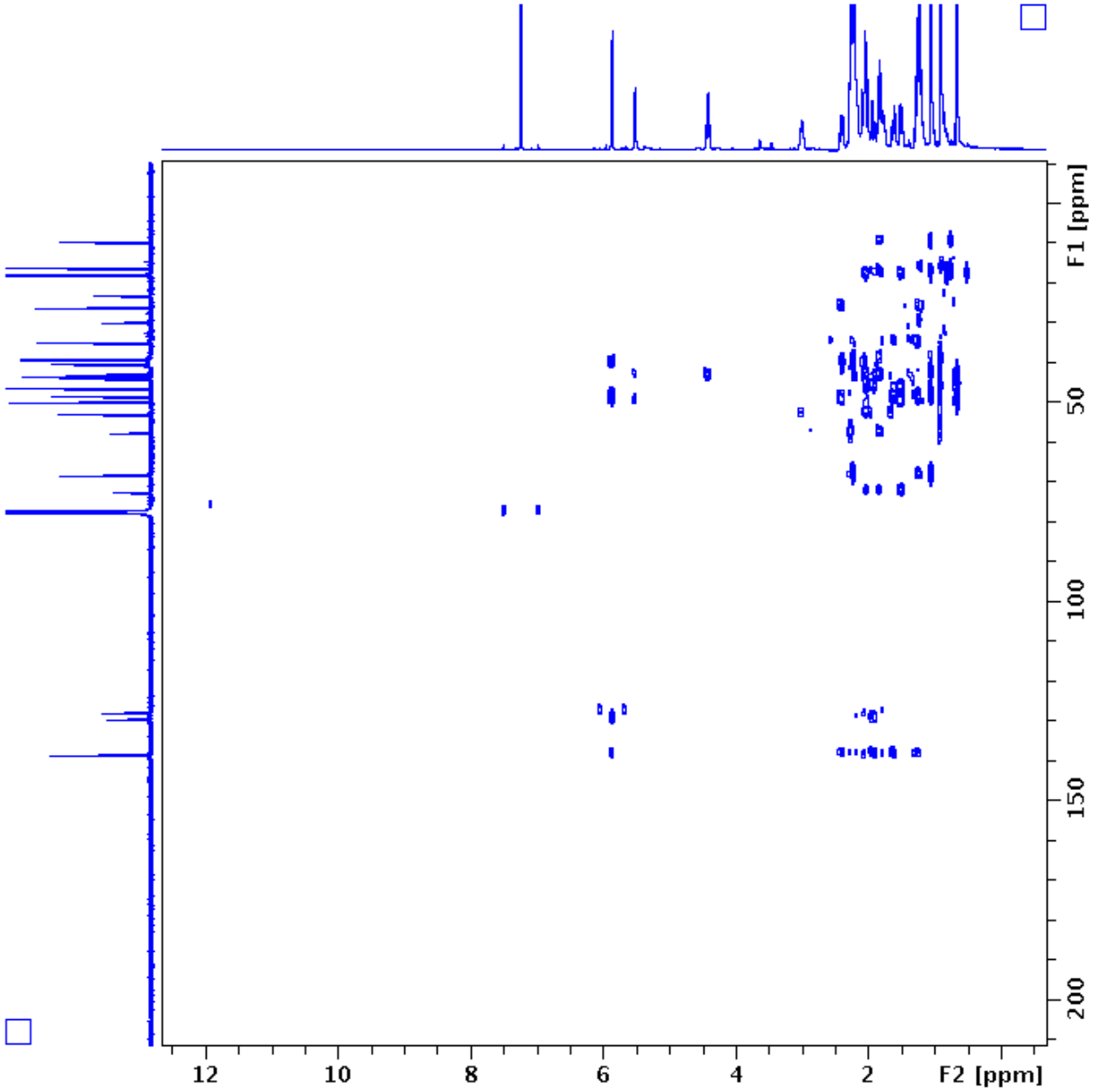

A29. HMBC spectrum of compound **(125)** in $CDCl_3$.

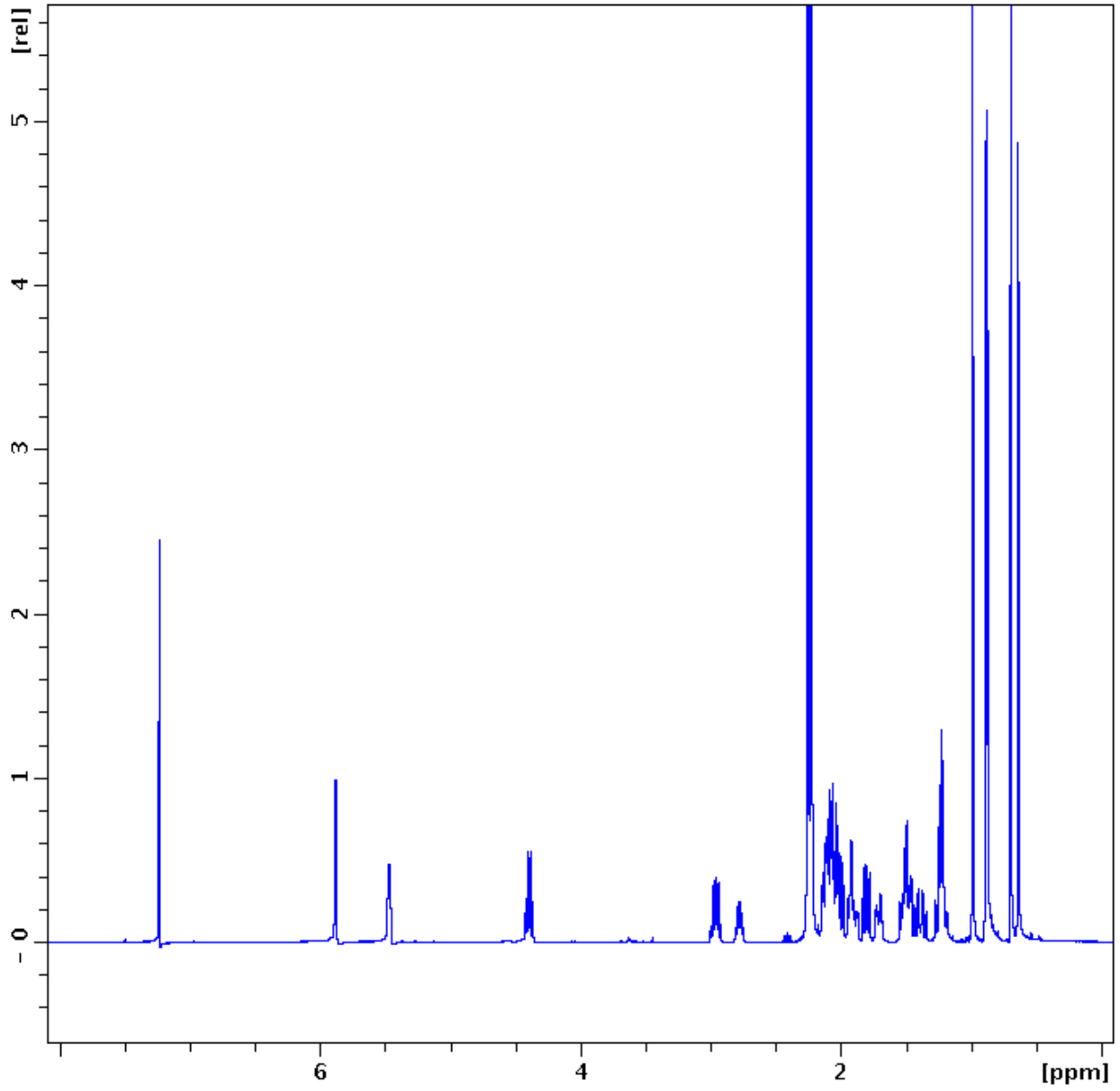

A30. ^{1}H-NMR spectrum of compound **(126)** in $CDCl_3$.

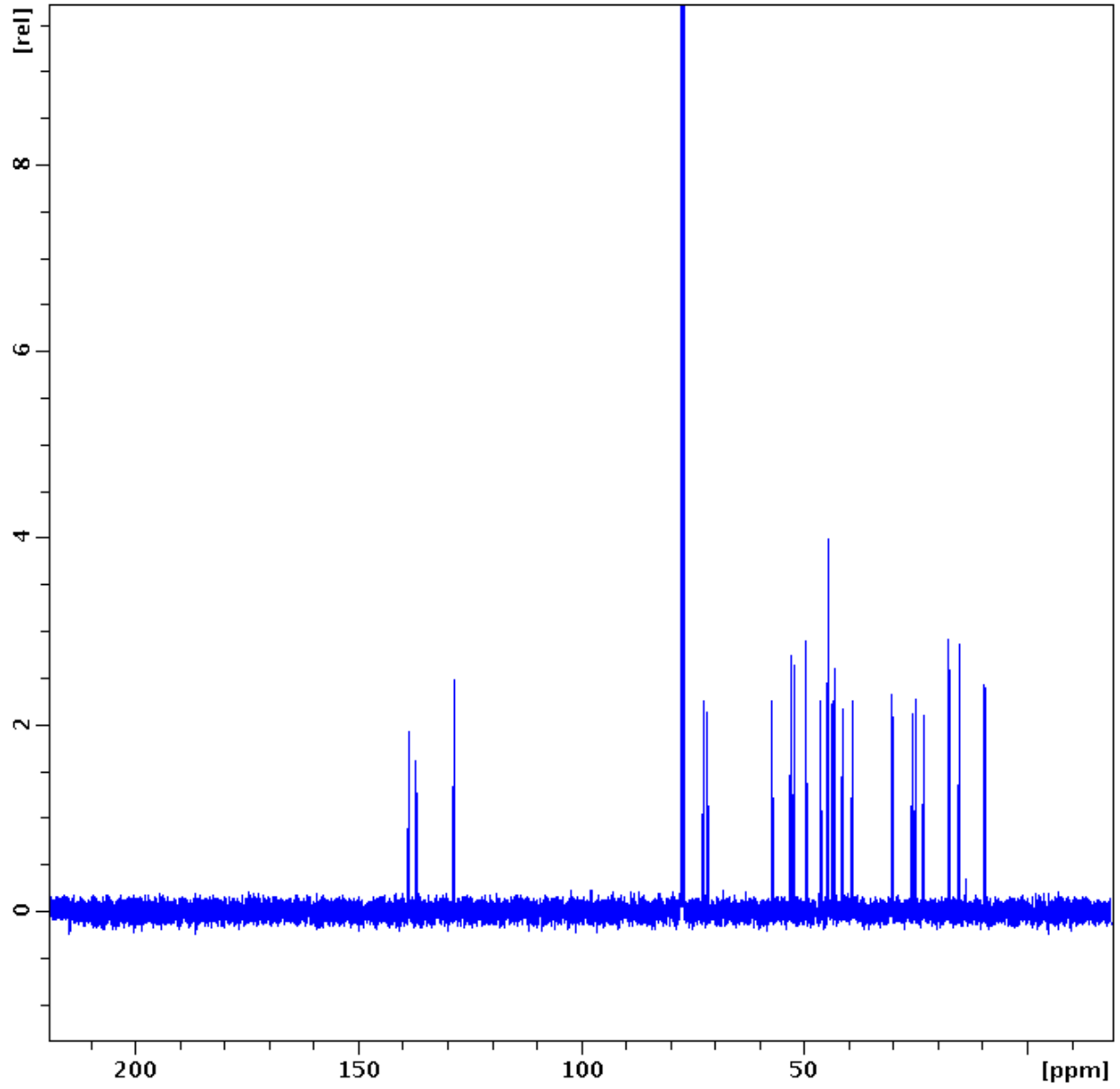

A31. ^{13}C-NMR spectrum of compound **(126)** in $CDCl_3$.

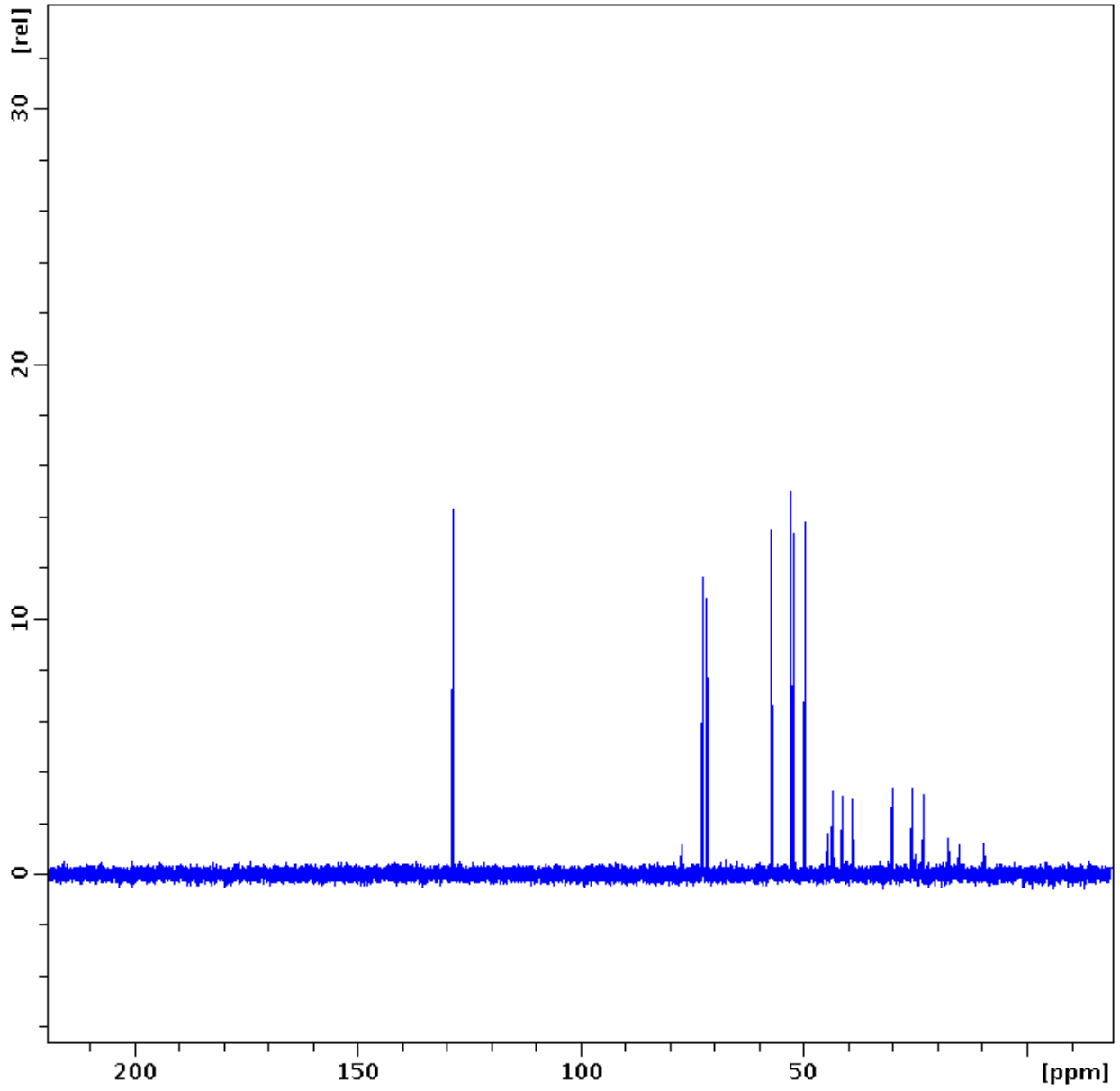

A32. DEPT 90 spectrum of compound **(126)** in $CDCl_3$.

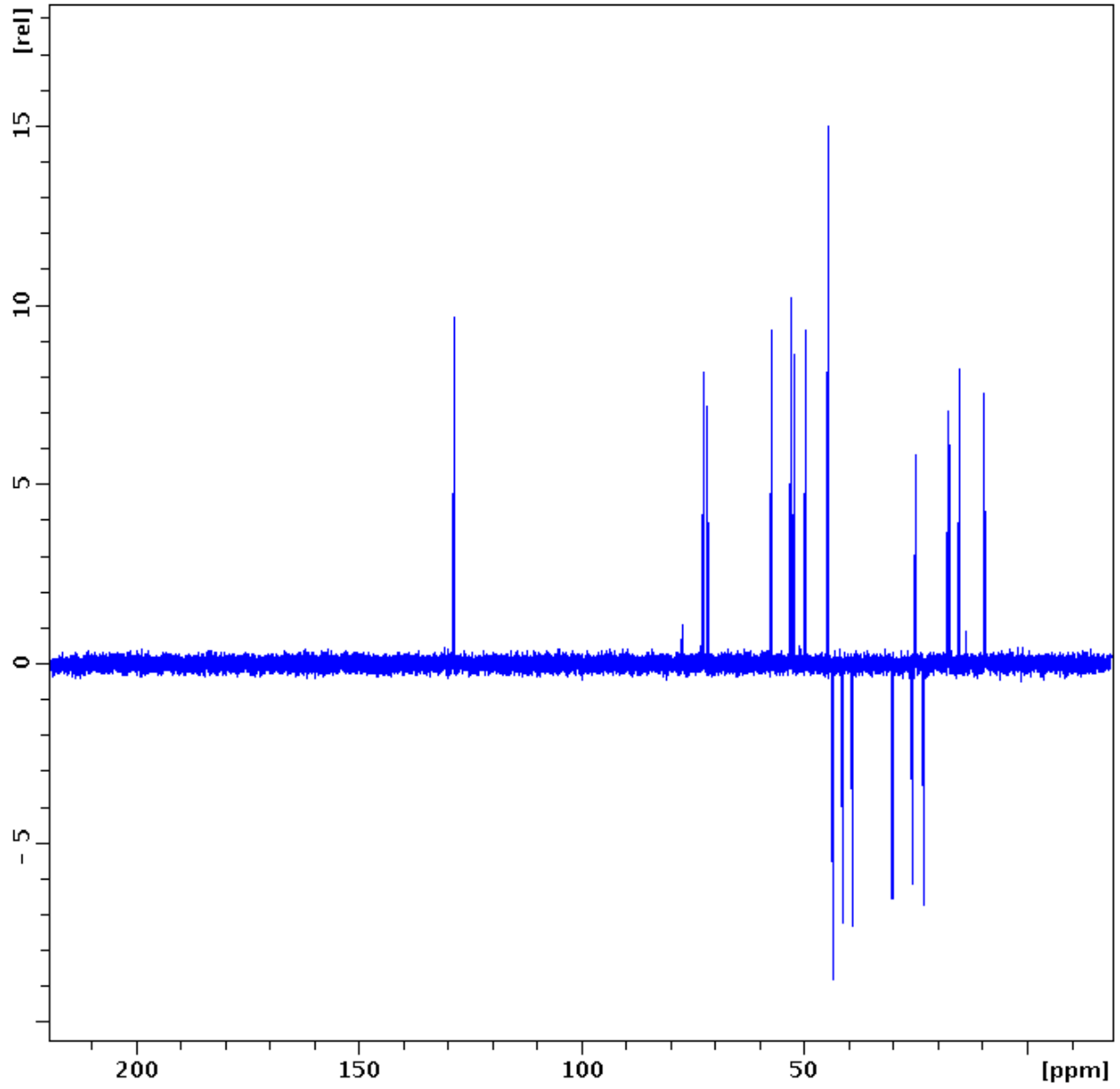

A33. DEPT 135 spectrum of compound **(126)** in $CDCl_3$.

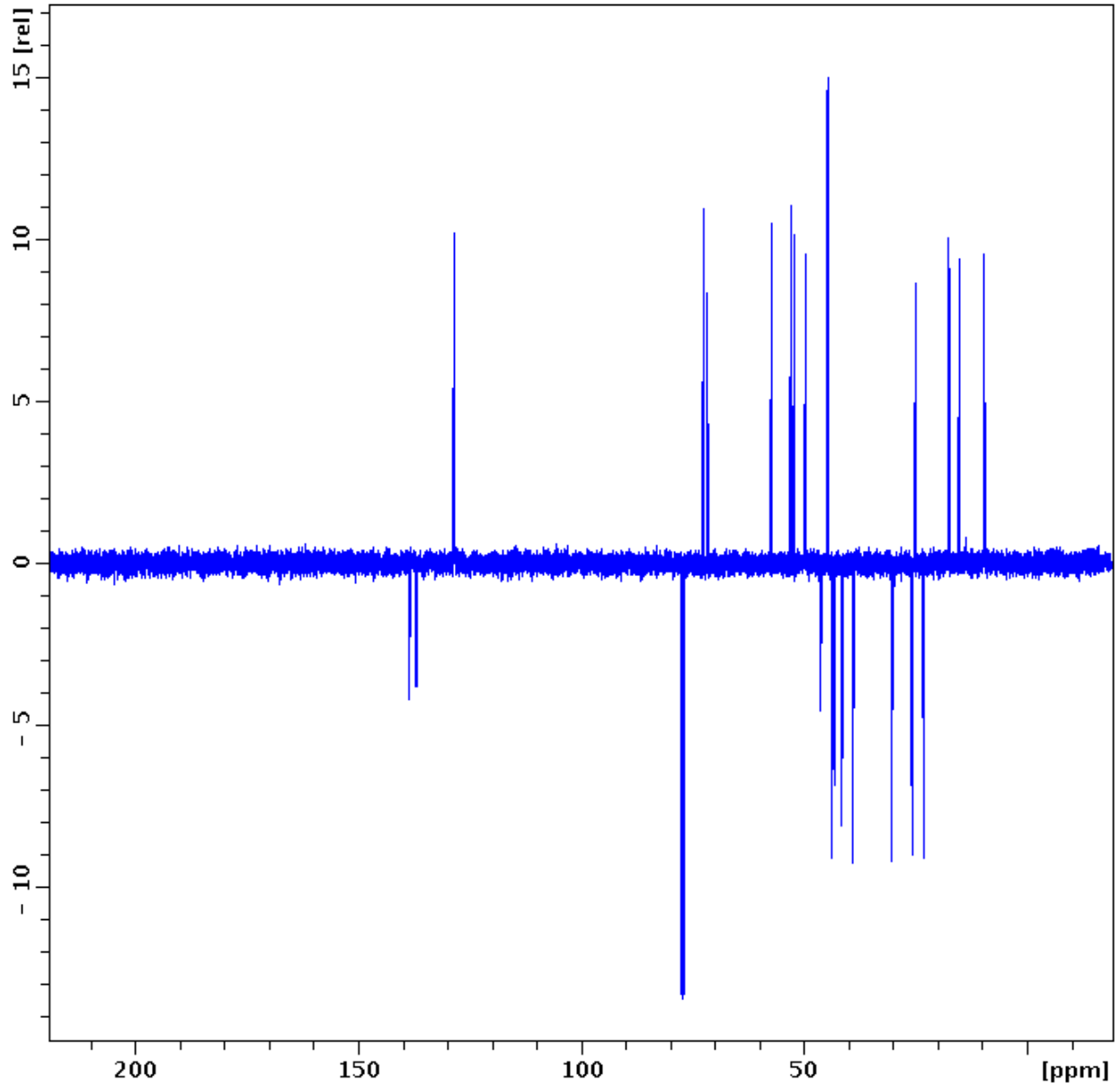

A34. APT spectrum of compound **(126)** in $CDCl_3$.

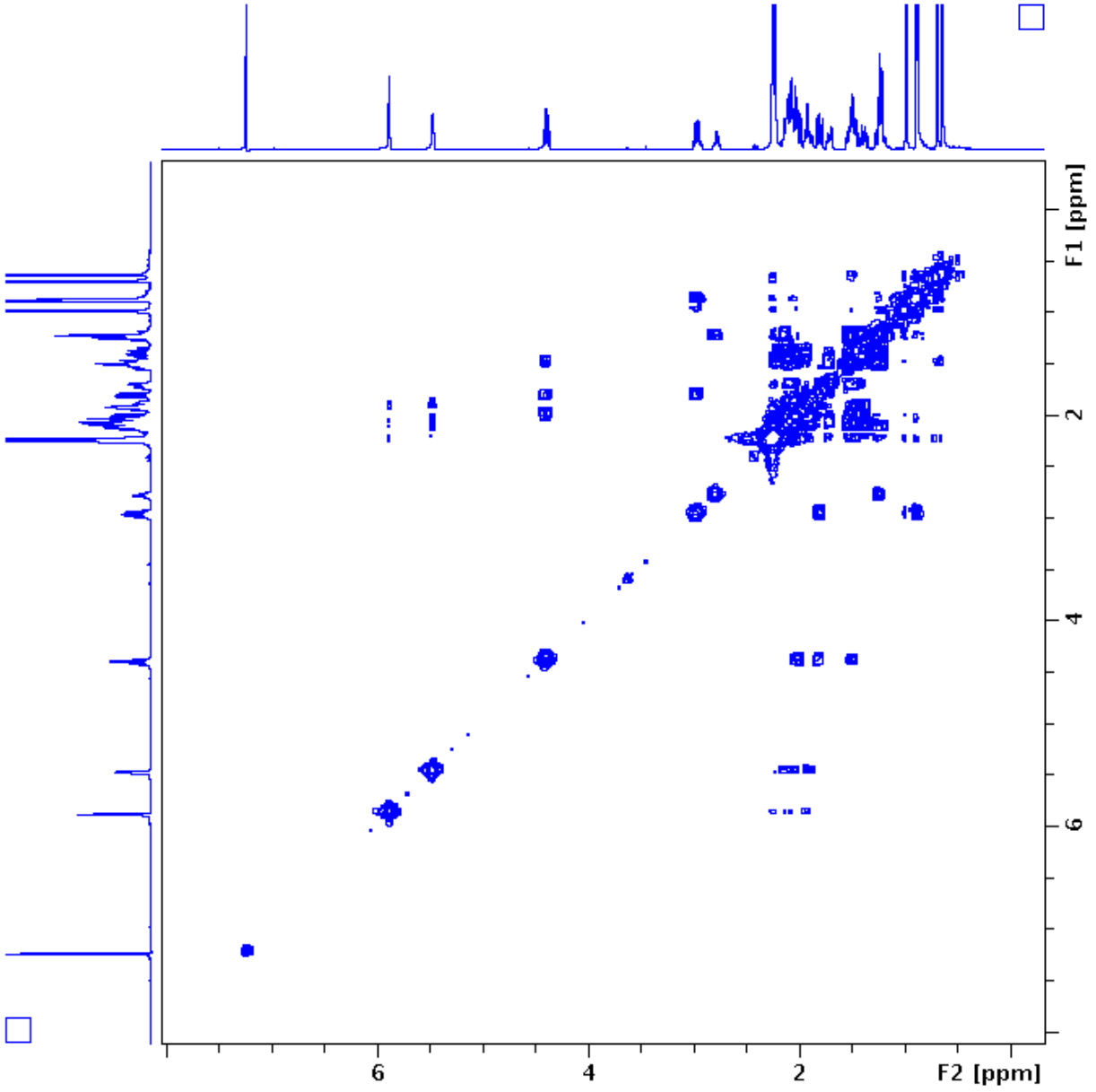

A35. COSY spectrum of compound **(126)** in $CDCl_3$.

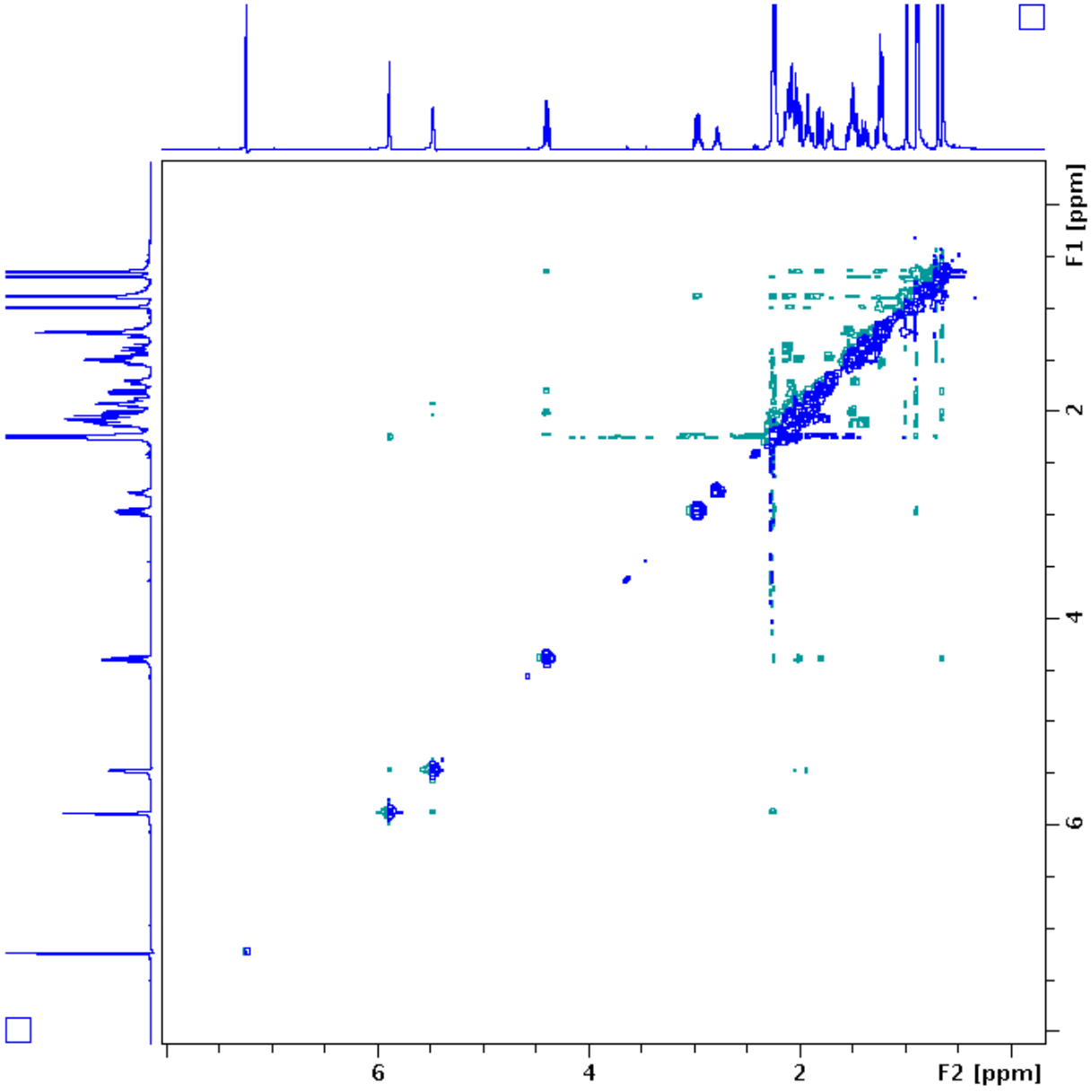

A36. NOESY spectrum of compound **(126)** in $CDCl_3$.

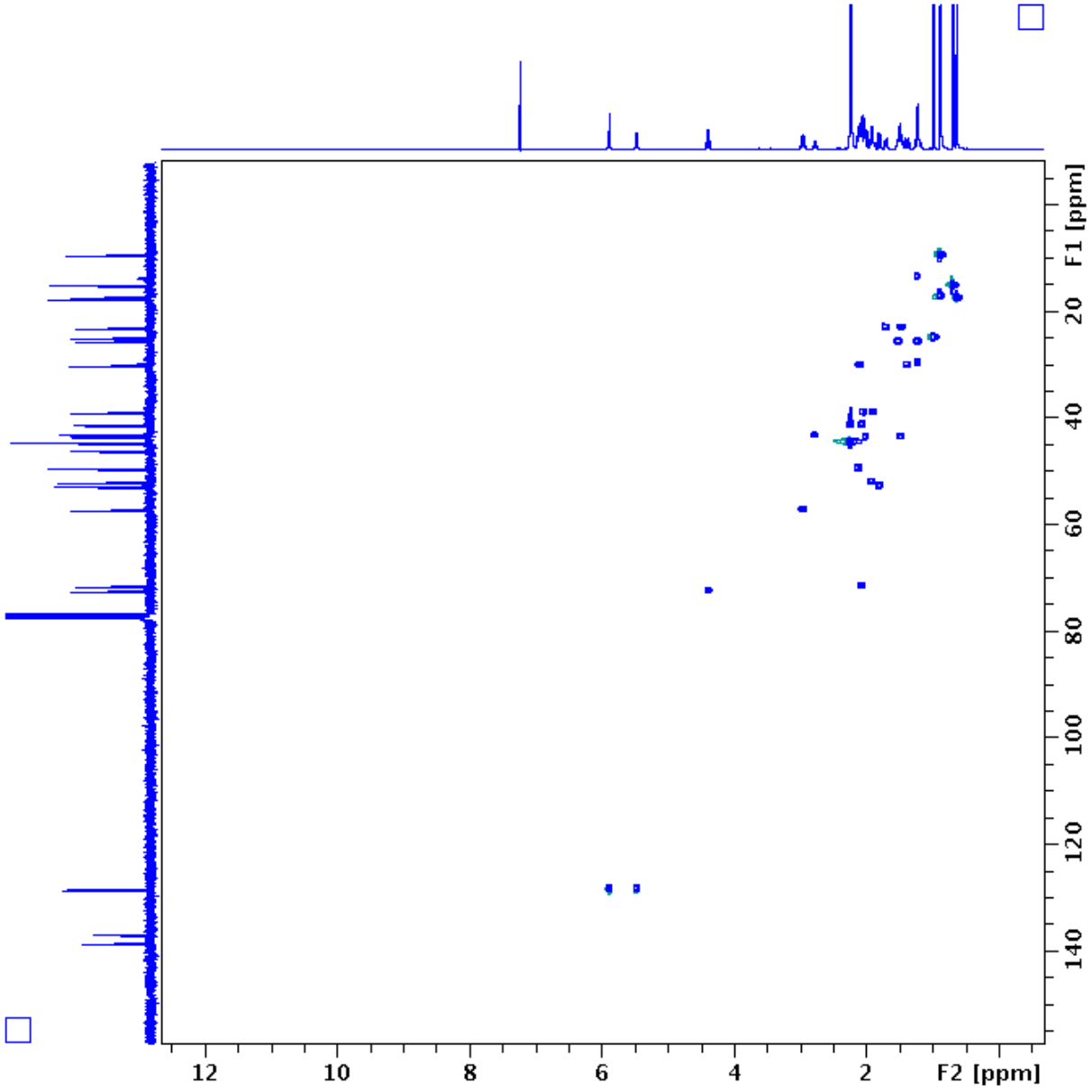

A37. HSQC spectrum of compound **(126)** in $CDCl_3$.

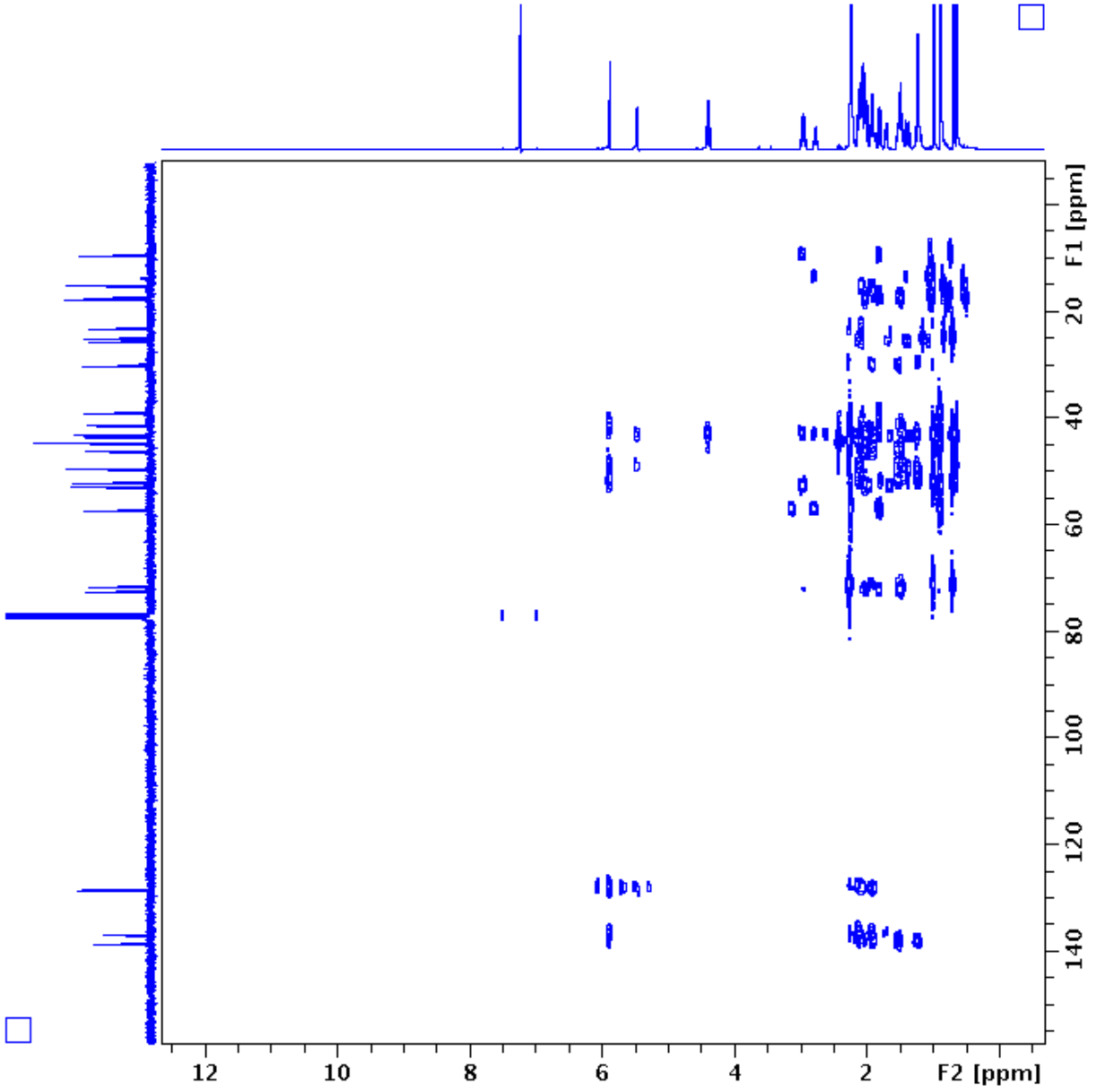

A38. HMBC spectrum of compound **(126)** in $CDCl_3$.

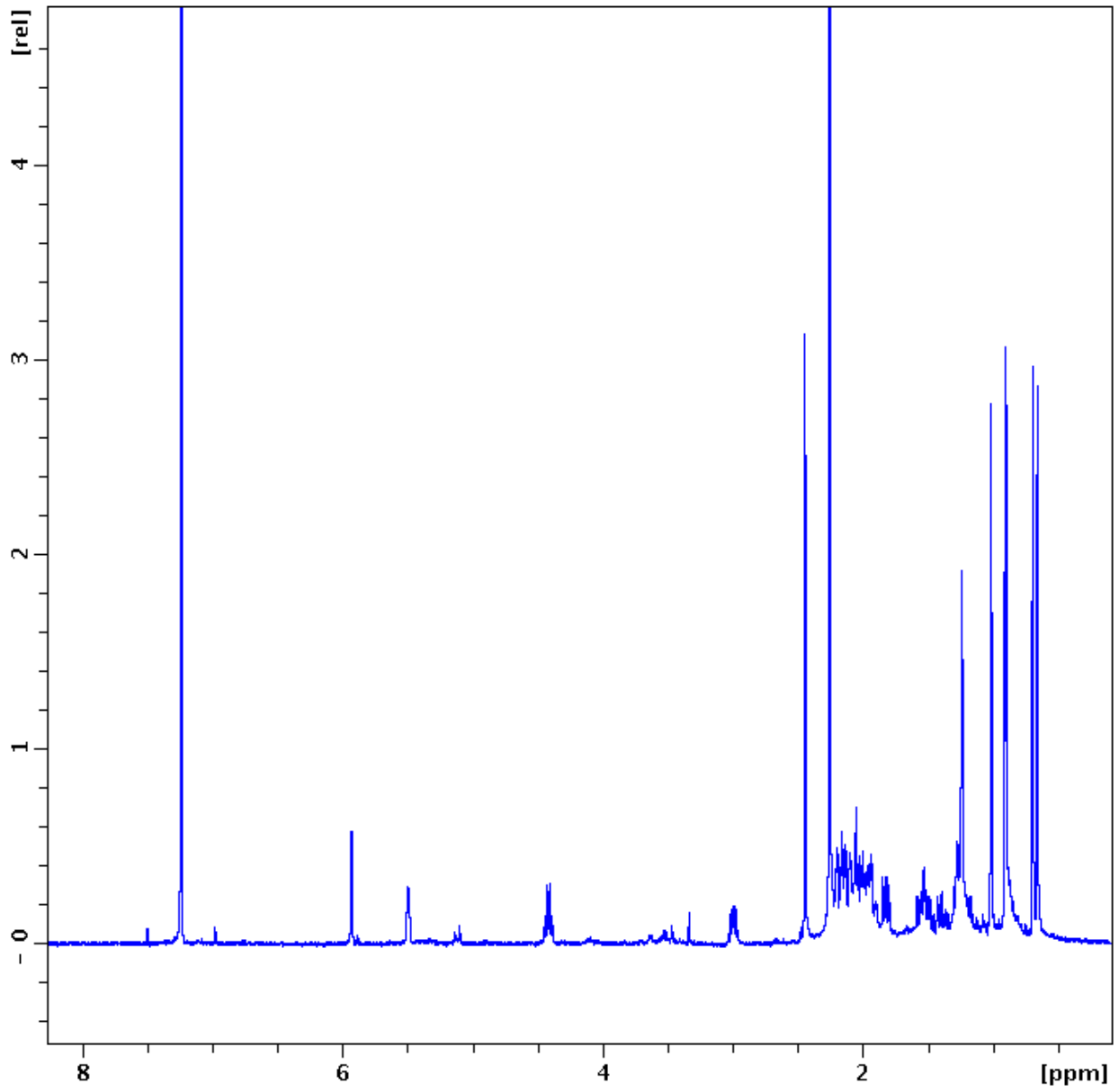

A39. ^{1}H-NMR spectrum of compound **(127)** in $CDCl_3$.

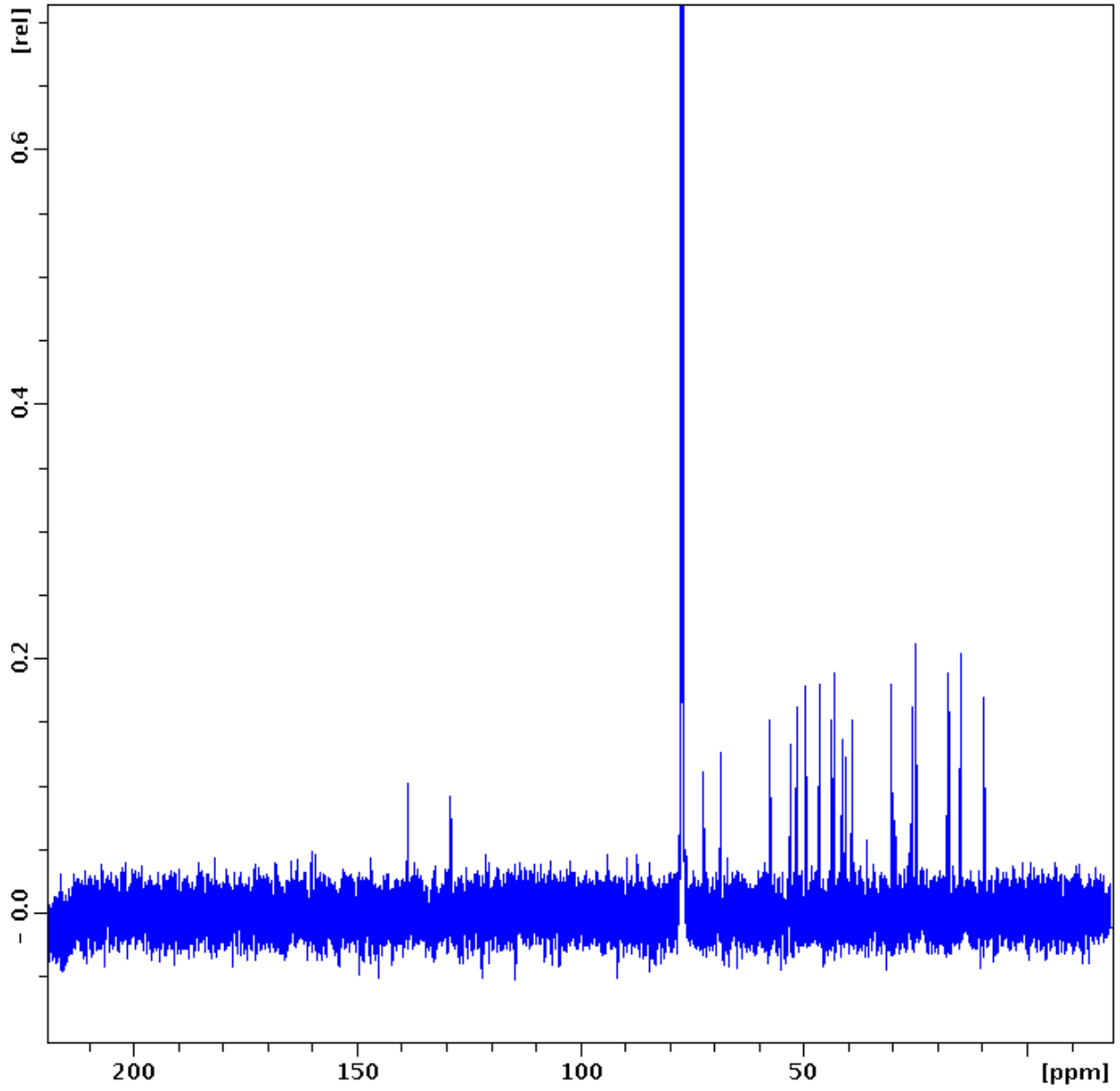

A40 ^{13}C-NMR spectrum of compound **(127)** in $CDCl_3$.

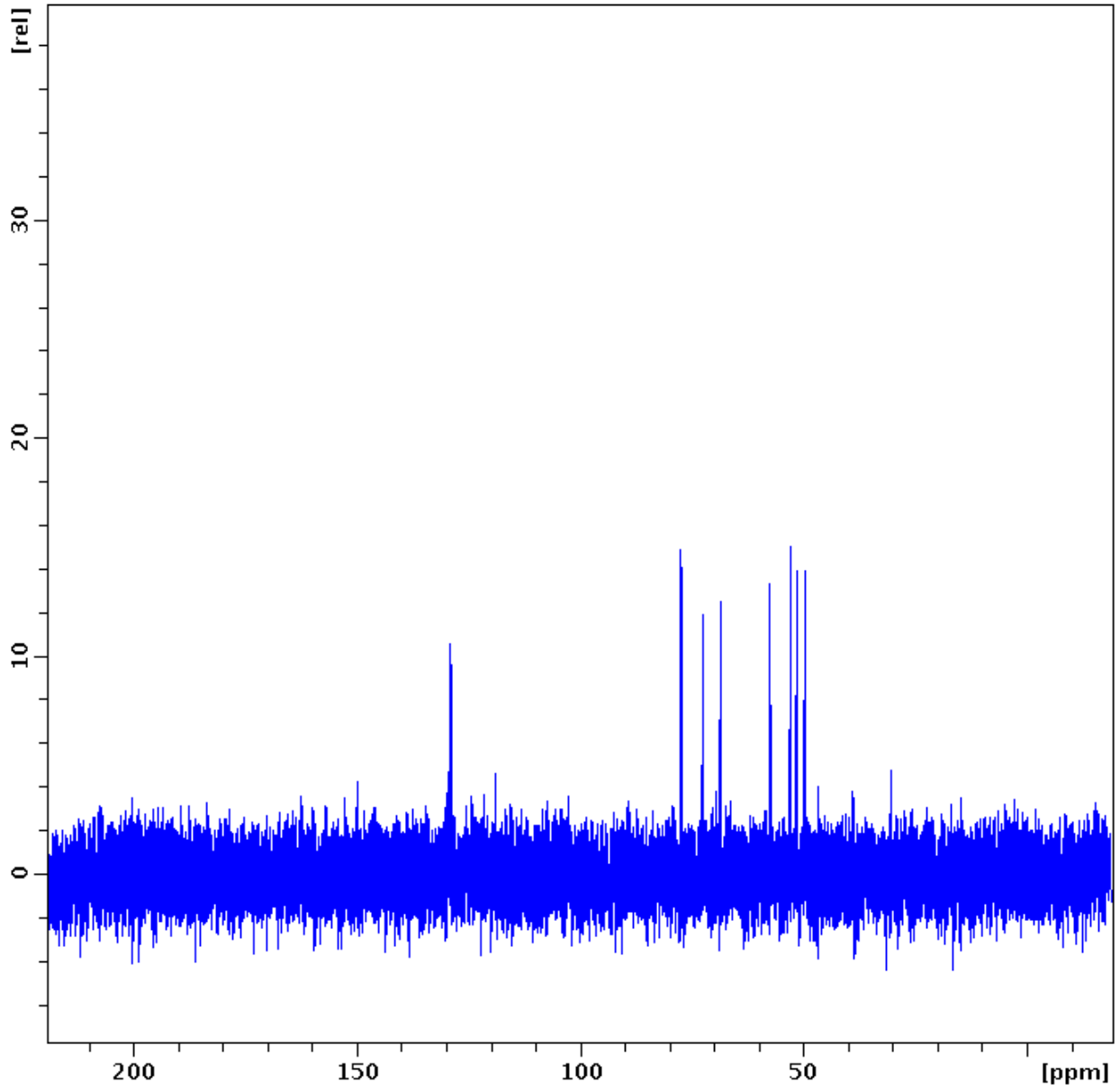

A41. DEPT 90 spectrum of compound **(127)** in $CDCl_3$.

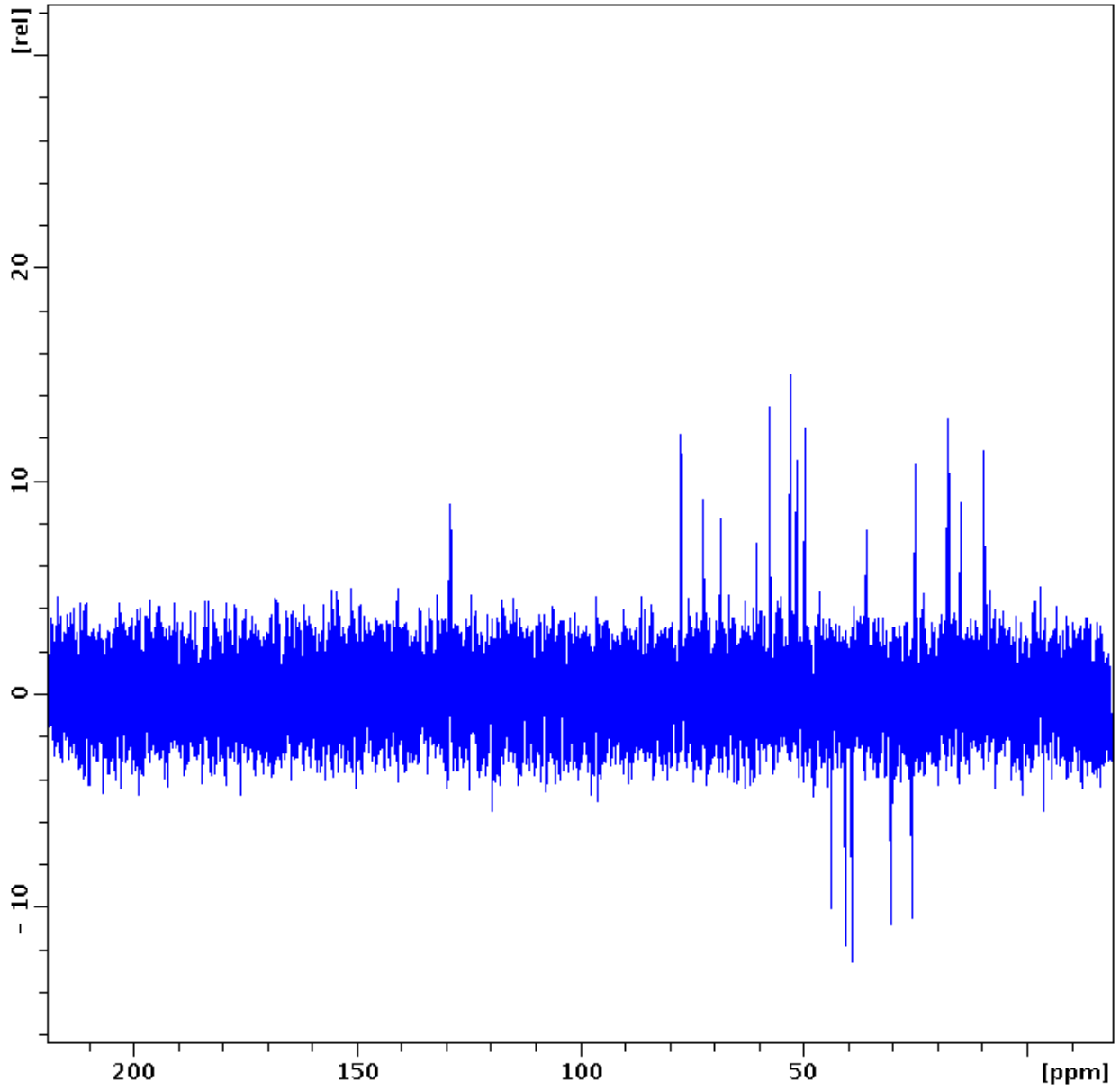

A42. DEPT 135 spectrum of compound **(127)** in $CDCl_3$.

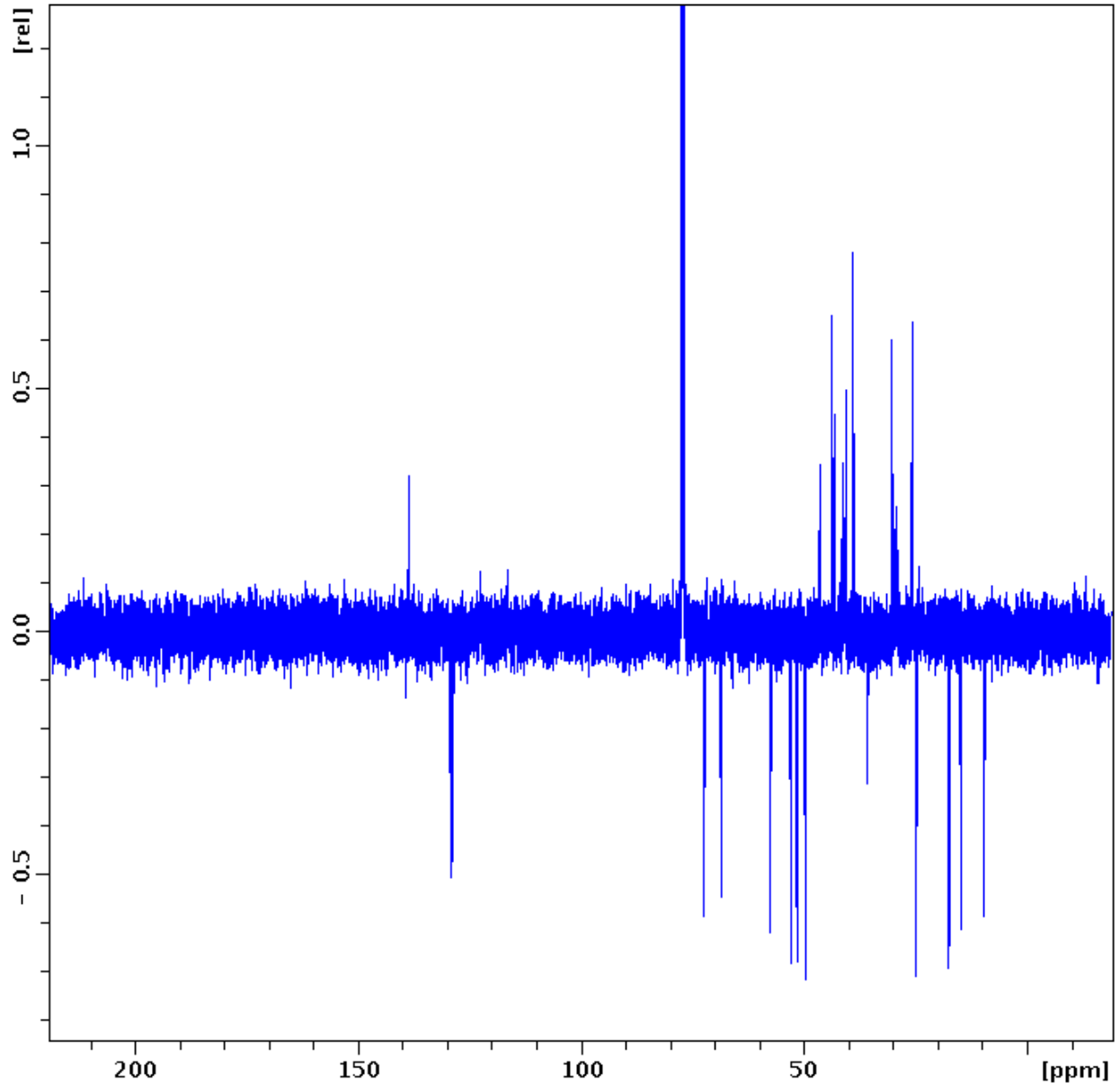

A43. APT spectrum of compound **(127)** in $CDCl_3$.

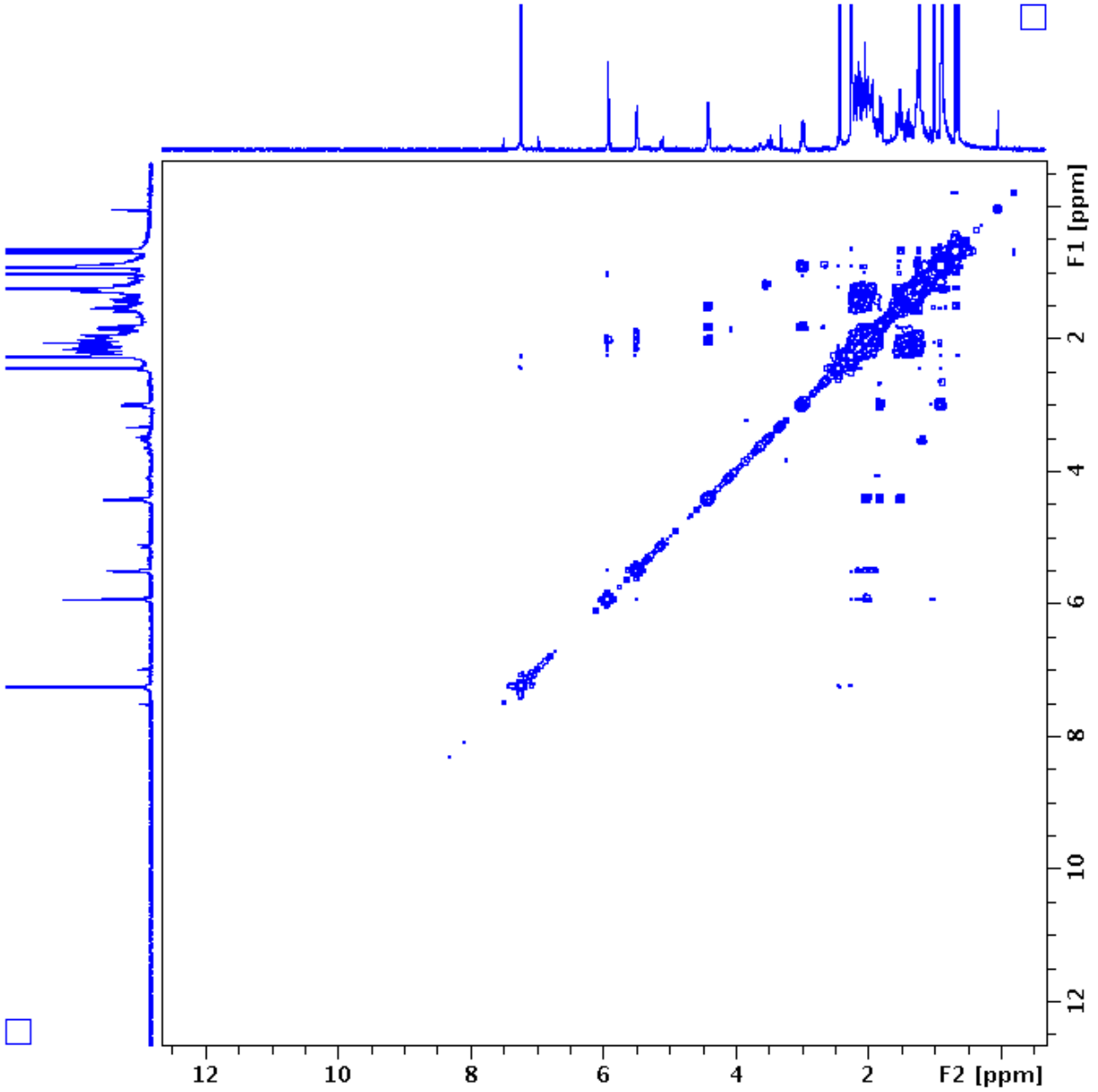

A44. COSY spectrum of compound **(127)** in $CDCl_3$.

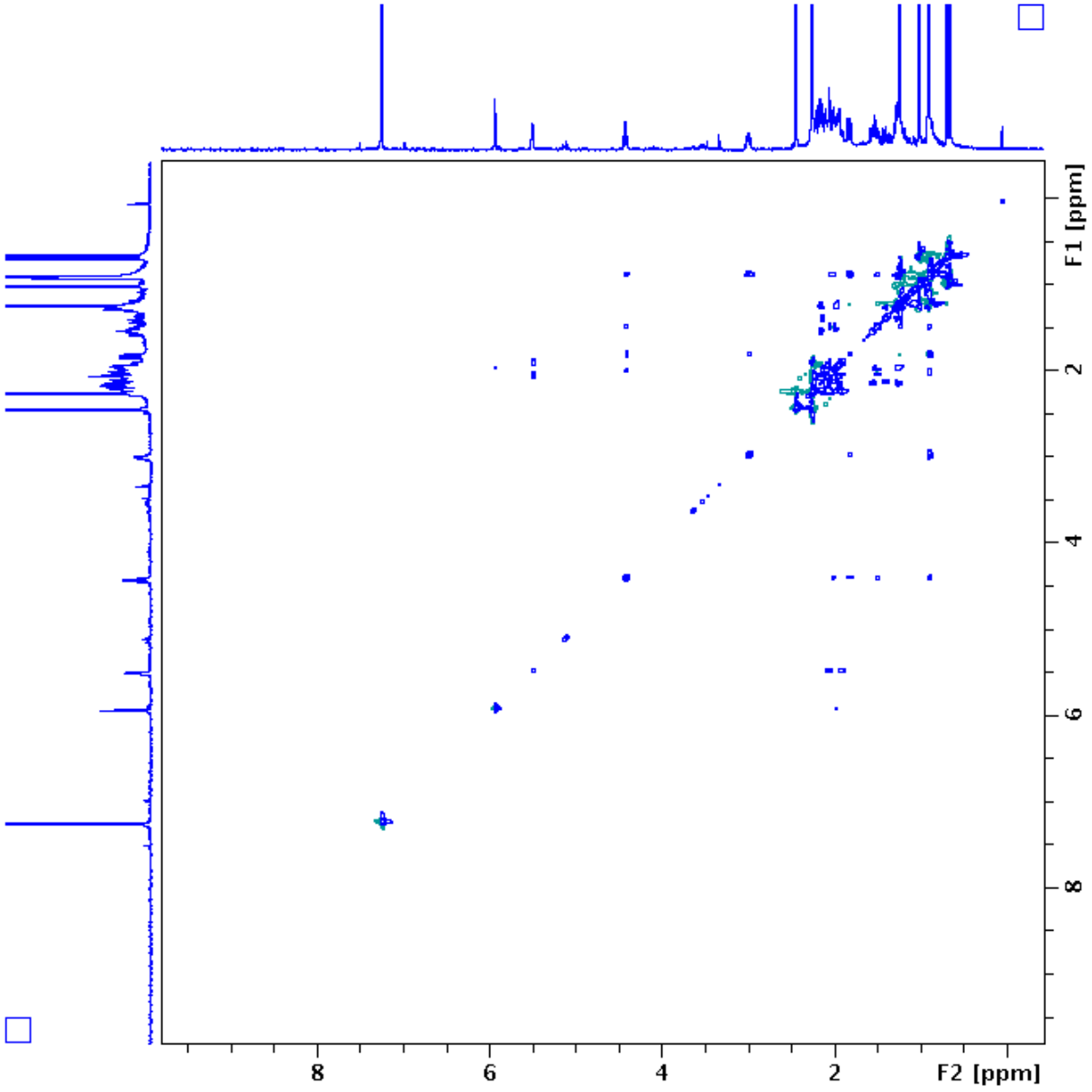

A45. TOCSY spectrum of compound **(127)** in $CDCl_3$.

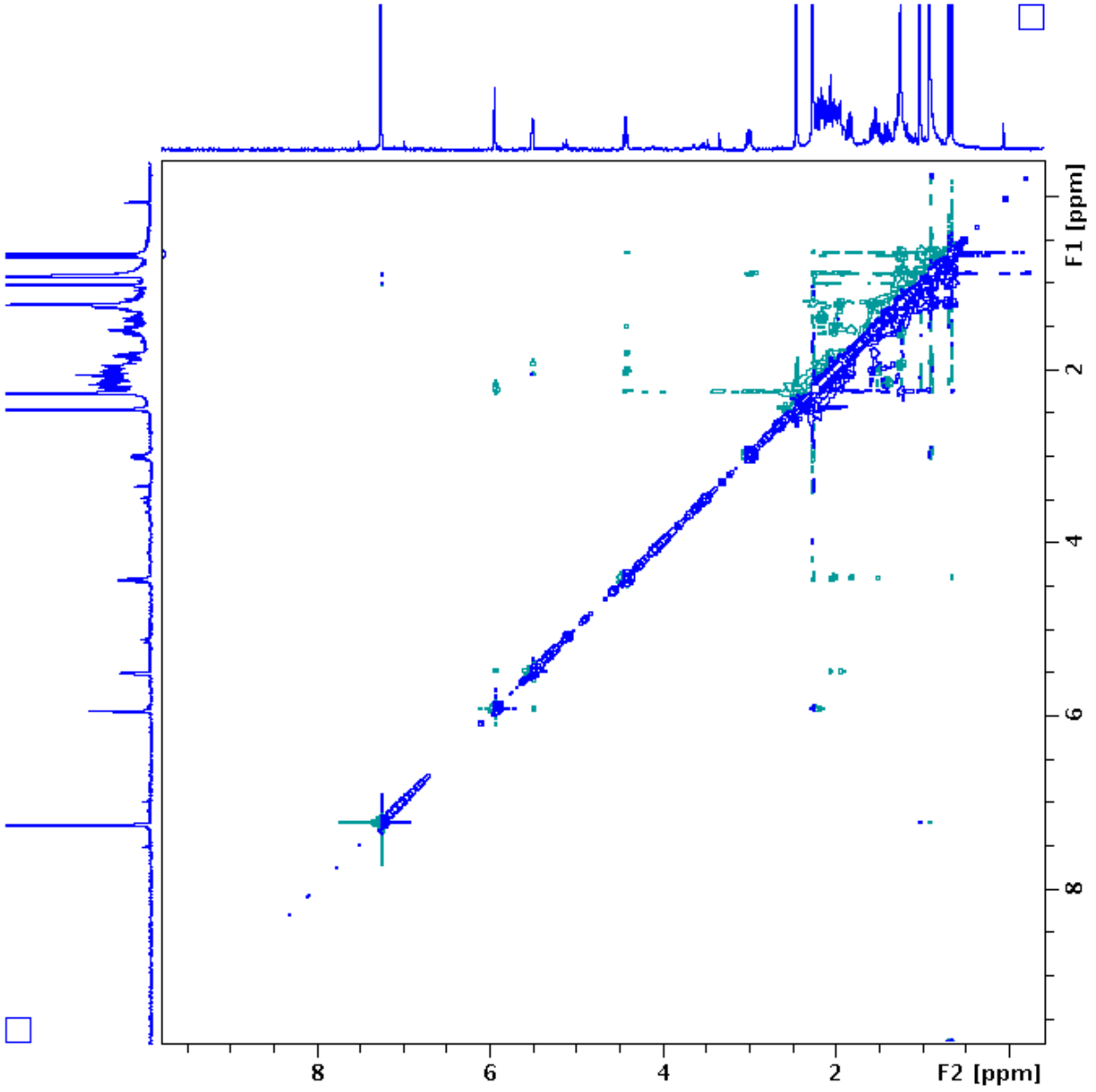

A46. NOESY spectrum of compound **(127)** in $CDCl_3$.

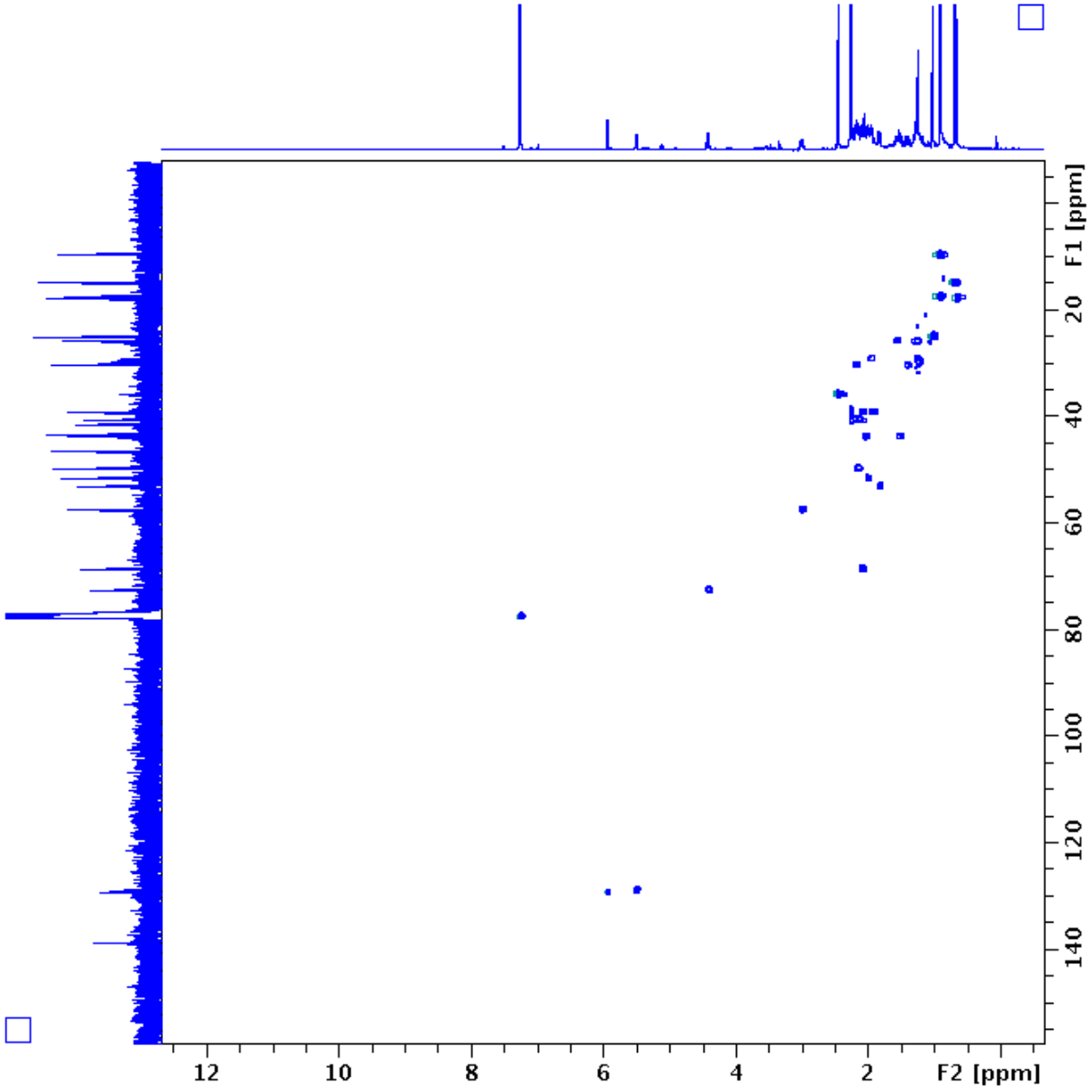

A47. HSQC spectrum of compound **(127)** in $CDCl_3$.

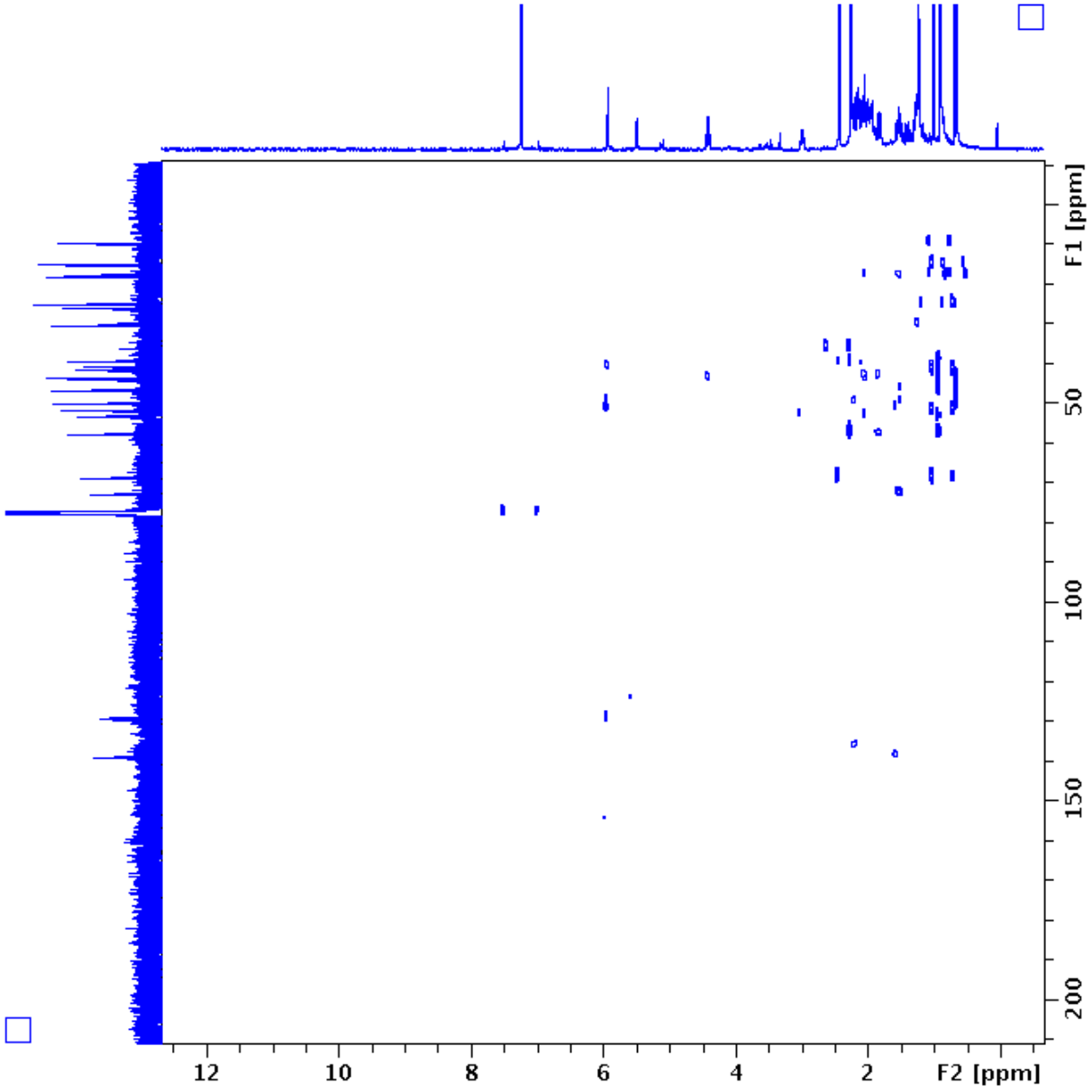

A48. HMBC spectrum of compound **(127)** in $CDCl_3$.

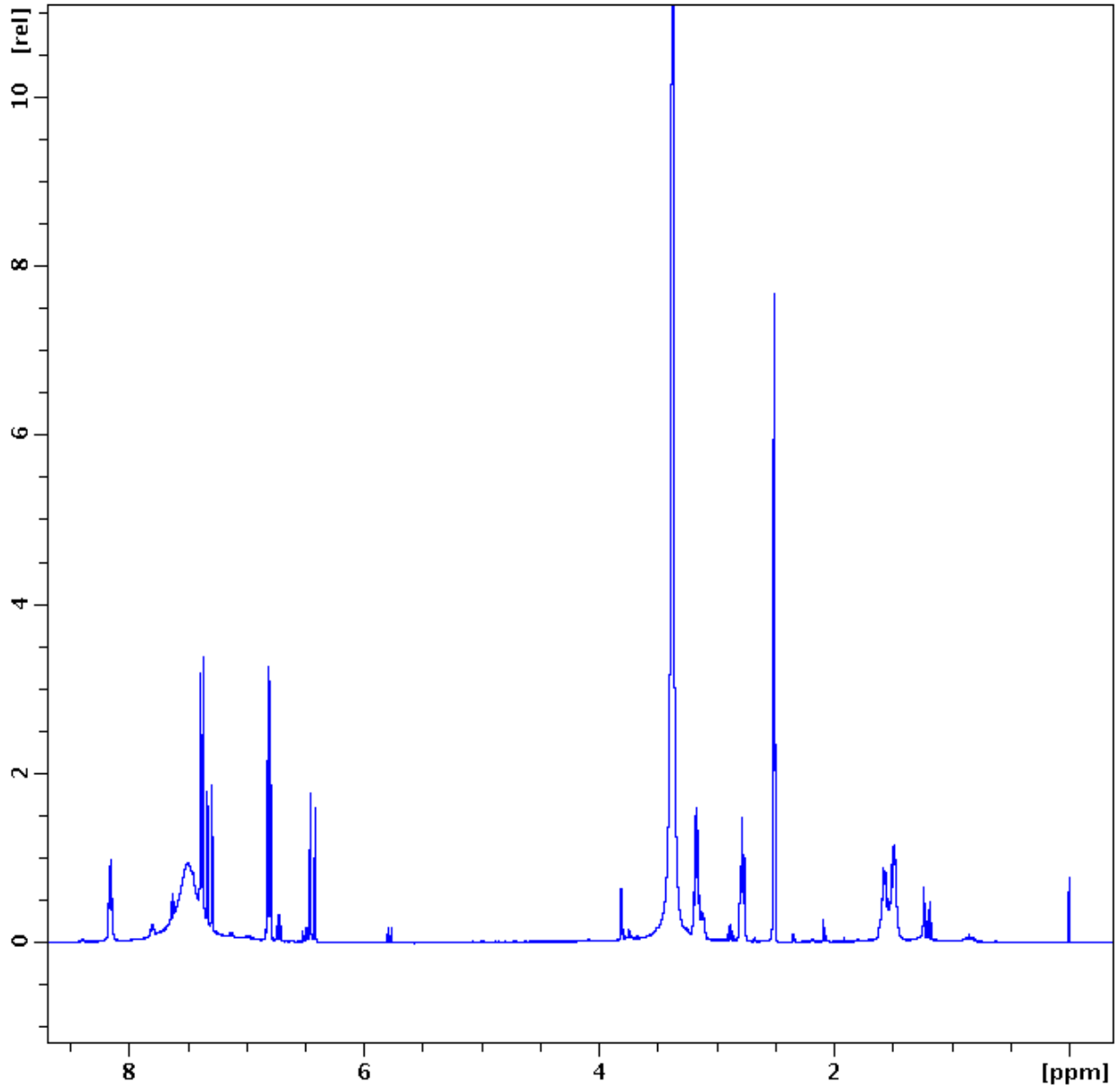

A49. ^{1}H-NMR spectrum of compound **(128)** in DMSO-d_6.

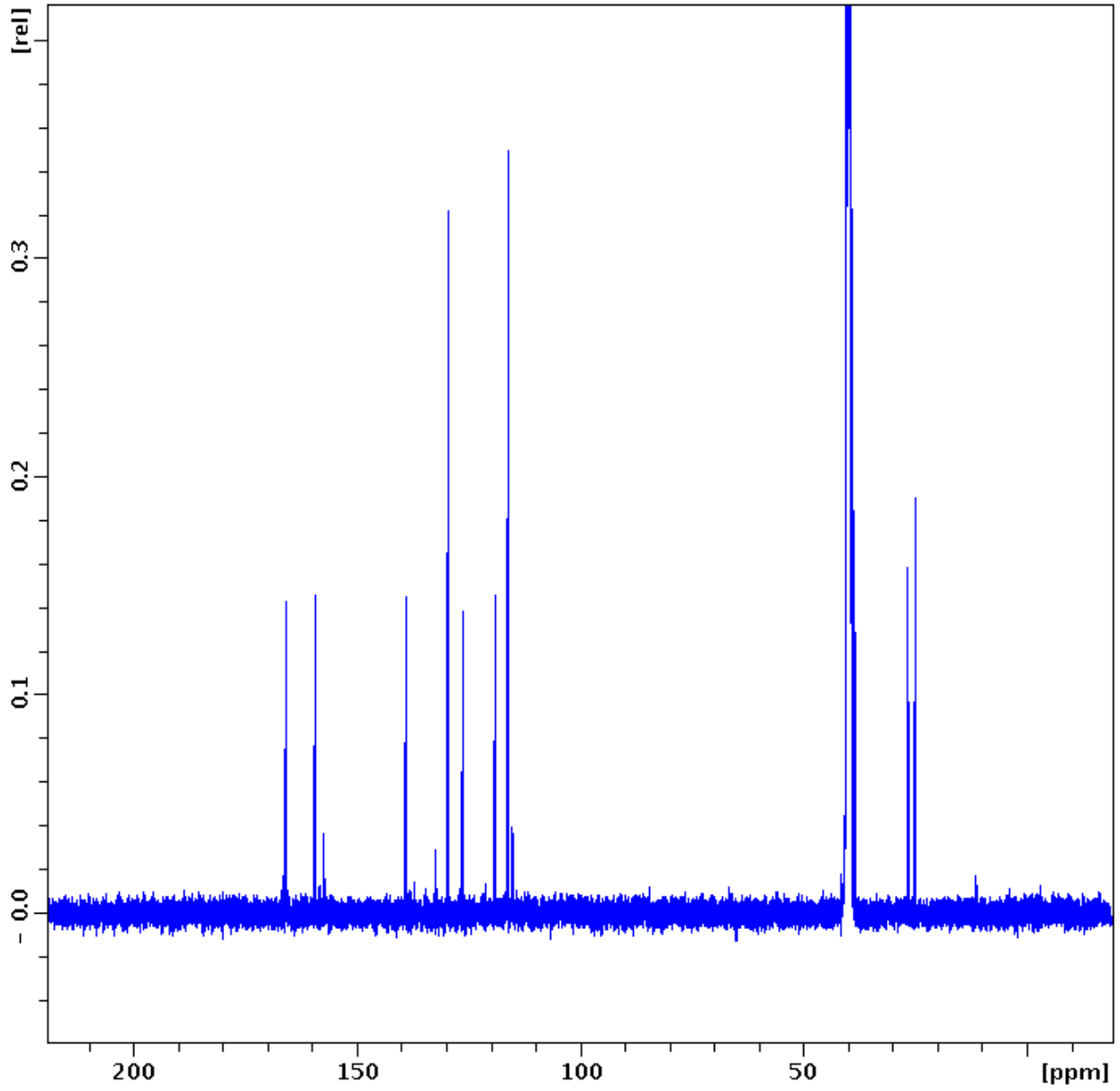

A50. ^{13}C-NMR spectrum of compound **(128)** in DMSO-d_6.

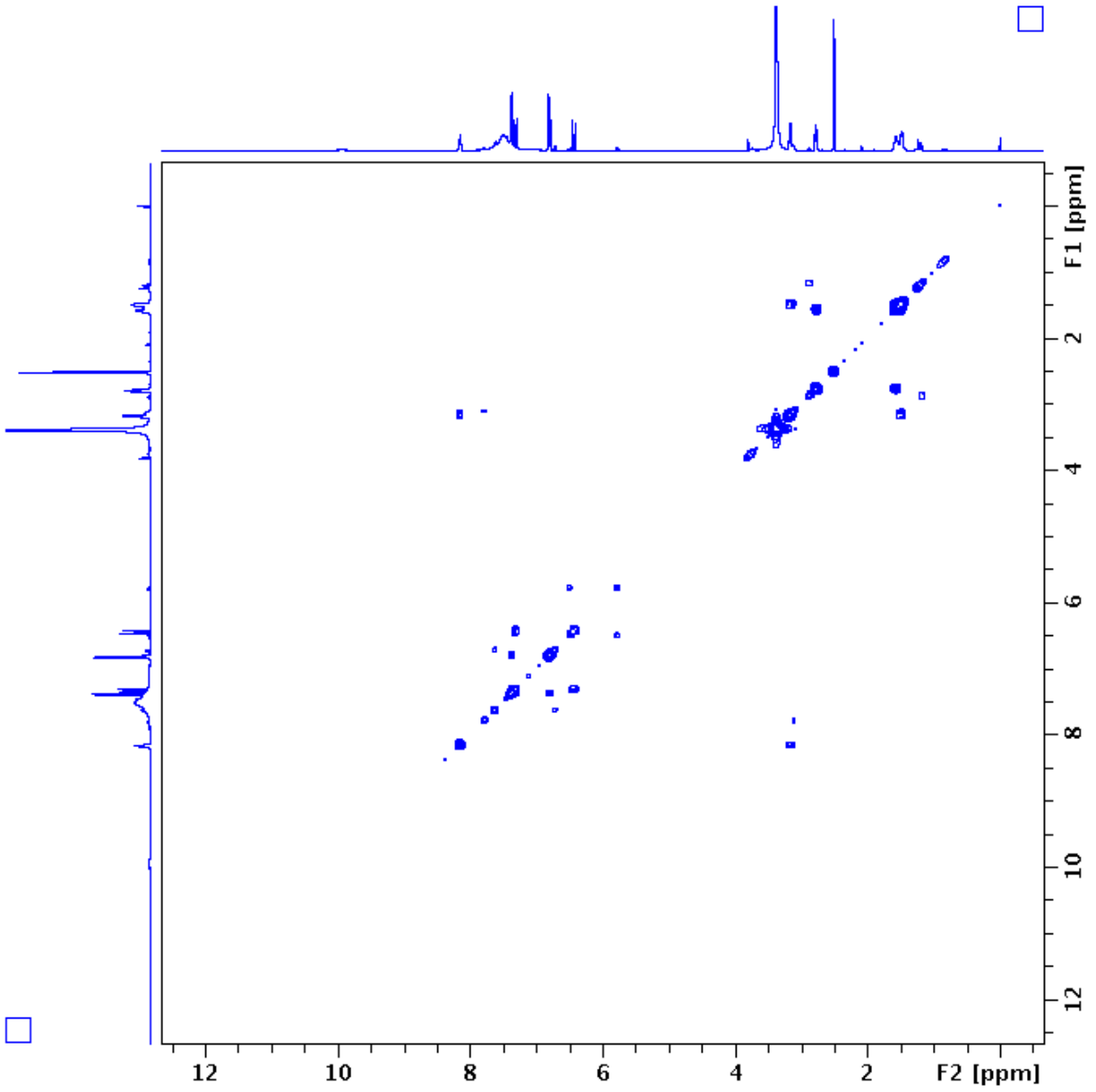

A51. COSY spectrum of compound **(128)** in DMSO-d_6.

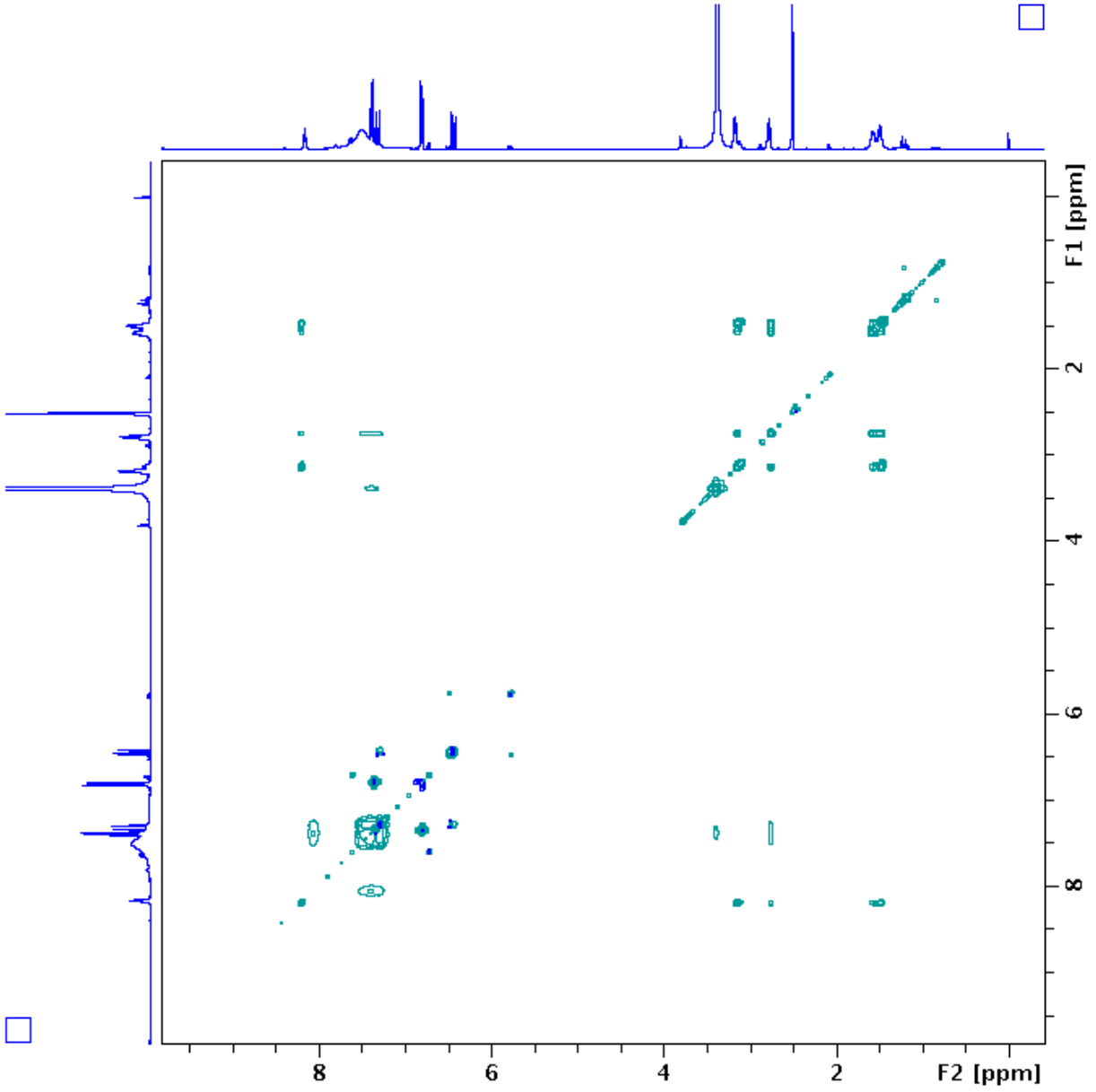

A52. TOCSY spectrum of compound **(128)** in DMSO-d_6.

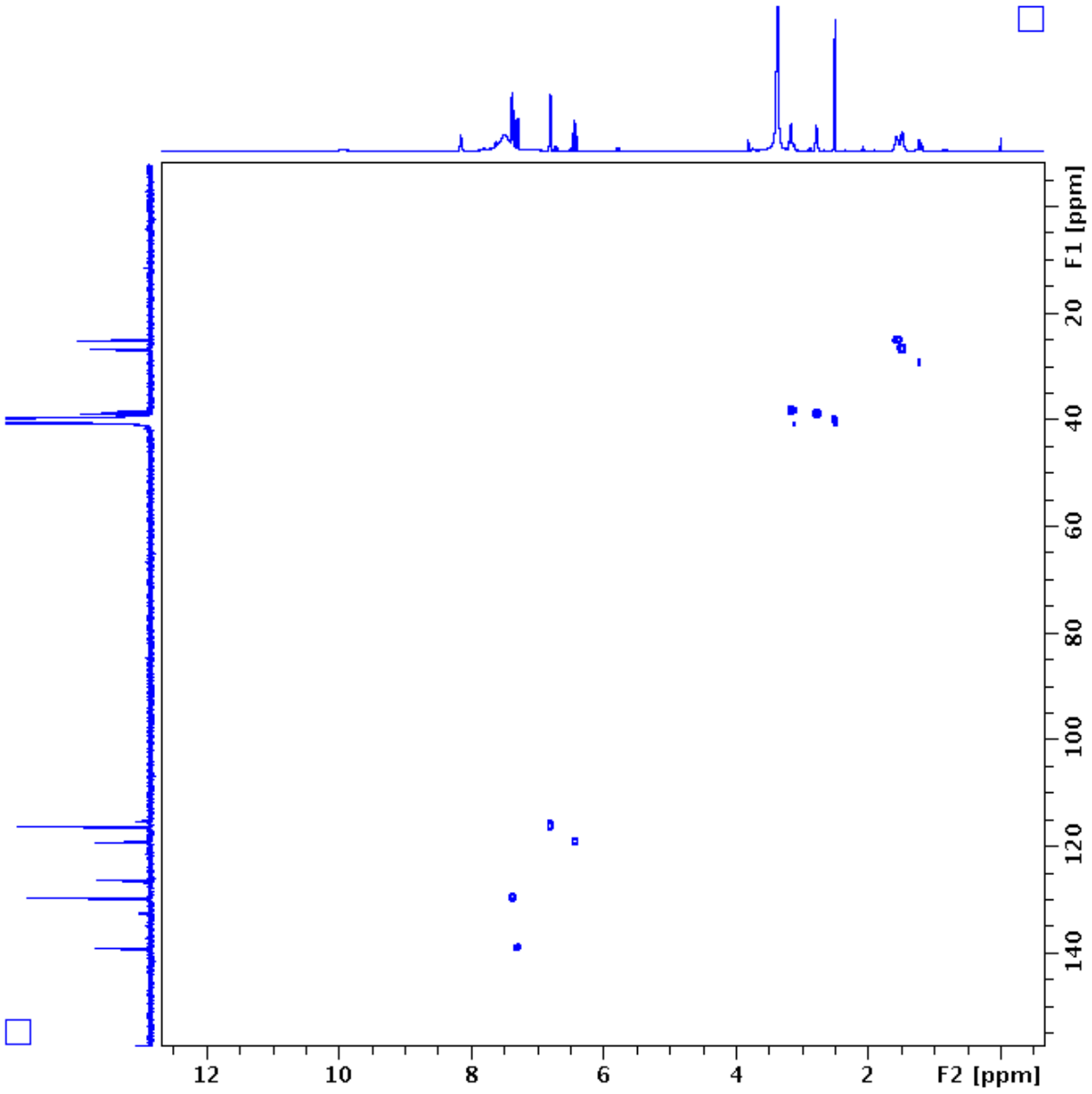

A53. HSQC spectrum of compound **(128)** in DMSO-d_6.

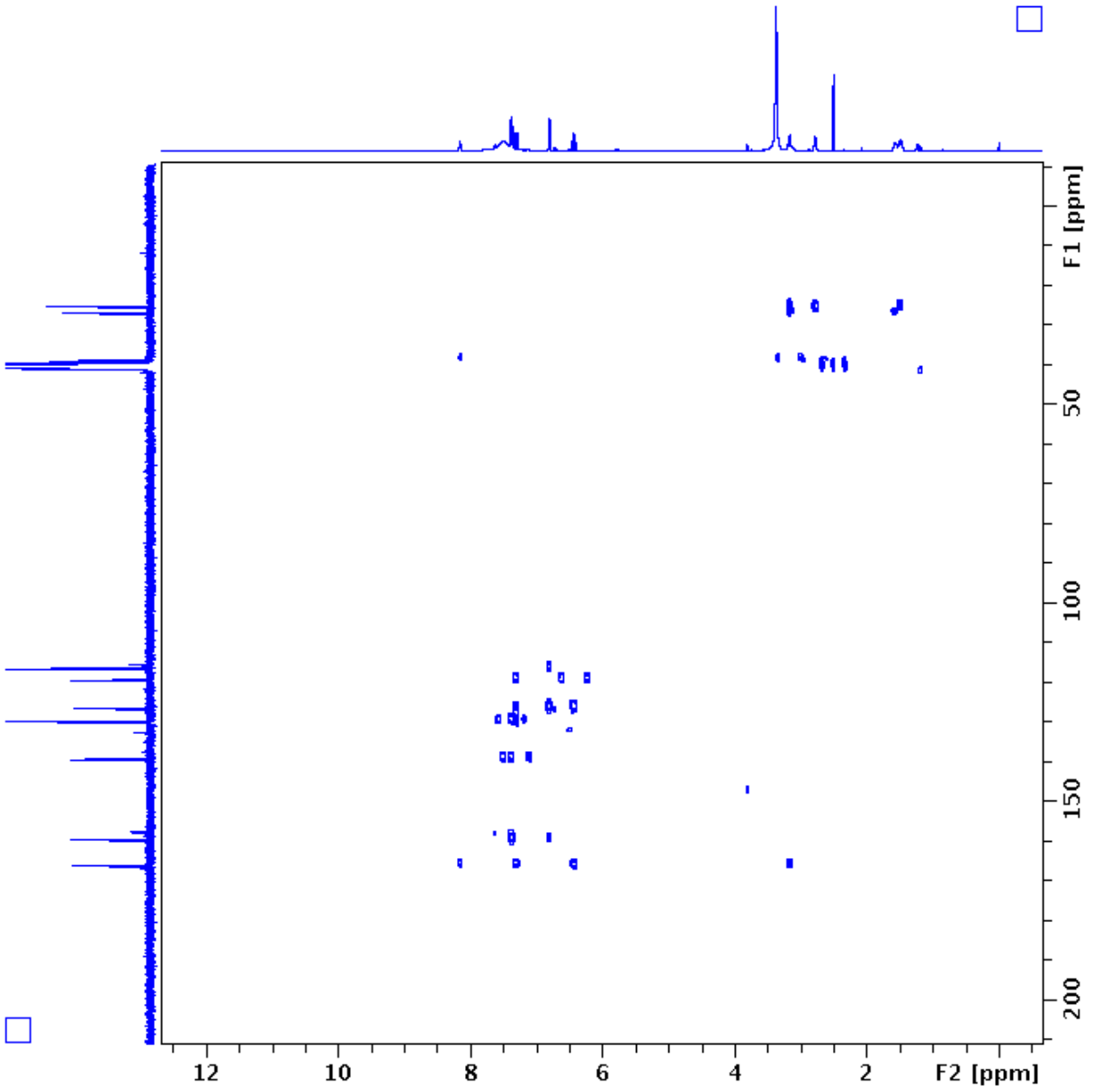

A54. HMBC spectrum of compound **(128)** in DMSO-d_6.

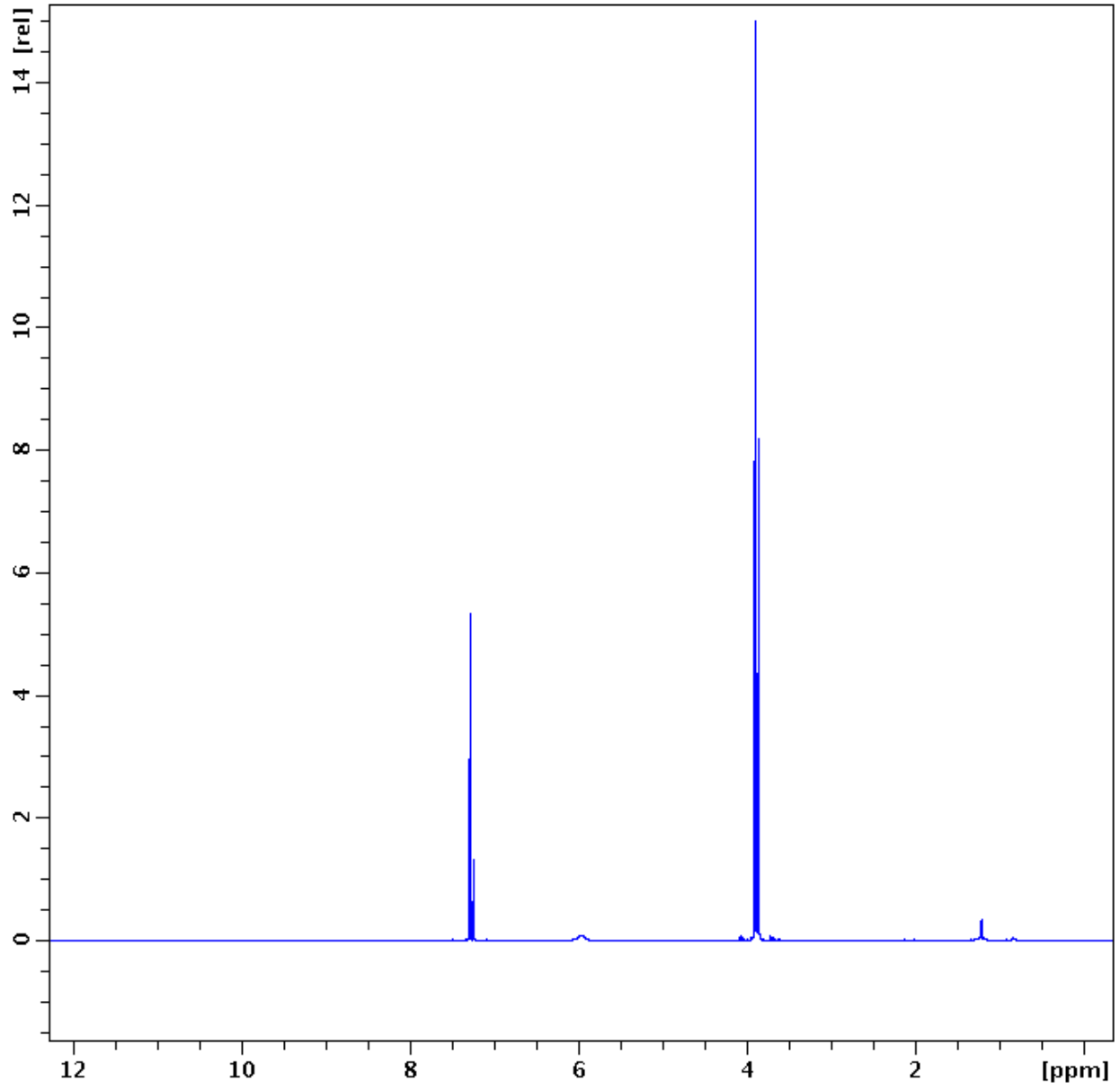

A55. ^{1}H-NMR spectrum of compound **(129)** in $CDCl_3$.

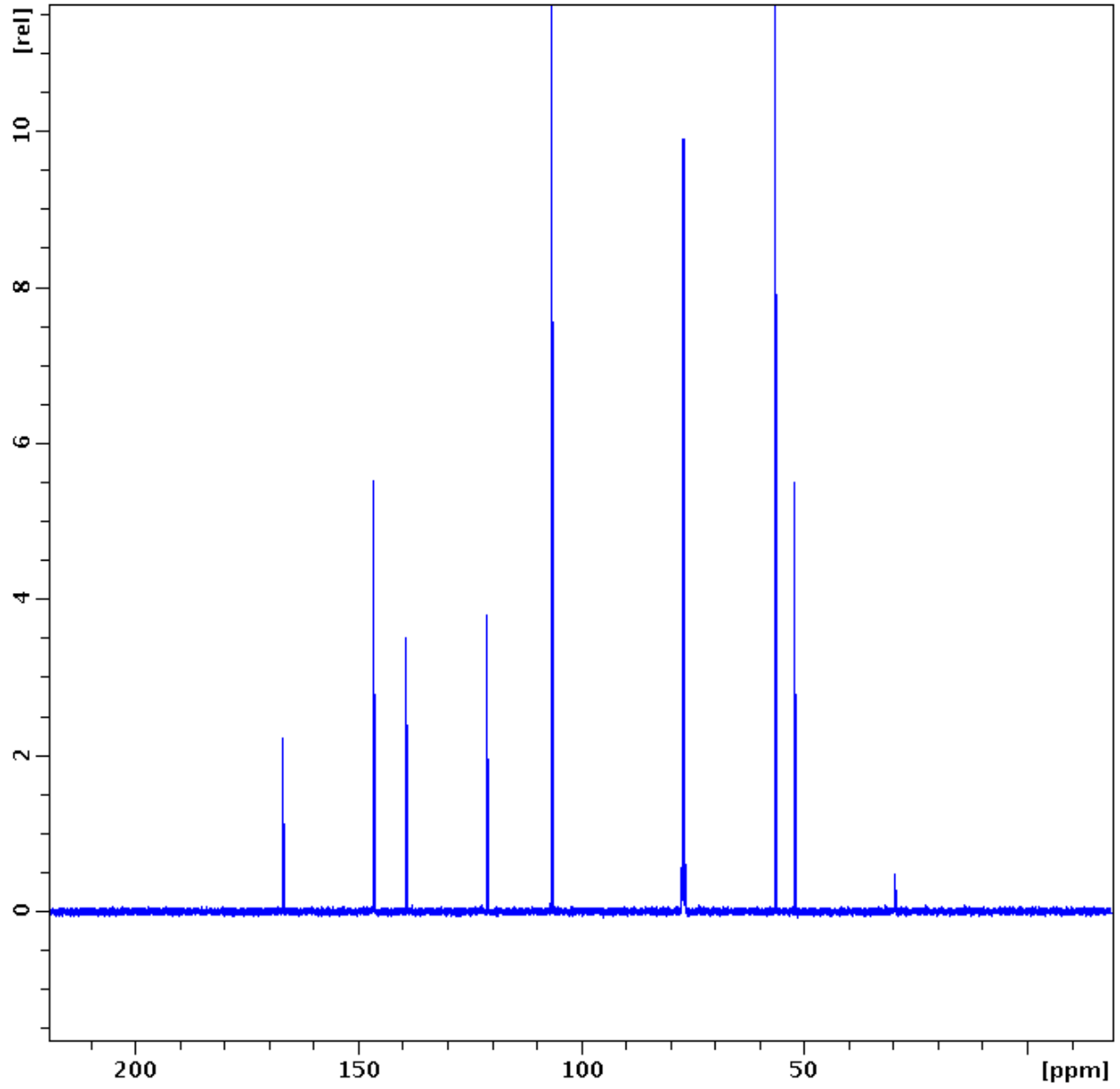

A56. ^{13}C-NMR spectrum of compound **(129)** in $CDCl_3$.

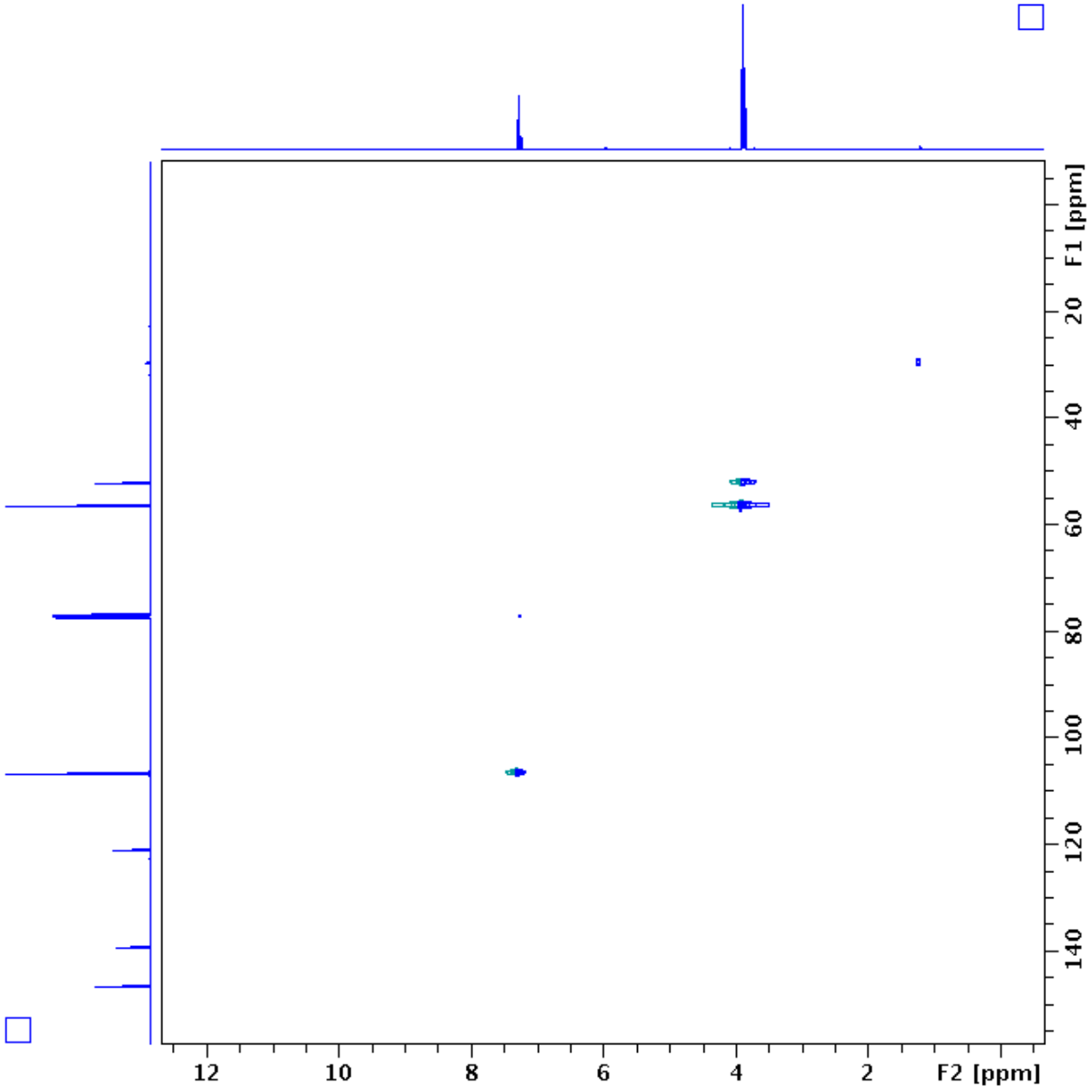

A57. HSQC spectrum of compound **(129)** in $CDCl_3$.

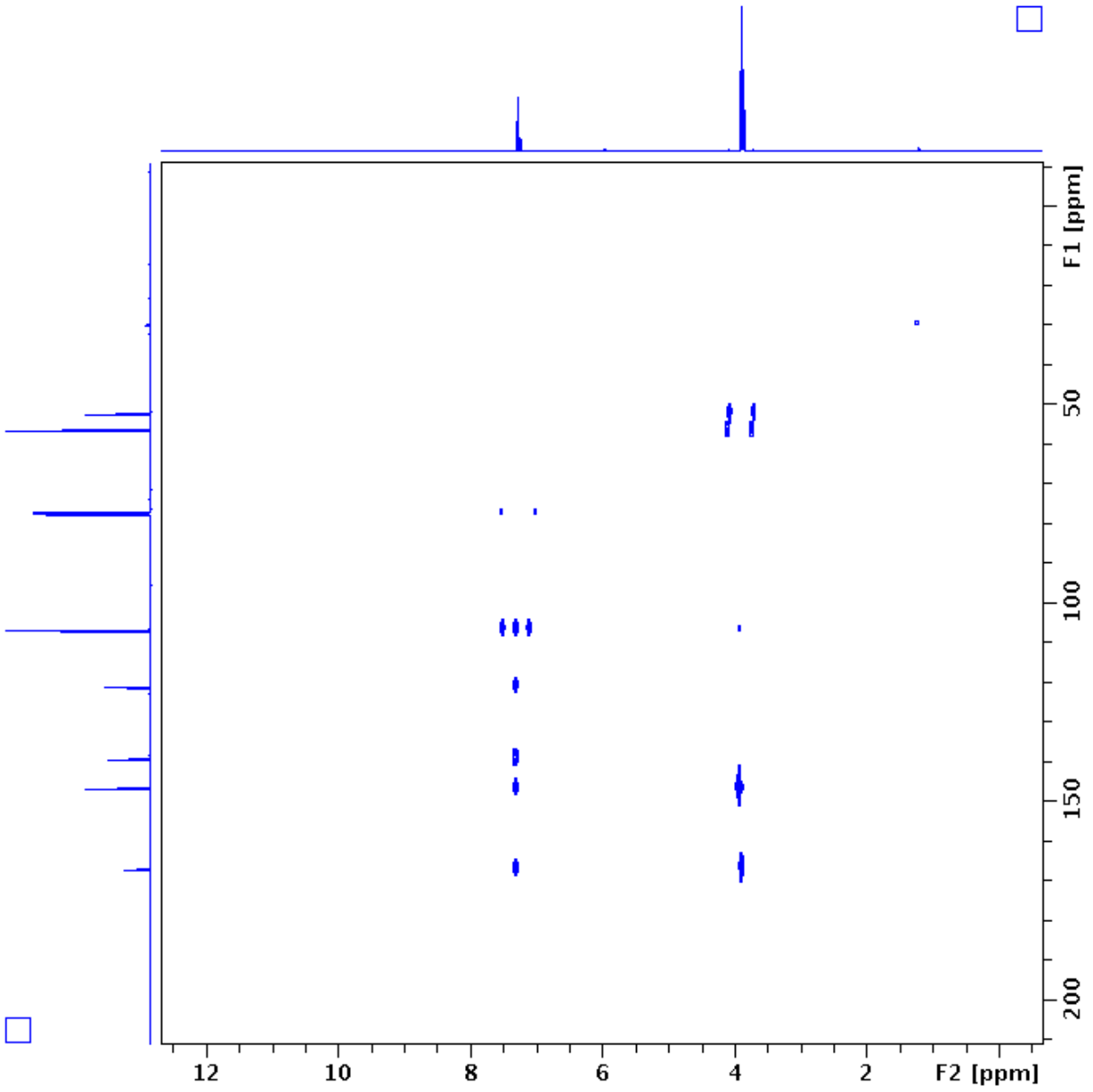

A58. HMBC spectrum of compound **(129)** in $CDCl_3$.

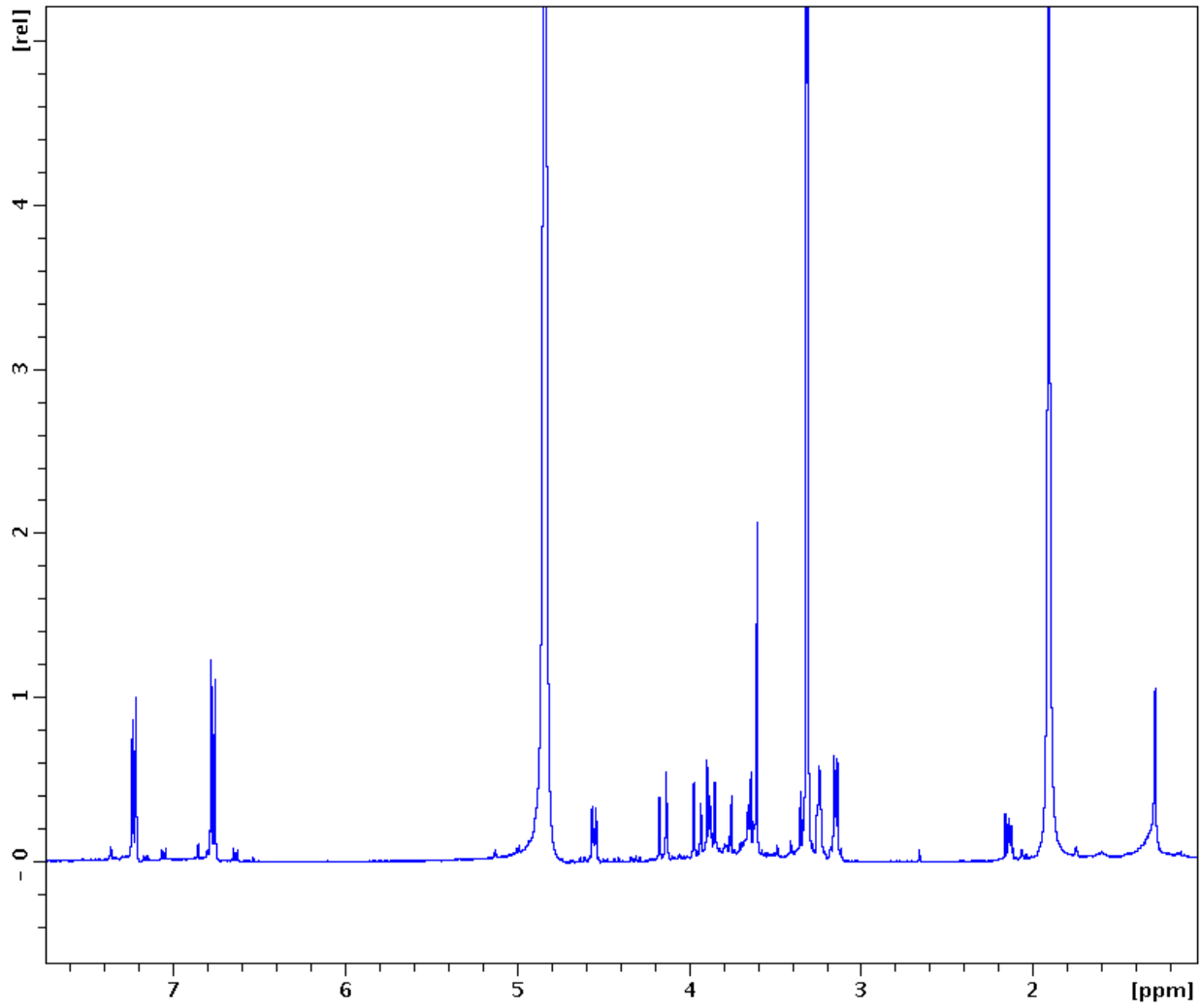

A59. ^{1}H-NMR spectrum of compound **(151)** in CD_3OD.

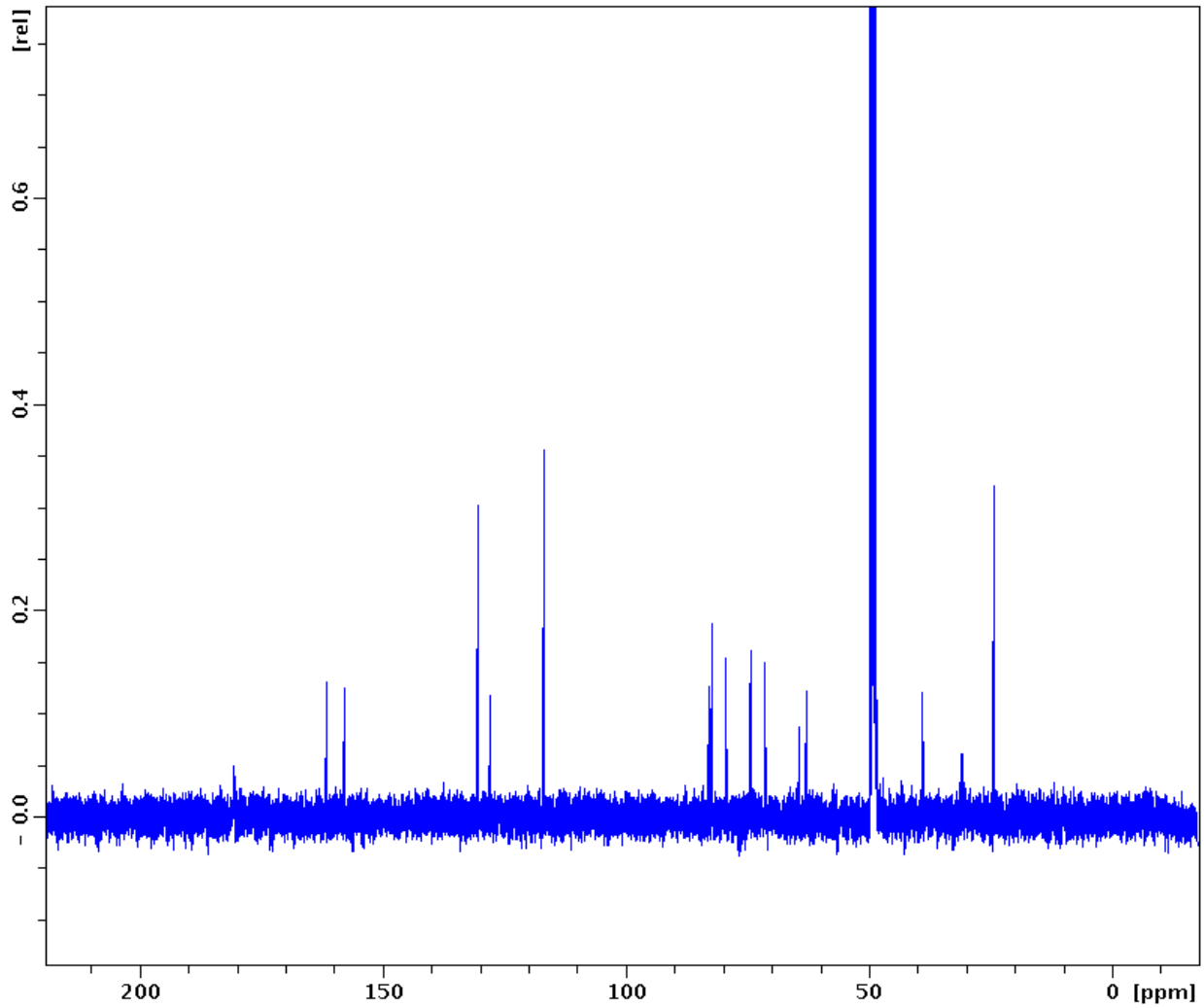

A60. ^{13}C-NMR spectrum of compound **(151)** in CD_3OD.

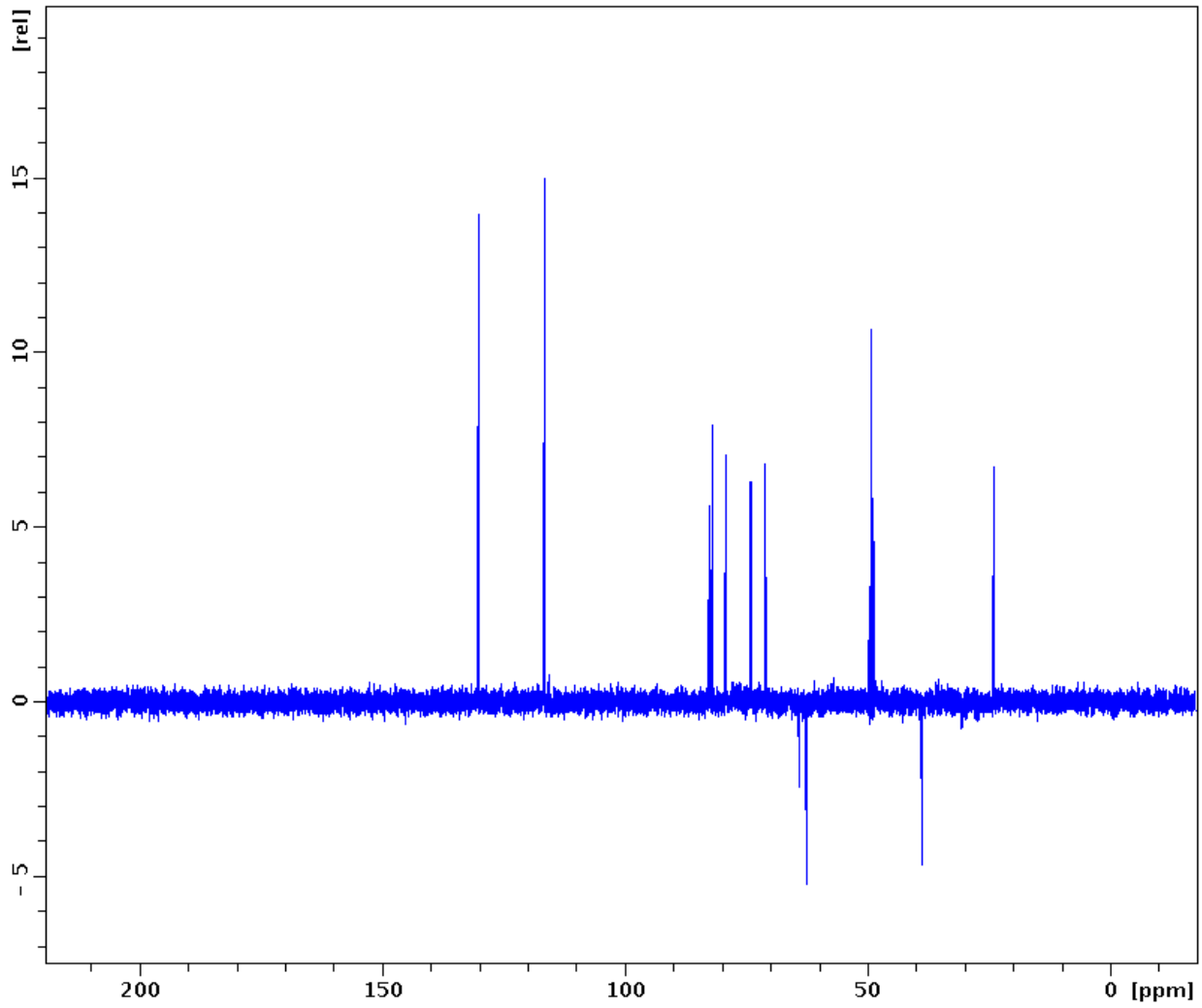

A61. DEPT 135 spectrum of compound **(151)** in CD_3OD.

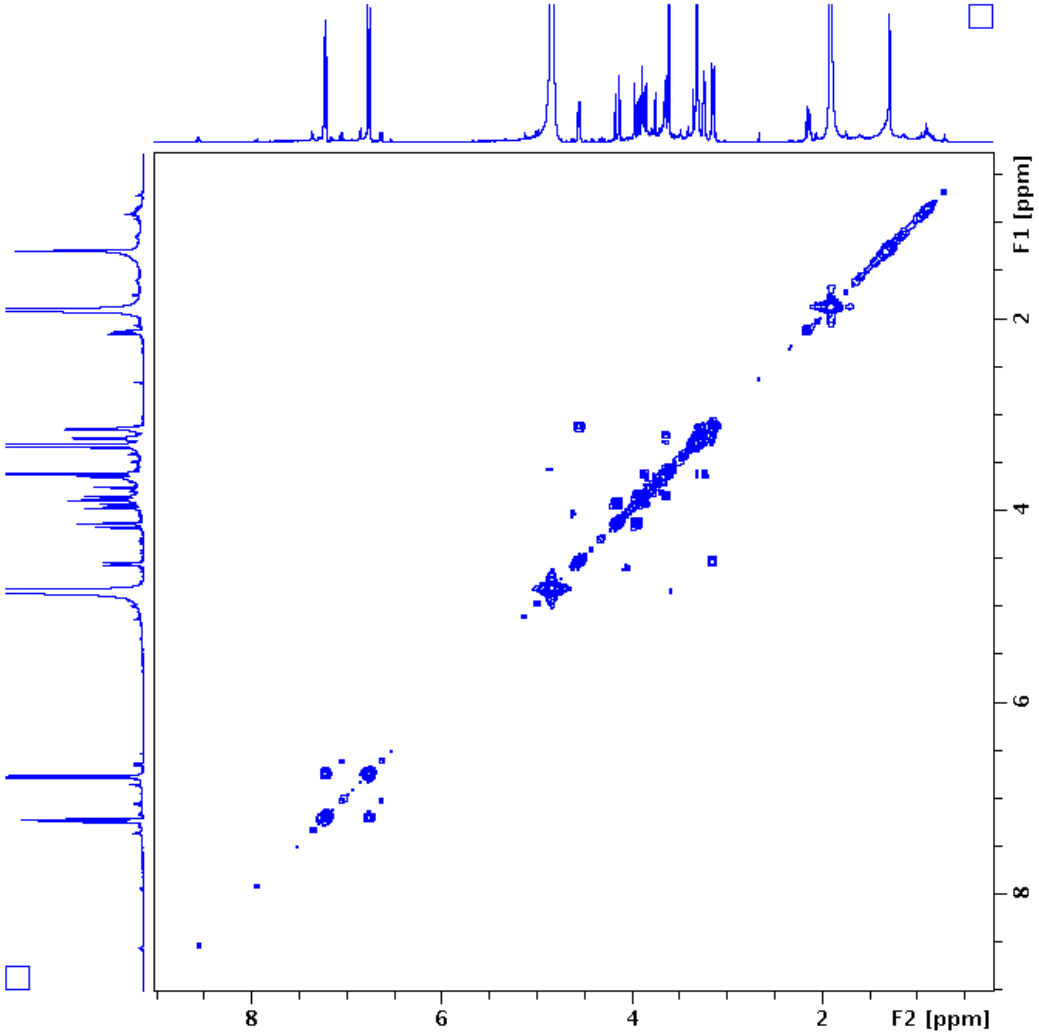

A62. COSY spectrum of compound **(151)** in CD_3OD.

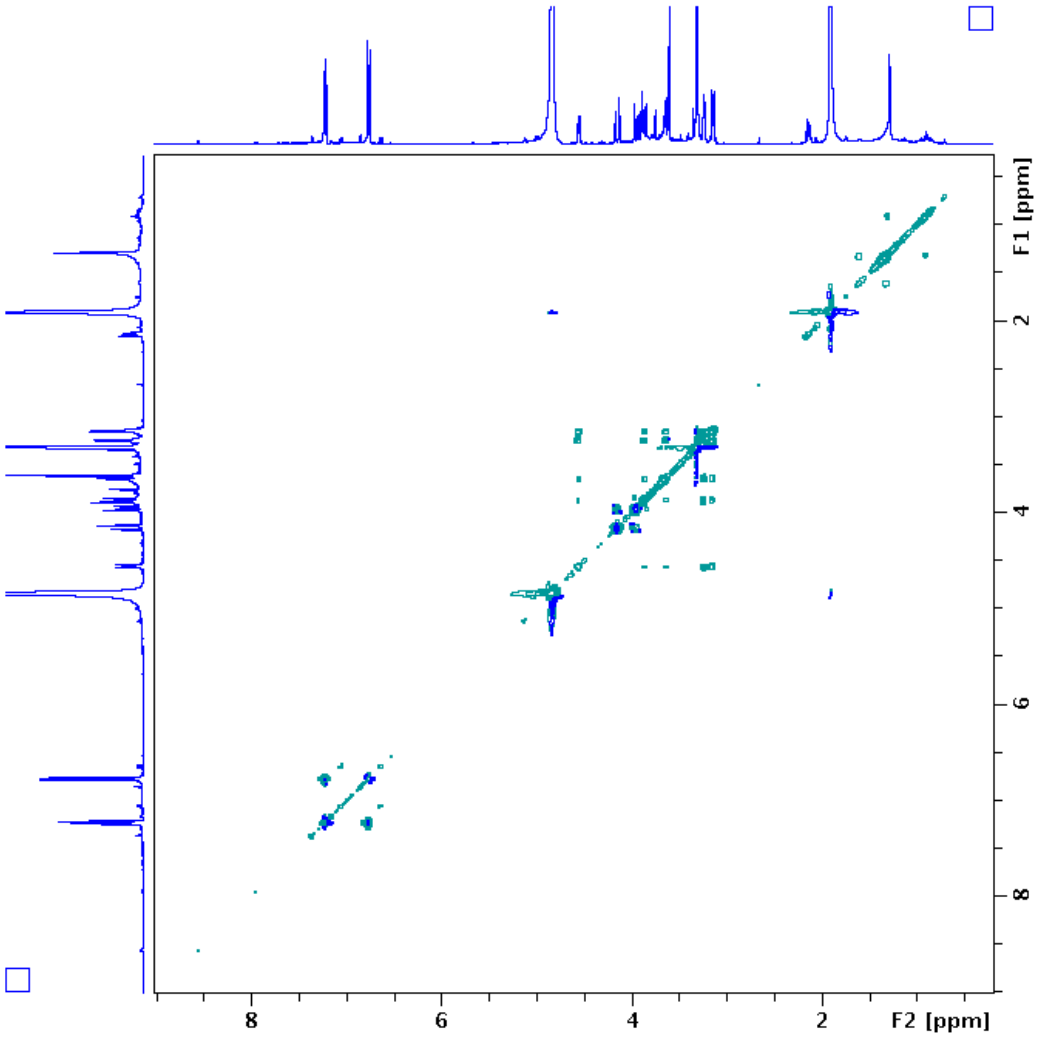

A63. TOCSY spectrum of compound **(151)** in CD_3OD.

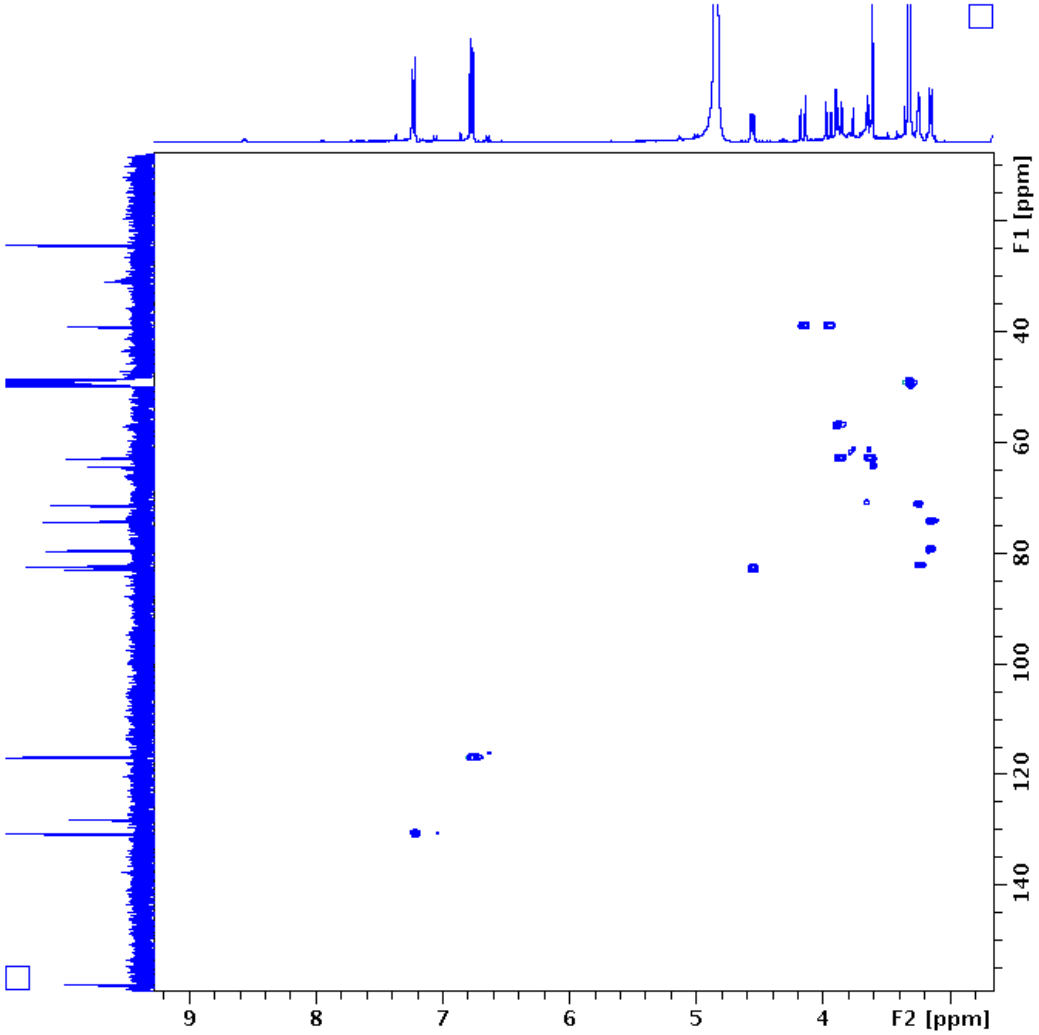

A64. HSQC spectrum of compound **(151)** in CD_3OD.

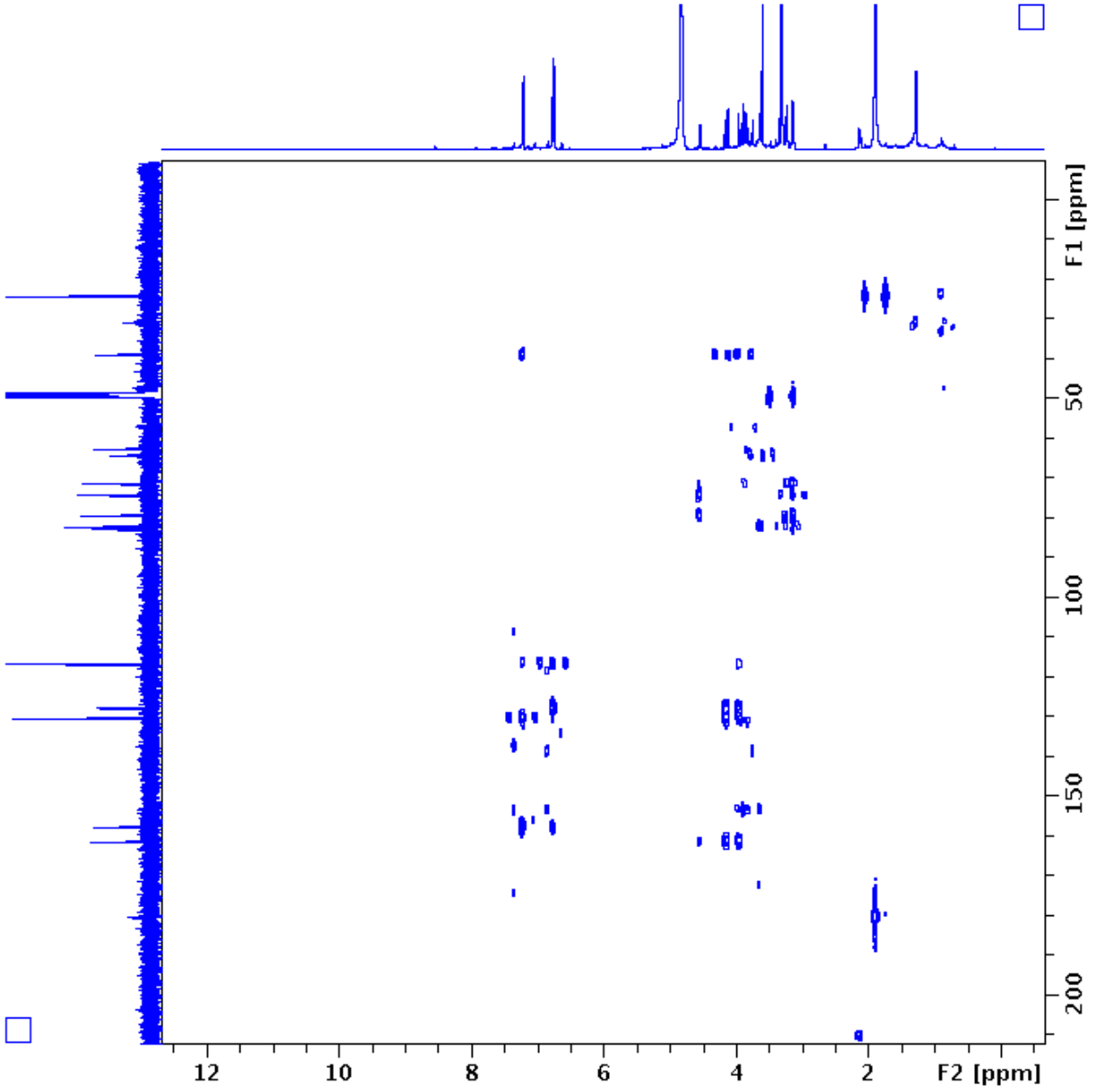

A65. HMBC spectrum of compound **(151)** in CD_3OD.

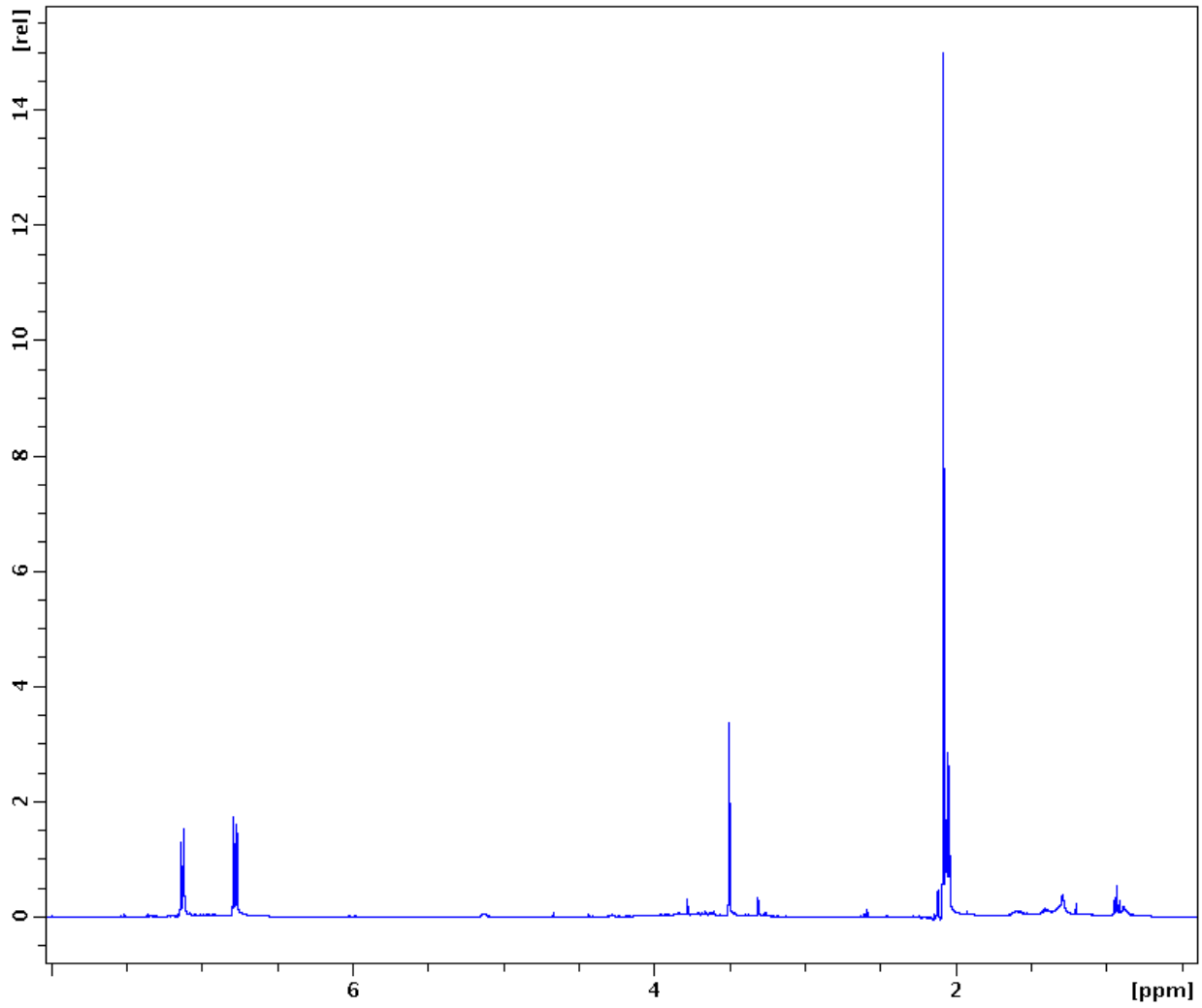

A66. ^{1}H-NMR spectrum of compound **(152)** in acetone-d_6.

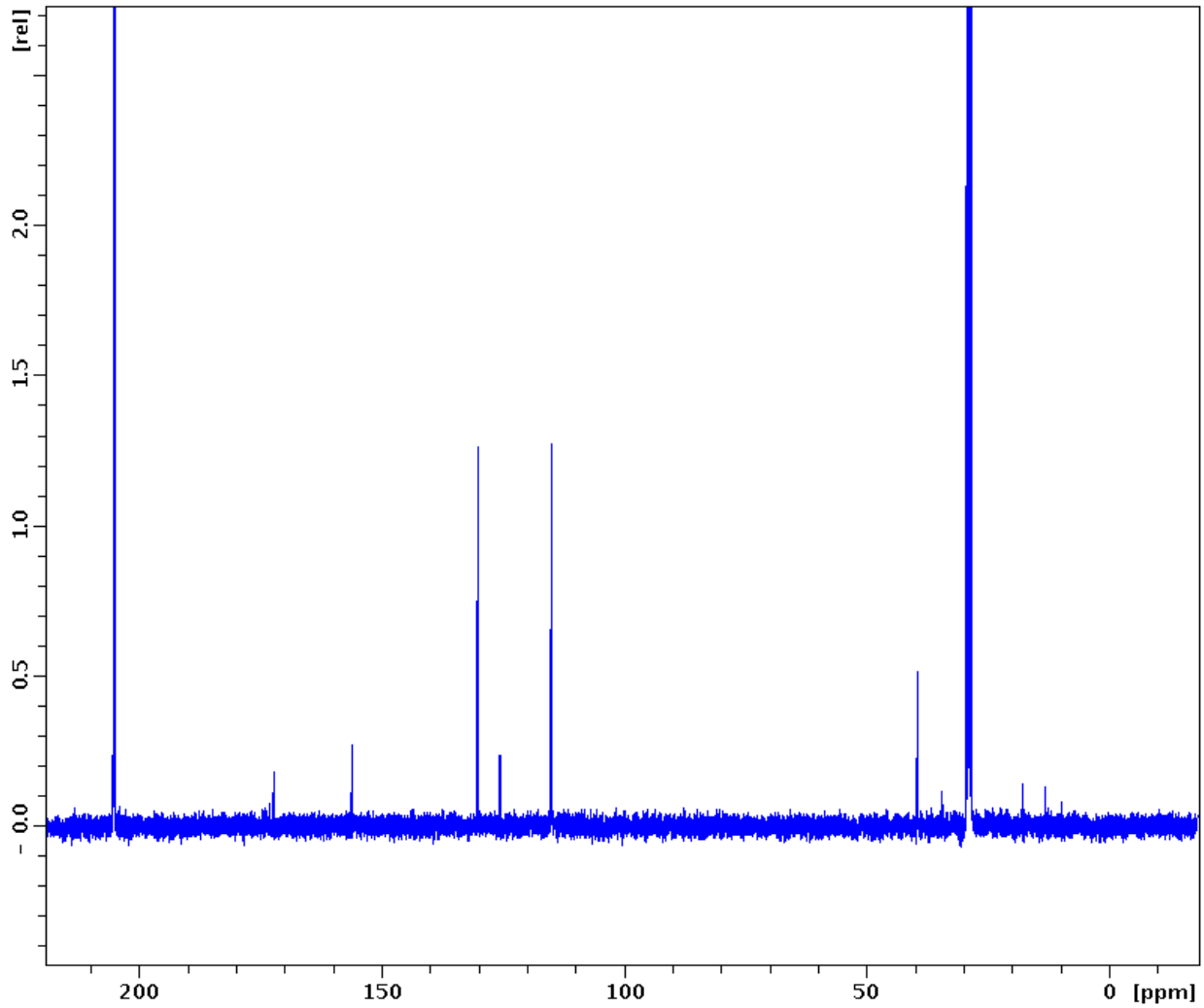

A67. ^{13}C-NMR spectrum of compound **(152)** in acetone-d_6.

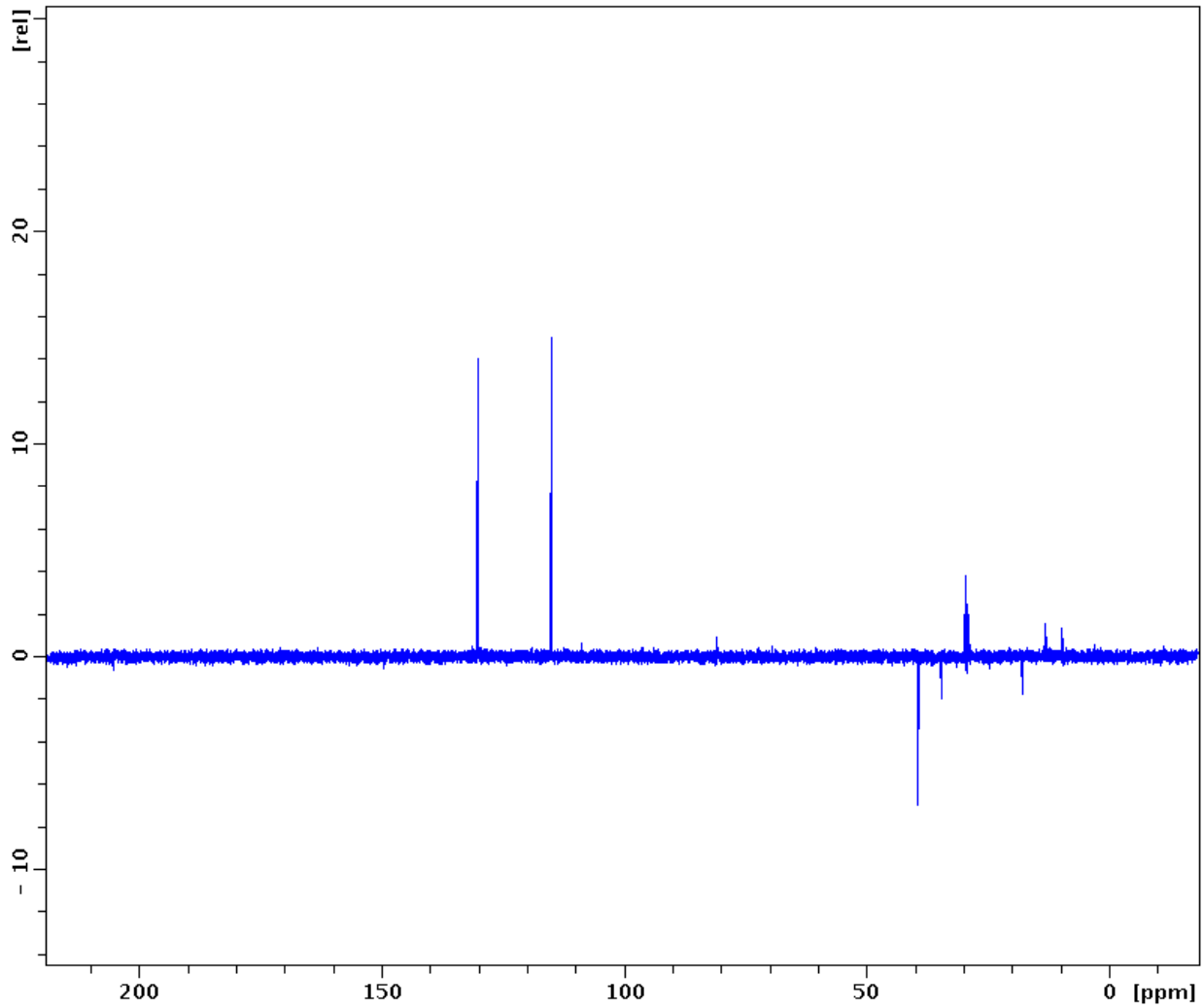

A66. DEPT 135 spectrum of compound **(152)** in acetone-d_6.

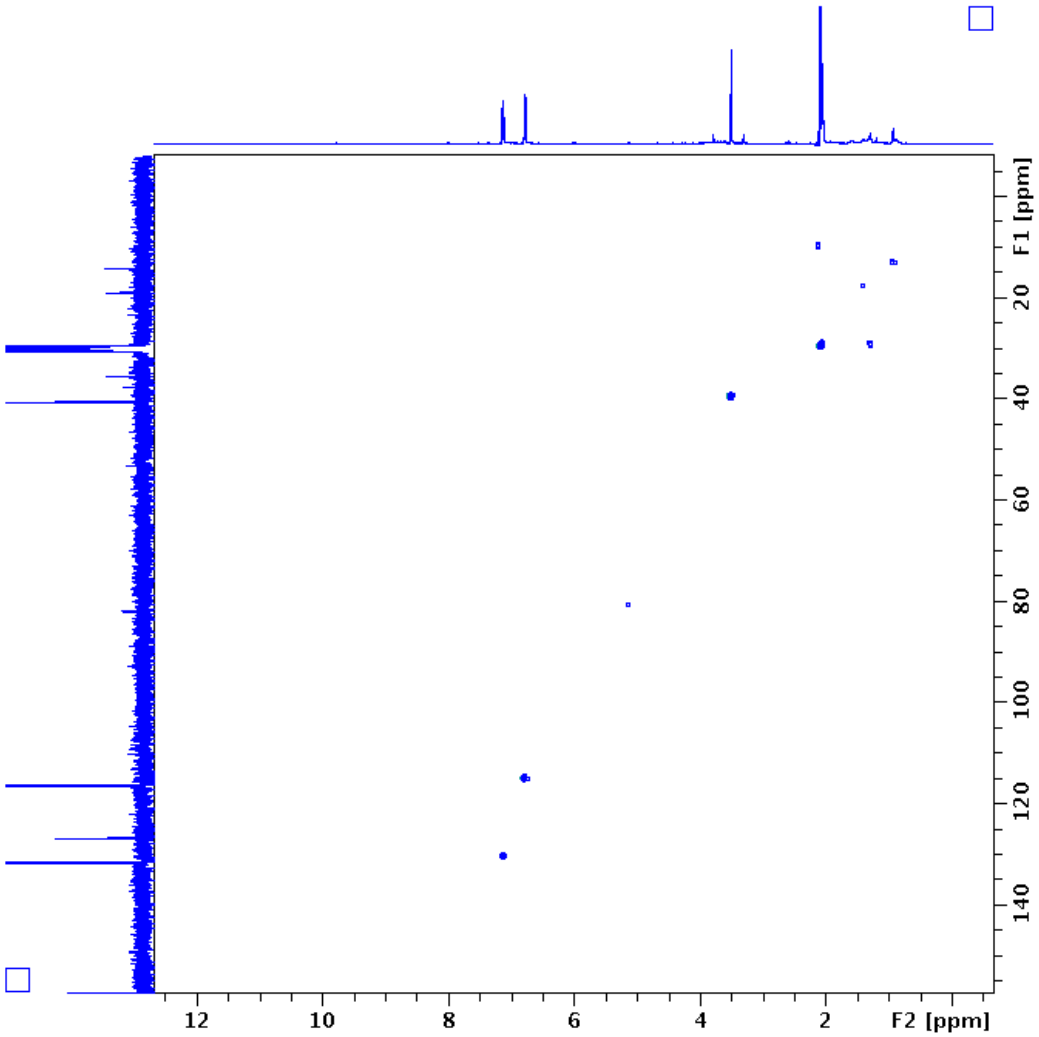

A69. HSQC spectrum of compound **(152)** in acetone-d_6.

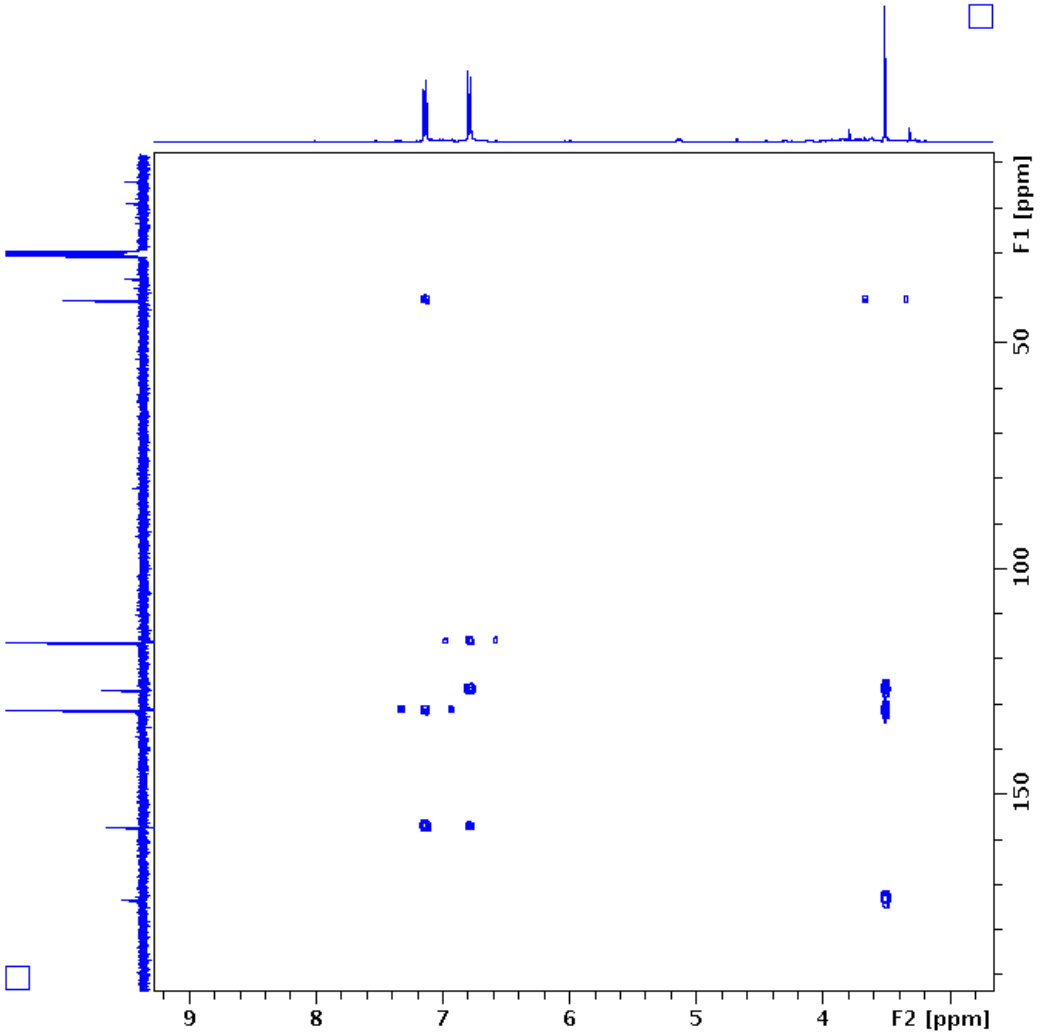

A70. HMBC spectrum of compound **(152)** in acetone-d_6.

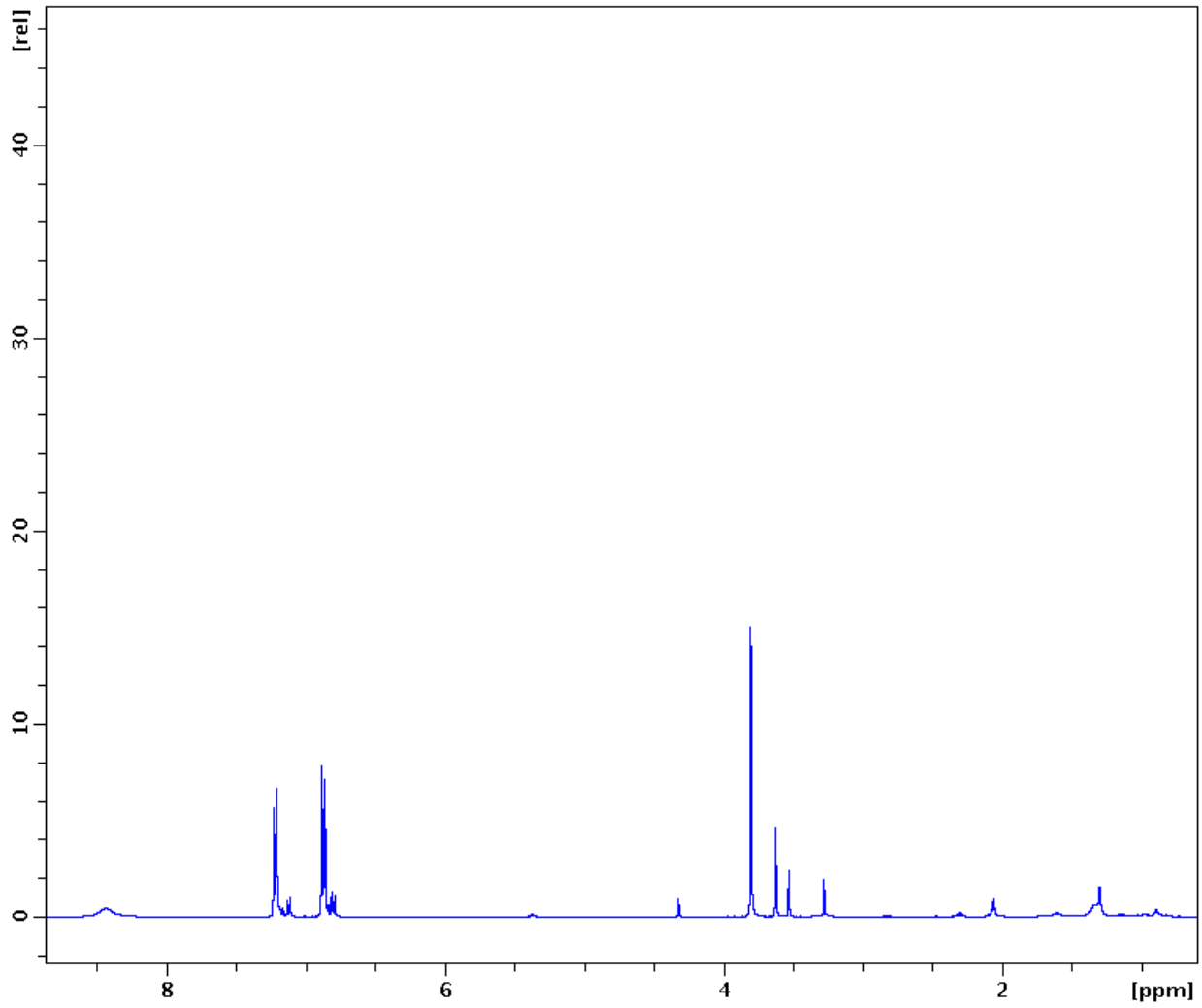

A71. ^{1}H-NMR spectrum of compound **(153)** in acetone-d_6.

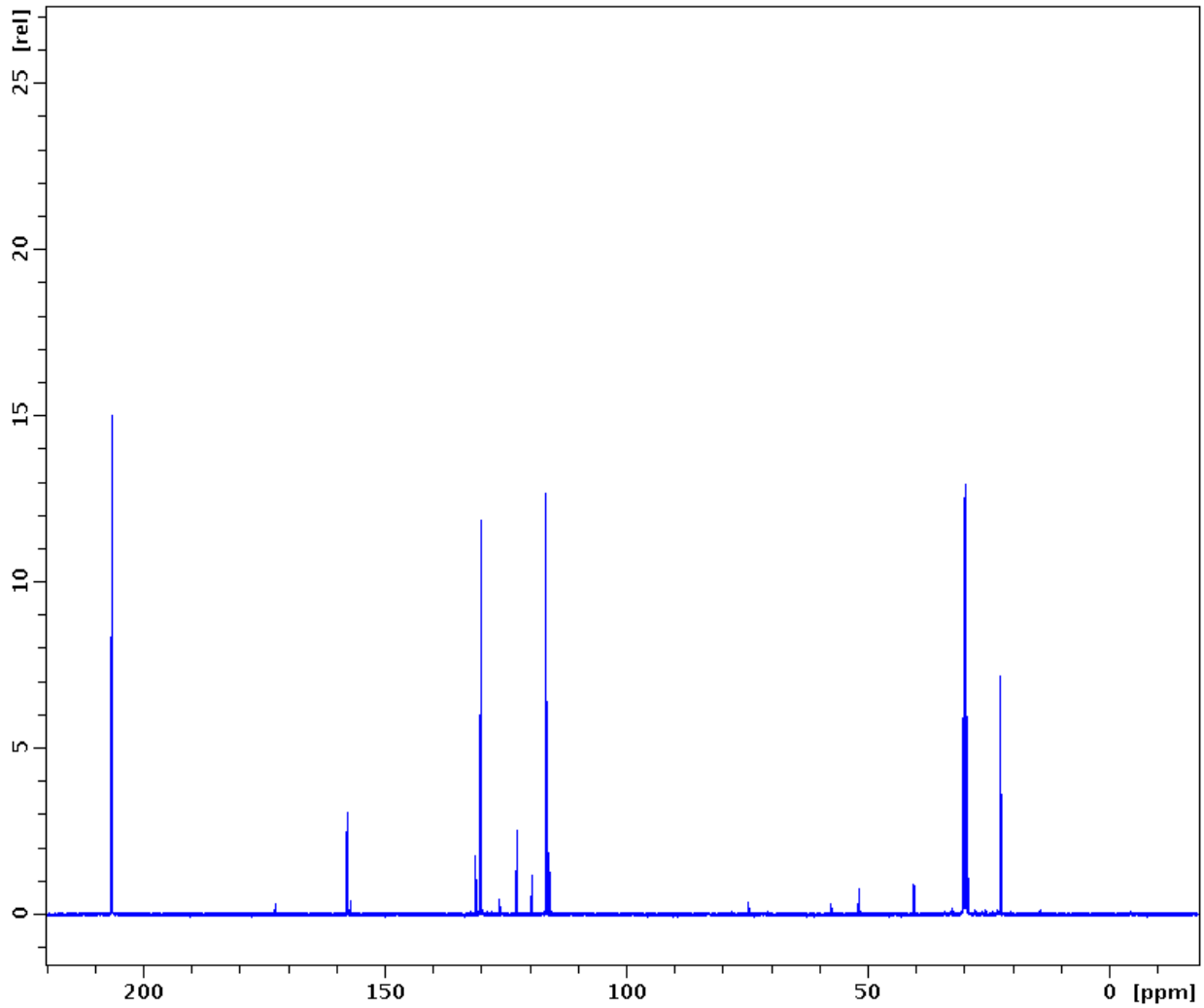

A72. ^{13}C-NMR spectrum of compound **(153)** in acetone-d_6.

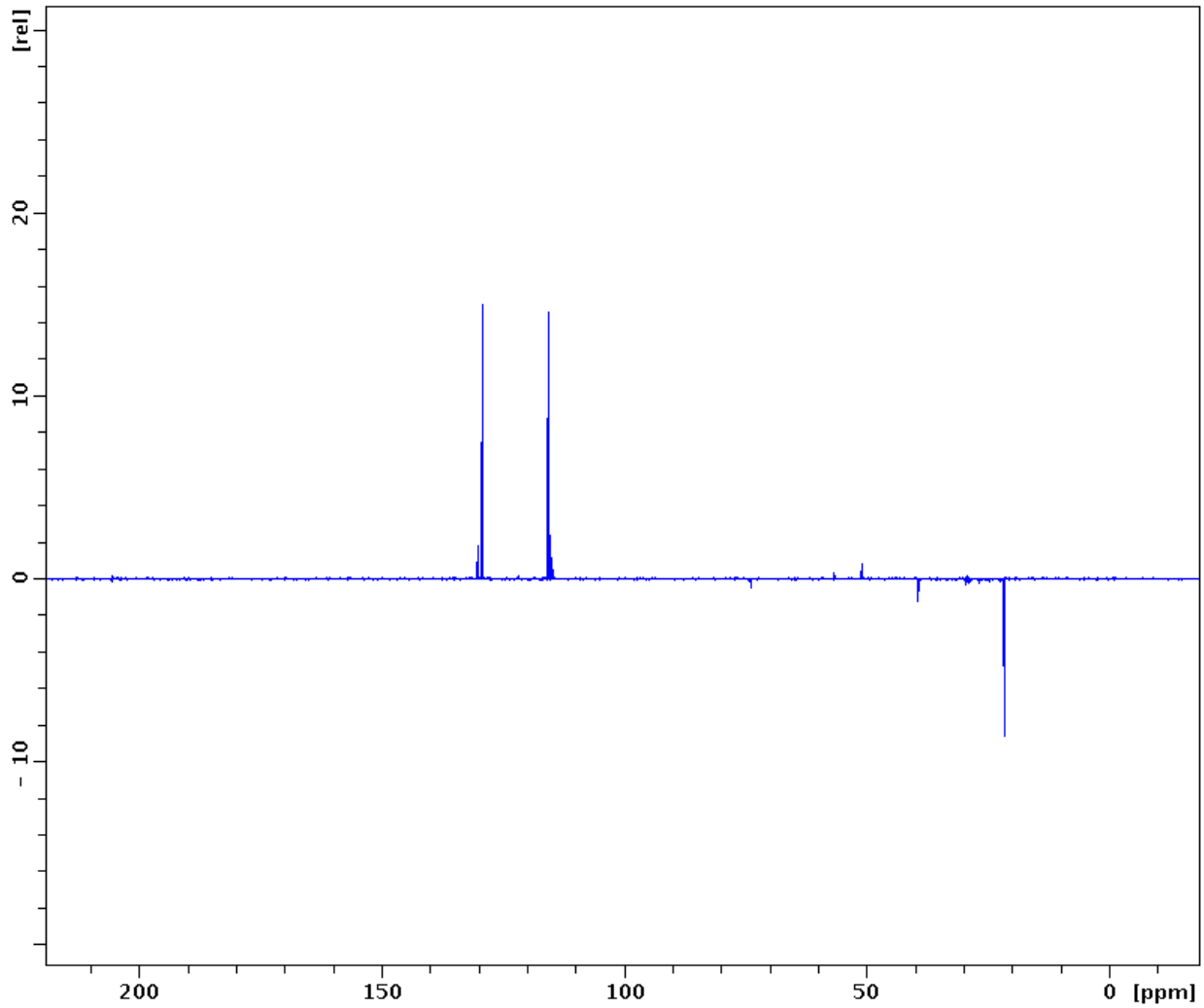

A73. DEPT 135 spectrum of compound **(153)** in acetone-d_6.

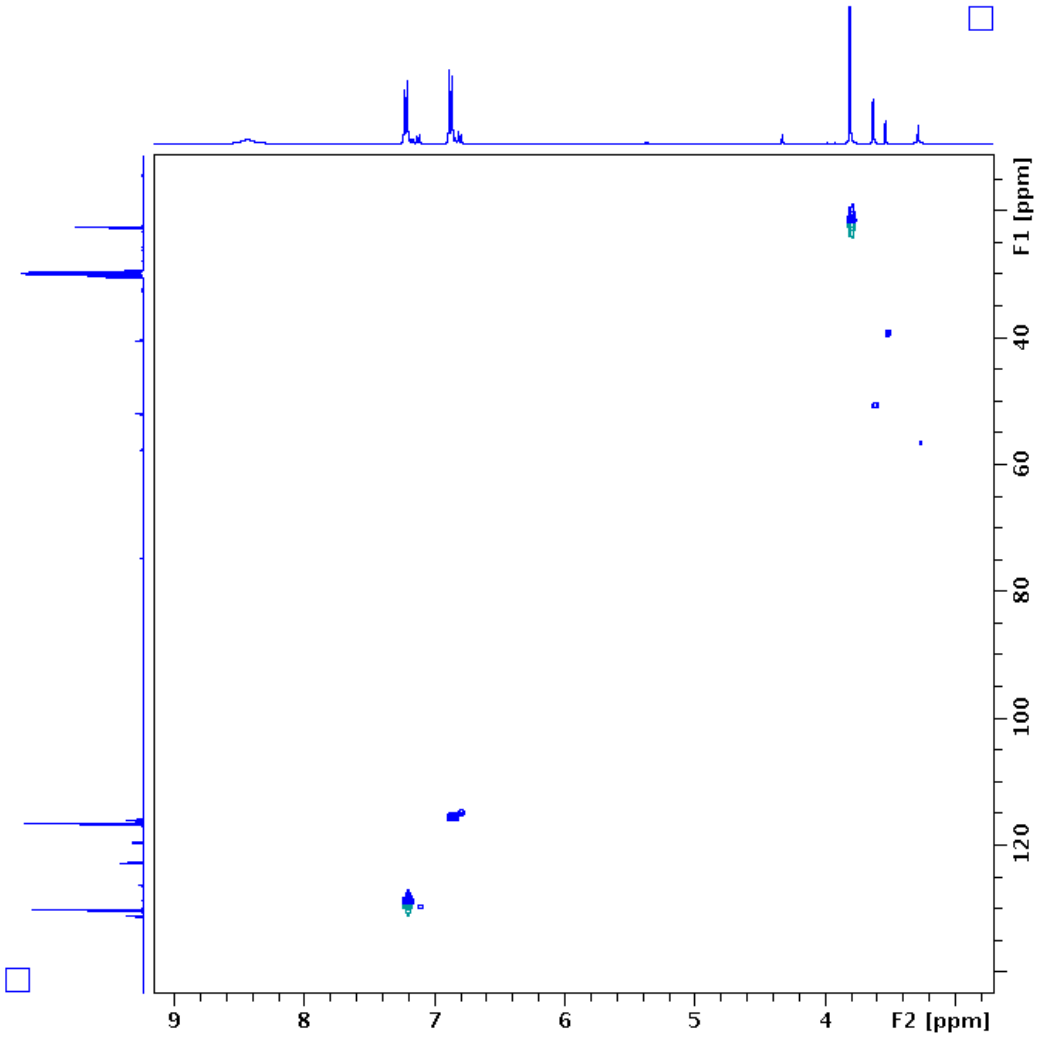

A74. HSQC spectrum of compound **(153)** in acetone-d_6.

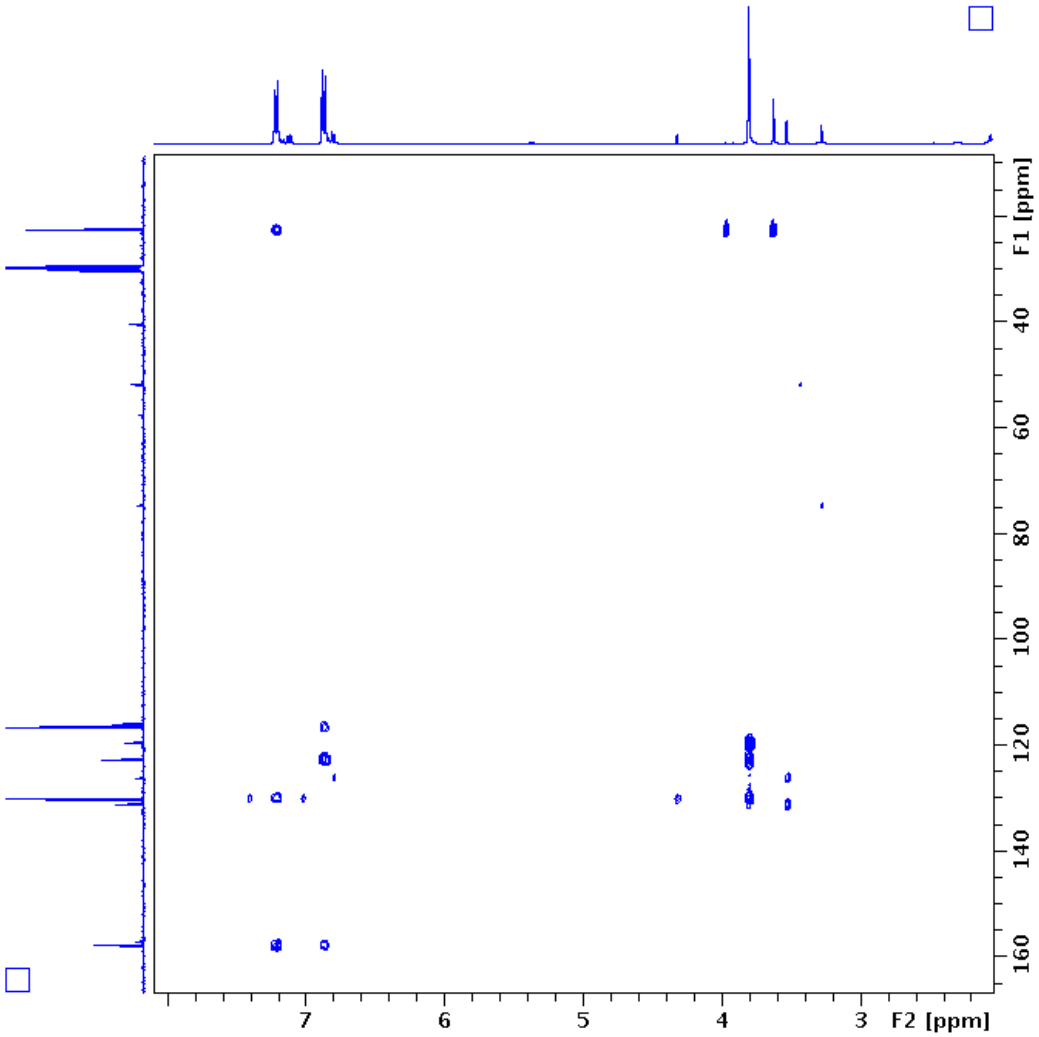

A75. HMBC spectrum of compound **(153)** in acetone-d_6.